

Equip GRID and GRIDSAT Tags with Accelerometers to Measure Ocean Waves

Wave Characterization Modules (WCMs)

Final Report

Bureau of Safety and Environmental Enforcement (BSEE)

Contract: E16PC00015

October 27, 2017

Prepared for:

Bureau of Safety and Environmental Enforcement (BSEE) E16PC00015
45600 Woodland Road
Sterling, VA 20166-9216

Prepared by:

Ben Schreib,¹ Manuel Sanchez,¹ Stephen Sporik,¹ Austin Vershel,¹ Sam McClintock,² Ted Hale,²
Elizabeth Skinner,² Navid Yazdi,³ Siva Aduri,³ Mark Hinders⁴

AECOM,¹ Midstream Technology,² Evigia Systems,³ College of William and Mary⁴

This final report has been reviewed by the Bureau of Safety and Environmental Enforcement (BSEE) and approved for publication. Approval does not signify that the contents necessarily reflect the views and policies of the BSEE nor does mention of the trade names or commercial products constitute endorsement or recommendation for use.

This study was funded by the BSEE, U.S. Department of the Interior, Washington, D.C., under Contract E16PC00015.

October 27, 2017

Point of Contact:

Ben Schreib
Project Manager
T: 410.379.5827
M: 301.305.8170
E: ben.schreib@aecom.com

AECOM
430 National Business Parkway
Annapolis Junction MD 20701
aecom.com

Table of Contents

Acronyms and Abbreviations	iv
1. Executive Summary	1-1
2. System Architecture	2-1
2.1 Commercial-off-the-Shelf Trade Study Summary	2-1
2.2 Design Report Summary	2-3
3. System Components	3-1
3.1 WCM, WCM-Sat, WCM-Buoy	3-1
3.1.1 Hardware Components	3-1
3.1.2 Enclosures	3-3
3.2 Embedded Software Development Platform	3-5
3.3 Wave Characterization Algorithms	3-5
3.4 Laboratory Testing	3-7
3.5 Field Testing: Albemarle Sound	3-9
3.6 Remote User Interface: Cloud Infrastructure and GIS Web Application	3-11
3.6.1 Software Tools	3-12
3.6.2 Cloud Infrastructure	3-12
3.6.3 Emulator	3-13
3.7 Local User Interface: Application Dashboard	3-13
3.7.1 Software Tools and Infrastructure	3-14
3.7.2 Emulator	3-14
4. Ohmsett Testing and Analysis	4-1
4.1 Facility and Equipment Setup and Configuration	4-1
4.2 Data Collection and Analysis	4-6
4.2.1 Wave Reflections	4-16
4.2.2 Oil Spray	4-16
4.2.3 Towed Test	4-18
4.3 Integrated System Demonstration	4-19
4.3.1 Test 13 – Chop, Stroke 12.0, CPM 30.0	4-20
4.3.2 Test 15 – Chop, Stroke 3.0, CPM 35.0	4-24
4.3.3 Test 17 – Sine, Stroke 18.0, CPM 10.0	4-28
4.3.4 Test 19 – Sine, Stroke 12.0, CPM, 25.0	4-33
4.3.5 Test 20 – Sine (Advancing), Stroke 7.5, CPM 35.0	4-39
5. Setup, Configuration, Operations, and Training	5-1
6. Conclusion	6-1
Appendix A Hardware and Firmware	
Appendix B Hardware Setup, Configuration and Operation	
Appendix C Local Application Dashboard User Guide	
Appendix D Remote GIS User Interface User Guide	
Appendix E RF Attenuation Analysis of Crude Oil	
Appendix F WCM-mounted Skimmer Significant Wave Heights	
Appendix G WCM-Buoy Significant Wave Heights	
Appendix H Difference in Significant Wave Height from Skimmer-Mounted WCM and Banners	
Appendix I Difference in Significant Wave Height between WCM-Buoy and Banners	

Appendix J Mean and Standard Deviation of Differences of the Significant Wave Height for WCM and WCM-Buoy Compared to Banner data

Appendix K Mean and Standard Deviation of Differences of the Significant Wave Height between Banners

Appendix L References

Figures

Figure 1-1: Wave Characterization Modules (WCMs) concept of operations 1-3

Figure 2-1: WCM system architecture block diagram..... 2-2

Figure 3-1: WCM, WCM-Sat, and WCM-Buoy hardware component architecture 3-1

Figure 3-2: WCM and WCM-Sat enclosure dimensions in millimeters (inches) 3-3

Figure 3-3: WCM and WCM-Sat enclosure with external WiFi antenna 3-3

Figure 3-4: WCM-Buoy enclosure with external antennas and counter-balance weight 3-4

Figure 3-5: WCM-embedded software development platform 3-5

Figure 3-6: Characteristics of ocean waves (height, length, and period)..... 3-6

Figure 3-7: Experimental setup using springs for laboratory testing..... 3-8

Figure 3-8: Plots of wave characterization algorithm steps from acceleration to heave 3-9

Figure 3-9: Mock weir skimmer with WCM-embedded software development platform 3-10

Figure 3-10: Field testing in Albemarle Sound 3-10

Figure 3-11: Web-based GIS user interface 3-11

Figure 3-12: iPad application dashboard viewing a WCM gateway report 3-13

Figure 3-13: iPad application dashboard viewing a WCM node report..... 3-14

Figure 4-1: Wave tank at Ohmsett 4-1

Figure 4-2: Ohmsett wave generator..... 4-2

Figure 4-3: Two WCMs, WCM-Sat, and WCM-embedded software development platform mounted to one of the Desmi Terminator’s floats 4-3

Figure 4-4: Craning the weir skimmer into the Ohmsett wave tank..... 4-3

Figure 4-5: Skimmer and WCM-Buoy deployments looking down from the auxiliary bridge 4-4

Figure 4-6: Ohmsett testing setup (top view) 4-4

Figure 4-7: Wave tank setup looking east 4-5

Figure 4-8: Varied significant wave height (H_{m0}) due to complex wave fields during Test 2 4-7

Figure 4-9: Significant wave height results from the skimmer for Test 19 4-8

Figure 4-10: Test 19 WCM on skimmer versus aux East Banner 4-9

Figure 4-11: WCM on skimmer mean and standard deviation by test..... 4-10

Figure 4-12: WCM-Buoy mean and standard deviation by test..... 4-11

Figure 4-13: Mean difference of main bridge Banner versus east aux bridge Banner..... 4-12

Figure 4-14: Difference between the WCM and the east auxiliary bridge Banner significant wave height calculations for Test 14 4-13

Figure 4-15: Difference between the WCM and the East Auxiliary Bridge Banner significant wave height calculations for Test 8 4-14

Figure 4-16: Albermarle Sound testing..... 4-15

Figure 4-17: Ohmsett Stroke 18, CPM 18 4-15

Figure 4-18: Oil-covered WCMs mounted to the skimmer 4-17

Figure 4-19: Oil-covered WCM-Buoy 4-17

Figure 4-20: Towed test.....	4-18
Figure 4-21: Test 13 Chop wave conditions – Stroke 12.0, CPM 30.0	4-20
Figure 4-22: Test 13 – Application dashboard screenshot of WCM 28988113 at 2:56 p.m.	4-21
Figure 4-23: Test 13 – Application dashboard screenshot of WCM-Sat 28988088	4-22
Figure 4-24: Test 13 – GIS user interface screenshot of WCM-Sat 28988088.....	4-23
Figure 4-25: Test 15 Chop wave conditions – Stroke 3.0, CPM 35.0	4-24
Figure 4-26: Test 15 – Application dashboard screenshot of WCM 28988113	4-25
Figure 4-27: Test 15 – Application dashboard screenshot of WCM-Sat 28988088	4-26
Figure 4-28: Test 15 – GIS user interface screenshot of WCM-Sat 28988088.....	4-27
Figure 4-29: Test 17 – Sine, Stroke 18.0, CPM 10.0	4-28
Figure 4-30: Test 17 – Application dashboard screenshot of WCM 28988113	4-29
Figure 4-31: Test 17 – Application dashboard screenshot WCM-Buoy 288988119.....	4-30
Figure 4-32: Test 17 – Application dashboard screenshot of WCM-Sat 28988088	4-31
Figure 4-33: Test 17 – GIS user interface screenshot of WCM-Sat 28988088.....	4-32
Figure 4-34: Test 19 – Sine, Stroke 12.0, CPM, 25.0	4-33
Figure 4-35: Test 19 – Application dashboard screenshot of WCM 28988113 at 10:51 a.m.	4-34
Figure 4-36: Test 19 –Application dashboard screenshot WCM-Buoy 288988119.....	4-35
Figure 4-37: Test 19 – Application dashboard screenshot of WCM-Sat 28988088	4-36
Figure 4-38: Test 19 – GIS user interface screenshot of WCM-Sat 28988088.....	4-37
Figure 4-39: Test 19 – Application dashboard screenshot of WCM 28988113 at 10:53 a.m.	4-38
Figure 4-40: Test 20 – Sine (Advancing), Stroke 7.5, CPM 35.0	4-39
Figure 4-41: Test 20–Application dashboard screenshot WCM-Buoy 288988119.....	4-40
Figure 4-42: Test 20 – Application dashboard screenshot of WCM 28988113	4-41
Figure 4-43: Test 20 – Application dashboard screenshot of WCM-Sat 28988088	4-42
Figure 4-44: Test 20 – GIS user interface screenshot of WCM-Sat 28988088 at the north end of the wave tank.....	4-43
Figure 4-45: Test 20 – GIS user interface screenshot of WCM-Sat 28988088 in the middle of the wave tank	4-44
Figure 4-46: Test 20 – GIS user interface screenshot of WCM-Sat 28988088 at the south end of the wave tank.....	4-45

Tables

Table 3-1: Primary Hardware Components	3-2
Table 4-1: Ohmsett Wave Settings Summary.....	4-5
Table 4-2: Mean Differences for All Tests for Each Banner	4-10
Table 4-3: H_{m0} for Test 13 – Chop, Stroke 12.0, CPM 30.0	4-20
Table 4-4: H_{m0} for Test 15 – Chop, Stroke 3.0, CPM 35.0	4-24
Table 4-5: H_{m0} for Test 17 – Sine, Stroke 18.0, CPM 10.0.....	4-28
Table 4-6: H_{m0} for Test 19 – Sine, Stroke 12.0, CPM 25.0.....	4-33
Table 4-7: H_{m0} for Test 20 – Sine (Advancing), Stroke 7.5, CPM 35.0	4-39

Acronyms and Abbreviations

6LoWPAN	internet protocol v6 over low-power wireless personal area networks	LQI	Link Quality Indicator
°C	degrees Celsius	MAC	medium access control
API	application program interface	MATLAB	matrix laboratory
ARM	advanced RISC [reduced instruction set computer] machine	MCU	microcontroller unit
BSEE	Bureau of Safety and Environmental Enforcement	min	minutes
CDIP	Coastal Data Information Program	MM	maintenance mode
cm	centimeter	mPa*sec	megaPascal second
COTS	commercial off-the-shelf	N/A	not applicable
cP	centiPoise	n.d.	no date
CPM	cycles per minute	PPS	pulse per second
CSV	comma-separated values	ppt	parts per thousand
dBm	decibel-milliwatts	RAM	random access memory
FFT	Fast Fourier Transform	RF	radio frequency
FIFO	first in first out	RSSI	relative received signal strength
g/mL	grams per milliliter	RTC	real-time clock
GHz	gigahertz	S	sulfur
GIS	geographical information system	SBD	short burst data
GPIO	general-purpose input/output	SO2	sulfur dioxide
GPS	global positioning system	SOCI2	thionyl chloride
GRID	Geo-Referencing Identification	SPI	serial peripheral interface
GRIDSAT	Geo-Referencing Identification Satellite	SSID	service set identifier
H _{1/3}	highest third of the wave heights	TCP/IP	transmission control protocol / Internet protocol
HCl	hydrogen chloride	TRL	Technology Readiness Level
H _{m0}	significant wave height	UDP	user datagram protocol
IEEE	Institute of Electrical and Electronics Engineers	URL	Uniform Resource Locator
IFFT	Inverse Fast Fourier Transform	USB	Universal Serial Bus
IMU	inertial measurement unit	UTC	Coordinated Universal Time
IP	ingress protection; Internet protocol	V	volt
JSON	JavaScript Object Notation	WAFO	Wave Analysis for Fatigue and Oceanography
kB	kiloByte	WCM	Wave Characterization Module
Li	lithium	WCM-Buoy	Wave Characterization Module – Buoy
LiCl	lithium chloride	WCM-Sat	Wave Characterization Module – Satellite

1. Executive Summary

The purpose of the project, Equip Geo-Referencing Identification (GRID) and Geo-Referencing Identification Satellite (GRIDSAT) Tags with Accelerometers to Measure Ocean Waves, was to develop a system that quantifies local wave characteristics.

The intended application of the system is the measurement of wave characteristics such as height, length, and period and to convey the information to local responders in real time via WiFi and remote reporting through a satellite network. The information will enhance situational awareness during an oil spill response, assisting stakeholders and mechanical skimming operations.

To accomplish the goal of the project, the AECOM team, which included Evigia Systems, Midstream Technology, and the College of William and Mary, created a family of devices and applications based on the successful GRID tagging system for the autonomous and long-term global tracking of remote assets without the need for local infrastructure. We equipped the GRID and GRIDSAT tags with accelerometers to measure ocean waves.

Based on the performance objectives of the project, we modified the baseline design, integrated, developed, fabricated, and tested the Wave Characterization Module (WCM), satellite-enabled Wave Characterization Module – Satellite (WCM-Sat), free-floating Wave Characterization Module – Buoy (WCM-Buoy), and local and remote user interfaces.

We successfully accomplished the following performance objectives of this project:

1. Enhance the latest generation of GRID and GRIDSAT tags with 3-axis accelerometers and other equipment/technology necessary to measure wave characteristics (e.g., wave height, wave length, wave period).
 - a. We successfully enhanced the GRID and GRIDSAT tags with an integrated inertial measurement unit (IMU) and associated microcontroller unit (MCU) with wave characterization algorithms to record, interpret, and report out wave data. The WCMs can be mounted on commercially available mechanical skimmers to measure the wave characteristics for use during oil spill response and recovery operations, providing quantitative feedback to operators and stakeholders. We tested several devices in the Albemarle Sound and field tested the entire system at the Ohmsett wave tank in Leonardo, NJ, advancing the technology from a Bureau of Safety and Environmental Enforcement (BSEE) Technology Readiness Level (TRL) 2—technology concept and speculative application formulated to a TRL 5—technology prototype demonstrated in relevant environment.
2. Use enhanced GRID and GRIDSAT tags to equip and test commercially available mechanical skimming units for wave characterization with accuracy within 4 inches, including choppy wave conditions and various sinusoidal wave conditions.
 - a. We mounted several WCMs and WCM-Sats on a weir skimmer along with a free-floating WCM-Buoy and successfully tested the system through various wave types and conditions such as sinusoidal and harbor chop, sprayed the devices with crude oil, and towed the skimmer through waves with successful operation and data communication. On average, the WCM attached on the skimmer was 2.7 inches higher and the buoy was 1.3 inches higher than the significant wave height calculated statistically using the raw data from the Ohmsett sensor Banner as a benchmark. The accuracy of our devices throughout all wave types and testing conditions was within the 4-inch performance objective.

3. Achieve satellite communication to transmit data for operational awareness.
 - a. Both the WCM-Sat and WCM-Buoy integrate a satellite modem for global coverage and reliable reporting of time, location, and wave information. We successfully designed and deployed a cloud-based solution to ingest and display the wave data on an Internet browser that has an accessible and user-friendly geographical information system (GIS) interface. This created a common operating picture for stakeholders and provided actionable intelligence at local and regional levels.
4. Create a user-friendly operator interface for a skimmer operator.
 - a. All three devices, WCM, WCM-Sat, and WCM-Buoy, have an integrated mesh network radio for device-to-device communication and a WiFi module for direct communication to a local user in real time, reporting wave characterization data. We successfully designed and tested a user-friendly tablet application dashboard to retrieve and display wave characterization reports to aid in situational awareness for skimmer operators.

The AECOM team envisions a suite of WCMs that provide wave condition data immediately to local operators and, when deployed throughout a region, collectively report actionable information to stakeholders. Figure 1-1 illustrates the concept of operations that corresponds to the project's purpose and application of assisting with oil spill response and recovery efforts.

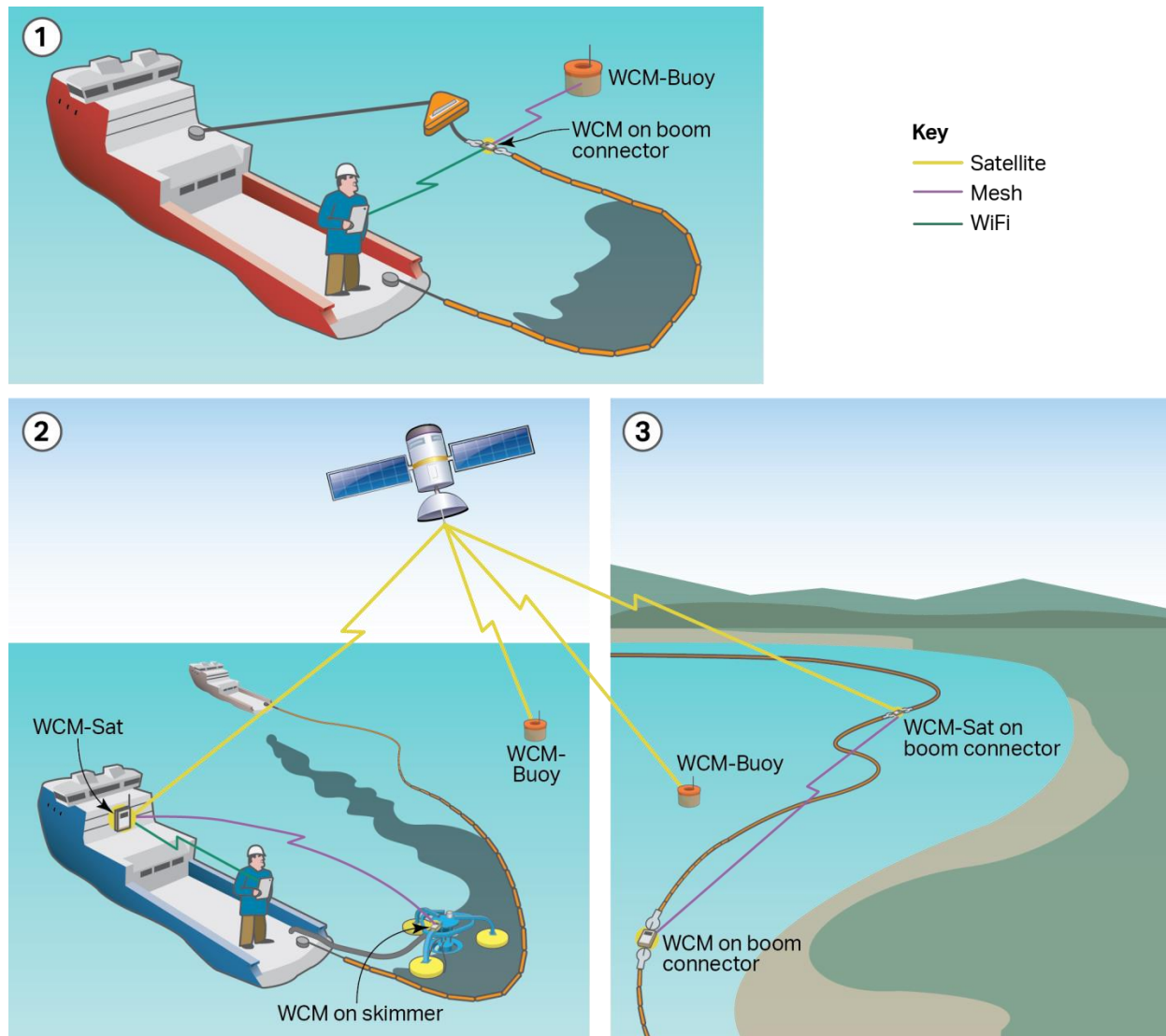


Figure 1-1: Wave Characterization Modules (WCMs) concept of operations

#1 shows a WCM-Buoy characterizing local wave conditions and transmitting information through the mesh network to a WCM. The WCM passes along the WCM-Buoy and its own data via WiFi for display on a local application dashboard, providing continuous updates to the response vessel's operators.

#2 shows a WCM attached to a skimmer transmitting wave conditions through the mesh network to a WCM-Sat for aggregation, summarization, and transmission via WiFi to a local user, as well as to the satellite gateway, onto the cloud database for display on the GIS user interface for remote stakeholders to view. The free-floating WCM-Buoy calculates local wave conditions and reports conditions through the satellite gateway for display on the GIS user interface.

#3 shows a boom protecting an environmentally sensitive shoreline with the WCM transmitting local wave conditions through the mesh network to a WCM-Sat, which then aggregates the wave conditions for transmission to the satellite gateway for display on the GIS user interface. Independently, WCM-Buoys deployed throughout the response area report their local wave conditions to the satellite gateway for viewing on the GIS user interface to provide a regional outlook.

2. System Architecture

Figure 2-1 shows the architecture of the system and interfaces between devices. The primary components and functionality of the deployed system are:

- **Wave Characterization Module (WCM)** – The WCM is intended to attach to a piece of equipment such as a skimmer and includes the hardware and software required to characterize wave conditions. The WCM includes a global positioning system (GPS) for accurate time keeping and location, radio frequency (RF) module for local mesh communications from device to device, and a WiFi module for direct communication to a local tablet for the display of wave characterization information on an application dashboard.
- **Wave Characterization Module – Satellite (WCM-Sat)** – The WCM-Sat includes all of the hardware and software of the WCM for wave characterization, GPS, mesh, and WiFi communications. The WCM-Sat is also intended to attach to high-value assets such as a vessel for remote reporting of location information, status, and wave conditions through the global satellite network.
- **Wave Characterization Module – Buoy (WCM-Buoy)** – The WCM-Buoy includes all of the hardware and software of the WCM-Sat but is intended to be free-floating and stay for an extended period on station reporting wave conditions.
- **Gateway and node configuration** – Each device can be configured in either gateway mode or node mode. When configured as a node, a WCM, WCM-Sat, or WCM-Buoy can only communicate its information through the mesh network to another device in the network. There is no pre-configuration required and joining to a network is autonomous with the ability to hop from device to device based on signal strength and availability to reach a gateway module.

When configured as a gateway, a WCM, WCM-Sat, or WCM-Buoy automatically reports its data and the data from the nodes in its mesh network to a user interface locally on a tablet application dashboard via WiFi and to the remote geographical information system (GIS) user interface through the satellite gateway via the Internet to a cloud-based server.

- **Local user interface** – The tablet application is used as a dashboard for local operators to view wave characterization reports via WiFi from a WCM, WCM-Sat, or WCM-Buoy configured in gateway mode.
- **Remote user interface** – The GIS user interface is intended for remote stakeholders to view wave characterization reports via satellite communications from a WCM-Sat or WCM-Buoy configured in gateway mode. The remote user interface is hosted in the cloud and is accessible from an Internet-connected web browser.

2.1 Commercial-off-the-Shelf Trade Study Summary

The AECOM team assessed available commercial-off-the-shelf (COTS) systems and performed a trade study of hardware, software, and protocols considered for the integrated WCM system.

To meet the project's performance objectives, a COTS wave characterization system must be able to meet the following criteria while measuring ocean wave characteristics:

- Operating while attached to a variety of booms, skimmers, buoys, and vessels. When attached to a boom or a skimmer, the device may have more than one degree of freedom reduced or eliminated, in which case additional modeling of the attached device data would be required to correctly characterize waves in operational conditions;
- Free-form operation, such as a floating buoy that has three axes of movement;

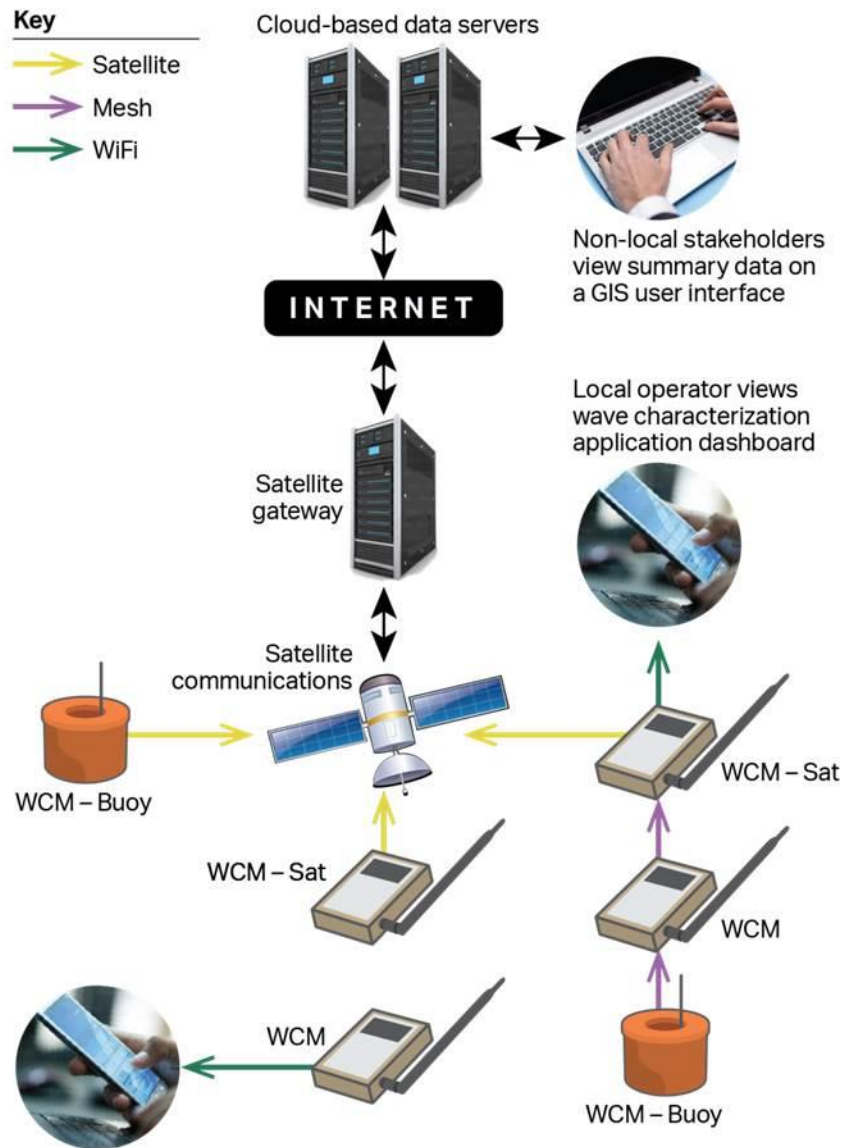


Figure 2-1: WCM system architecture block diagram

- A local mesh network for extended range communication among all devices within the wave characterization system. Each device in the system needs to be configurable as a node to pass along measurement information or as a gateway to report the collected data;
- Local communication and display of the wave characterization information through a dashboard; and
- Non-local communication and reporting through a global satellite network for remote viewing of the wave characterization data.

There were no existing wave-characterization COTS devices that met all of the performance objectives. Therefore, a trade study was performed to provide recommendations on the components, software, and protocols that should be considered for the design and development of the WCMs and reporting applications. These components, software and protocols included the inertial measurement unit (IMU); the primary sensor, which is used to record wave motion; sensor microcontroller unit that interprets and processes the IMU sensor data; device microcontroller, which packages and directs where the processed

data is sent; local wireless protocols and hardware components to communicate the information locally to a mobile device application dashboard; and the type of mobile device. The trade study facilitated the selection of the best components, devices, software, and protocols, as well as alternates in case integration or product issues were discovered during the design, production, and testing phases. The trade study findings are the foundation for both the embedded software development platform used as a pre-prototype to develop and test our algorithms and for the design of the wave characterization modules. The items that were selected were used in developing the design and documented in the design report.

2.2 Design Report Summary

The technology survey and trade study laid the foundation for determining the components, software, and protocols to use in detailing the design and functionality of the WCM, WCM-Sat, and WCM-Buoy and included the cloud infrastructure, remote web-based GIS user interface, and local wireless application dashboard.

The purpose of the design report was to:

- Provide a description of the pre-prototype WCM-embedded software development platform, its components, operation, algorithm development, and test results that influenced the design of the WCM family of devices,
- Outline the major components used in the WCM, WCM-Sat, and WCM-Buoy,
- Detail the functionality provided by each component or group of components,
- Show how various components interact and interface as designed,
- Provide a baseline for the WCM, WCM-Sat, and WCM-Buoy detailed design and development, and
- Show how the information is sent and displayed to remote and local operators and stakeholders.

At the design meeting, it was discussed that the several hundred feet of direct line-of-sight communication via WiFi may not provide the desired range for field operations. Through a design modification as documented in the external WiFi antenna memo, it was determined to address this challenge from two fronts:

- Swap out the WiFi module with integrated antenna internal to the enclosures with a WiFi module and external antenna to increase local communication range, and
- Strategically use the mesh radio network to extend the effective range from one WCM, WCM-Sat, or WCM-Buoy in node mode by inserting an additional device between the target node and gateway, allowing it to hop through one or more intermediate nodes to the final destination of a WCM, WCM-Sat, or WCM-Buoy configured as the gateway.

3. System Components

This section describes the design elements, modifications, and component integration to the baseline design for the WCM, WCM-Sat, and WCM-Buoy along with the methodology and approach to the embedded wave characterization algorithms, development, and deployment of the local wireless application dashboard and remote GIS user interface.

3.1 WCM, WCM-Sat, WCM-Buoy

Figure 3-1 describes the hardware components and communication interfaces within the WCM, WCM-Sat and WCM-Buoy.

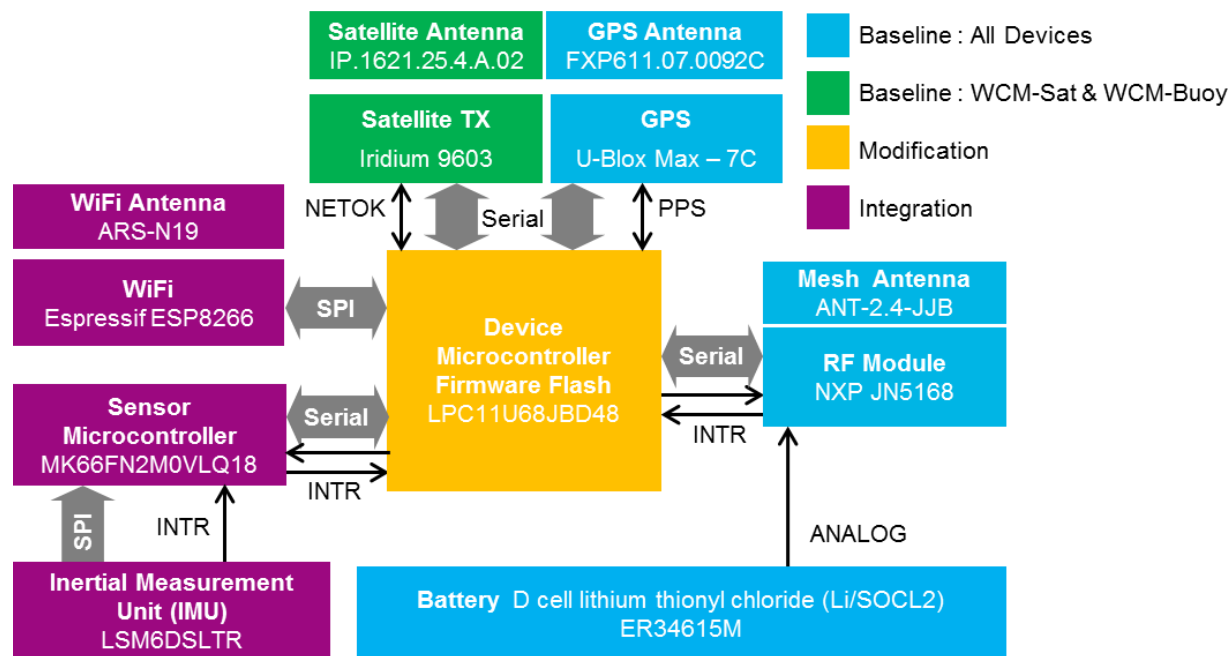


Figure 3-1: WCM, WCM-Sat, and WCM-Buoy hardware component architecture

Baseline: All Devices – Components based on the GRID and GRIDSAT tags, common to all wave characterization modules.

Baseline: WCM-Sat & WCM-Buoy – Components based on the GRIDSAT tag, common to the WCM-Sat and WCM-Buoy.

Modification – The device MCU firmware modified for the WCM system and sensor MCU messages and commands.

Integration – Hardware components and associated firmware integrated to characterize and report ocean wave information.

3.1.1 Hardware Components

The primary hardware modules for the WCM, WCM-Sat, and WCM-Buoy are detailed in Table 3-1.

The device MCU powers on the sensor MCU and IMU. Upon initialization, the sensor MCU starts to collect data from the IMU and processes the raw sensor data through the wave characterization algorithms. The resultant wave information is sent to the device MCU for packing into a predefined message format. The device MCU powers off the sensor MCU and IMU and powers on the GPS module to receive the current time and location. If the device is in node mode, the message is set out through the RF module via the mesh network to a gateway device. If the device is in gateway mode, the device MCU receives all node messages through the RF module and generates a wave characterization report, sending the message first via WiFi, then satellite for WCM-Sats and WCM-Buoys. See **Appendix A** for details regarding each component, its interfaces, and sequence of communication.

Table 3-1: Primary Hardware Components

Component	Model	Interface	Description
IMU	LSM6DSLTR	SPI and interrupt	3-axis accelerometer and 3-axis gyroscope with 4 kB FIFO
Sensor MCU	MK66FN2M0VLQ18	<ul style="list-style-type: none"> • GPIO for interrupt • Serial port communication to the device MCU 	Runs algorithms on IMU data to calculate wave parameters and transfers results to the device MCU
WiFi Module	ESP8266	<ul style="list-style-type: none"> • SPI bus • Power on/off digital signal 	WiFi chipset to deliver wave characterization data locally
Device MCU	LPC11U68JBD48	Serial ports for communications with the GPS, satellite modem, local wireless module, sensor MCU and RF module	Low-power ARM-based MCU that coordinates the activity of each hardware component
RF Module	JN5168-001-M06	Serial interface and interrupt	2.4 GHz 6LoWPAN module with support for application tasks built into its firmware
GPS	MAX_7C	<ul style="list-style-type: none"> • Asynchronous serial port and 1 PPS signal to connect to the device MCU • Power on/off digital signal 	Low power and voltage GPS module
Satellite Modem	Iridium 9603	<ul style="list-style-type: none"> • Network ready signal to connect to the device MCU • Asynchronous serial port for data • Power on/off digital signal 	Satellite modem module for communications to cloud server and GIS interface

6LoWPAN = Internet protocol v6 over low-power wireless personal area networks
 ARM = advanced RISC [reduced instruction set computer] machine
 FIFO = first in first out
 GHz = gigahertz
 GIS = geographical information system
 GPIO = general-purpose input/output

GPS = global positioning system
 IMU = inertial measurement unit
 kB = kiloByte
 MCU = microcontroller unit
 PPS = pulse per second
 RF = radio frequency
 SPI = serial peripheral interface

3.1.2 Enclosures

Figure 3-2 shows the dimensional drawings of the WCM and WCM-Sat. The enclosure uses thick-walled polycarbonate plastic with pressurized screws to provide ingress protection (IP) 67 sealing, which provides protection for immersion in up to 1 meter of water for 30 minutes.

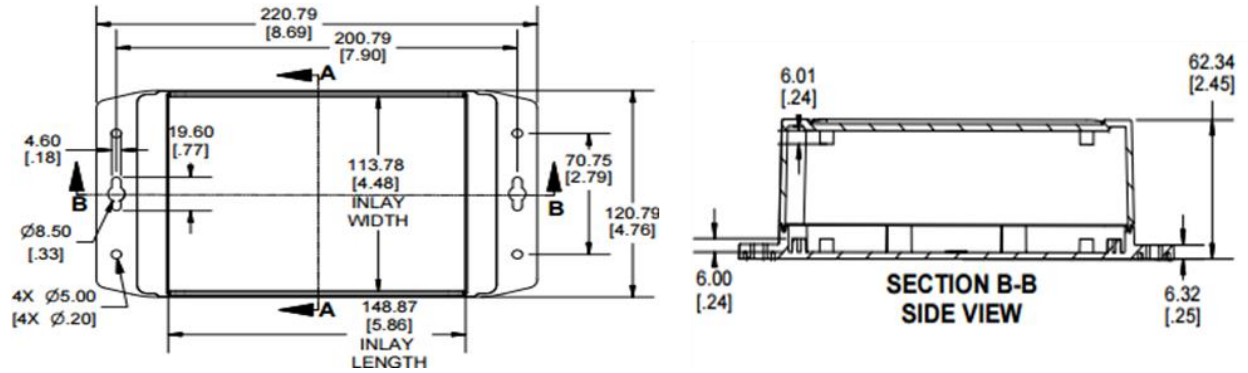


Figure 3-2: WCM and WCM-Sat enclosure dimensions in millimeters (inches)

Figure 3-3 shows the WCM and WCM-Sat enclosure with the external WiFi antenna.



Figure 3-3: WCM and WCM-Sat enclosure with external WiFi antenna

The WCM-Buoy enclosure shown in Figure 3-4 is constructed of polypropylene and painted to be resistant to ocean environments and can withstand being dropped without damage to the case material. The material is almost the same density of water ($\times 1.1$), so a minimal amount of air captured in the circuitry compartment is enough to keep it afloat. The WCM-Buoy is designed so that approximately 75 percent is submerged to minimize wind impact on measurements. The bottom has several attachment points for tethering and for various weights to dampen unwanted motion when deployed. The satellite, WiFi, and GPS antennas are epoxied (with marine-grade epoxy) into a recessed lid compartment, with a 1/16-inch plastic cover epoxied over the antennas.



Figure 3-4: WCM-Buoy enclosure with external antennas and counter-balance weight

3.2 Embedded Software Development Platform

After the COTS assessment, technology survey, and trade study, we fabricated several pre-prototype WCMs for embedded software development and component testing. As pictured in Figure 3-5, we were able to quickly bread-board together the primary hardware components including WiFi and Bluetooth versions for further local wireless communication evaluation, ultimately selecting WiFi for its flexibility and transmission range. We were also able to test the wireless protocols and data transfer with our tablets. The most important enabler from the embedded software development platform was the ability to stream raw data from the IMU to develop and refine the wave characterization algorithms in parallel with the full design and fabrication of the WCM, WCM-Sat, and WCM-Buoy.

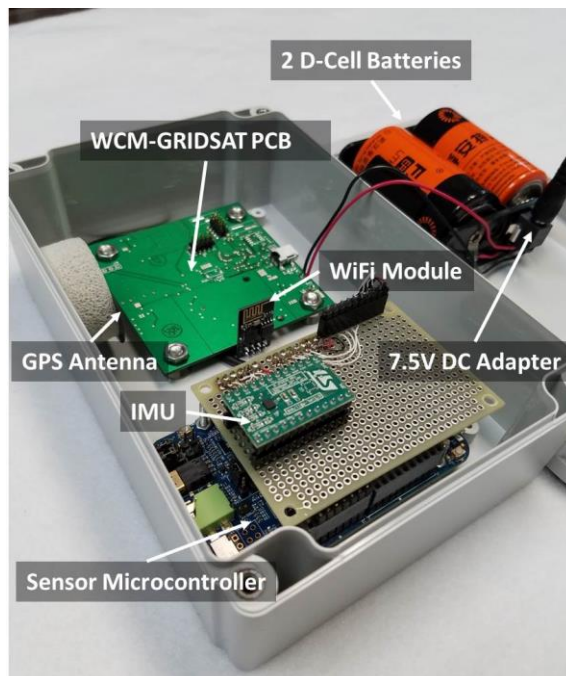


Figure 3-5: WCM-embedded software development platform

3.3 Wave Characterization Algorithms

In order to report wave characterization data, we first defined which measurements the IMU could make and how the measurements would be used to determine wave characteristics such as height, length, and period.

An ocean wave is the flow of energy traveling from its source, not the water itself, and therefore, anything floating on top of a wave, such as a buoy, moves in a circular rise-and-fall pattern (CDIP, n.d.). This allows us to measure wave elevation from the surface of the ocean. A WCM-Buoy or WCM attached to an object such as a skimmer floating on the ocean's surface can be equipped with an accelerometer to measure its own movement from crest to trough, which translates to the same movement of the wave at that particular point.

Figure 3-6 highlights the anatomy of a wave and the basis of characterizing a wave or wave train through its height, length, and period.

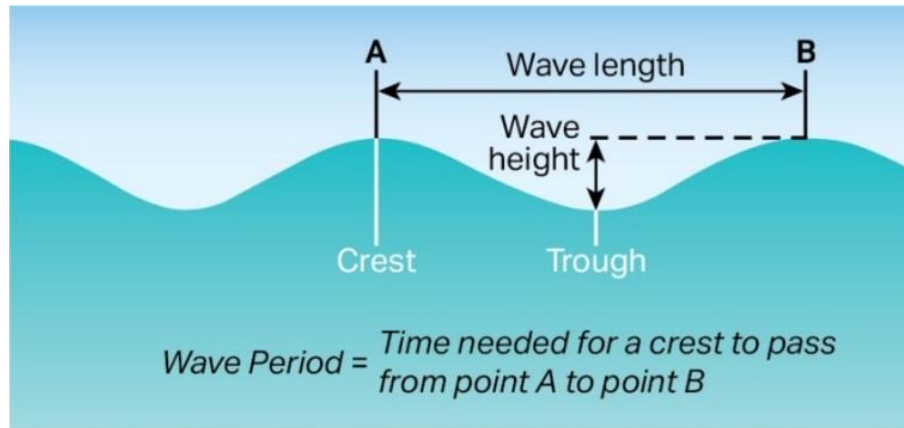


Figure 3-6: Characteristics of ocean waves (height, length, and period)

Although “simple” waves, well-defined sinusoidal motions, are readily analyzed by elementary methods, their regularity does not approximate the variability of ocean waves. Outside of a wave tank, one never sees a constant progression of identical waves. Instead, the sea surface is a superposition of waves of varying heights and periods moving in differing directions. When the wind blows and the waves swell in response, a wide range of heights and periods is produced. When the WCM measures waves at a fixed location on the ocean, the wave signals it outputs will be irregular, and although individual waves could be identified, there will always be significant variability in height and period from wave to wave. Consequently, it is necessary to treat the characteristics of the sea surface in statistical terms.

The ocean surface comprises many wave components that are generated by the wind in different regions of the ocean and then propagated to the point of observation. Complex wave distributions are difficult to obtain in explicit form from a random wave model, but numerical algorithms based on the regression approximation work well. This method of calculating wave distributions is the only known method that gives correct answers that are valid for general spectra. In particular, we selected the open-source matrix laboratory (MATLAB) software Wave Analysis for Fatigue and Oceanography (WAFO) toolbox, a third-generation package of MATLAB routines for statistical analysis and simulation of random waves, to calculate the distributions of wave characteristics from observed power spectra of the sea as measured by the WCM. WAFO provides a comprehensive set of validated computational tools for statistical analysis of random waves and a marine structure’s responses to them (Lund University, 2007). In a random wave model, the distribution of wave characteristics, such as wave period and crest-trough wave height, can be calculated with high accuracy for almost any spectral type.

To determine the wave characterization information sent to the user, the WCM first uses the onboard IMU and sensor MCU to record and process the raw data. The IMU reports the acceleration and angular velocity at a given sampling rate from the 3-axis accelerometer and gyroscope. We found through our initial laboratory and field testing that the majority of the motion of the WCM is up and down or heave motion. We simplified the displacement calculation to use the scalar magnitude of the 3-axis accelerometer data instead of complicated calculations using the gyroscope data. We then integrated the acceleration of the heave signal component twice to get the total heave of the sea. Using the heave measurements, we performed the standard oceanography spectral and statistical analysis to calculate the wave characterization values sent to the user.

To convert the accelerometer data to heave, we first took a Fast Fourier Transform (FFT). This converts the data from the time domain into the frequency domain. We then filtered the data to isolate the wave

frequencies of interest. The filtering process determines the ω values of the data. We used this information to calculate the period in seconds that will be sent to the user. Then, the frequency data were divided by ω^2 , and an Inverse Fast Fourier Transform (IFFT) was performed to calculate the heave of the WCM. Using the heave data, we used WAFO to run the spectral and statistical analysis of the heave to determine the wave characteristics, including wave height reported as significant wave height (H_{m0}), presently defined as four times the standard deviation of the wave surface or four times the square root of the zeroth-order moment of the wave spectrum.

3.4 Laboratory Testing

Testing with several different IMUs, including the WCM-embedded software development platform, we took systematic measurements first in the lab and then in the field to refine the algorithms and optimize them for the WCM platform.

We mounted the sensors on several spring-mass combinations to simulate ocean waves in a controlled laboratory environment. We choose the spring-mass combinations that would give displacements and frequencies in the range of interest for ocean waves in the region where the decisions need to be made about continuing to skim or instead to disperse. We released the sensors from a determined distance from the ground and allowed the system to oscillate until little motion was evident.

We began with simple harmonic motion, using a single weighted spring setup to collect data. The photograph on the left in Figure 3-7 shows the experimental set up, where the WCM is mounted in the weighted basket hanging off a single spring. The basket was released at a variety of heights, and the motion was recorded with both the IMU and a GoPro camera. Each band on the witness pole hanging next to the basket represents 10 cm. Using the recordings from the GoPro camera, we found the peaks and troughs of the harmonic motion and compared them to the calculations of the IMU.

Once we were convinced the heave calculations for the simple harmonic motion were consistent with the physical heave, we introduced more complexity in the experiment. We used combinations of springs and fixtures that have multi-frequency responses, as one would expect in actual wave conditions. The photograph on the right in Figure 3-7 shows one of these more complex experimental setups. Here we mounted the WCM on the top of the board that is weighted at one end. We also suspended the board using a spring on either side. Mounting the WCM to a board connected to two springs and varying both (1) the weight in the basket and (2) the mounting locations of the springs and weights allowed us to create wave motion with multiple frequencies. The two spring experiments generated more complex motion with multiple frequencies in the data. We again recorded the motion with a GoPro camera, releasing the board from different heights indicated by the witness pole. We then repeated the measurements using multiple mounting positions for both the springs and weights.

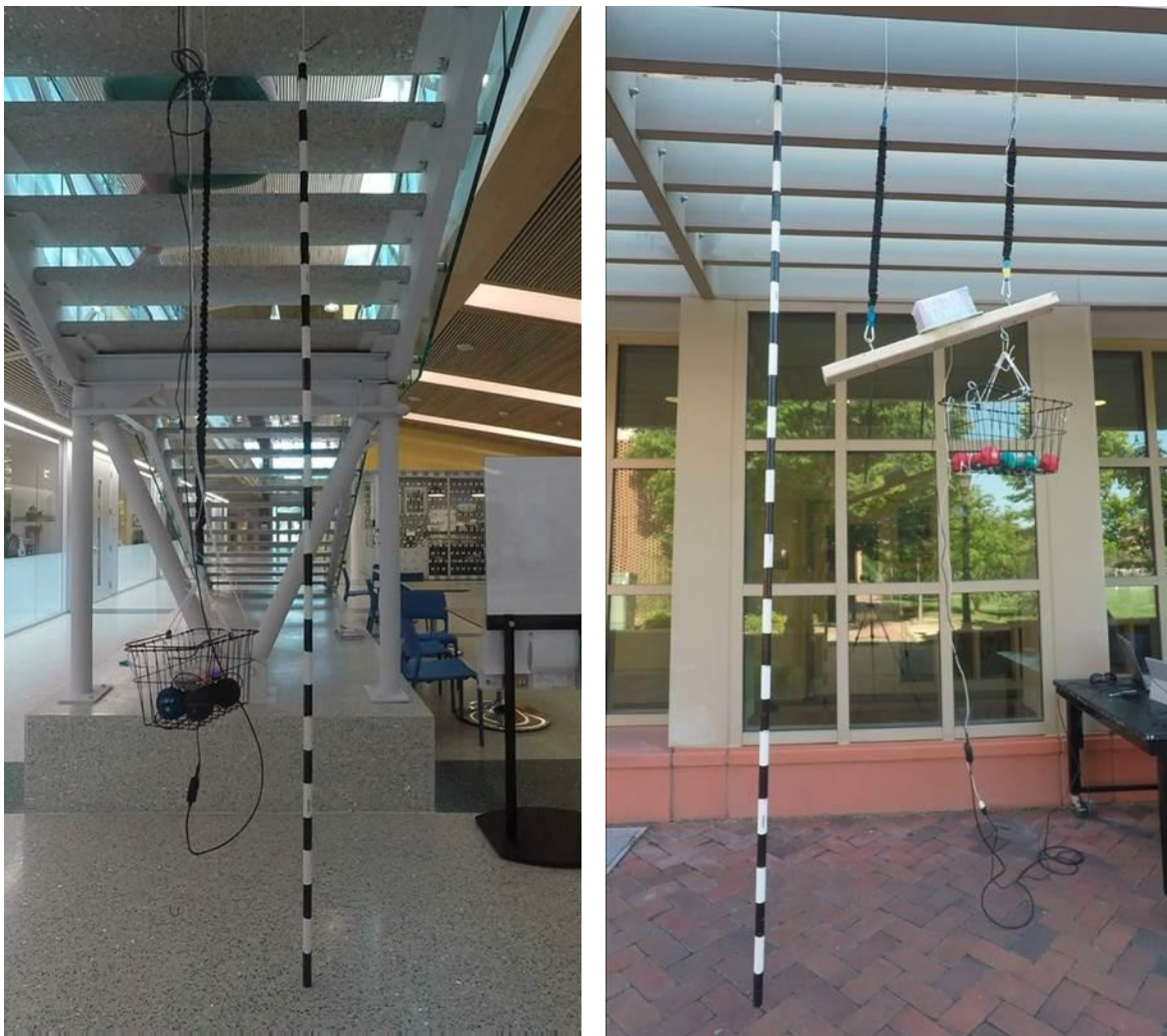


Figure 3-7: Experimental setup using springs for laboratory testing

The laboratory testing showed that we could accurately calculate the heave motion of the simple harmonic motion and more complicated motion with multiple frequencies. We started by fixing the z-axis to isolate the heave component to one dimension. We later found that using the scalar magnitude of the raw data from all three accelerometers axes gave a close approximation to the heave, allowing us to remove some complexity in the algorithm and removing the need for the gyroscope data.

Figure 3-8 shows the steps of the algorithm to determine the heave of the sensor. For this test, we sighted the maximum displacement at approximately 0.9 meters. The top left graph shows the raw accelerometer data from the z-axis. The top right shows the frequency spectrum of the data after an FFT has been performed. We then filtered the frequency data to isolate the wave frequencies and removed the noise, as seen in the bottom left plot. Then, the frequency data were divided by ω^2 , and an IFFT was performed to create the plot in the bottom right of the heave. Here, the maximum heave was approximately 0.39 meter, and the minimum heave was approximately -0.49 . The heave plot shows a total displacement of about 0.88 meter, which is less than 1 inch in difference to the displacement noted visually during the data acquisition. We did not observe any significant noise or notice any discernable drift in the sensor during our data capture.

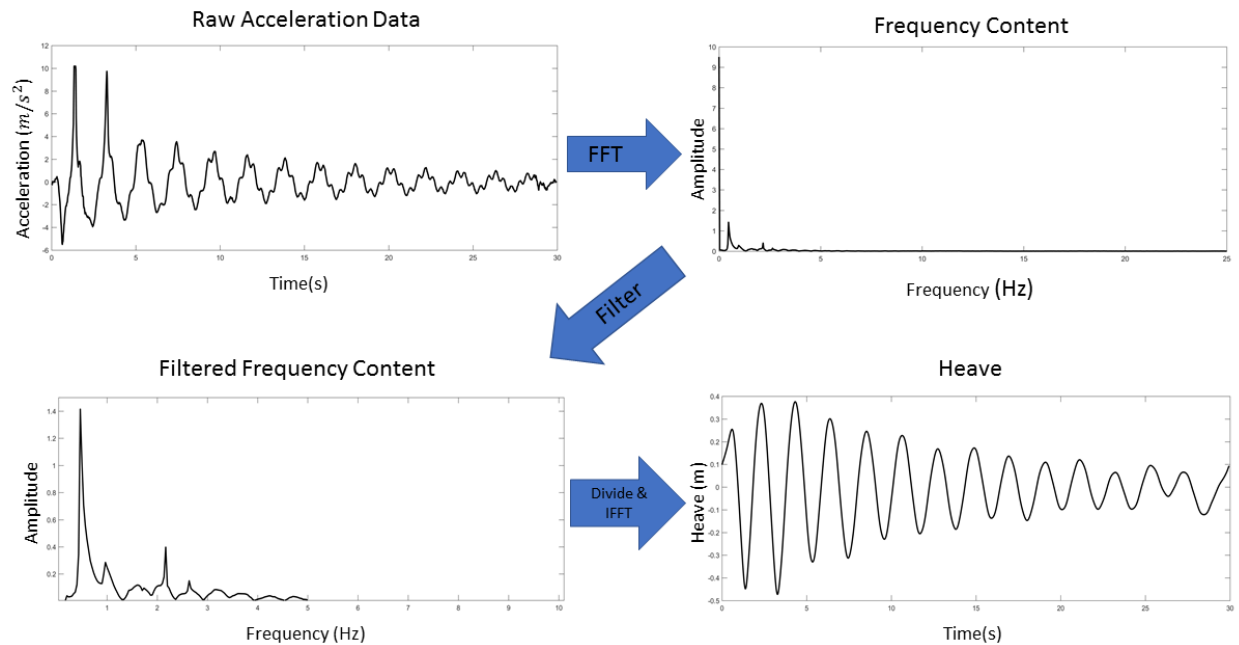


Figure 3-8: Plots of wave characterization algorithm steps from acceleration to heave

Using the heave data, we ran the standard ocean wave spectral analysis and statistics to calculate the wave data sent to the end user using the WAFO software for MATLAB. Once the MATLAB algorithms were finalized, they were converted to C code and programmed on the sensor MCU. By using the scalar magnitude of the acceleration, we removed the need to store any gyroscope data on the sensor MCU, which allowed for a higher sampling rate and longer data collection period on the final device.

3.5 Field Testing: Albemarle Sound

In order to collect real-world data for refining the wave characterization algorithms for the WCM and WCM-Sat, we fabricated a mock weir skimmer as shown in Figure 3-9. The skimmer mockup approximated the buoyancy and dynamics of the actual skimmer, both in terms of the float geometry and the weight. The mock weir skimmer shown in Figure 3-9 is built from modular square tubing to provide a range of attachment points for WCMs, but the figure does not show that we attached buckets/sandbags filled with local sand to approximate the total weight of the real skimmer. The use of local sand allowed us to transport and deploy the mock skimmer without heavy equipment. We simply hung the sandbags from the frame once the mock skimmer was in the water.



Figure 3-9: Mock weir skimmer with WCM-embedded software development platform

One of the embedded software development platforms was also placed inside a buoy for streaming data collection over WiFi to compare results. The testing setup is shown deployed in Figure 3-10. We deployed a witness pole in the water near the mockup skimmer. Using a witness pole, we noted the wave height periodically while streaming the raw data from the mockup skimmer and buoy to the boat. We do not have any expertise in visually assessing wave heights, so there was some uncertainty in what we observed using the witness pole. Even with the uncertainty, we found that the significant wave heights that were calculated were mostly within the performance criteria.

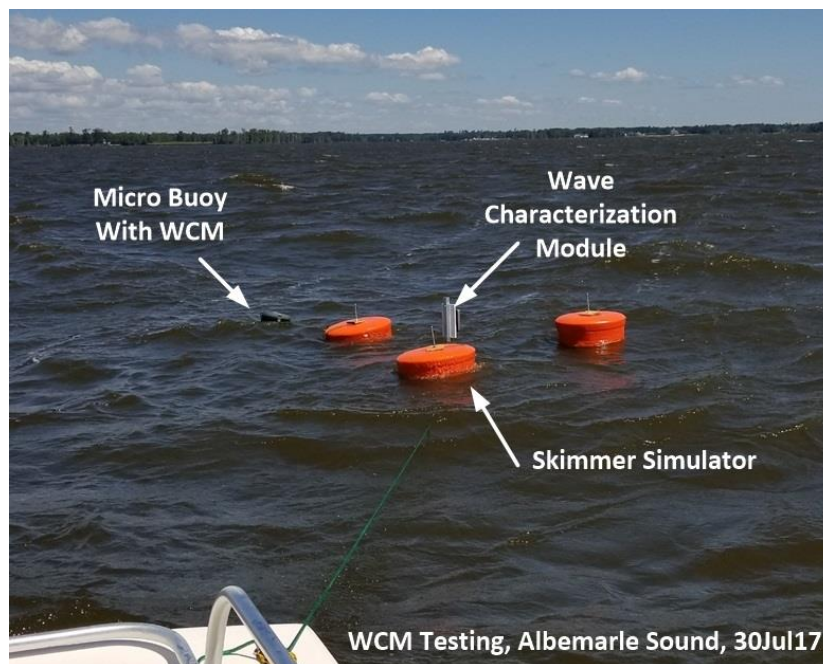


Figure 3-10: Field testing in Albemarle Sound

3.6 Remote User Interface: Cloud Infrastructure and GIS Web Application

The cloud infrastructure provides backend data acceptance from the satellite gateway, processing, and interpretation of WCM information such as time, location, and wave characteristics to a web-accessible GIS user interface.

Figure 3-11 is a screenshot from our deployed GIS user interface. A WCM-Buoy with ID 9090 in gateway mode is shown reporting a message that includes its wave characterization data along with information about the other WCMs in node mode. The other WCMS in node mode would communicate through WCM-Buoy 9090's mesh network. Additional documentation and a user guide are in **Appendix D**.

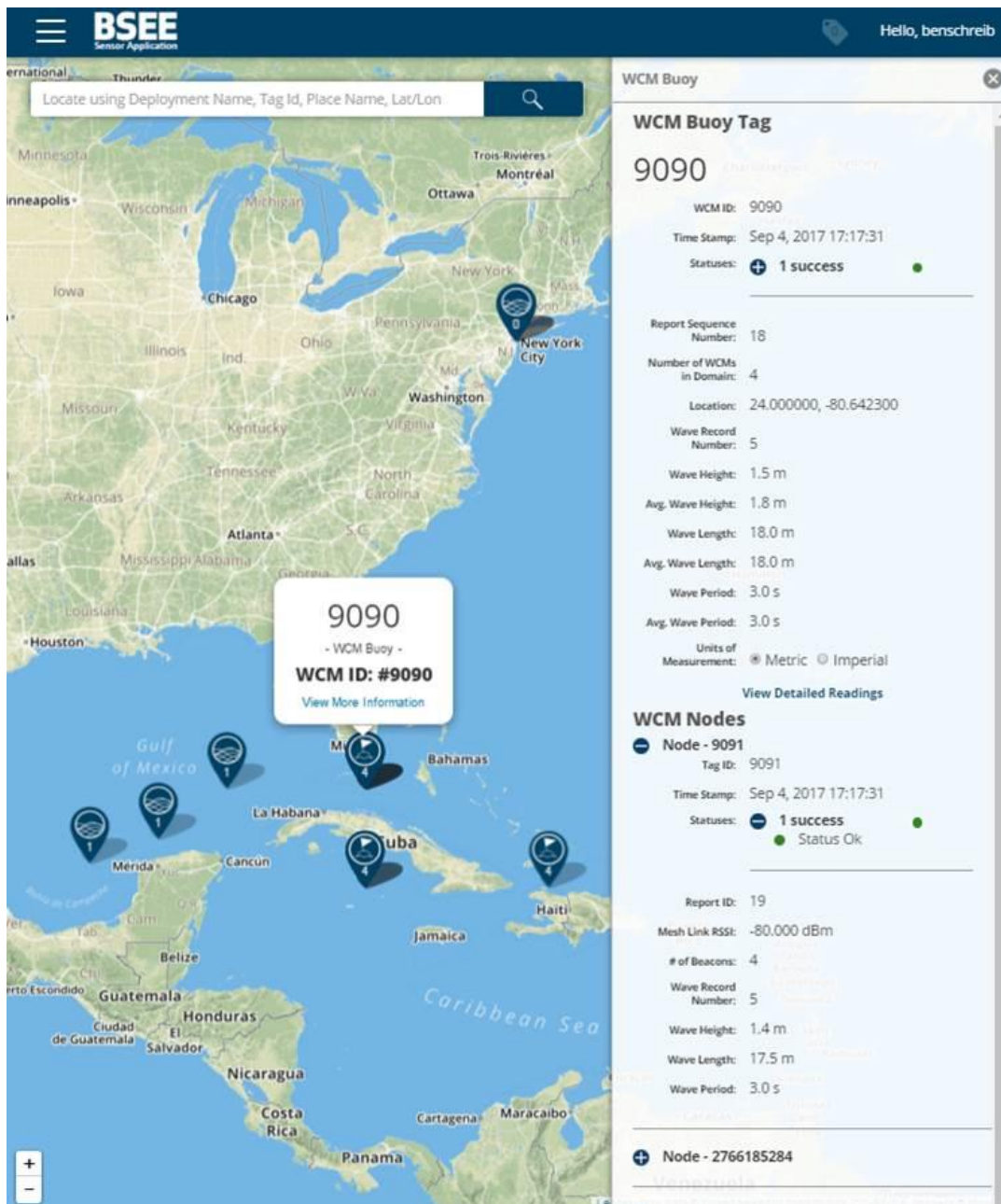


Figure 3-11: Web-based GIS user interface

3.6.1 Software Tools

The remote cloud infrastructure consists of the software components listed below that process the WCM gateway report messages sent to the satellite gateway and are run on Amazon Web Services cloud servers:

- **NginX** – Used as a reverse proxy to manage incoming requests from the gateway. It will facilitate which ports are open and what systems (Node application program interface [API], Node Gateway Receiver) can communicate through those ports. It works in tandem with the firewall. It is also used as the web server for the GIS web application.
- **Node Gateway Receiver** – Listens for packages sent by the satellite, and once received starts the processing engine.
- **JavaScript Object Notation (JSON) Entity Mapper** – Configuration file used by the node ingestion server to translate the messages into database entities. If the gateway changes protocols or the gateway provider changes, the entity mapper is updated and the rest of the subsystem should be unaffected.
- **Node Ingestion Server** – Processing engine used to receive incoming messages and translate them into MongoDB database entities.
- **MongoDB Database** – Used to store the translated entities from the node ingestion server. The database structure defines what the entities are and the data type formats of each attribute in the entities.
- **Apache Solr** – Indexing engine that provides fast search capabilities.
- **Node API Server** – Same server as the Node Ingestion Server, but is used as an API server for the mapping application.
- **Koop** – Data translation engine that can format the database entities into a consumable format for open web-based systems.
- **Turf.js** – Spatial data manipulation engine used to conduct spatial queries and format MongoDB data into GeoJSON.
- **Leaflet** – Web-based GIS mapping user interface that displays interactive features that represent the WCMs in the field and the messages and status that they send over time.

3.6.2 Cloud Infrastructure

The first component of this subsystem is the satellite gateway. The gateway is the conduit for the WCMs to relay information from the device to the cloud infrastructure to where it is stored. The gateway enables the system to communicate worldwide and outputs information directly into a cloud-hosted database.

The cloud subsystem translates the gateway messages into a normalized format and stores the information in the database. Once the byte formatted message is received from the gateway, the cloud infrastructure executes the node gateway receiver engine, which parses the message, retrieves all the relevant data needed for the system, and invokes the node processing server.

Amazon cloud servers offer scalability and provide confidence that what is done on a small scale using the platform can be upgraded to support a larger production-ready environment with high availability. The hardware that was chosen is suitable to support all server components of this project including NginX, node ingestion server and MongoDB database and displayed using Leaflet.

3.6.3 Emulator

We also created an emulator to mimic the satellite messages received from the WCM-Sat and WCM-Buoy and their associated nodes to test our approach, and we deployed tools before the hardware was fully completed and unit tested.

3.7 Local User Interface: Application Dashboard

The native iOS application is designed to run on an iPad and ingest the same WCM gateway report and WCM node report messages as the GIS user interface for the user in a simple, easy-to-read dashboard.

Figure 3-12 is a screenshot of the application dashboard report from a gateway. The app displays which device we are connected to through the WiFi service set identifier (SSID), the type of device (WCM, WCM-Sat, or WCM-Buoy), which ID we are viewing and at what time, along with its status and wave characteristics. Note that the SSID is automatically updated to the current device connected to, but the ID panel in the top right corner needs to be selected to view the current gateway or other nodes that are available. All data are stored on the tablet locally until deleted and can be exported via email in a comma-separated values format. Additional features and definitions are provided in **Appendix C**.

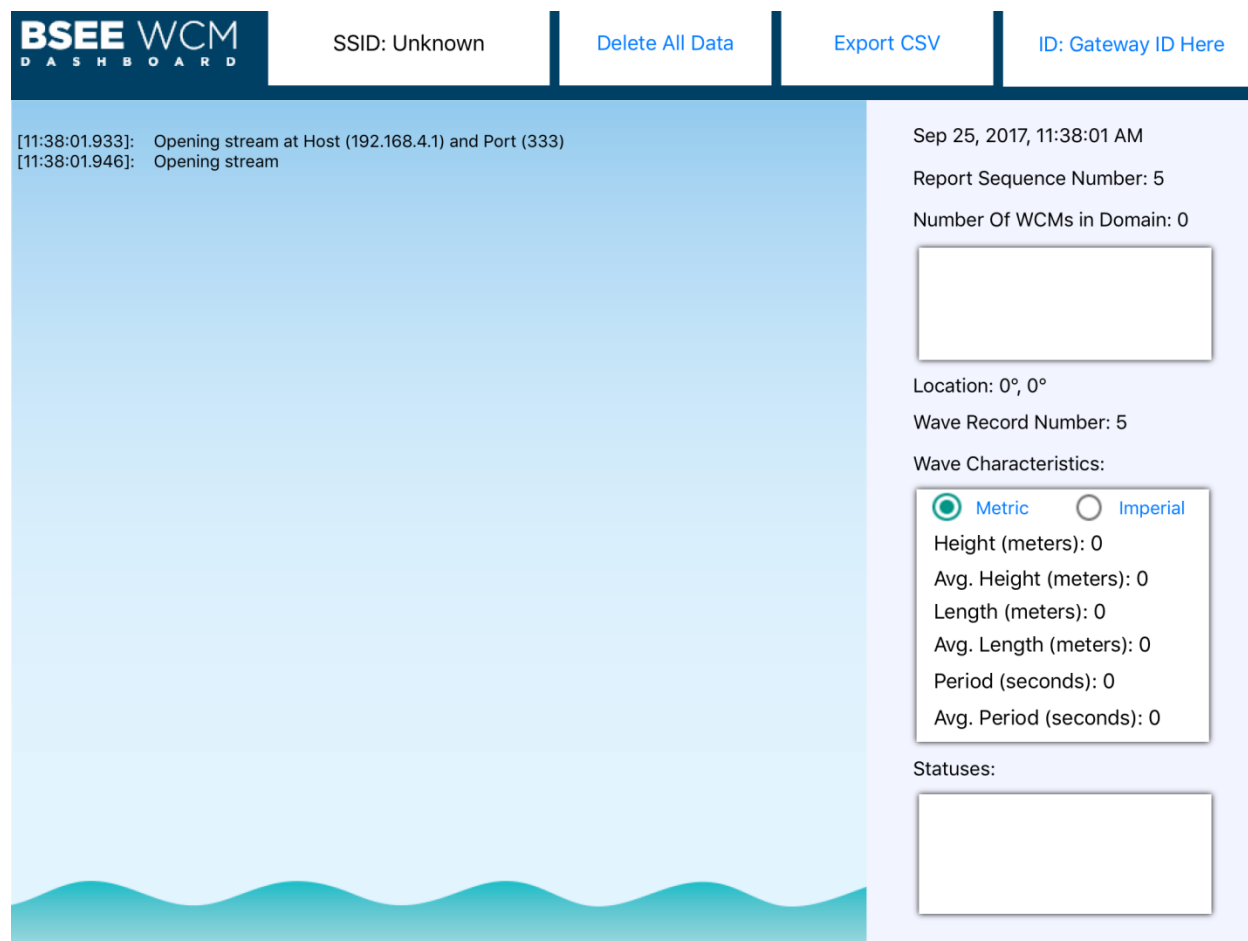


Figure 3-12: iPad application dashboard viewing a WCM gateway report

Figure 3-13 shows the node report view when an ID in node mode is selected.

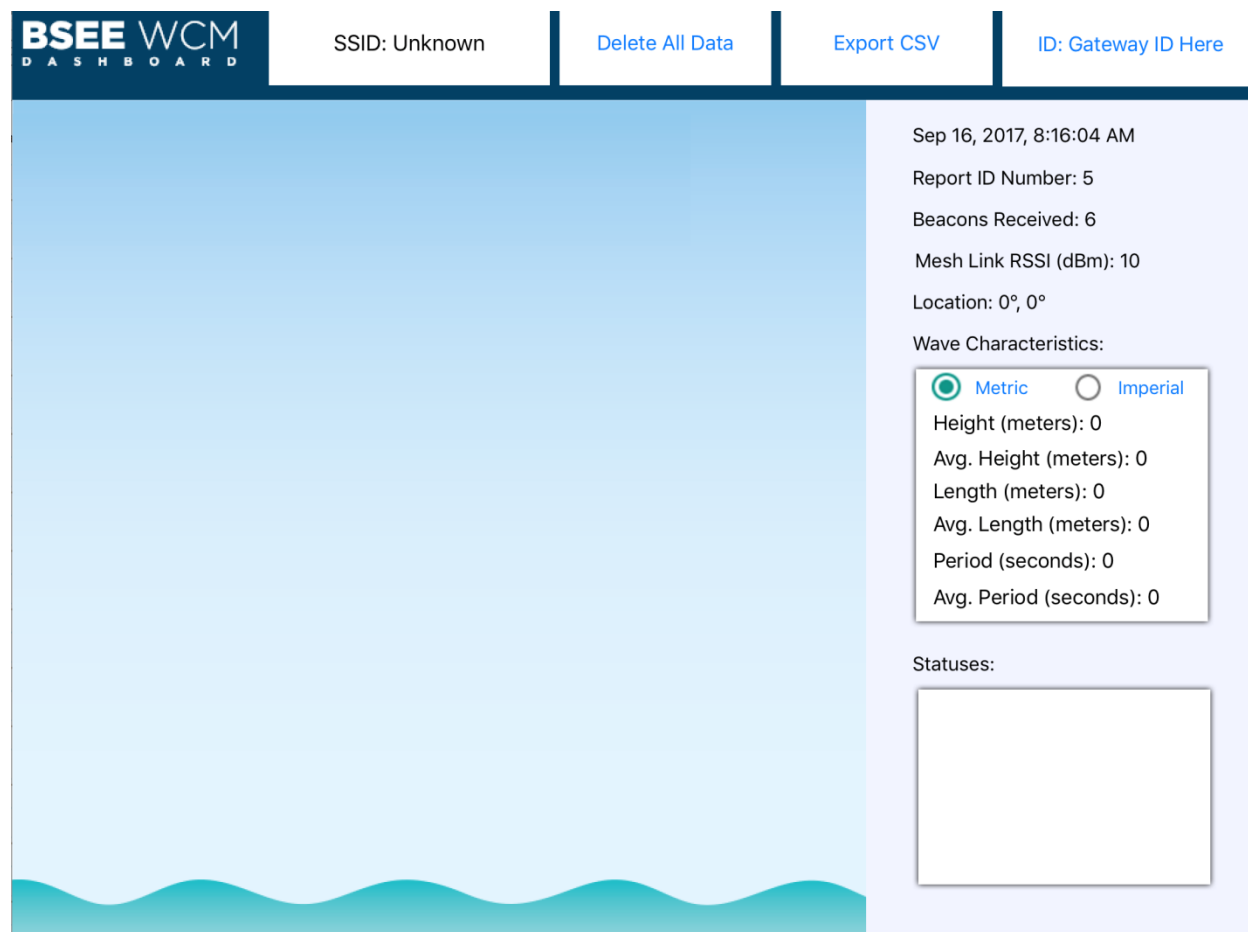


Figure 3-13: iPad application dashboard viewing a WCM node report

3.7.1 Software Tools and Infrastructure

The native application was developed using the Swift programming language and standard APIs for connection and handling of data packets between the WCM WiFi and display on an iOS device. All the hardware required is built into the iPad tablet.

The iPad needs to be preconfigured with the SSID and password in settings before launching the application. Once the WCM, if in gateway mode, powers up its WiFi module, the iPad will automatically connect to the WCM. The iPad will create a socket at the specified Internet protocol (IP) and port number using the transmission control protocol / Internet protocol (TCP/IP) protocol to handshake with the WCM for data transfer and confirmation.

3.7.2 Emulator

We adapted the GIS user interface to send messages over WiFi to the iPad for unit testing the local user application dashboard.

4. Ohmsett Testing and Analysis

Each piece of the system architecture, starting with the embedded software development platform; message emulators to the WCM, WCM-Sat, and WCM-Buoy; mesh networking; and local and remote reporting were unit tested and system tested to check the accuracy and correct configuration of the reported data. We conducted field unit tests at Albemarle Sound for data collection to refine the wave characterization algorithms and conducted full WCM system testing at Ohmsett on September 5, 2017, through September 8, 2017.

4.1 Facility and Equipment Setup and Configuration

The Ohmsett wave tank shown in Figure 4-1 is 203 meters long, 20 meters wide, and 3.5 meters deep.

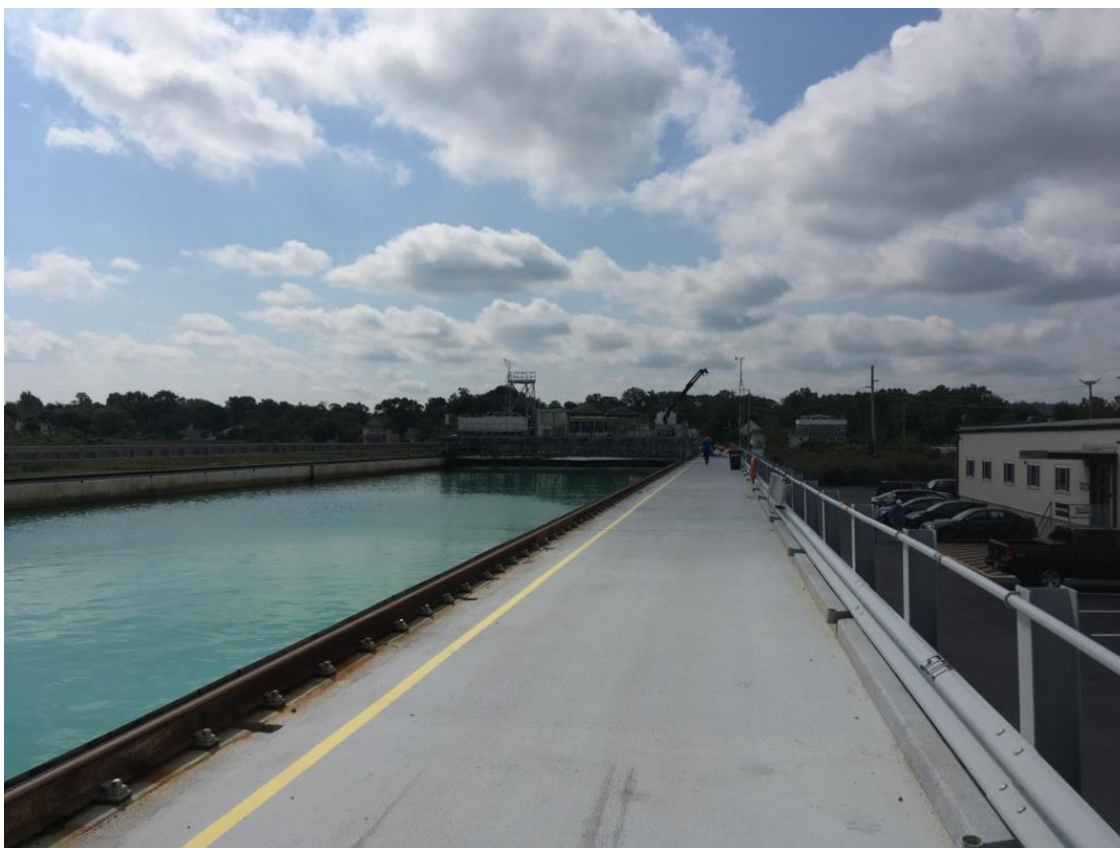


Figure 4-1: Wave tank at Ohmsett

The wave generator as pictured in Figure 4-2 has the capability of creating sine waves as high as 1 meter and simulated harbor chop waves. The waves are generated by varying the stroke length (inches) of the hydraulic arms and the cycles per minute (CPM) of the stroke movement in and out.



Figure 4-2: Ohmsett wave generator

The AECOM team provided WCMs, WCM-Sats, WCM-Buoys, embedded software development platforms, batteries, mounting hardware, iPads, and laptops for data collection. The WCMs, WCM-Sats, and embedded development platforms were secured to a vertical bracket attached to a round plate mounted on a Desmi Terminator weir skimmer float provided by Ohmsett, as shown in Figure 4-3.



Figure 4-3: Two WCMs, WCM-Sat, and WCM-embedded software development platform mounted to one of the Desmi Terminator's floats

The Desmi Terminator weir skimmer was craned in and out of the tank, as shown in Figure 4-4.

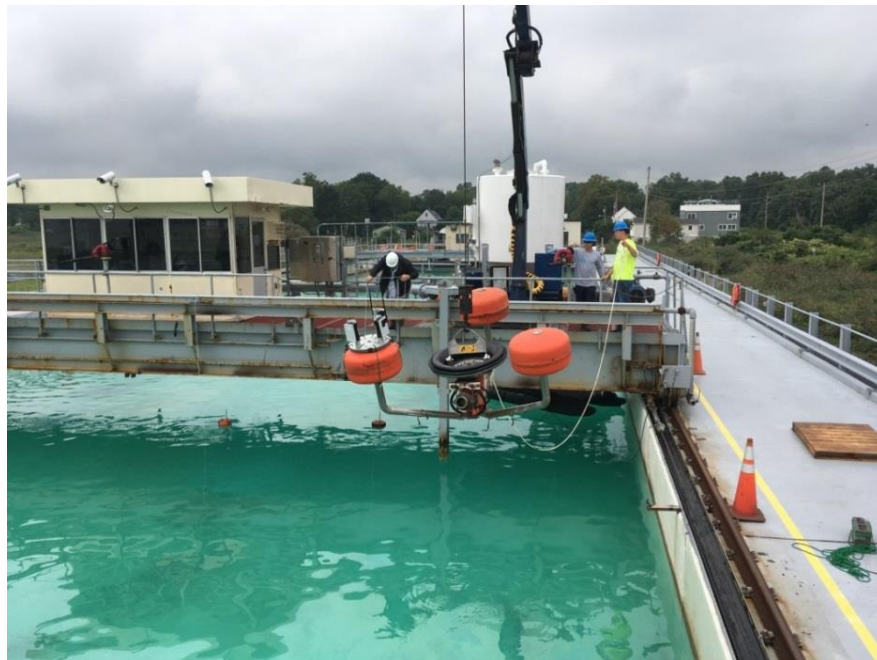


Figure 4-4: Craning the weir skimmer into the Ohmsett wave tank

After the WCM-Buoys were lowered into the water, the skimmer and WCM-Buoys were secured to the main bridge to prevent excessive drift from the testing area between the main and auxiliary bridges, as shown in Figure 4-5. Altimeter Banner sensors extending over the water were used for measuring distance to the water's surface, and a MATLAB program was used to calculate significant wave height, wavelength, and period. One of the auxiliary bridge sensors is shown in Figure 4-5.



Figure 4-5: Skimmer and WCM-Buoy deployments looking down from the auxiliary bridge

Figure 4-6 provided by Ohmsett illustrates the testing system setup and configuration with Banner sensors.

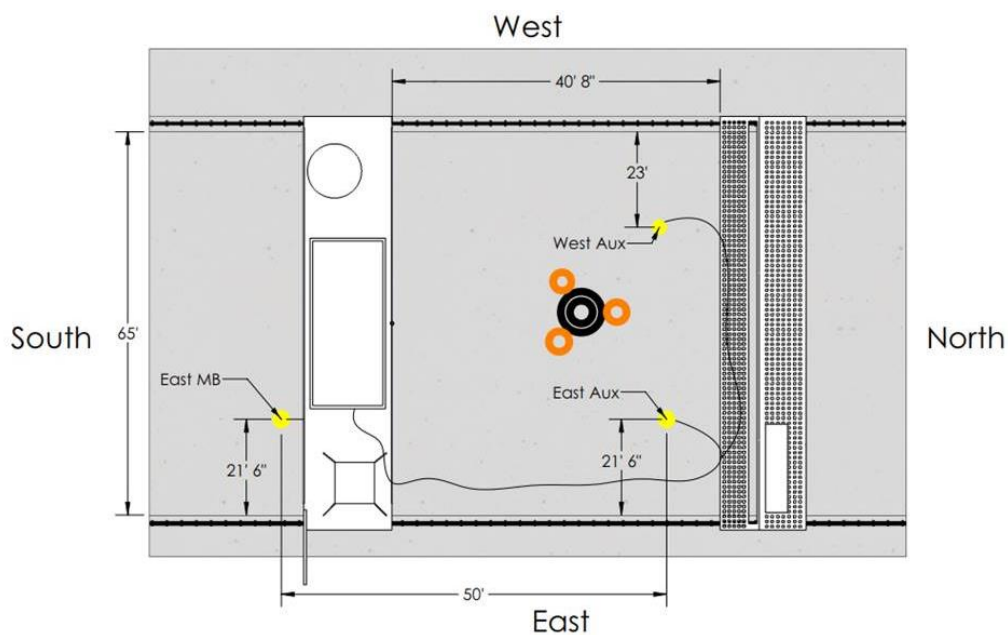


Figure 4-6: Ohmsett testing setup (top view)

Figure 4-7 is a side view of the testing setup looking to the east with the auxiliary bridge on the left side and main bridge on the right. We also deployed an anchored witness pole with 10 cm markings and a GoPro pointed at the pole to record the wave heights.



Figure 4-7: Wave tank setup looking east

Table 4-1 summarizes the wave conditions for all the tests performed at Ohmsett.

Table 4-1: Ohmsett Wave Settings Summary

Test No.	Date	Start Time	Stroke (inches)	CPM	Wave Type
1	9/5	1:00 p.m.	18.0	18.0	Sine
2	9/5	2:00 p.m.	18.0	20.0	Sine
3	9/5	2:52 p.m.	7.5	35.0	Sine
4	9/5	3:30 p.m.	7.5	35.0	Sine
5	9/6	10:44 a.m.	18.0	18.0	Sine
6	9/6	11:23 a.m.	18.0	18.0	Sine
7	9/6	12:00 p.m.	18.0	20.0	Sine
8	9/6	2:45 p.m.	12.0	30.0	Sine
9	9/6	3:33 p.m.	12.0	30.0	Sine
10	9/6	4:03 p.m.	6.0	40.0	Sine
11	9/7	12:10 p.m.	6.0	40.0	Sine
12	9/7	12:53 p.m.	12.0	30.0	Chop
13	9/7	2:48 p.m.	12.0	30.0	Chop
14	9/7	3:33 p.m.	3.0	35.0	Chop
15	9/7	4:01 p.m.	3.0	35.0	Chop
16	9/8	9:10 a.m.	15.0	20.0	Chop
17	9/8	10:02 a.m.	18.0	10.0	Sine
18	9/8	10:22 a.m.	4.5	35.0	Sine
19	9/8	10:46 a.m.	12.0	25.0	Sine (Oil applied)
20	9/8	11:46 a.m.	7.5	35.0	Sine (Advancing)
21	9/8	1:10 p.m.	12.0	30.0	Sine
22	9/8	1:37 p.m.	18.0	18.0	Sine

4.2 Data Collection and Analysis

Once powered up, each device measured and reported wave characterization data. The embedded software development platform mounted to the skimmer and in a buoy streamed 1 minute of raw data during each data collection time window. The WCM, WCM-Sat, and WCM-Buoy each calculated and reported wave height, wave length, and wave period. The data transmitted from each device via WiFi were displayed on an iPad, stored on local memory, and exported via email in a comma-separated values file with the option of a dashboard screenshot. Data transmitted from the WCM-Sat and WCM-Buoy via satellite were stored in a MongoDB database and displayed on the GIS user interface. The raw gateway log was saved into a text file with a unique URL that can be accessed via the Internet.

The WCM reports sea-state features of significant wave height, period, and wavelength to the end user. These features are calculated by first recording 1 minute of 3-axis acceleration data and then computing the surface elevation of the sea. Once we have calculated the surface elevation, we perform statistical analysis to calculate the sea-state features. The statistical analysis was generated using MATLAB WAFO, a well-established software toolbox for analyzing waves (Brodtkorb et al., 2000).

Significant wave height corresponds to the average wave height the human eye would visually estimate (Massel, 2013). Historically, significant wave height refers to the average of the highest third of the wave heights, and when calculated this way, it is denoted as $H_{1/3}$. Significant wave height (H_{m0}) is presently defined as four times the standard deviation of the wave surface or four times the square root of the zeroth-order moment of the wave spectrum. Both $H_{1/3}$ and H_{m0} are referred to as significant wave height and generally have a difference in the magnitude of a few percent.

The WCM reports significant wave height as H_{m0} . We performed the statistical analysis based on the WAFO software package. In contrast, the MATLAB program used at Ohmsett calculates the significant wave height using $H_{1/3}$. WAFO removes spikes that are over the maximum variation amplitude, then sorts the peak to trough amplitudes, and finally calculates the mean of the top third of the data.

There will also be some difference between raw data from the WCM versus the raw data from Ohmsett. The wave measurements from Ohmsett instrumentation are made with a Banner U-Gauge QT50U series transducer versus the WCM accelerometer (Banner, n.d.). The Ohmsett transducer readings are collected at a different frequency, and Ohmsett is using a different calculation for the wave height. So, some differences between Ohmsett and WCM data were expected. To compensate for these differences, our team analyzed the Ohmsett data using the statistical algorithms developed from WAFO to calculate H_{m0} . This provided some normalization between the two data sets.

Another reason for variation between raw data from the WCM versus raw data from the Ohmsett Banners is the spatial differences in the locations of the devices. The reflections of the waves from the sides of the tank create a complex wave field at different locations.

Figure 4-8 shows the significant wave height (H_{m0}) calculation for the WCM buoy, the WCM-mounted to the skimmer, and all three Banner locations for Test 2. Here the Buoy is represented by the crosses, the skimmer is represented by the stars, the main bridge Banner is represented by the dots, the west auxiliary bridge Banner is represented by the squares, and the east auxiliary bridge Banner is represented by the diamonds. Figure 4-8 shows that there is variation due to the location of the data collection device.

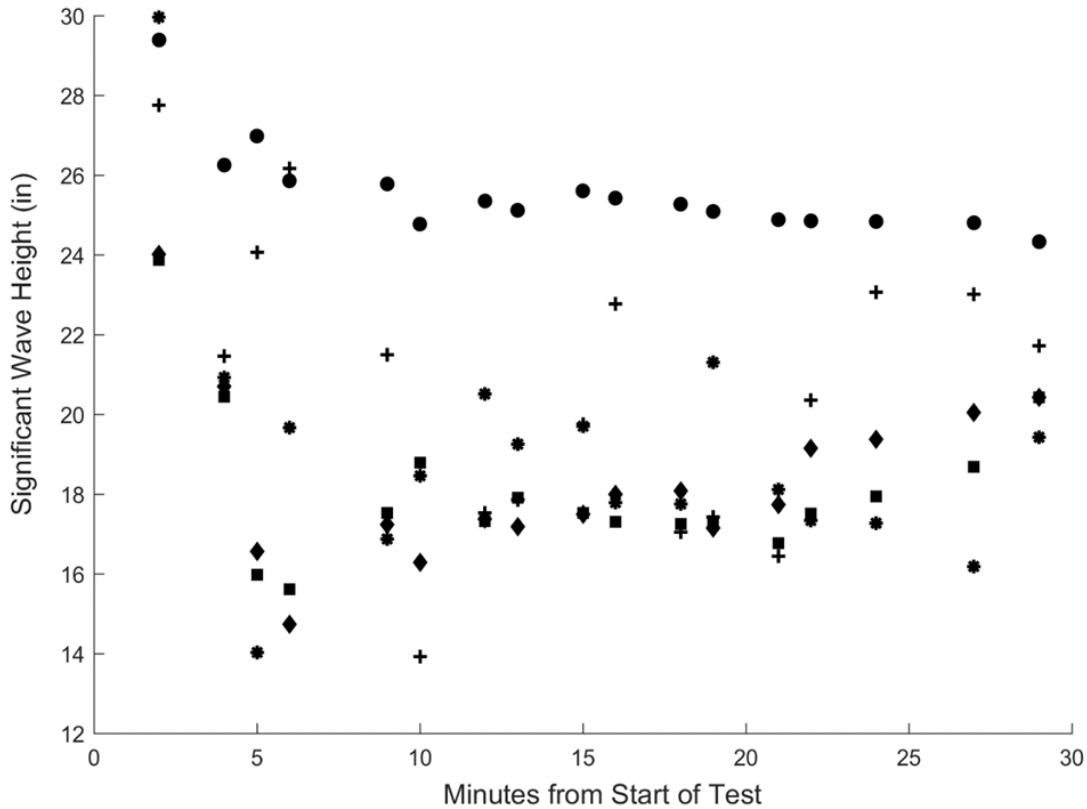


Figure 4-8: Varied significant wave height (H_{m0}) due to complex wave fields during Test 2

This plot shows the significant wave height (H_{m0}) calculation for the WCM buoy, the WCM mounted to the skimmer, and all three Banner locations for Test 2. Here the Buoy is represented by the crosses, the skimmer is represented by the stars, the main bridge Banner is represented by the dots, the west auxiliary bridge Banner is represented by the squares, and the east auxiliary bridge Banner is represented by the diamonds. Here it can be seen that there is variation in the significant wave height due to location in the tank.

Figure 4-9 shows the significant wave height results from the skimmer for Test 19. Similar plots for each test and each Banner location can be found in **Appendix F** and **Appendix G**. We used the raw data from the east Banner transducer on the auxiliary bridge because the data were physically closest to the skimmer during the testing. The crosses are the significant wave heights (H_{m0}) calculated using the WCM data. The triangles represent the significant wave height calculated statistically (H_{m0}) using the Banner data, and the dots are the wave heights ($H_{1/3}$) calculated using the algorithm from Ohmsett. We found that calculating the wave height statistically (H_{m0}) produces a result on average 3.5 inches higher than the wave height generated ($H_{1/3}$) by the code from Ohmsett.

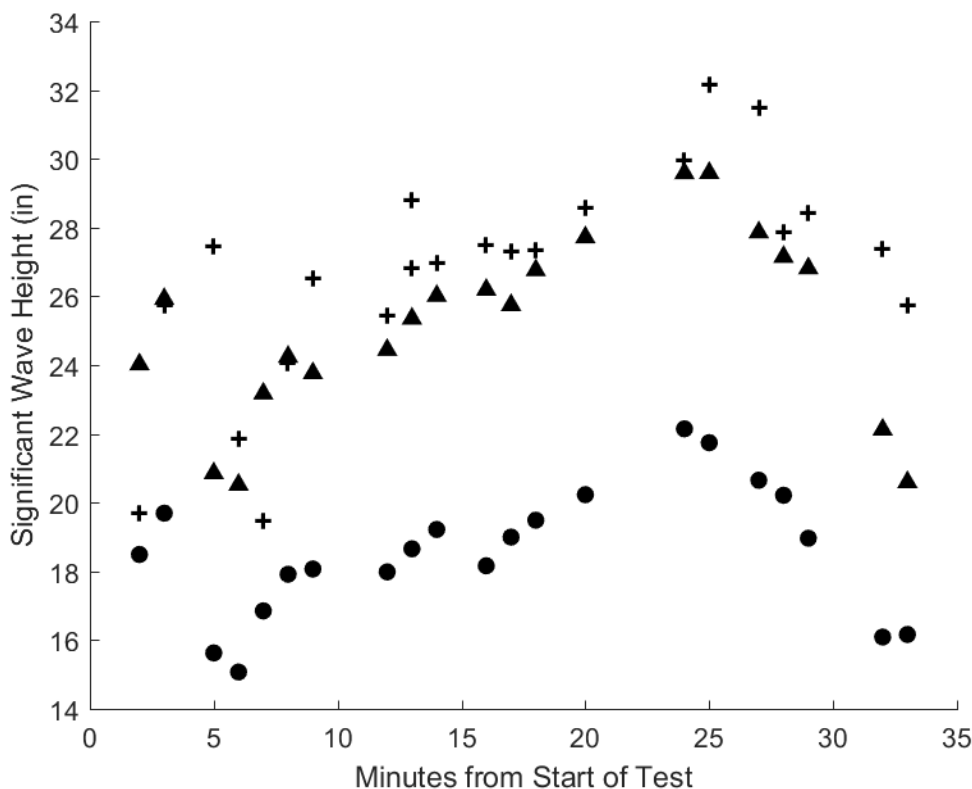


Figure 4-9: Significant wave height results from the skimmer for Test 19

This plot shows the significant wave heights for Test 19. The plus signs indicate the significant wave height (H_{m0}) calculated statistically using the raw data from the WCM. The triangles represent the significant wave height (H_{m0}) calculated statistically using a segment of time corresponding to the WCM data from the raw Banner data. The dots represent the wave heights calculated using the average of the top third wave height from the same segments ($H_{1/3}$). Each data point represents a calculation of the significant wave height from approximately 60 seconds of raw data.

Based on the closer agreement between calculating wave heights statistically and physical position of the east Banner, the rest of our analysis uses the significant wave heights (H_{m0}) calculated using the statistical algorithm from the east Banner on the auxiliary bridge.

Figure 4-10 shows the difference between the significant wave heights calculated using the WCM data and the Banner data for Test 19. Here it can be seen that for this test, most of the WCM results are within the 4-inch performance criteria, with two outliers. Plots showing the significant wave height (H_{m0}) for each test and Banner location are in **Appendix H** and **Appendix I**.

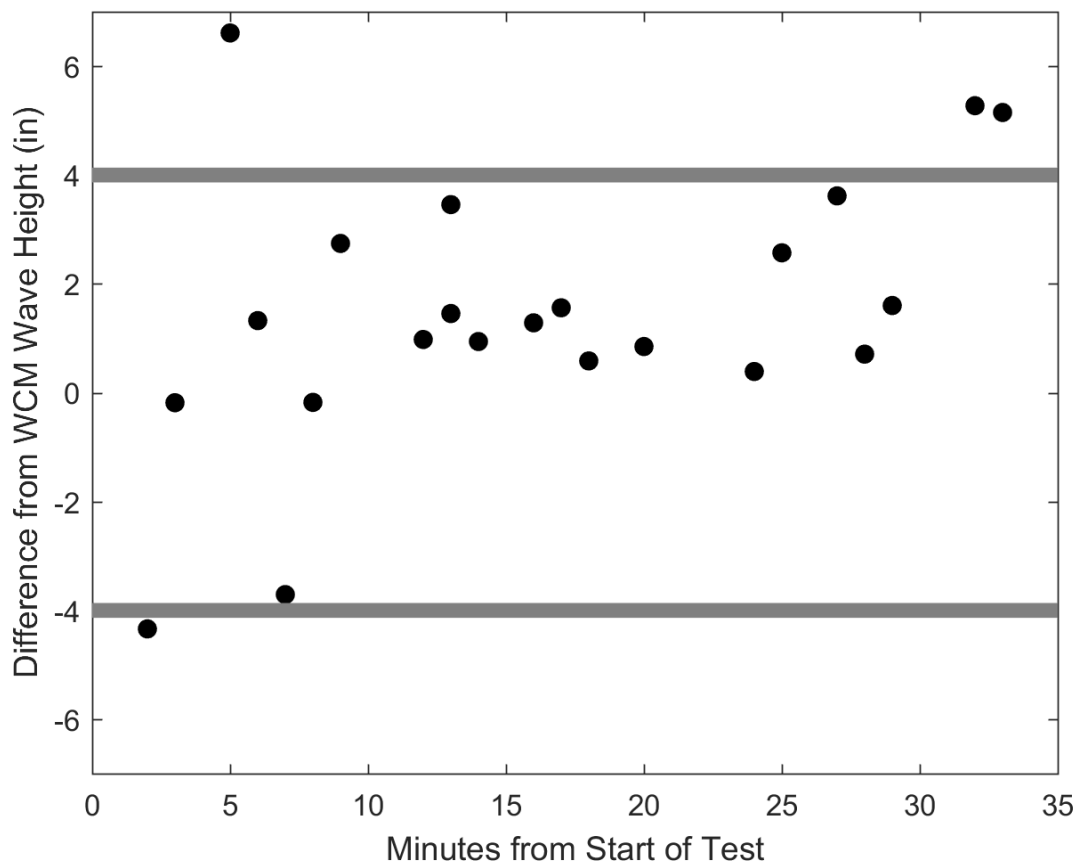


Figure 4-10: Test 19 WCM on skimmer versus aux East Banner

This plot shows the difference of the significant wave heights calculated for Test 19. The plus signs indicate the difference between the significant wave height calculated statistically using the raw data from the WCM and the significant wave height calculated statistically using a segment of time corresponding to the WCM data from the raw Banner data. Each data point represents a calculation from approximately 60 seconds of raw data.

We are using the Banner data as our gold standard for comparing our results. The Banner itself has an error of 0.2 percent, which results in approximately ± 0.1 inch for the wave heights that were generated. We have introduced additional error in the way we segmented the raw data from Ohmsett. To segment the data, we first determined the minute of data collected by the WCM by looking at the timestamp of the data file. We then found that minute in the raw data file from Ohmsett and the minute plus 10 seconds before the minute, and 10 seconds after the minute.

Table 4-2 shows the mean differences for all the tests for each Banner. On average, the WCM attached on the skimmer was 2.7 inches higher and the buoy 1.3 inches higher than the significant wave height calculated statistically using the raw data from the east auxiliary bridge Banner.

Table 4-2: Mean Differences for All Tests for Each Banner

	Mean Difference (inches)		
	From Main Bridge Banner	From West Aux Bridge Banner	From East Aux Bridge Banner
Skimmer	3.3	3.5	2.7
Buoy	2.7	2.5	1.3

Figure 4-11 shows the mean and standard deviation of the difference between the significant wave height from the WCM mounted on the skimmer and the east auxiliary bridge Banner data for each test. Differences against the other Banner data are in **Appendix J**.

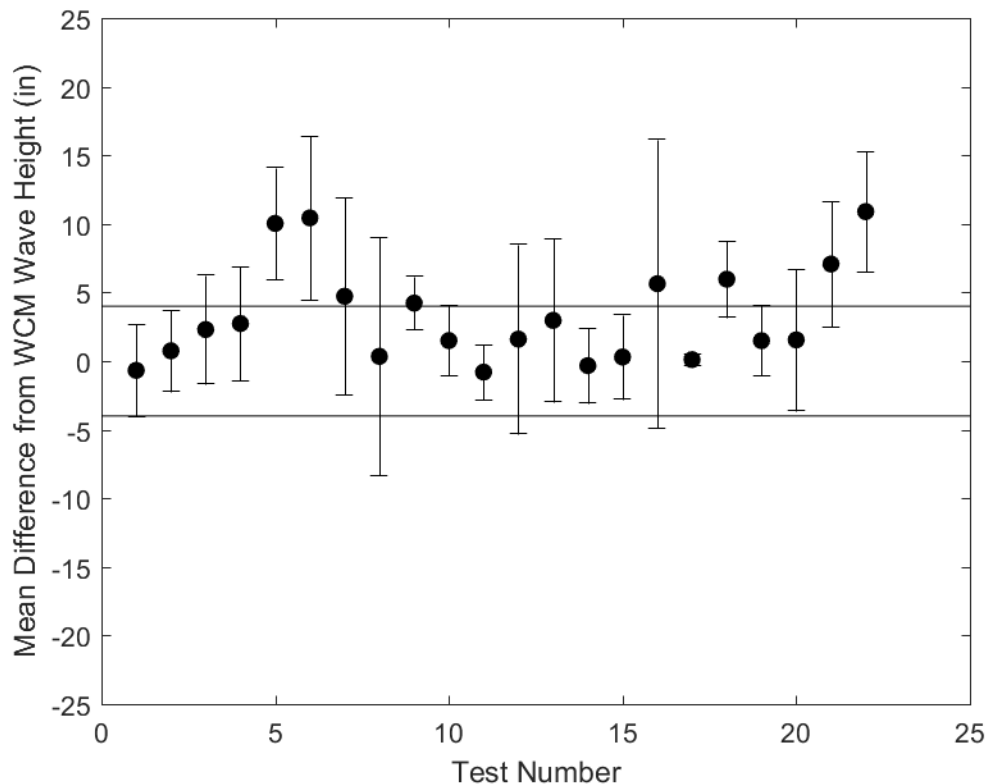


Figure 4-11: WCM on skimmer mean and standard deviation by test

This plot shows the mean and standard deviation of differences of the significant wave height for each test using the WCM attached to the skimmer. Each data point represents the mean of the difference between the significant wave height calculated statistically using the raw data from the WCM and the significant wave height calculated statistically using a segment of time corresponding to the WCM data from the raw Banner data for each test.

Figure 4-12 shows the mean and standard deviation of the difference between the significant wave height from the WCM Buoy and the east auxiliary bridge banner data for each test. Note that the buoy did not report raw data on the last day of testing. For both plots, the mean of a test is represented by the dot, and the whiskers are the standard deviation of that test. Here, it can be seen that for all except a few cases, the WCM data and the Banner were within 4 inches of each other.

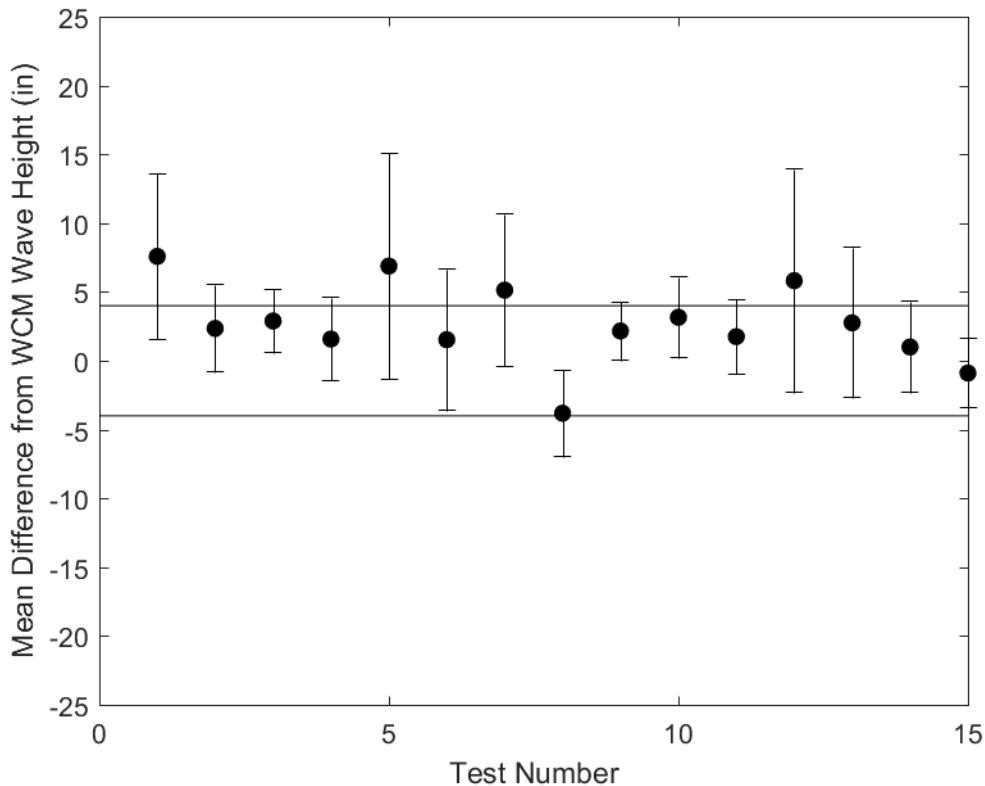


Figure 4-12: WCM-Buoy mean and standard deviation by test

This plot shows the mean and standard deviation of differences of the significant wave height for each test using the WCM Buoy. Each data point represents the mean of the difference between the significant wave height calculated statistically using the raw data from the WCM and the significant wave height calculated statistically using a segment of time corresponding to the WCM data from the raw Banner data for each test.

Again, it is important to note the spatial differences in the locations of the devices and Banner measurement locations. The reflections of the waves from the sides of the tank create a complex wave field at different locations throughout the wave tank, where each point in the tank is unique and experiences different wave conditions. To demonstrate this, Figure 4-13 compares the main bridge Banner sensor to the east auxiliary bridge Banner sensor. We observe several outliers and large standard deviations between the two Banner sensors on a number of tests. A comparison of the Banners is provided in **Appendix K**.

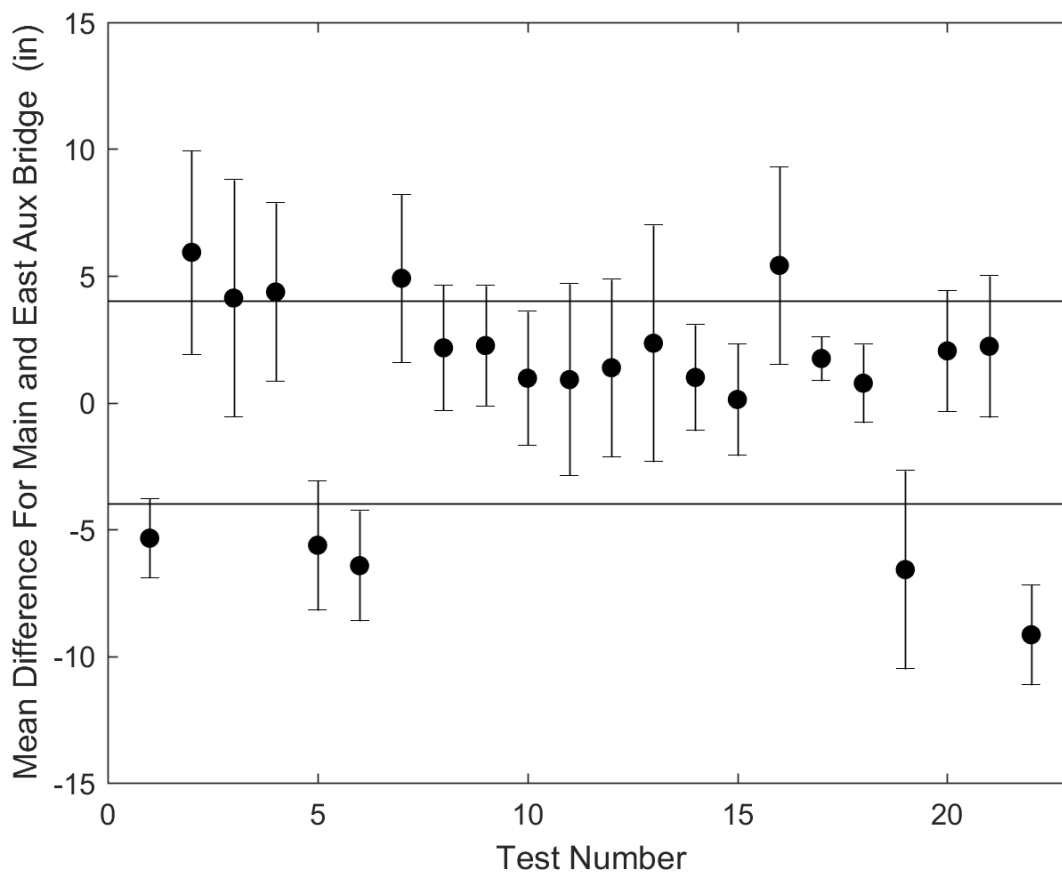


Figure 4-13: Mean difference of main bridge Banner versus east aux bridge Banner

This plot shows the mean and standard deviation of differences of the significant wave height for each test between the main bridge Banner and the east auxiliary bridge Banner. Each data point represents the mean of the difference between the significant wave height calculated statistically using 80-second segments of the raw Banner data from Ohmsett. While there is small measurement error in the wave heights being measured by the Banner devices, there is a measurement uncertainty in the wave height due to the location of the device collecting data. This is due to the complex wave field generated in the tank.

Each test had on average 14 periods of data collection, with the lowest number of data points 5 and the largest number of data points 23. The mean was calculated first by finding the difference between the significant wave height of the WCM and the Banner data for a given minute in the test. We then took the mean and standard deviation of these differences for each test. Test 14 and Test 8 have similar mean differences between the WCM and the east auxiliary bridge Banner at 0.3 inches but large discrepancies in the standard deviation, where the standard deviation for Test 14 is 2.7 inches and Test 8 is 8.7 inches.

Figure 4-14 shows the plot of the difference between the WCM and the east auxiliary bridge Banner significant wave height calculations for Test 14. Figure 4-15 shows the plot of the difference between the WCM and the east auxiliary bridge Banner significant wave height calculations for Test 8. Here it can be seen that there was little variation in the significant wave height difference in Test 14, while Test 8 had a few outliers that increased the standard deviation.

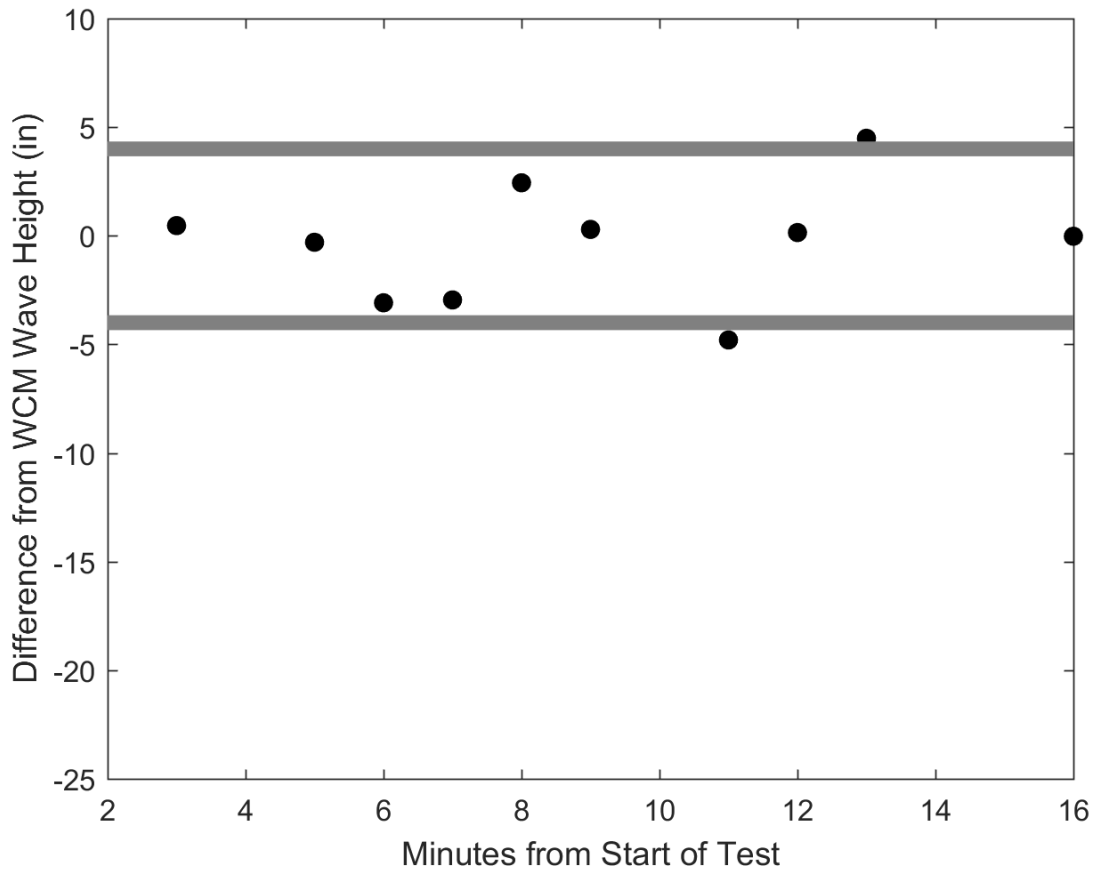


Figure 4-14: Difference between the WCM and the east auxiliary bridge Banner significant wave height calculations for Test 14

Figure 4-15: This is a plot of the difference between the WCM and the East Auxiliary Bridge Banner significant wave height calculations for Test 8.

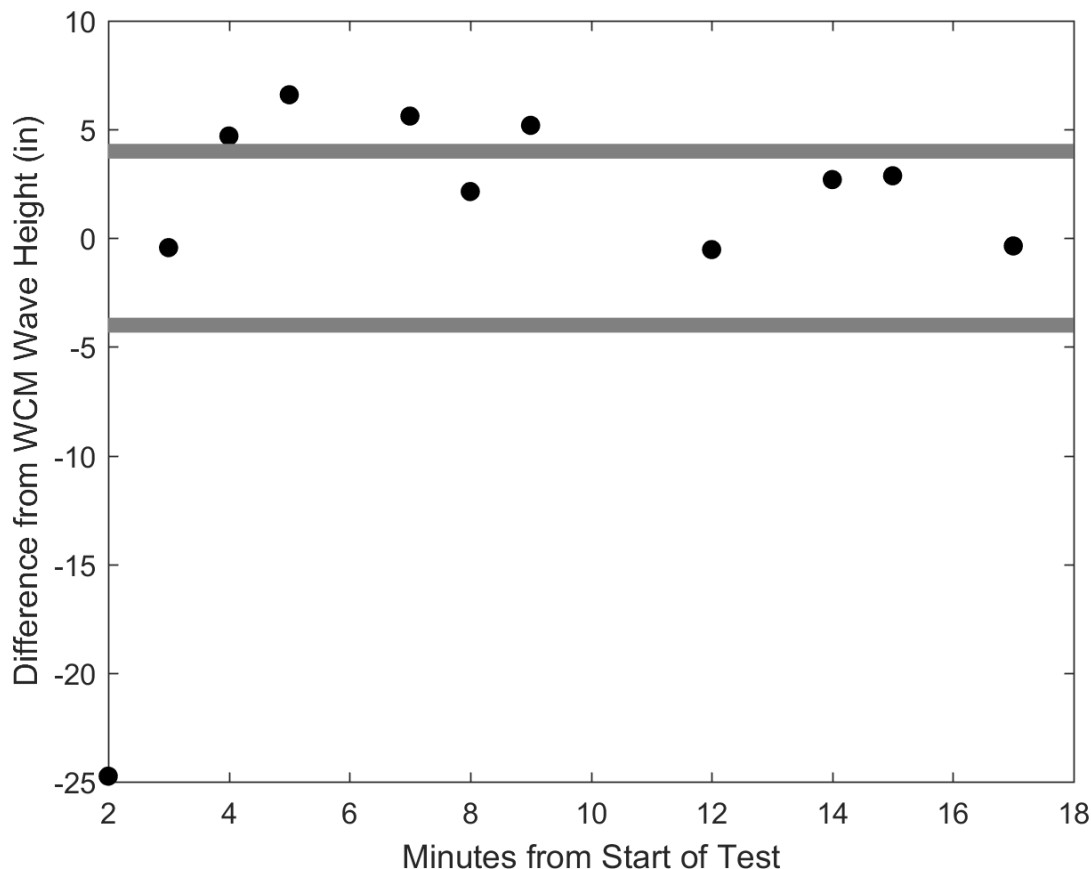


Figure 4-15: Difference between the WCM and the East Auxiliary Bridge Banner significant wave height calculations for Test 8

For both skimmer and buoy, the mean values furthest from the performance criteria were calculated for the waves created by the 18-inch stroke and 18 CPM setting of the wave generator. This creates a large sinusoidal wave with a significant wave height of approximately 22 inches. We believe the discrepancy between the wave heights is due to the evenness of the waves in the tank. Figures 4-16 and 4-17 are pictures of the wave tank compared to the conditions we used for training our algorithms. We collected data in open water under complex conditions using both the buoy and a mockup skimmer. The open water conditions were deep-water waves with a water depth of approximately 20 feet, while the water depth at Ohmsett was 8 feet. Except in the choppy conditions, the wave tank produced sinusoidal waves with all of the energy moving in one direction. This created more lateral motion on the skimmer than in the open waves. We used the scalar magnitude of the three axes to calculate wave height, so this lateral motion was not taken into account and was folded into the wave height calculation.



Figure 4-16: Albermarle Sound testing



Figure 4-17: Ohmsett Stroke 18, CPM 18

Pictures from data collection on the Albermarle Sound, Figure 4-16 versus the Ohmsett wave tank, Figure 4-17. The top picture shows the wave condition on the Albermarle Sound. We used the buoy and a WCM connected to a mockup of a terminator skimmer to collect wave data from deep water waves in complex conditions. The bottom picture shows the waves generated at Ohmsett. We collected data from the buoy and a WCM attached to a terminator skimmer. The waves generated at Ohmsett were consistent sinusoidal waves in shallower water conditions.

We calculated the period by dividing the zeroth-order moment of the wave spectrum by the first-order moment of the wave spectrum. We found that this was equivalent to the periods calculated by Ohmsett.

We calculated the wave length by dividing the significant height by the significant wave steepness. This resulted in shorter wavelengths than measured on the side of the tank or calculated at Ohmsett. The code used at Ohmsett estimates the wavelength based on the first-order dispersion equation. Wavelength does not seem to be used much in determining sea state. In the next phase, we recommend changing the value to steepness as a value that may prove more useful for skimmer operations.

4.2.1 Wave Reflections

The variation observed by Ohmsett in calculated $H_{1/3}$ and the height of a single wave is typically 10 to 40 percent. It also appears that in general, the longer periods show a larger difference. In addition to interference from reflections (constructive and deconstructive interference), wavelengths greater than twice the water depth (8 feet for the Ohmsett tank) experience friction on the bottom of the basin, which influences the wave speed and profile as the waves travel toward the north. Harbor chop waves also sometimes have “hot spots” and can create higher values and greater variances between Banner measurement locations during a test run. According to Ohmsett staff, hot spots are likely due to the constructive/destructive interference of the waves. For example, Test 6 (Stroke 18, CPM 18) had a significant wave height difference between bridge Banner sensors of more than 7 inches for the same 1-minute time window. This large variance accounts for some of the large standard deviations and averages seen from the skimmer-mounted WCM and WCM-Buoy, which were positioned between the main, east, and west auxiliary bridge Banner sensors.

We conclude that the WCM, WCM-Sat, and WCM-Buoy performed remarkably well and were able to accurately report localized wave conditions. As the variation observed between the main bridge Banner and auxiliary bridge Banner sensors show, complex wave fields create very localized conditions. Our wave characterization modules demonstrate why localized sensors on skimmers and around recovery areas are critical in making informed decisions because other methods to access wave-field characteristics will have an uncertainty due to spatial variations in the waves, even if the measurement is nearby.

4.2.2 Oil Spray

Prior to Test 19, Ohmsett staff sprayed crude oil on all devices attached to the skimmer, as shown in Figure 4-18, and the buoy in Figure 4-19 to see whether there was any degradation in operation.

The crude oil did not have any discernable effect on the operation, communications, or reporting ability of the devices. Any residue or coating of material on the enclosure or antennas has potential to attenuate the radio frequency (RF) signals including GPS, WiFi, RF mesh, and satellite. Typically, non-electrically conductive residues such as oil have a lower attenuation factor and impact on RF communication degradation. We also increased the separation of the internal antennas from the enclosure by a few inches to further reduce RF attenuation. See **Appendix E** for further details and analysis.

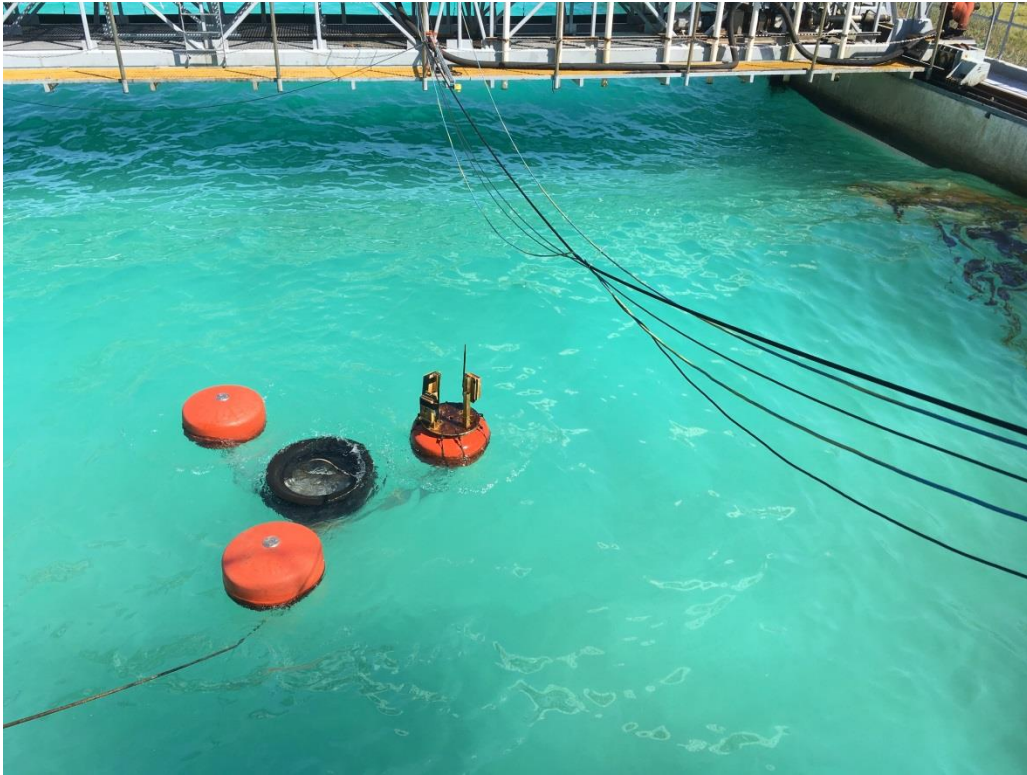


Figure 4-18: Oil-covered WCMs mounted to the skimmer

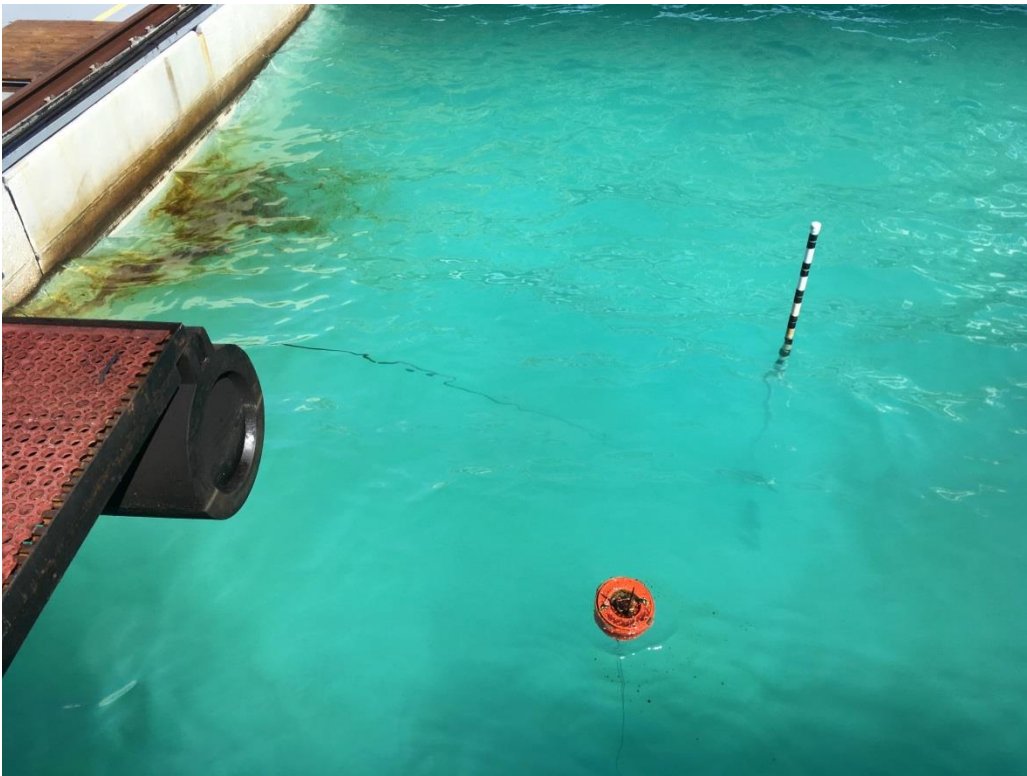


Figure 4-19: Oil-covered WCM-Buoy

4.2.3 Towed Test

Prior to Test 20, we positioned the bridges to the northern-most side of the wave tank. During Test 20, we started towing the skimmer with WCMs and WCM-Buoy at 0.75 knots toward the south end of the tank as pictured in Figure 4-20. We did not observe or record any issues with reporting wave data during the towing operation. The mean significant wave height and standard deviation were similar compared to the same wave types in Tests 3 and 4.



Figure 4-20: Towed test

4.3 Integrated System Demonstration

The AECOM team tested several configurations and device settings during our 4 days at Ohmsett. In order to increase the number of data points during each test, we configured a WCM attached to the skimmer and a buoy to stream raw data, as analyzed in the previous section. We also deployed a WCM, WCM-Sat, and WCM-Buoy configured for onboard calculation of wave characteristics and autonomous reporting of wave data to the local application dashboard via WiFi and remote GIS user interface via satellite to showcase a complete, end-to-end wave characterization solution.

Several tests with varied wave types and conditions are highlighted below. The significant wave height (H_{m0}) calculated from the Ohmsett Banner sensors is shown with data sent through WiFi to the iPad application with screenshots and data sent through satellite captured by the GIS user interface. The iPad application screenshots are in Coordinated Universal Time (UTC). Each device has a unique ID and associated WiFi service set identifier (SSID). The ID and SSID are:

- WCM (ID: 288988113, SSID: WCME243),
- WCM-Sat (ID: 28988088, SSID: WCM7FE3), and
- WCM-Buoy (ID: 288988119, SSID: WCM4320).

The WCM, WCM-Sat, and WCM-Buoy “Report timestamp” column in Tables 4-3 through 4-7 is the timestamp when the iPad application received the wave characterization data over WiFi. The “Hm0 Calculation Time Window” column is the one minute time windows from each of the Banner sensors to cover the timestamps of each WCM, WCM-Sat and WCM-Buoy. The GPS was disabled on the WCM and the GPS and satellite modem was disabled on the WCM-Buoy to allow for more frequent wave data updates because the GPS and satellite modem add several minutes of latency.

The WCM-Sat acquires a GPS signal after recording wave data but prior to WiFi and satellite transmission. Therefore, the WCM and WCM-Buoy report timestamps lag the actual significant wave height calculation time window by only a few seconds. However, the GPS initialization can take between 60 and 90 seconds; therefore, this time offset from the calculation time window is added to the timestamp recorded through the WiFi message.

4.3.1 Test 13 – Chop, Stroke 12.0, CPM 30.0

Figure 4-21 shows the testing configuration and harbor chop wave conditions present during Test 13. There were large and varied wave fronts throughout the tank as noted by the witness pole being nearly submerged by the oncoming wave and the sizeable peak created between the witness pole and the buoy.



Figure 4-21: Test 13 Chop wave conditions – Stroke 12.0, CPM 30.0

Table 4-3 summarizes a portion of Test 13 comparing the skimmer-attached WCM and WCM-Sat reported significant wave heights to the significant wave heights calculated from the Ohmsett Banners. The harbor chop and wave generator settings created large and varied wave heights throughout the tank as shown during the 2:56 to 2:57 time period in which the difference between the main and auxiliary east Banners was more than 10 inches. The WCM and WCM-Sat reported significant wave heights in line with the wave heights observed.

Table 2-3: H_{m0} for Test 13 – Chop, Stroke 12.0, CPM 30.0

H_{m0} Calculation Time Window	Main (inches)	Aux West (inches)	Aux East (inches)	Device	Report Timestamp	H_{m0} (inches)
2:54 – 2:55	37.0754	31.0411	28.6106	WCM	2:56:04	36.6141
2:55 – 2:56	28.3820	21.5642	20.2099	WCM-Sat	2:56:34	30.7086
2:56 – 2:57	36.6519	26.4310	26.0352	WCM	2:57:59	31.8897
2:57 – 2:58	27.5223	28.0460	22.0279			

Figure 4-22 is a screenshot of the application dashboard from an iPad of WCM with ID 28988113 and SSID WCME243. The timestamp is in UTC (-5 Eastern Standard Time) with no other reported nodes. The location is missing because the GPS was disabled, generating a “No GPS Fix” error in the status window. The wave height in meters was reported as 0.93 meter or 36.61 inches. The overlay of data on the left side is the debug mode to view the data retrieve events and byte stream from the WCM to the iPad.

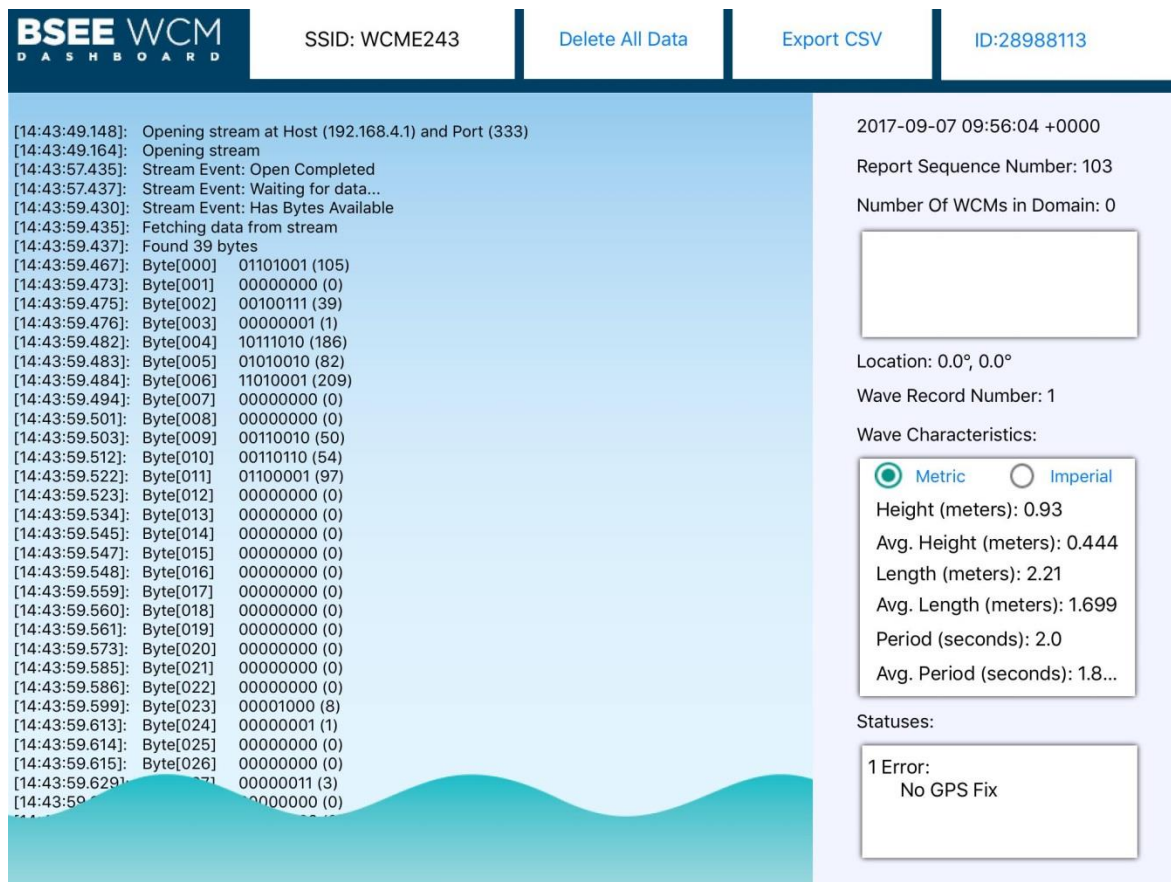


Figure 4-22: Test 13 – Application dashboard screenshot of WCM 28988113 at 2:56 p.m.

Figure 4-23 is a screenshot of the application dashboard from an iPad of WCM-Sat with ID 28988088 and SSID WCM7FE3 wave characterization report through WiFi. Here the longitude and latitude are reported because a GPS signal was acquired during the WCM-Sat reporting sequence. A height of 0.78 meter or 30.71 inches was reported at 2:56:34 p.m. local time.

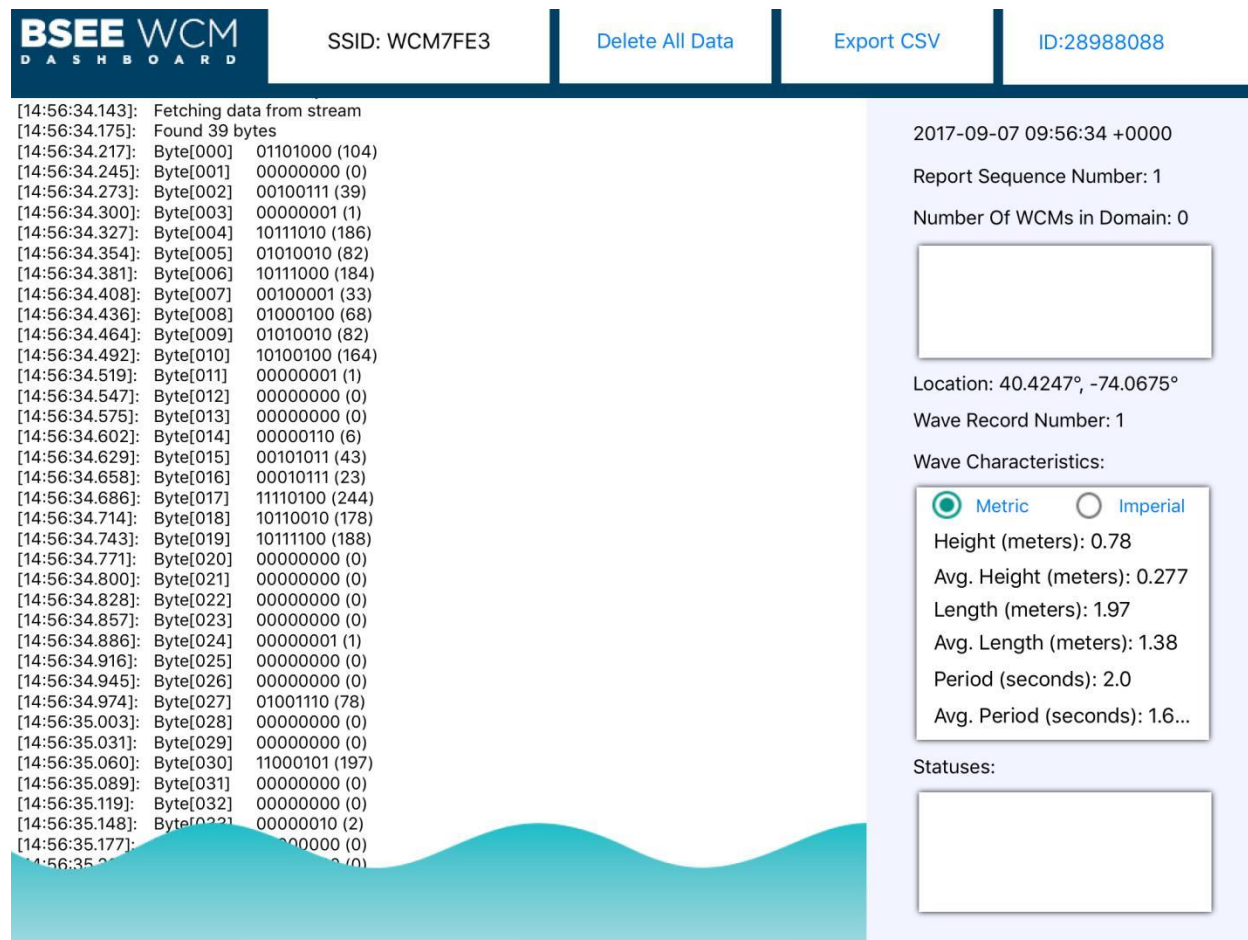


Figure 4-23: Test 13 – Application dashboard screenshot of WCM-Sat 28988088

Figure 4-24 shows the same data as Figure 4-23 from WCM-Sat ID 28988088 but reported via satellite to the remote GIS user interface. This figure shows its location in the Ohmsett wave tank with a reported timestamp of 2:55:32 p.m. when a GPS lock was achieved, which is before the wave characterization report was sent out through WiFi or sent via satellite. The wave height is reported to the nearest tenth of a meter.

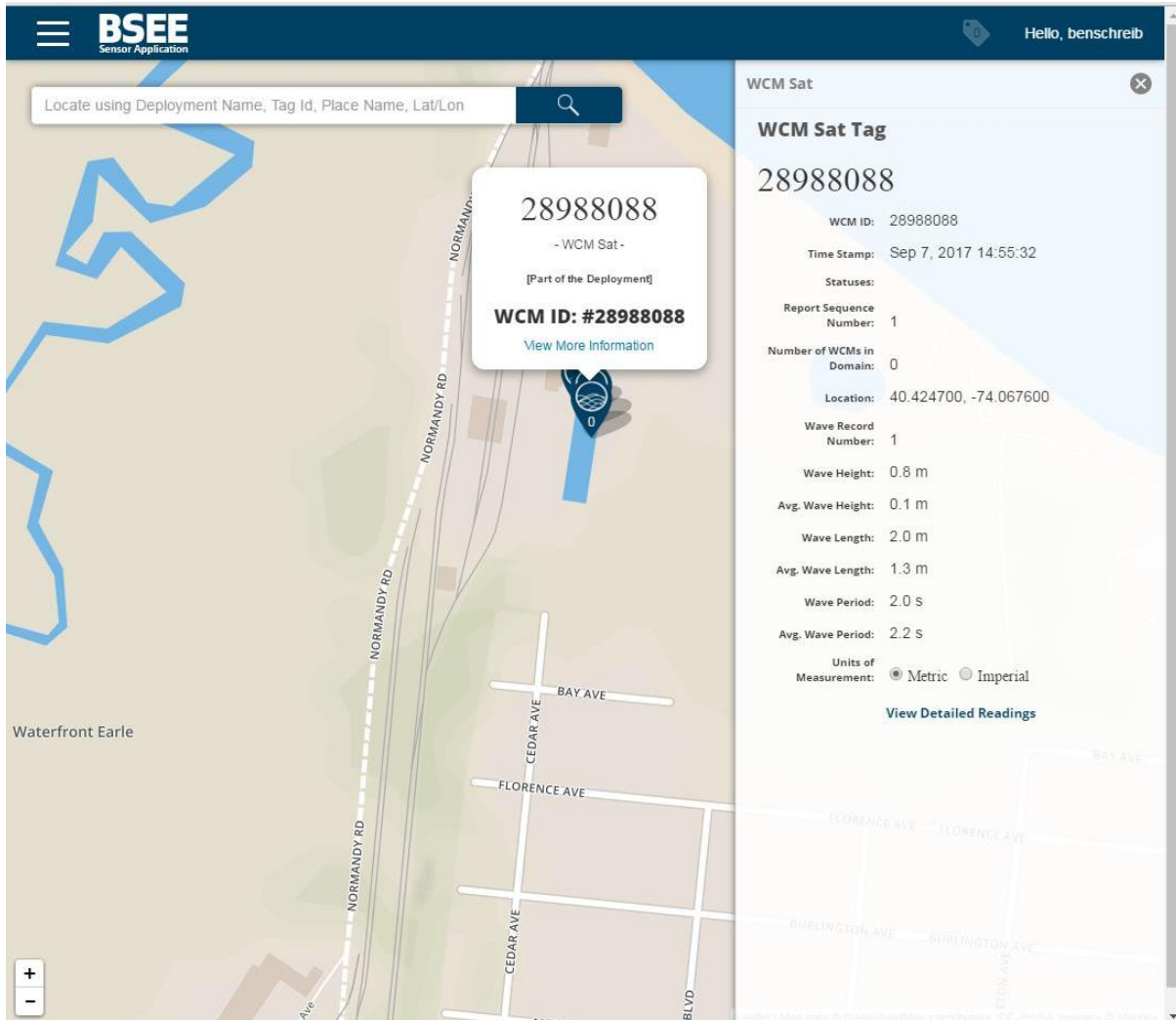


Figure 4-24: Test 13 – GIS user interface screenshot of WCM-Sat 28988088

4.3.2 Test 15 – Chop, Stroke 3.0, CPM 35.0

Figure 4-25 shows the testing configuration and harbor chop wave conditions present during Test 15. The stroke was relatively short, producing moderately sized waves.

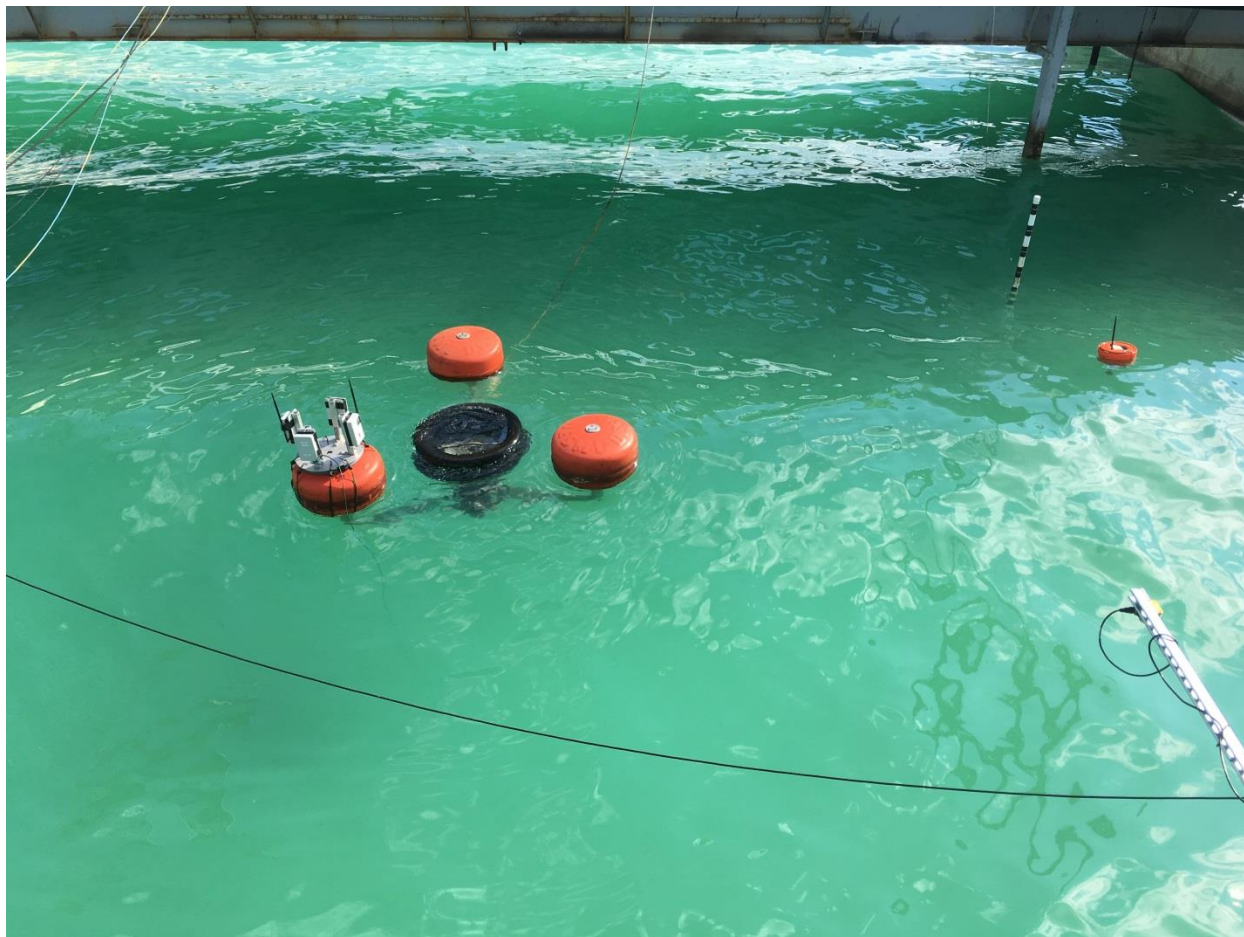


Figure 4-25: Test 15 Chop wave conditions – Stroke 3.0, CPM 35.0

Table 4-4 highlights a few of the wave characterization reports during Test 15 showing significant wave heights for the WCM and WCM-Sat near the significant wave heights generated from the Banner sensors.

Table 4-4: H_{m0} for Test 15 – Chop, Stroke 3.0, CPM 35.0

H_{m0} Calculation Time Window	Main (inches)	Aux West (inches)	Aux East (inches)	Device	Report Timestamp	H_{m0} (inches)
4:08 – 4:09	14.0213	15.5726	12.2604	WCM	4:08:51	14.1732
4:09 – 4:10	10.5187	9.9354	12.2864	WCM-Sat	4:09:42	10.6299
4:10 – 4:11	12.9406	10.1315	14.6415	WCM	4:10:47	9.8425
4:16 – 4:17	12.2832	13.0043	13.3524	WCM	4:17:07	15.7480
4:17 – 4:18	10.6827	12.2256	10.1522	WCM-Sat	4:17:55	15.7480

Interestingly, both the WCM and WCM-Sat recorded wave data between approximately 4:16 and 4:17 p.m. The WCM-Sat reported via WiFi approximately 60 seconds after the WCM or the amount of time it takes for the GPS to acquire a signal and then send out a wave characterization report. Therefore, since both devices were recording data during close to the same time window and both were mounted to the skimmer, the significant wave height was the same for both devices, only approximately 2.4 inches higher than what was measured by the auxiliary east Banner sensor.

Figure 4-26 is a screenshot of this report from the WCM.

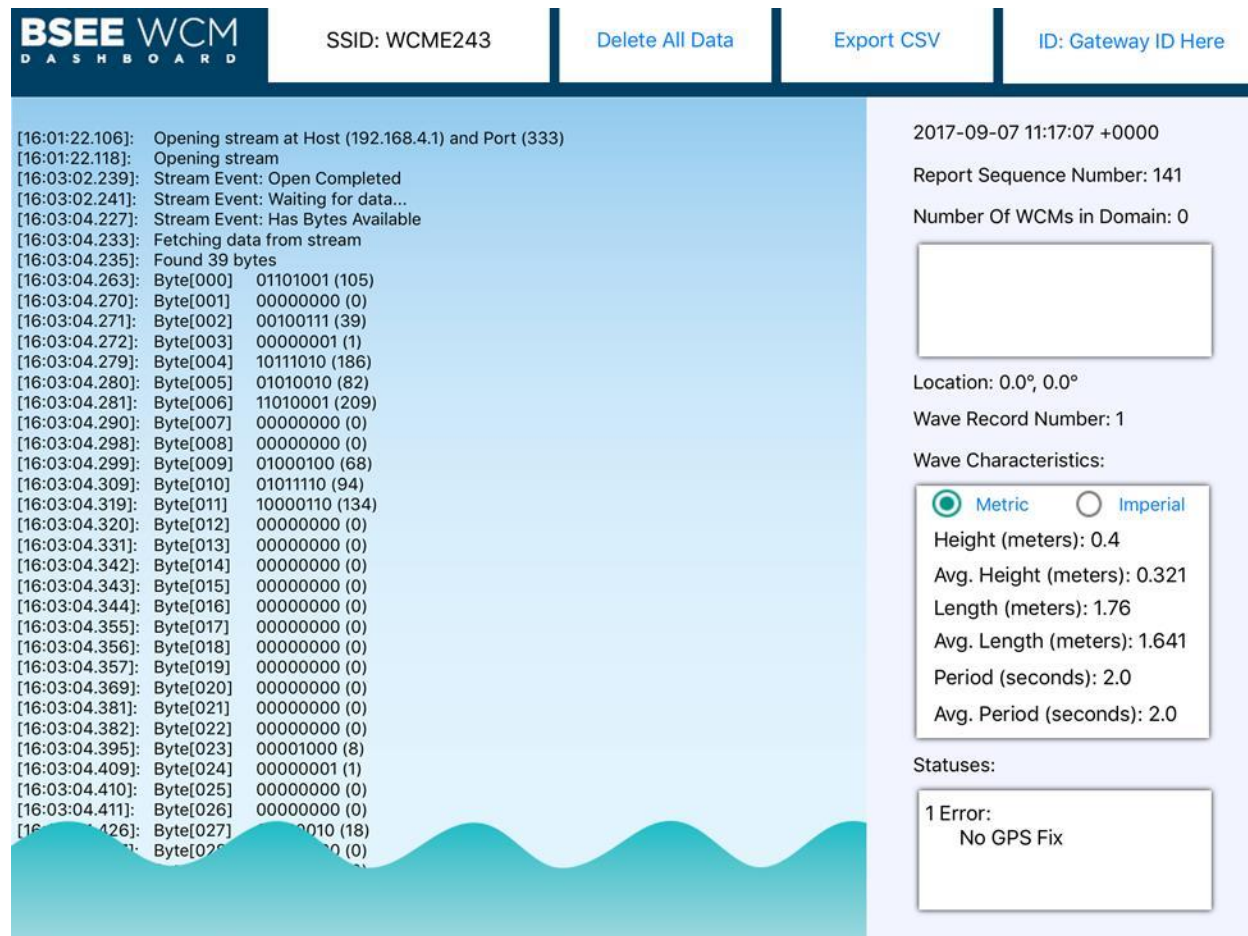


Figure 4-26: Test 15 – Application dashboard screenshot of WCM 28988113

Figure 4-27 is a screenshot of this report from the WCM-Sat.

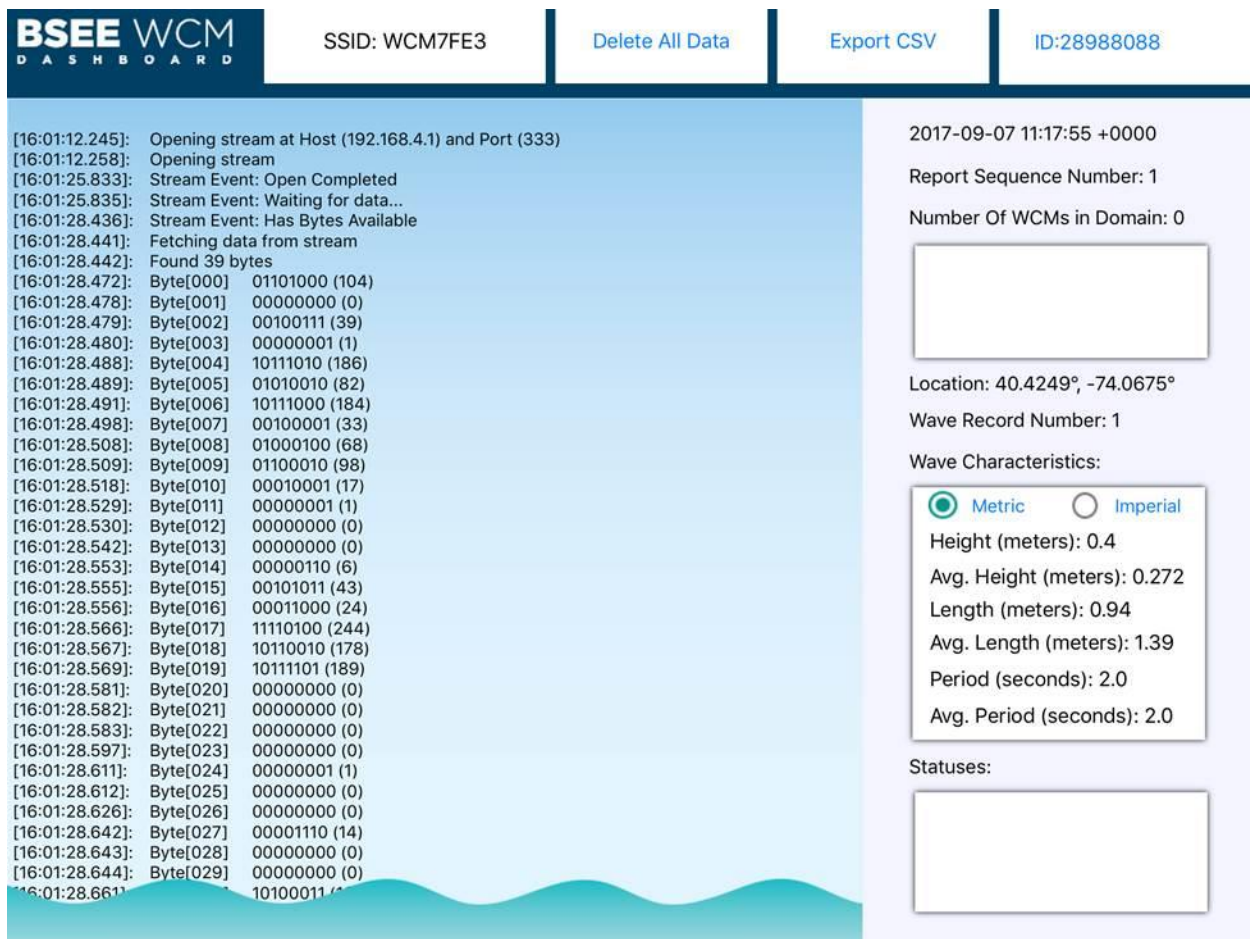


Figure 4-27: Test 15 – Application dashboard screenshot of WCM-Sat 28988088

Figure 4-28 shows this report on the GIS user interface.

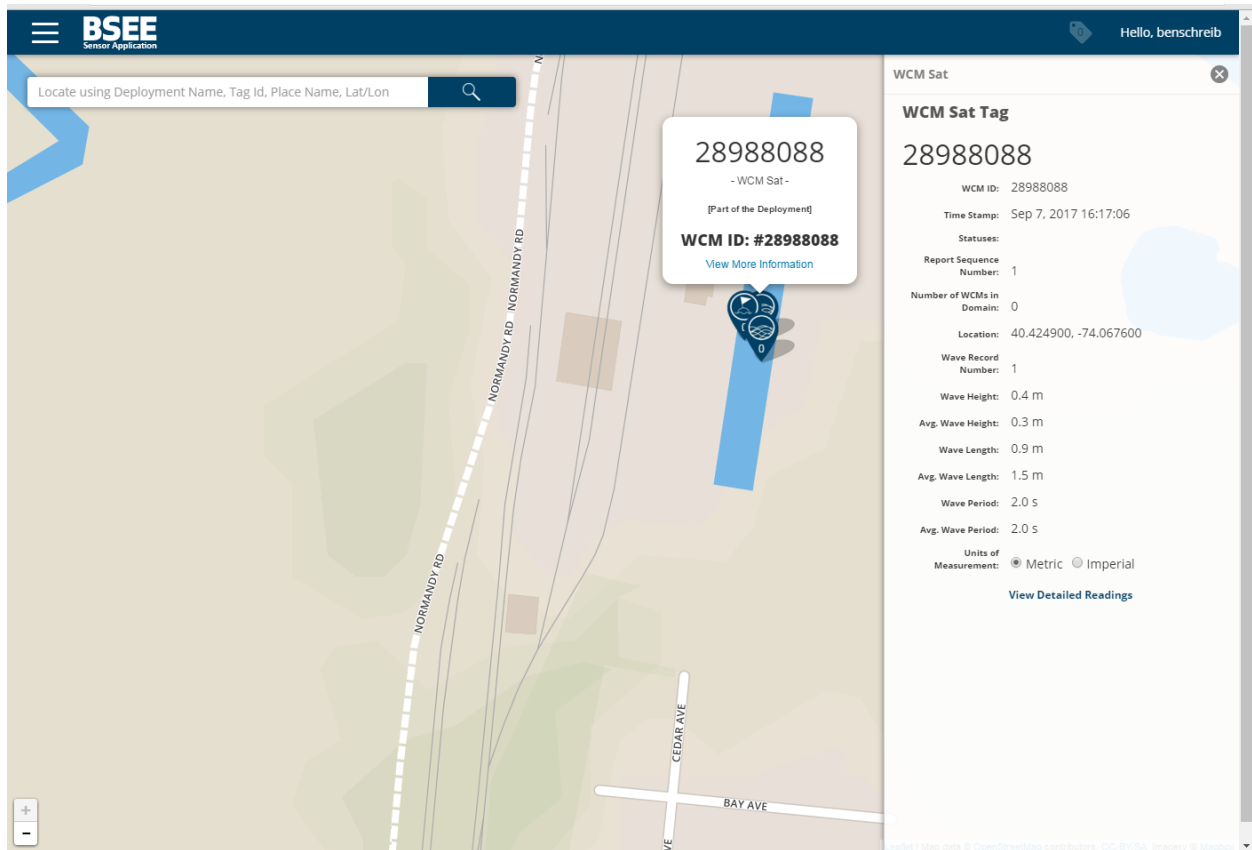


Figure 4-28: Test 15 – GIS user interface screenshot of WCM-Sat 28988088

4.3.3 Test 17 – Sine, Stroke 18.0, CPM 10.0

Figure 4-29 is a picture of the relatively small sine waves generated during Test 17.

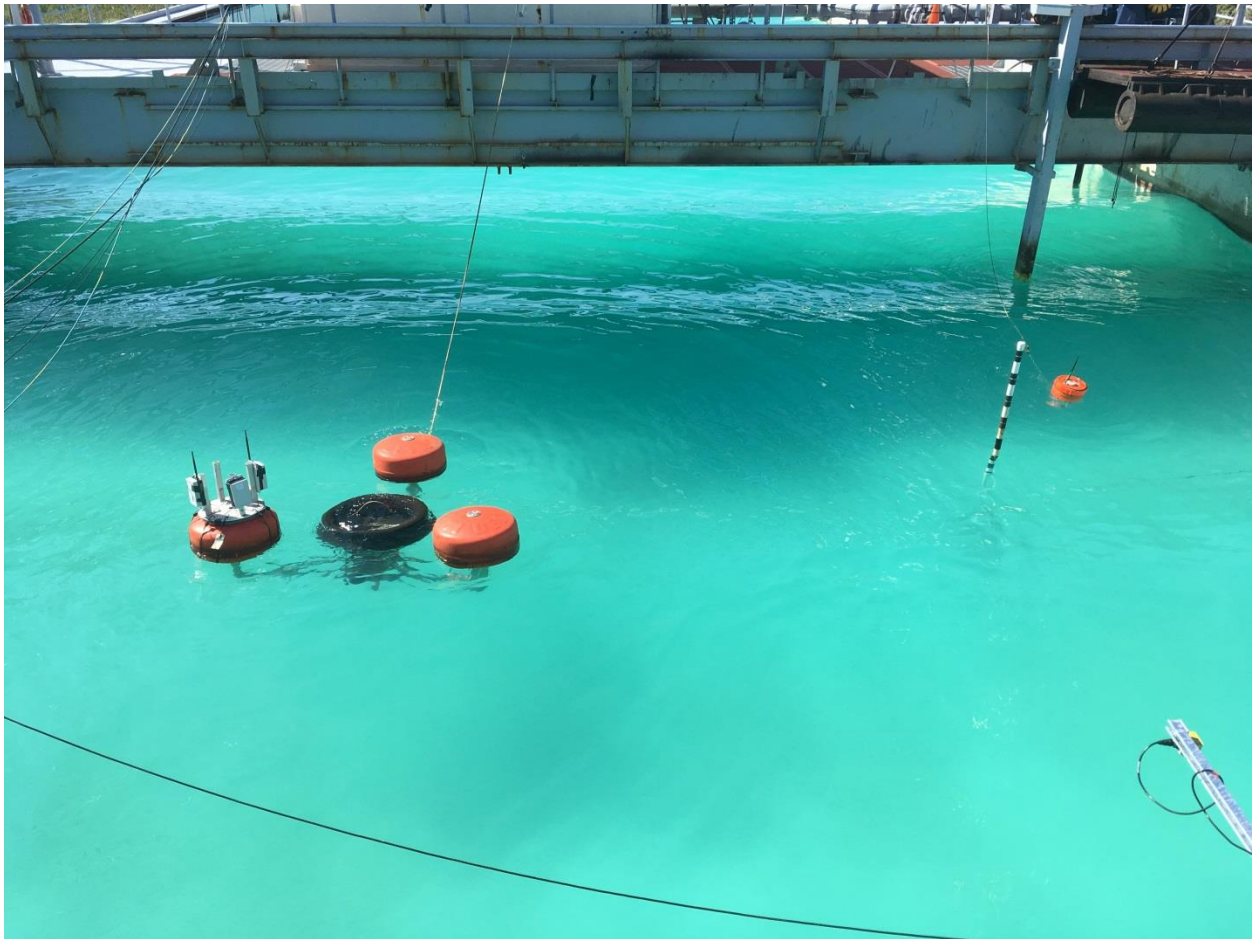


Figure 4-29: Test 17 – Sine, Stroke 18.0, CPM 10.0

Table 4-5 highlights wave characterization reports from Test 17 showing significant wave heights. Again, the WCM and WCM-Sat located on the skimmer generated the same significant wave height due to the approximately 60-second delay in the WCM-Sat report through WiFi to the application dashboard because of the GPS initialization sequence. The WCM-Buoy also reports a similar wave height with all three reports within 1 inch of several Banner sensors.

Table 4-5: H_{m0} for Test 17 – Sine, Stroke 18.0, CPM 10.0

H_{m0} Calculation Time Window	Main (inches)	Aux West (inches)	Aux East (inches)	Device	Report Timestamp	H_{m0} (inches)
10:14 – 10:15	5.3056	3.2253	3.1773	WCM	10:15:17	2.3622
10:15 – 10:16	3.4383	2.1018	2.0757	WCM-Buoy	10:15:32	3.1496
				WCM-Sat	10:16:28	2.3622

Figure 4-30 is a local application dashboard screenshot of the wave characterization report from the WCM as listed in Table 4-5.

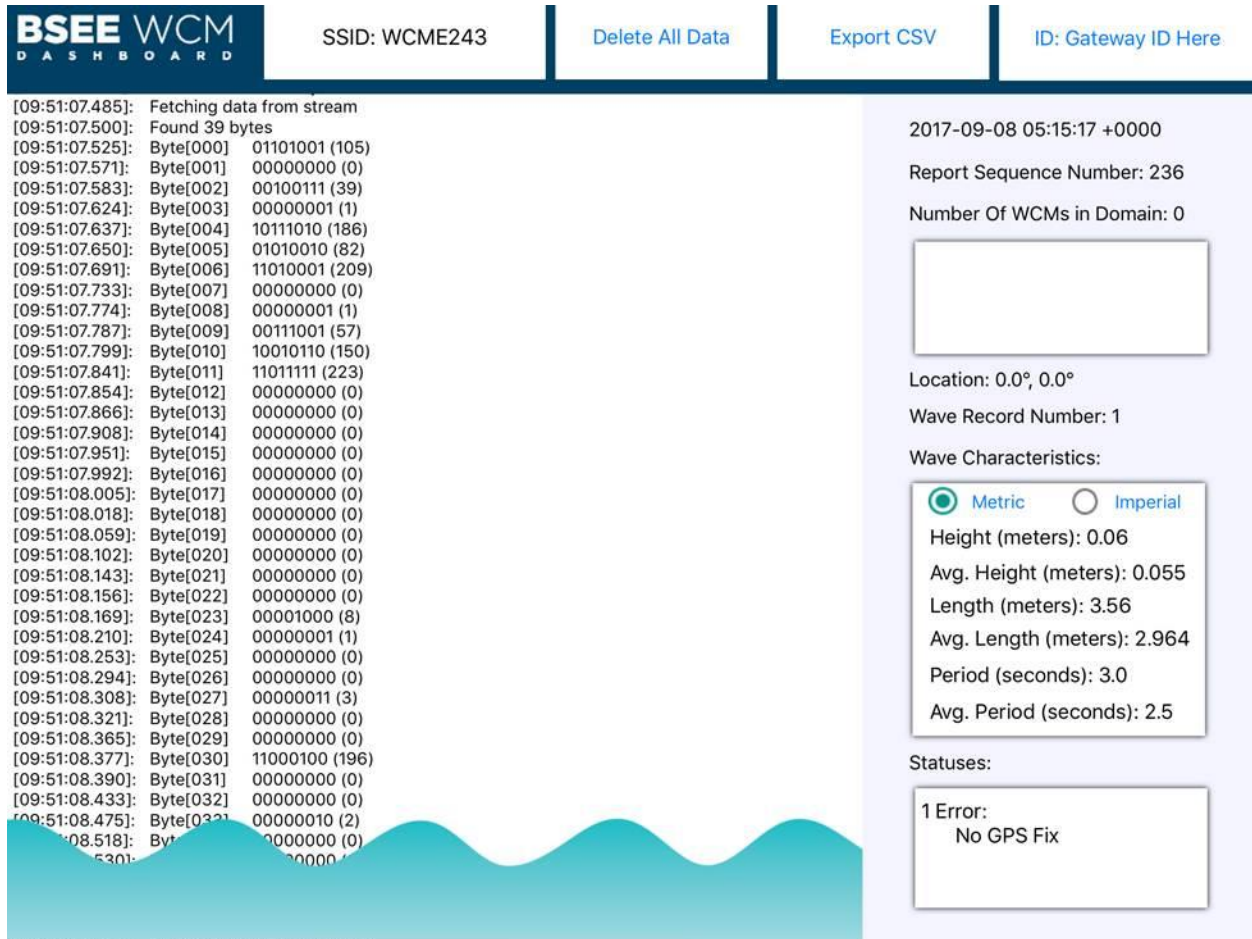


Figure 4-30: Test 17 – Application dashboard screenshot of WCM 28988113

Figure 4-31 is a screenshot of the WCM-Buoy wave characterization report.

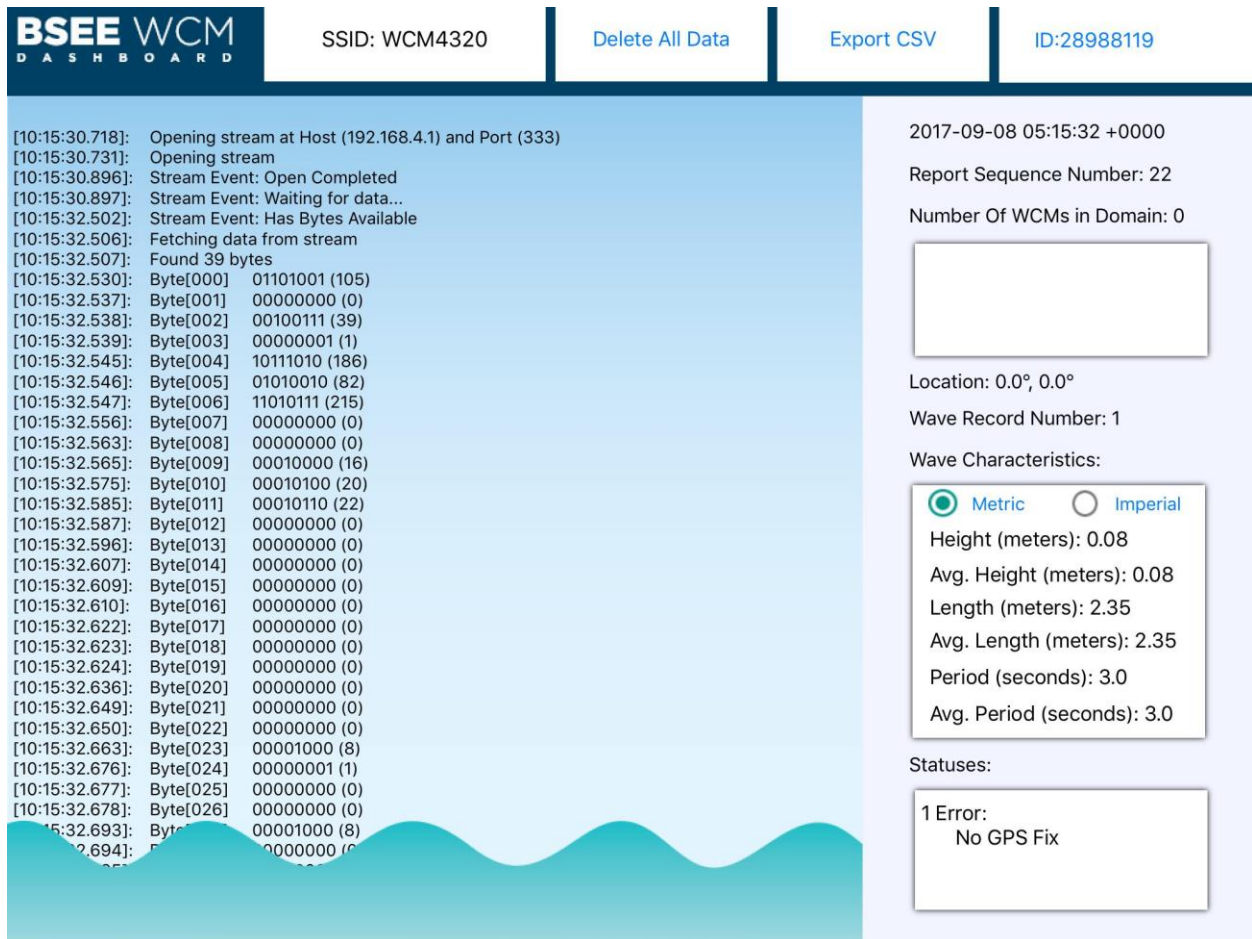


Figure 4-31: Test 17 – Application dashboard screenshot WCM-Buoy 288988119

Figure 4-32 is a screenshot of the WCM-Sat report from the local application dashboard.

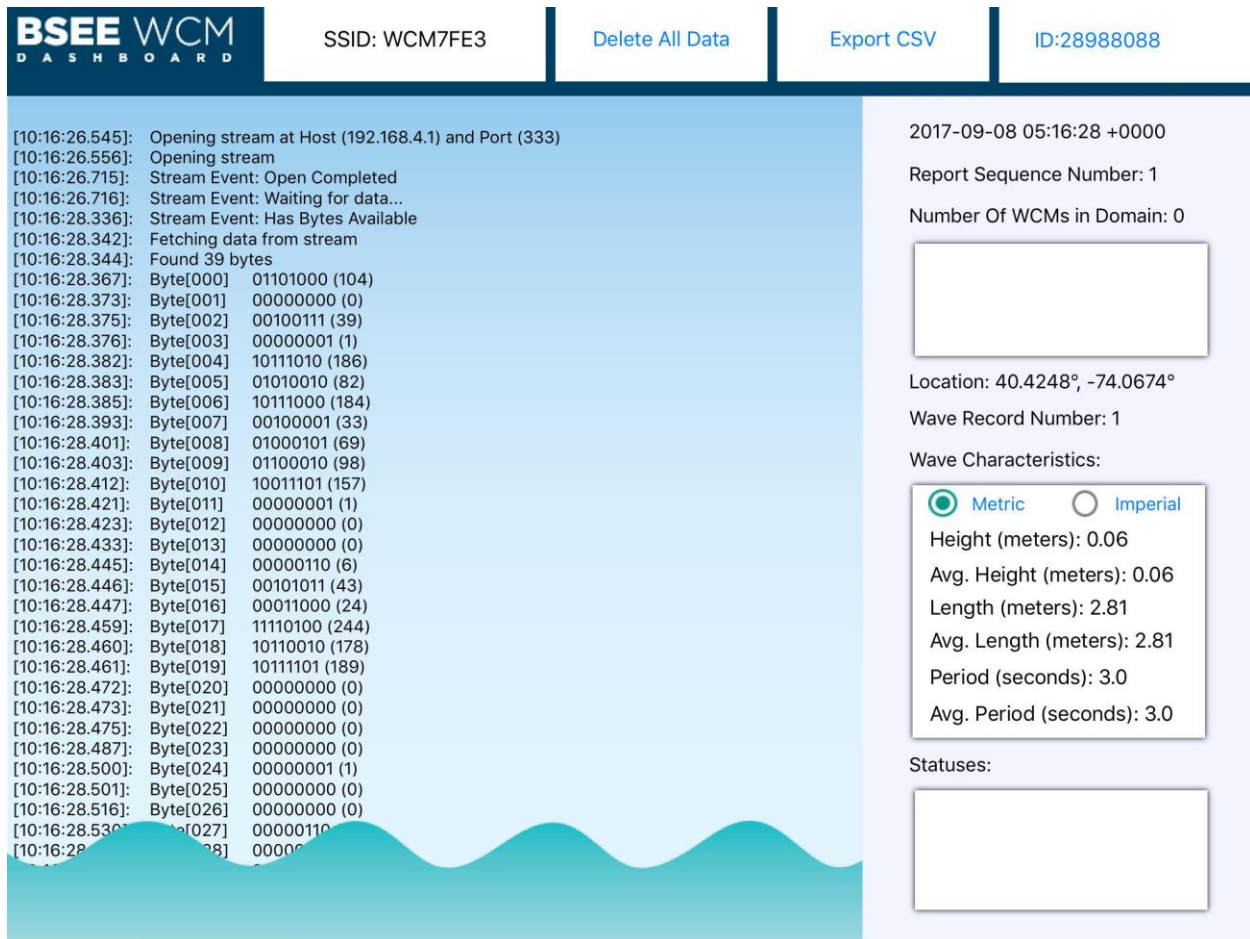


Figure 4-32: Test 17 – Application dashboard screenshot of WCM-Sat 28988088

Figure 4-33 shows the same WCM-Sat wave characterization report but reported via satellite to the remote GIS user interface. The wave height is rounded to the nearest tenth of a meter, and the GPS accuracy is within a few meters. The nearby bridges and wave action during the GPS signal acquisition may have contributed to some errors in the location, as shown on the map.

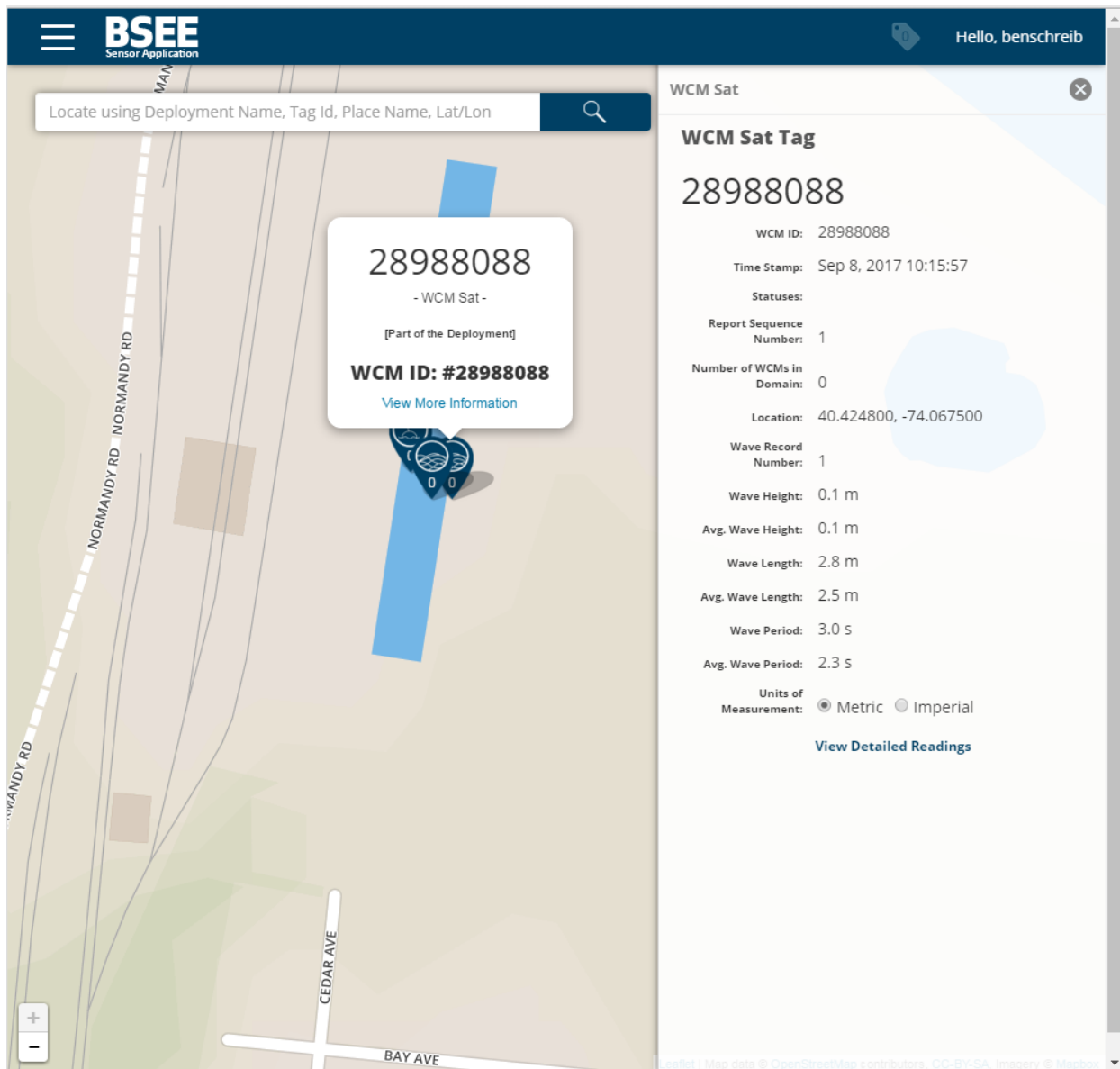


Figure 4-33: Test 17 – GIS user interface screenshot of WCM-Sat 28988088

4.3.4 Test 19 – Sine, Stroke 12.0, CPM, 25.0

Figure 4-34 shows the wave conditions during Test 19.



Figure 4-34: Test 19 – Sine, Stroke 12.0, CPM, 25.0

Table 4-6 summarizes a sample of the wave characterization reports from Test 19. Of particular note, the WCM-Buoy, as pictured in Figure 4-34, is closer to the main and aux west Banners than the skimmer, whereas the WCM and WCM-Sat mounted on the skimmer are closer to the auxiliary east Banner. This relative positioning of the WCM-Buoy is reflected in the slightly lower significant wave height experienced by the WCM-Buoy, similar to the main and auxiliary west Banner references. The auxiliary east Banner is 2 to 5 inches higher over these time periods, reflected by a similar trend in the WCM and WCM-Sat significant wave heights.

Table 4-6: H_{m0} for Test 19 – Sine, Stroke 12.0, CPM 25.0

H_{m0} Calculation Time Window	Main (inches)	Aux West (inches)	Aux East (inches)	Device	Report Timestamp	H_{m0} (inches)
10:51 – 10:52	16.5516	19.8027	23.3146	WCM	10:51:38	22.04724
10:52 – 10:53	18.5393	17.8026	20.5176	WCM-Buoy	10:52:40	16.92913
				WCM-Sat	10:53:16	18.50394
				WCM	10:53:30	19.29134

Figures 4-35 through 4-39 show the user interface screenshots for the four reports listed in Table 4-6.

BSEE WCM DASHBOARD | SSID: WCME243 | Delete All Data | Export CSV | ID:28988113

[09:51:07.485]: Fetching data from stream
 [09:51:07.500]: Found 39 bytes
 [09:51:07.525]: Byte[000] 01101001 (105)
 [09:51:07.571]: Byte[001] 00000000 (0)
 [09:51:07.583]: Byte[002] 00100111 (39)
 [09:51:07.624]: Byte[003] 00000001 (1)
 [09:51:07.637]: Byte[004] 10111010 (186)
 [09:51:07.650]: Byte[005] 01010010 (82)
 [09:51:07.691]: Byte[006] 11010001 (209)
 [09:51:07.733]: Byte[007] 00000000 (0)
 [09:51:07.774]: Byte[008] 00000001 (1)
 [09:51:07.787]: Byte[009] 00111001 (57)
 [09:51:07.799]: Byte[010] 10010110 (150)
 [09:51:07.841]: Byte[011] 11011111 (223)
 [09:51:07.854]: Byte[012] 00000000 (0)
 [09:51:07.866]: Byte[013] 00000000 (0)
 [09:51:07.908]: Byte[014] 00000000 (0)
 [09:51:07.951]: Byte[015] 00000000 (0)
 [09:51:07.992]: Byte[016] 00000000 (0)
 [09:51:08.005]: Byte[017] 00000000 (0)
 [09:51:08.018]: Byte[018] 00000000 (0)
 [09:51:08.059]: Byte[019] 00000000 (0)
 [09:51:08.102]: Byte[020] 00000000 (0)
 [09:51:08.143]: Byte[021] 00000000 (0)
 [09:51:08.156]: Byte[022] 00000000 (0)
 [09:51:08.169]: Byte[023] 00001000 (8)
 [09:51:08.210]: Byte[024] 00000001 (1)
 [09:51:08.253]: Byte[025] 00000000 (0)
 [09:51:08.294]: Byte[026] 00000000 (0)
 [09:51:08.308]: Byte[027] 00000011 (3)
 [09:51:08.321]: Byte[028] 00000000 (0)
 [09:51:08.365]: Byte[029] 00000000 (0)
 [09:51:08.377]: Byte[030] 11000100 (196)
 [09:51:08.390]: Byte[031] 00000000 (0)
 [09:51:08.433]: Byte[032] 00000000 (0)
 [09:51:08.475]: Byte[033] 00000010 (2)
 [09:51:08.517]: Byte[034] 00000000 (0)
 [09:51:08.559]: Byte[035] 00000000 (0)

2017-09-08 05:51:38 +0000
 Report Sequence Number: 255
 Number Of WCMs in Domain: 0

Location: 0.0°, 0.0°
 Wave Record Number: 1
 Wave Characteristics:
 Metric Imperial
 Height (meters): 0.56
 Avg. Height (meters): 0.387
 Length (meters): 2.69
 Avg. Length (meters): 2.007
 Period (seconds): 2.0
 Avg. Period (seconds): 2.0

Statuses:
 1 Error:
 No GPS Fix

Figure 4-35: Test 19 – Application dashboard screenshot of WCM 28988113 at 10:51 a.m.

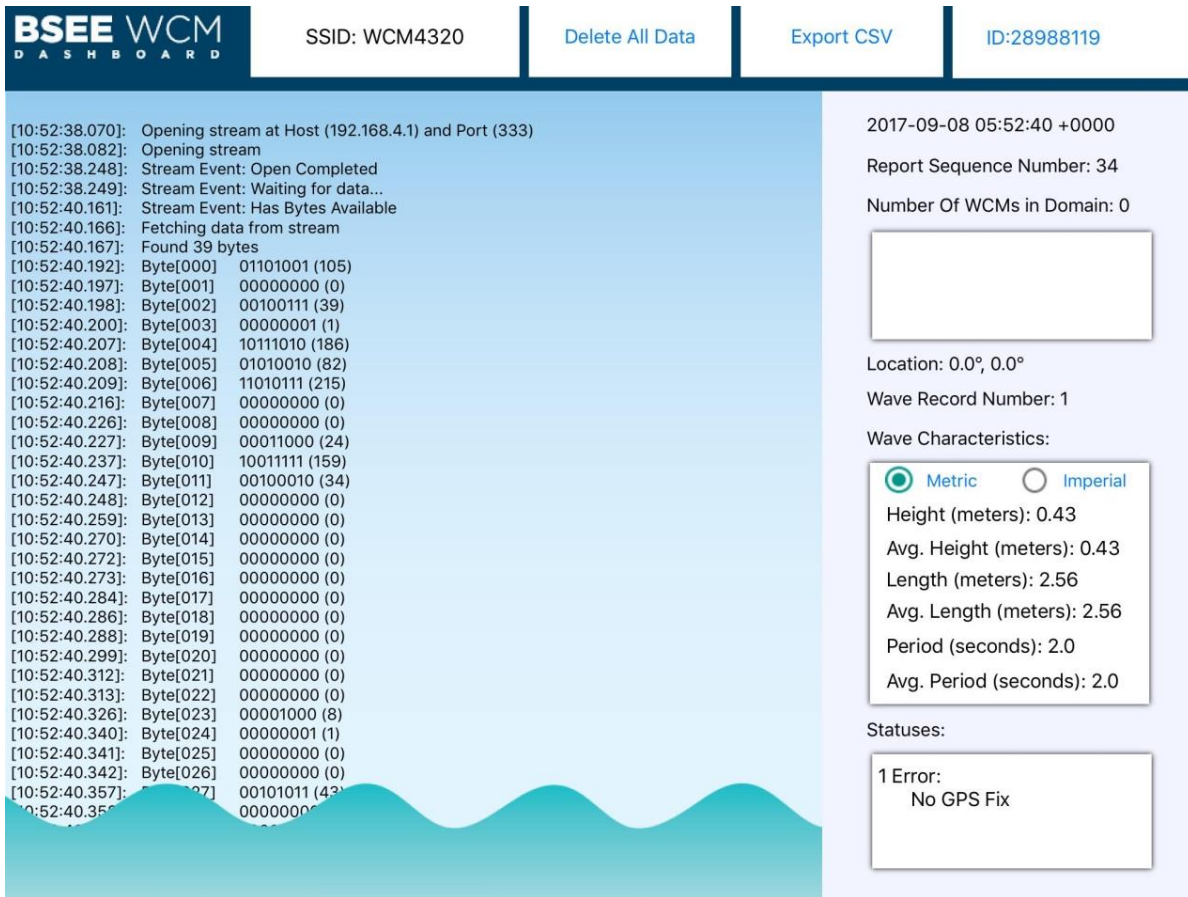


Figure 4-36: Test 19 –Application dashboard screenshot WCM-Buoy 288988119

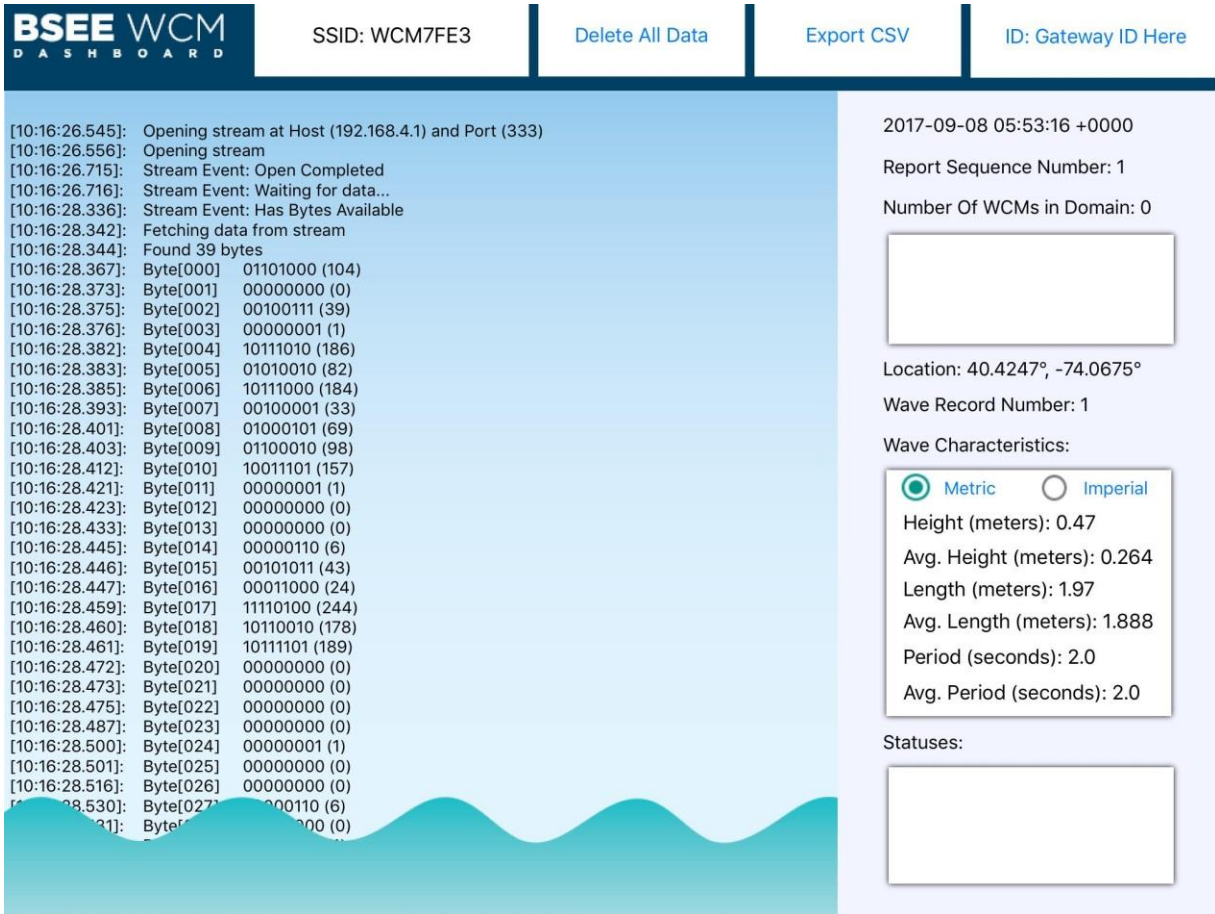


Figure 4-37: Test 19 – Application dashboard screenshot of WCM-Sat 28988088

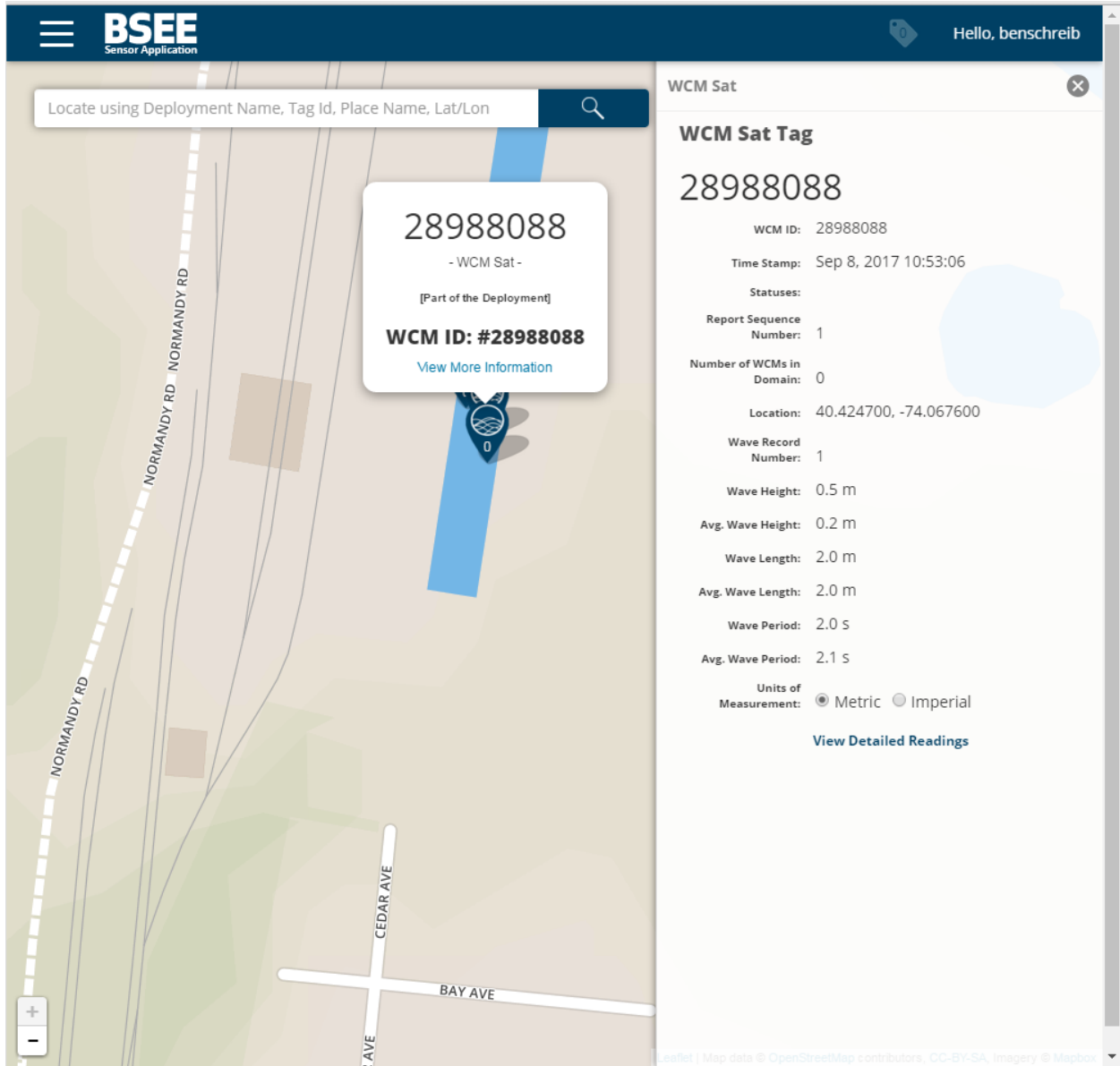


Figure 4-38: Test 19 – GIS user interface screenshot of WCM-Sat 28988088

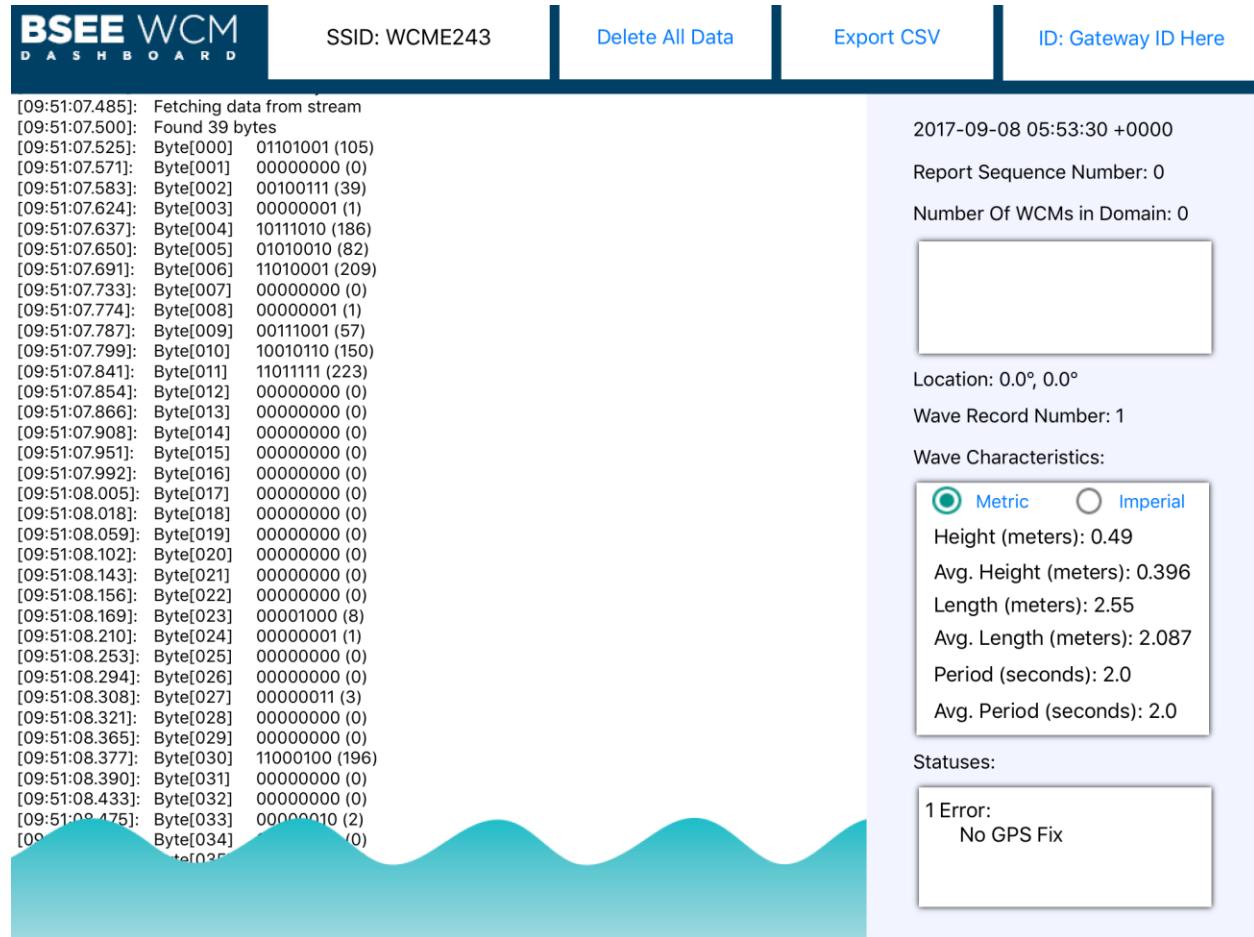


Figure 4-39: Test 19 – Application dashboard screenshot of WCM 28988113 at 10:53 a.m.

4.3.5 Test 20 – Sine (Advancing), Stroke 7.5, CPM 35.0

Figure 4-40 shows the north-to-south advance of the bridges pulling the skimmer and buoy at 0.75 knots during Test 20 with some large and complex wave action.



Figure 4-40: Test 20 – Sine (Advancing), Stroke 7.5, CPM 35.0

Table 4-7 shows the wave characterization reports collected during the bridge advance and towing the skimmer and buoy down the wave tank. All WCM, WCM-Sat, and WCM-Buoy significant wave heights are within 1 to 3 inches of a Banner data point for their respective time periods. Some variation is expected with the more complex the wave fields because each point in the wave tank was experiencing something different during the time window when data are being collected.

Table 4-7: H_{m0} for Test 20 – Sine (Advancing), Stroke 7.5, CPM 35.0

H_{m0} Calculation Time Window	Main (inches)	Aux West (inches)	Aux East (inches)	Device	Report Timestamp	H_{m0} (inches)
11:56 – 11:57	17.1766	15.9392	16.6479	WCM-Buoy	11:56:54	17.7165
11:57 – 11:58	15.921	16.2095	14.7043	WCM	11:57:00	19.6850
11:58 – 11:59	14.0613	10.9290	12.5594	WCM-Sat	11:58:14	14.1732
11:59 – 12:00	16.1601	11.9118	12.3986	WCM	11:58:58	20.0787
12:00 – 12:01	17.8194	15.2444	14.5168	WCM-Buoy	11:59:55	19.6850
12:01 – 12:02	19.0378	15.582	14.5867	WCM	12:00:57	20.4724
12:02 – 12:03	22.6512	16.8445	17.8917	WCM-Sat	12:02:02	17.7165
				WCM-Buoy	12:02:51	23.2283
				WCM	12:02:55	23.6220

Figures 4-41 through 4-43 show a few of the screenshots from Table 4-7. Figure 4-41 is an application dashboard screenshot from an iPad for the first row in Table 4-7 (WCM-Buoy).

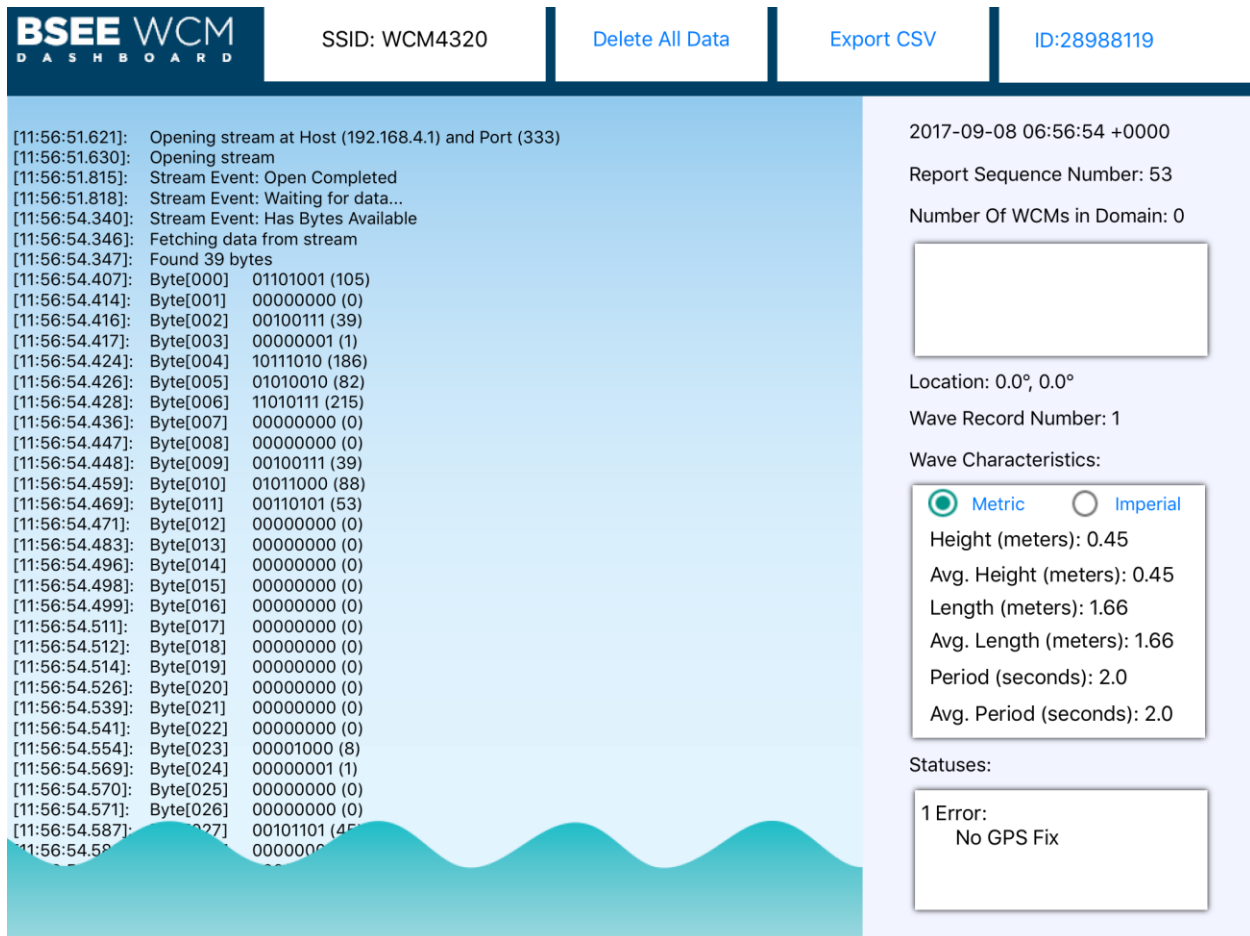


Figure 4-41: Test 20–Application dashboard screenshot WCM-Buoy 288988119

Figure 4-42 shows the screenshot from the first WCM report in Table 4-7.

The screenshot displays the BSEE WCM Dashboard for SSID: WCME243. The dashboard includes navigation links for 'Delete All Data', 'Export CSV', and 'ID: Gateway ID Here'. The main content area is divided into two sections: a data log on the left and a summary panel on the right.

Data Log:

Timestamp	Byte	Value (Count)
[11:06:32.863]:	Byte[004]	10111010 (186)
[11:06:32.883]:	Byte[005]	01010010 (82)
[11:06:32.929]:	Byte[006]	11010001 (209)
[11:06:32.944]:	Byte[007]	00000000 (0)
[11:06:32.991]:	Byte[008]	00000001 (1)
[11:06:33.006]:	Byte[009]	01001010 (74)
[11:06:33.024]:	Byte[010]	11100110 (230)
[11:06:33.071]:	Byte[011]	00000111 (7)
[11:06:33.086]:	Byte[012]	00000000 (0)
[11:06:33.105]:	Byte[013]	00000000 (0)
[11:06:33.153]:	Byte[014]	00000000 (0)
[11:06:33.167]:	Byte[015]	00000000 (0)
[11:06:33.215]:	Byte[016]	00000000 (0)
[11:06:33.230]:	Byte[017]	00000000 (0)
[11:06:33.249]:	Byte[018]	00000000 (0)
[11:06:33.297]:	Byte[019]	00000000 (0)
[11:06:33.312]:	Byte[020]	00000000 (0)
[11:06:33.361]:	Byte[021]	00000000 (0)
[11:06:33.375]:	Byte[022]	00000000 (0)
[11:06:33.394]:	Byte[023]	00001000 (8)
[11:06:33.442]:	Byte[024]	00000001 (1)
[11:06:33.486]:	Byte[025]	00000000 (0)
[11:06:33.500]:	Byte[026]	00000000 (0)
[11:06:33.549]:	Byte[027]	01000101 (69)
[11:06:33.564]:	Byte[028]	00000000 (0)
[11:06:33.612]:	Byte[029]	00000000 (0)
[11:06:33.627]:	Byte[030]	11110100 (244)
[11:06:33.645]:	Byte[031]	00000000 (0)
[11:06:33.694]:	Byte[032]	00000000 (0)
[11:06:33.709]:	Byte[033]	00000010 (2)
[11:06:33.758]:	Byte[034]	00000000 (0)
[11:06:33.773]:	Byte[035]	00000000 (0)
[11:06:33.791]:	Byte[036]	00000000 (0)
[11:06:33.839]:	Byte[037]	00000000 (0)
[11:06:33.854]:	Byte[038]	00000000 (0)
[11:06:45.978]:	Stream Event:	Error Occurred
[11:06:46.1...]	to Connect	
[11:06:...	eam	

Summary Panel:

- 2017-09-08 06:57:00 +0000
- Report Sequence Number: 32
- Number Of WCMs in Domain: 0
- Location: 0.0°, 0.0°
- Wave Record Number: 1
- Wave Characteristics:
 - Metric Imperial
 - Height (meters): 0.5
 - Avg. Height (meters): 0.255
 - Length (meters): 2.1
 - Avg. Length (meters): 1.723
 - Period (seconds): 2.0
 - Avg. Period (seconds): 2.0
- Statuses:
 - 1 Error: No GPS Fix

Figure 4-42: Test 20 – Application dashboard screenshot of WCM 28988113

Figure 4-43 shows the screenshot from the first WCM-Sat report in Table 4-7.

The screenshot displays the BSEE WCM Dashboard for SSID: WCM7FE3. The interface includes navigation links for 'Delete All Data', 'Export CSV', and 'ID: Gateway ID Here'. The main content area is split into two panels. The left panel shows a log of stream events from 10:16:26.545 to 10:16:28.530, including messages like 'Opening stream at Host (192.168.4.1) and Port (333)', 'Stream Event: Open Completed', and a list of 39 bytes with their binary representations and counts. The right panel shows report metadata: '2017-09-08 06:58:14 +0000', 'Report Sequence Number: 1', 'Number Of WCMs in Domain: 0', 'Location: 40.4256°, -74.0672°', 'Wave Record Number: 1', and 'Wave Characteristics' with 'Metric' selected. The characteristics include: Height (meters): 0.36, Avg. Height (meters): 0.372, Length (meters): 2.18, Avg. Length (meters): 2.302, Period (seconds): 2.0, and Avg. Period (seconds): 2.1. A 'Statuses' section is also present but empty.

Figure 4-43: Test 20 – Application dashboard screenshot of WCM-Sat 28988088

Figures 4-44 through 4-46 show the time lapse of the skimmer with WCM-Sat being towed from the north end of the tank to the south end over approximately 6 minutes during Test 20.

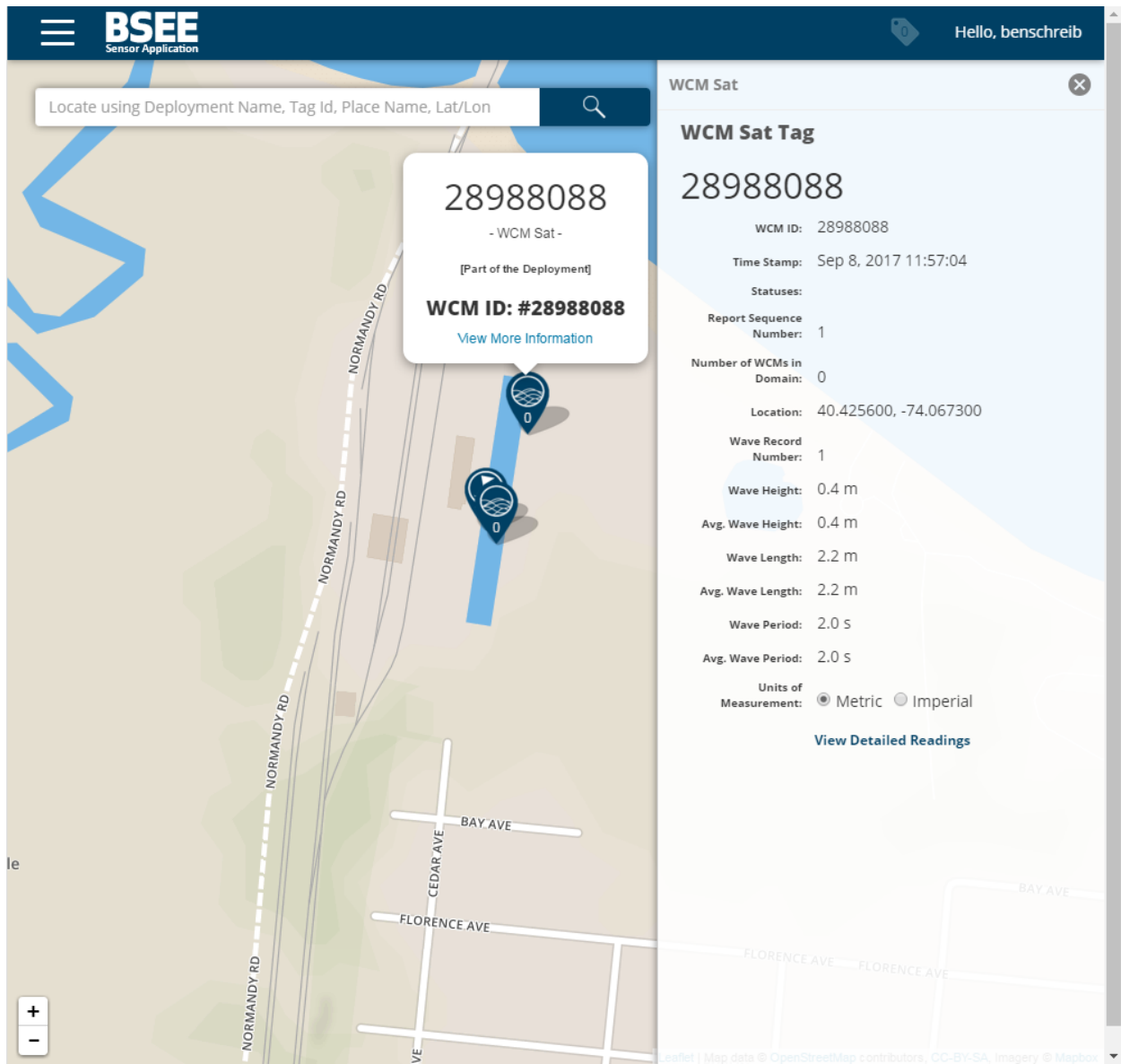


Figure 4-44: Test 20 – GIS user interface screenshot of WCM-Sat 28988088 at the north end of the wave tank

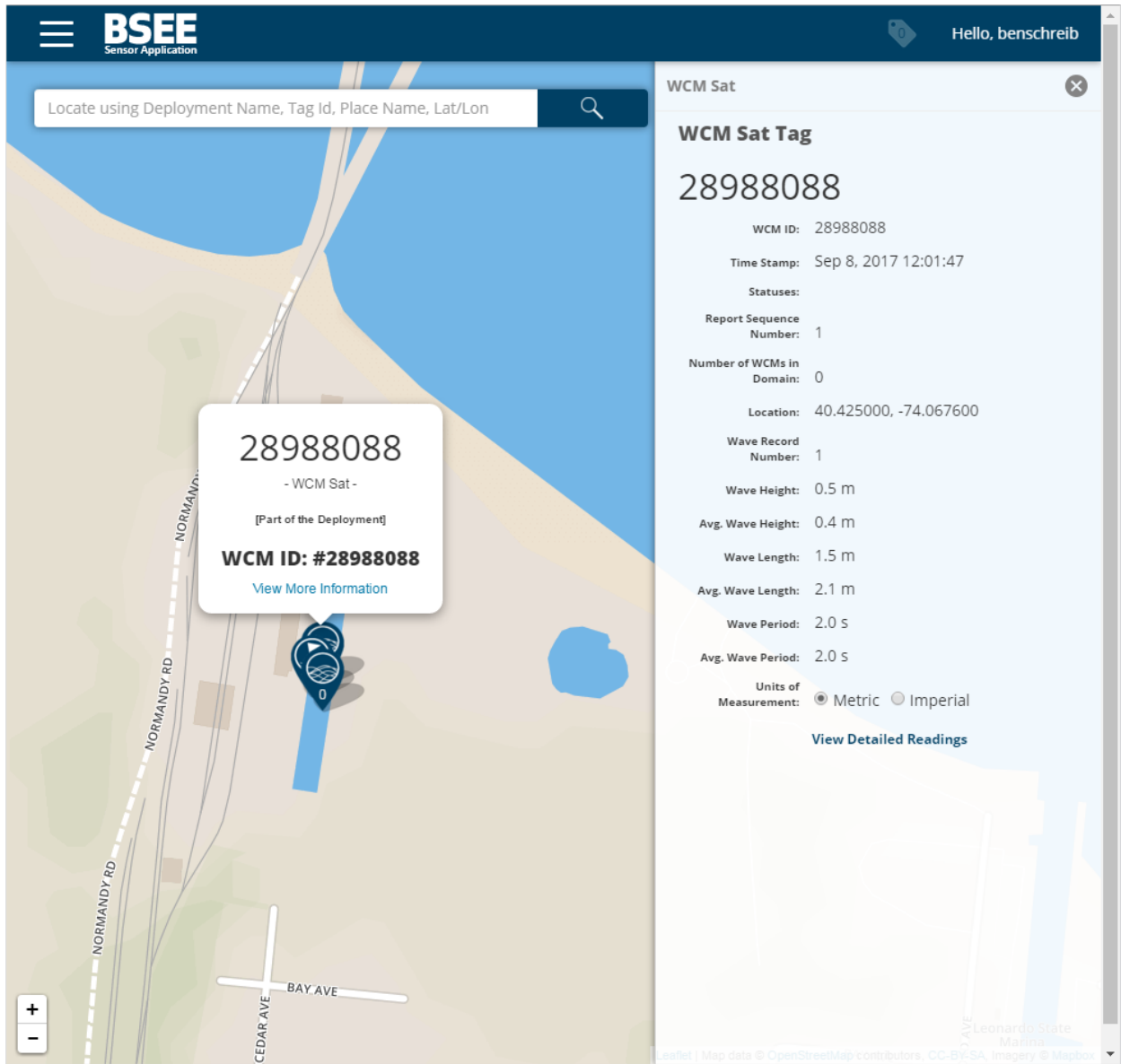


Figure 4-45: Test 20 – GIS user interface screenshot of WCM-Sat 28988088 in the middle of the wave tank

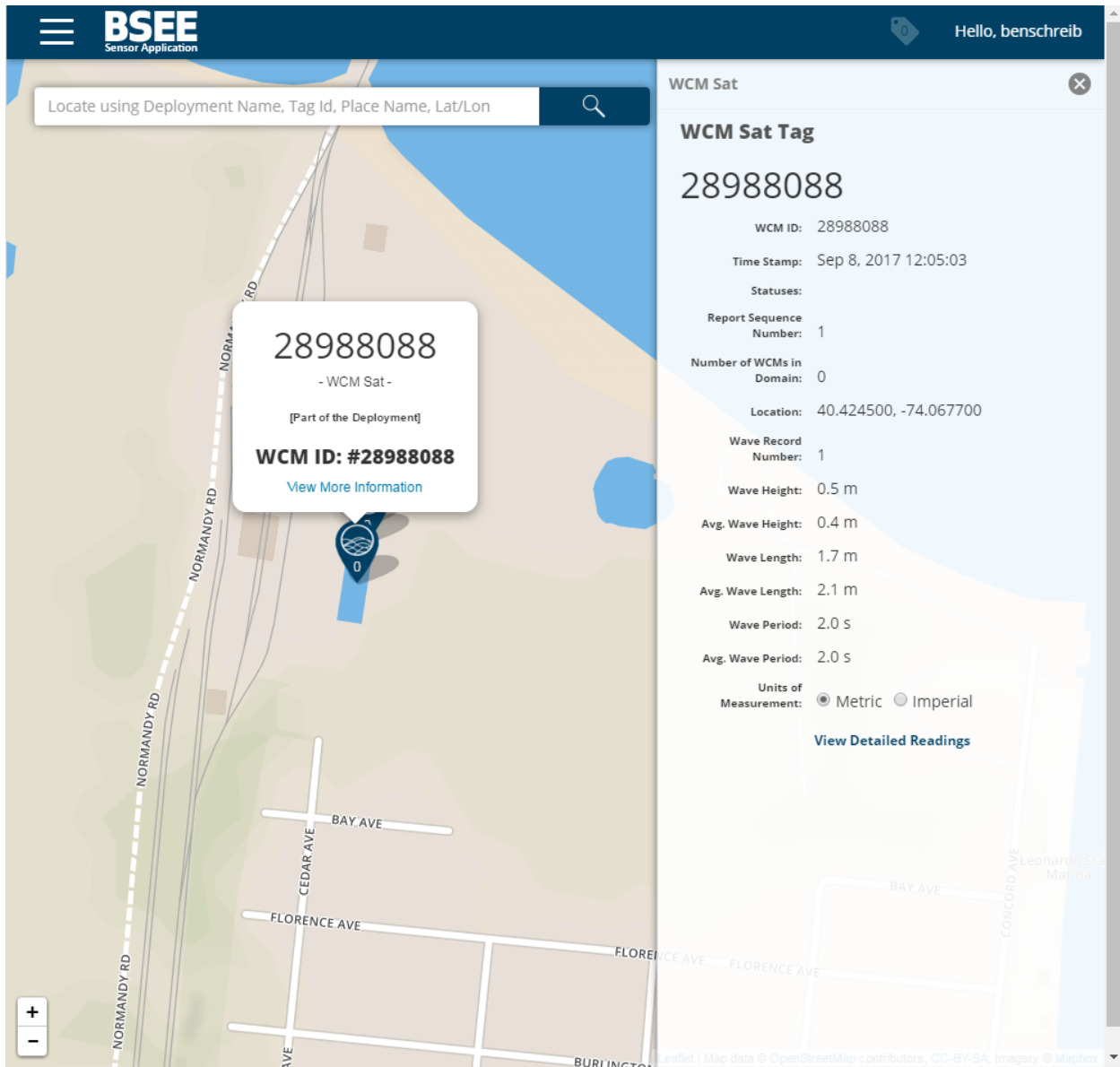


Figure 4-46: Test 20 – GIS user interface screenshot of WCM-Sat 28988088 at the south end of the wave tank

5. Setup, Configuration, Operations, and Training

For setup, configuration, operation, and training user guides, see the following appendices:

- Appendix B: Hardware Setup, Configuration, and Operation
- Appendix C: Local Application Dashboard User Guide
- Appendix D: Remote GIS User Interface User Guide – BSEE Sensor Application

6. Conclusion

Based on the purpose of the project, to develop a system that quantifies local ocean wave characteristics, the AECOM team delivered an assessment of available COTS systems and a technology survey with a trade study of components, software, protocols, and tools that when integrated, met or exceeded the project's goal and performance objectives.

After an analysis and selection of components, software, and protocols a pre-prototype embedded software development platform was fabricated to gather data and develop and refine wave characterization algorithms and unit test ancillary parts of the system while the design of the WCM, WCM-Sat and WCM-Buoy was completed in parallel. Through an iterative process, we adjusted our designs and functionality to meet the flow-down requirements as they evolved from the high-level project goals and system performance objectives. The designs were developed and fabricated into an operational system that included the WCM, WCM-Sat, WCM-Buoy, local wireless application dashboard, and remote GIS user interface.

We successfully developed a system that characterizes ocean waves and accomplishes the performance objectives. We were able to leverage and modify our existing technology with the sensors and software to measure wave characteristics and advance the TRL from 2 to 5. Our testing at Ohmsett showed an accuracy of within 4 inches, including when testing in a variety of wave types and conditions such as oil spray and towing. We showed successful satellite communication of data to the cloud and GIS user interface as well as a user-friendly mobile application for local viewing of wave characteristics for enhanced quantitative situational awareness.

Next steps in the development of a wave characterization system are to enhance a next generation of wave characterization modules and supporting user interfaces. Enhancements would include:

- Bringing in additional metrological data to the user interfaces to create a fully local and quantifiable view of the surrounding weather and environmental conditions,
- By adapting the mesh network and user interfaces to ingest local wind speed and direction, air and water temperature, barometric pressure, and other predictive wave condition data such as wave steepness to help determine skimmer efficiency during recovery operations,
- Enhancing modules through additional testing including offshore operational scenarios,
- Flexible and adaptable time windows for wave data collection,
- Smaller and more energy-efficient packaging, next generation buoy designs,
- Expansion of operating systems such as Android for the local application dashboard; and
- Refinement of the algorithms for additional skimmer types, booms, and other response and recovery equipment.

These enhancements will help provide critical data in real-time to emergency response personnel, mechanical recovery equipment operators and stakeholders to create a more complete and localized common operating picture.

Appendix A: Hardware and Firmware

Hardware Component Descriptions

Device Microcontroller Unit

The NXP LPC11U68JBD48 device microcontroller unit (MCU) interfaces with the other hardware components and communicates to coordinate their activity. The device MCU is the primary control and connection node for sensor data capture and processing components (sensor MCU and inertial measurement unit [IMU]), global positioning system (GPS), and the wireless communication through the long-range mesh, Iridium satellite link, and local WiFi. The device MCU supports configuring the WCM-Sat as a mesh node or gateway. In the mesh node, it aggregates the processed data generated by the sensor MCU, initiates GPS data capture and storage, creates a report database, and transmits through radio frequency (RF) mesh based on its predefined message format. In gateway mode, it aggregates the sensor information from the network-connected mesh nodes, and from its sensor MCU and GPS location, creates a report and then transfers the report via WiFi and through satellite link for the WCM-Sat and WCM-Buoy.

The device MCU has a multitasking environment and implements tasks to generate and send a message format containing wave characterization information to both local and remote user interfaces. These tasks include periodically receiving a GPS fix; handling communications with the RF module and WiFi module; monitoring system status; receiving wave characterization data from the sensor MCU; checking for an Iridium satellite fix; and formatting, packaging, and sending a message to the geographical information system (GIS) user interface and local wireless device application. Firmware and user set parameters will define polling rates for each component and the calibration / conversion coefficients.

The device MCU also has built-in communication ruggedness features such as automatic retries in the case of message transmission failure. The device MCU provides report transmission intervals, RF transmission power, and local communication link/pairing credentials, configured through a Universal Serial Bus (USB) port.

Inertial Measurement Unit

The STMicrosystems LSM6DSL inertial measurement unit (IMU) is a system-in-package containing a 3-axis digital accelerometer and 3-axis digital gyroscope. The unit features 4 Kbyte data buffering and fully configurable event-detection interrupts such as wakeup, activity, and inactivity recognition. The IMU passes its sensor data to the sensor MCU for storage and processing.

Sensor Microcontroller Unit

The NXP MK66FN2M0VLQ18 features an ARM M4 chip running at 180 MHz clock speed with 256 kB of RAM. The sensor MCU sends commands to the IMU chip and transfers and stores raw motion data captured from the IMU for processing. The captured data are processed to generate wave characterization parameters that can be transferred to the device MCU for packaging into a message format sent through the available wireless communication methods to the remote GIS user interface and/or WiFi to the local wireless device application.

Radio Frequency Module

The NXP JN5168-001-M06 RF module is configured as a border router and is the coordinator for the mesh network. It maintains tables of all WCMs joined to its network; passes a message between the device MCU and the other modules in the mesh network, sending network beacons to synchronize mesh

communications; and notifies the device MCU of changes to the network (wave characterization module join and drop). It interfaces with the device MCU over an asynchronous serial interface using an NXP defined protocol and has a digital output signal to wake the device MCU when the module needs to communicate.

The RF module also monitors the battery voltage and passes this information to the device MCU. The RF module computes the battery voltage and compares it to a low threshold to detect low voltage and sets a fault status. The analog converter uses the modules 1.2 V internal voltage reference. The RF module provides a multitasking environment that supports a 6LoWPAN mesh network stack.

When in node mode, the RF module uses network discovery to identify the strongest router signal and the closest WCM, WCM-Sat, or WCM-Buoy gateway to decide which network to join. The network is self-healing; when a module in node mode loses contact with its router to the gateway, it returns to discovery to find a new route or new network to join.

Global Positioning System Module

The GPS module is powered on during the server update cycle. The time to the first fix is expected to take 30 to 90 seconds. After receiving a stable fix, the device MCU powers down the GPS and adds the coordinates to the message.

WiFi Module

The Espressif ESP8266 is the local wireless communication module using the WiFi protocol. This module provides competitive performance specifications at a relatively low cost. The WCM, WCM-Sat, and WCM-Buoy when in gateway mode send formatted messages to the local wireless module via SPI to transmit to a WiFi-connected tablet for display on the application dashboard.

Satellite Modem

The Iridium 9603 satellite modem is used for communications with the cloud server and GIS user interface, periodically sending wave characterization messages. The satellite modem operates in the frequency range of 1616 to 1626.5 MHz and implements the short burst data (SBD) protocol with a message payload size of 340 bytes.

Firmware Descriptions

Firmware on the WCM, WCM-Sat, and WCM-Buoy makes it possible for a user to configure the device in gateway or node mode, as described in Section 2. The firmware defines operation of the mesh networking communication and external reporting through the WiFi module and satellite modem. WCM, WCM-Sat, and WCM-Buoy firmware implements the mesh networking communication protocol, power management functions, sensor MCU coordination, GPS fix, WiFi, and satellite communications.

Device Microcontroller Unit

The device MCU sleeps most of the time but wakes up to process messages from the mesh RF module, store sensor MCU readings, and process periodic local communication via the WiFi module. The server update cycle is when the device MCU gathers the information needed to create the WCM gateway or node report messages containing wave characterization data and includes checking system status and waiting for a GPS fix.

The protocol steps are as follows:

- Device MCU handling of messages from the mesh RF module:
 - Receives WCM node report messages and updates information in the WCM table

- Receives join / drop notifications and updates WCM table
- Receives battery level and updates WCM status

The sensing and signal processing software and firmware for wave characterization are programmed into the sensor MCU. The device MCU powers up and then communicates with the sensor MCU through a serial asynchronous interface. The device MCU receives the wave characterization data from the sensor MCU firmware through the communication interface in a predefined message format. The proper message handling and integration of the message reporting are handled by the device MCU.

- Device MCU communicates with sensor MCU:
 - Stores wave characterization data from the sensor MCU
 - Provides an interface to change configuration settings of the sensor MCU
 - Device MCU accepts a change in default configurations to the IMU, sensor MCU, and device MCU through USB. To change the configuration parameters, a request parameter is sent by the device MCU, and the report parameter is sent by the sensor MCU. After a write or read command, the sensor MCU reports the final value of the parameter requested to be changed and result code of the transaction through the report parameter. The messages are created when the sensor MCU is in maintenance mode.
- For each update cycle, the device MCU performs the following operations:
 1. Power on sensor MCU and wait for wave characterization data, then power off sensor MCU
 2. Power on GPS and wait for a stable fix, then power off GPS
 3. Generate WCM report messages (gateway or node report)
 4. Power on Iridium modem (only for WCM-Sat and WCM-Buoy)
 - a. Wait for satellite to be detected
 - b. Connect to satellite and open channel for communications
 - c. Send WCM report using short burst data protocol
 - d. Wait for packet acknowledgment
 - e. Power down Iridium modem
 5. Sleep until the next update cycle or message from RF module
- Device MCU to WiFi module:
 1. Device MCU switches on WiFi module after update cycle is complete
 2. Device MCU configures WiFi module with the required configuration to setup a valid network
 3. Device MCU looks for any connected devices within a specified amount of time
 4. If devices are found, WCM establishes a Transmission Control Protocol/Internet Protocol (TCP/IP) connection to transmit WCM gateway report message with wave characterization data
 5. Powers down WiFi module

Sensor Microcontroller Unit

The firmware includes drivers for capturing sensor data from the LSM6DSLTR IMU.

1. Sensor MCU is in sleep mode

2. IMU raises a general-purpose input/output (GPIO) output line high into an interrupt input on sensor MCU
3. Sensor MCU wakes on the interrupt and sets a GPIO output high to notify ready for data (has serial line open)
4. IMU opens serial line and outputs raw data with the following parameters for all records in the IMU first-in first-out (FIFO) memory
 - Linear acceleration x
 - Linear acceleration y
 - Linear acceleration z
 - Rate-of-rotation x
 - Rate-of-rotation y
 - Rate of rotation z
5. Sensor MCU reads the message and sets GPIO output back to low to notify read complete
6. IMU closes serial port
7. This process is repeated until the amount of data transferred or timing conditions are met to trigger the wave characterization algorithms

The sensor MCU firmware then initializes the wave characterization algorithms:

1. Use transferred IMU data to calculate the wave characterization parameters for the given time period
2. Generate device MCU and sensor MCU inter-processor message format
3. Sensor MCU goes back to sleep mode based on its other tasks and the scheduled timings

RF Mesh Functions

The RF module has the following functions for mesh communications:

- Network stack functions
 - 802.15.4 medium access control (MAC) layer
 - Network joining
 - Point-to-point communications
 - User datagram protocol (UDP), Internet protocol (IP), and Internet control message protocol
 - Send network announcements for network discovery
 - Send network beacon polls to sync communication windows of network
 - 6LoWPAN layer for configured as a border router
 - Maintain routing tables and neighbor lists
 - Maintain table of all nodes joined to the network
- Functions when in gateway mode
 - Initialize and configure network stack
 - In deployed (active) state

- Pass to device MCU notifications of wave characterization modules in mesh node mode joining the network
- Pass to device MCU notifications of wave characterization modules in mesh node mode dropping from the network
- Pass to device MCU all UDP packets (wave characterization reports) received from the network.
 - To maintain timing and network connection, a payload of UDP packets is sent over the mesh network. UDP packet format and mesh protocol have routing and cyclic redundancy check fields and are not duplicated in payload fields. Most communications on the mesh network are these beacon messages.
- Send over network all UDP packets (e.g., parameter get / set) received from device MCU
- Process command messages from device MCU for WCM-Sat functions (e.g., read battery voltage)
- Send notifications to device MCU of motion detect
- Functions when in mesh node mode
 - Act as a router node to pass wave characterization messages to the nearest mesh node or gateway

Local Wireless Module

- Network stack functions for WiFi:
 - 802.11 MAC layer
 - Network joining
 - Point-to-point communications
 - TCP/IP protocol
- Functions when in gateway mode:
 1. Initialize and configure network stack.
 2. Power on local wireless module based on trigger from device MCU (after IMU, sensor MCU, and RF functions have been completed).
 3. In deployed (active) state:
 - a. Check to see if any device is connected or if any device is actively listening at the specified port number. If so, proceed with the next steps. If not, wait a predetermined amount of time for a connection and then power off.
 - b. Send over network wave characterization message formats received from device MCU.
 - c. Wait for confirmation from wireless device, resend twice if message send failed.
 - d. Device MCU powers off local wireless module.

Time Synchronization

The WCMs when in gateway mode use the GPS Coordinated Universal Time (UTC) to set and maintain their real-time clocks, which is GPS time plus the correction for leap seconds. A WCM timestamps incoming node WCM messages when received and adds the current UTC time to sync beacons, which

allows node WCMs to maintain their real-time clock (RTC). Therefore, network-wide RTC time is accurate to approximately 1 second.

Firmware Segment for Controlling Iridium Modem Module

The device MCU communicates with the satellite modem over an asynchronous serial interface. Control of the modem uses attention (AT) commands. Data packets are sent as SBD messages to the Iridium network. The Iridium gateway sends the messages to the cloud server and GIS interface as mobile-originated directIP transfers.

The payload for SBD messages is 340 bytes, which allows sending a gateway report message with 8-wave characterization modules in a single packet. If a mesh network has more than eight joined nodes, the satellite gateway report message is sent as a multi-block message that can be interpreted by the GIS user interface.

Appendix B: Hardware Setup, Configuration, and Operation

Setup

Before using the WCM system, the user activates the satellite data service plan on the WCM-Sat units through an authorized service provider. The modem number (International Mobile Equipment Identity [IMEI]) is noted on the tag cover. The satellite data are routed to the pre-defined cloud infrastructure server IP address and port number.

Startup

When the battery needs to be installed or replaced in a WCM or WCM-Sat, the cover is removed to expose the battery compartment. The cover is secured with four screws in the back as shown in Figure B-1. Three D size lithium/thionyl chloride batteries are inserted into the holder as shown in Figure B-2. Once the batteries are installed as shown in Figure B-3 and the cover is fastened again, the device will start functioning autonomously; the device does not have an external power button. IDs are assigned as factory default and are imported into the cloud infrastructure database as part of the standard node messages.

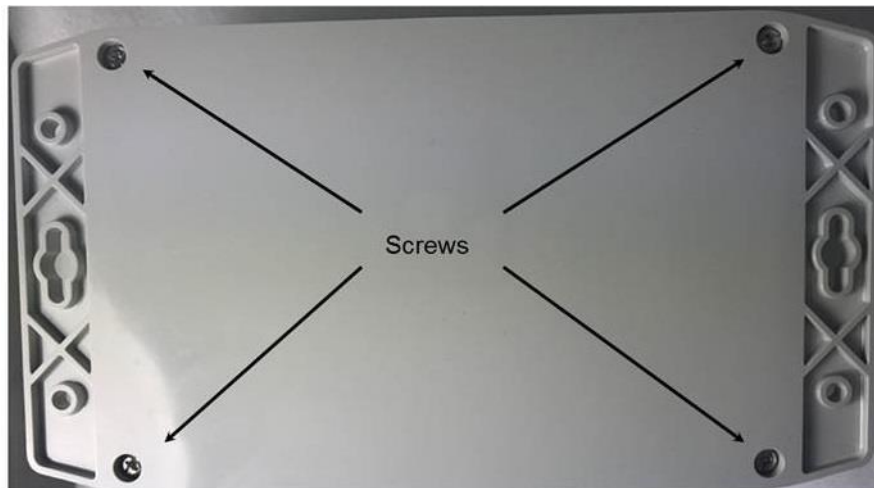


Figure B-1: Back of WCM/WCM-Sat showing four screws to access the battery compartment

Equip GRID and GRIDSAT Tags with Accelerometers to Measure Ocean Waves



Figure B-2: USB port and battery holder



Figure B-3: Installed WCM-Sat batteries

The recommended mounting position and orientation of the WCM and WCM-Sat tags are shown in Figure B-4. This position promotes the best communication because of internal global positioning system (GPS) and satellite antenna placement.



Figure B-4: Recommended WCM-Sat tag mounting position and orientation

Configuration

Modes of Operation

The tags operate in four modes:

1. **Active mode.** WCM devices operate in active mode during deployment. All devices can calculate wave statistics. A device configured as a node calculates wave statistics and participates in a mesh network communicating its data through a device configured as a gateway. A device configured as a gateway calculates wave statistics, acts as a network coordinator and host to send sync beacons such that nodes in the mesh network can identify, connect, and send their respective wave statistics and GPS location periodically and send node reports through a satellite or WiFi connection. Any device can be configured to act as a node or gateway. WCM, WCM-Sat, and WCM-Buoy default in gateway mode. To configure as a node, the WCM device is started via maintenance mode (see #2) and use command N (shown below in Table B-1).
2. **Maintenance mode (MM).** MM can be initiated by connecting a USB cable to an opened WCM device (USB Type A Male to USB Type A Male cable required). In this mode, the configuration parameters on the nodes can be retrieved and set using a command-line interface displayed on a terminal emulator (such as Tera Term) as shown for the WCM in Figure B-5 and WCM-Sat in Figure B-6.

- a. Plug in the USB cable
- b. Insert the batteries
- c. Deploy Tera Term on the computer
- d. Hit return to start
- e. Enter ? and return to see menu
- f. Start entering commands

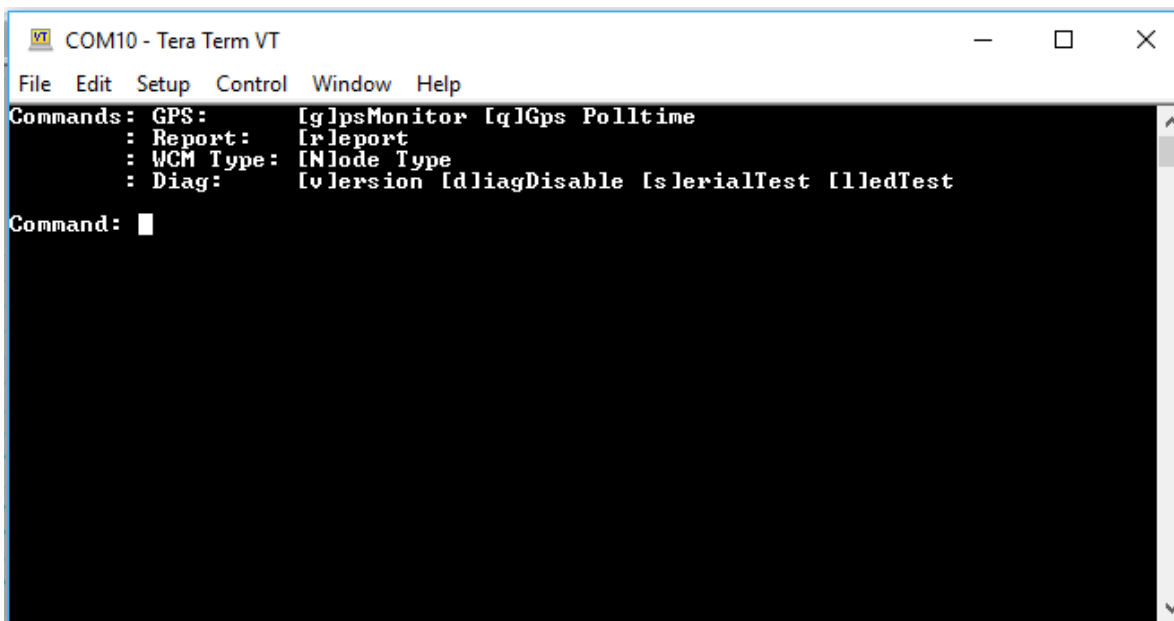


Figure B-5: Tera Term command line interface to configure a WCM

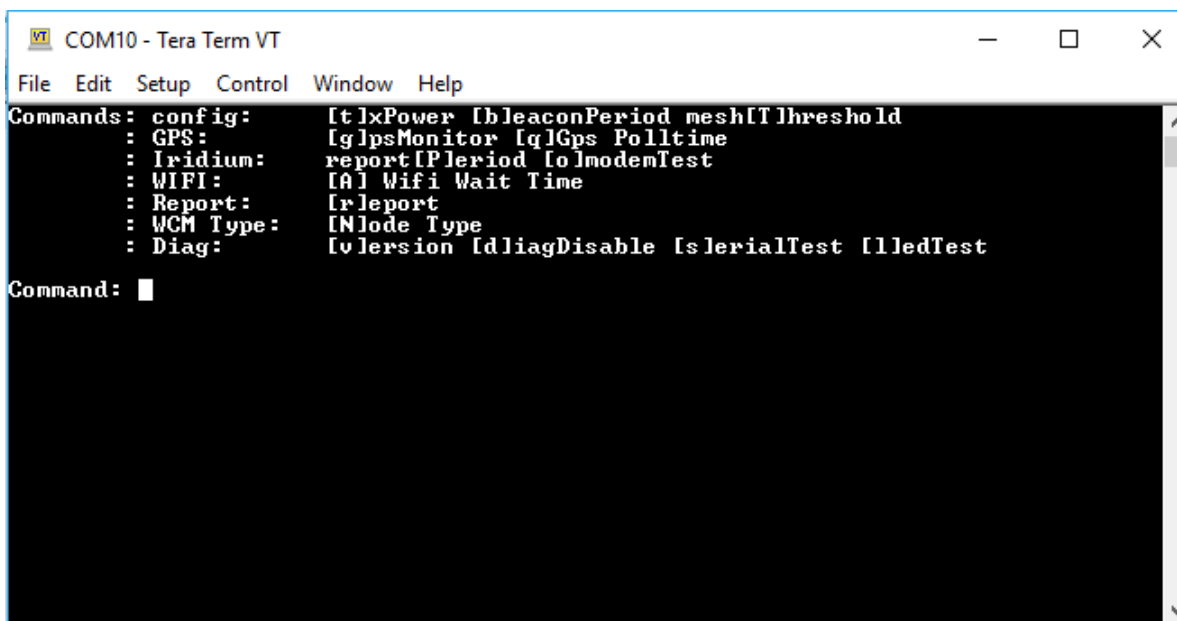


Figure B-6: Tera Term command line interface to configure a WCM-Sat or WCM-Buoy

To disconnect and power down from MM:

1. Enter option d[iagDisable] in Tera Term.
2. Go to Tera Term File tab, hit disconnect, or close Tera Term.
3. Disconnect the USB cable.
4. If the WCM device is to remain deployed, keep batteries in and attach cover. The settings will be retained.
5. If the WCM device is to be powered down, remove WCM device batteries. The settings will be lost and will return to default values when powered on again.

Configuration Parameters

Gateway configuration parameters, node configuration parameters, and default parameter values are presented in Tables B-1 through B-3.

Table B-1: Gateway Configuration Parameters

Command	Description	Parameter
b	Beacon Period: Defines the beacon rate of the network associated with the Gateway module in seconds	Valid range: 1 – 600 Time in seconds
T (shift t)	Mesh Threshold: Sets the Link Quality Indicator (LQI) parameter threshold for rebroadcast of beacons. If a module receives a beacon in the network with its LQI below this threshold, the module rebroadcasts the beacon. Setting a value 0 disables this feature	Valid range: 0 – 255 counts 0 disables rebroadcast feature
P (shift p)	Iridium Report Period: Sets the WCM-Sat or WCM-Buoy automatic reporting period.	Valid range : 0 – 3e5 minutes Time in minutes 0 disables the automatic reporting to manual
g	GPS Monitor: Monitor GPS and get a location fix	N/A
q	GPS Polltime: Sets the maximum time GPS module will look for a fix	Valid range: 0 – 3e5 seconds 0 – disables, no fix
A	WiFi Wait Time: Sets time for which WiFi network switches on and looks for a device to connect before switching off.	Valid range: 0 – 3e5 minutes 0 – disables
N	Node type: Sets function of device	103 – node mode 104 – gateway mode
r	Starts a reporting sequence in manual mode (when P=0)	N/A
D	Enable debug output	N/A
d	Disable maintenance	N/A
V	Version	N/A
S	Serial test	N/A
L	Led test	N/A

N/A = not applicable

Table B-2: Node Configuration Parameters

Command	Description	Parameter
P (shift p)	Report Period: Sets the WCM automatic reporting period to collect sensor data	Valid range : 0 – 3e5 minutes Time in minutes 0 disables the automatic reporting to manual
g	GPS Monitor: Monitor GPS and get a location Fix	N/A
q	GPS Polltime: Sets the maximum time GPS module will look for a fix	Valid Range: 0 – 3e5 seconds 0 – disables, no fix
N	Node type: Sets type of device	103 – node mode 104 – gateway mode
r	Starts a WCM node report in manual mode (when P=0)	N/A
D	Enable debug output	N/A
d	Disable maintenance	N/A
V	Version	N/A
S	Serial test	N/A
L	Led test	N/A

N/A = not applicable

Default Configuration Parameters

Table B-3 is a list of the default configuration parameters for the devices. These are the values that are loaded when the system is powered on. Resetting the power (through removing the batteries) resets all configured values to their default.

Table B-3: WCM-Sat and WCM-Buoy Default Parameter Values

Description	Default Value
Tx Power	Setting 6 (13 dBm)
Beacon Period	60 sec
Mesh Threshold	60 sec
Iridium Report Period	6 min
GPS Poll Time	180 sec
WiFi Wait Time	90 sec

dBm = decibel-milliwatts
min = minutes
sec = seconds
Tx = Transmit

Understanding report periods:

- Time taken to finish a report is variable, which is subject to availability of GPS satellites, Iridium satellites, and WiFi devices. Hence, a sample calculation is presented below with default parameters to highlight the effects of changing report parameters.
- WCM-Sat at the end of 6 mins (Iridium report period) starts the following process:

Case 1

Time taken to calculate wave data	2 min
Time to get a GPS fix (maximum no fix)	3 min
Time to transmit data over WiFi (maximum, no devices)	1.5 min
Time to transmit data over satellite (maximum, no satellite)	1 min
Total.....	7.5 min

Because our report period is 6 minutes, WCM-Sat will attempt to generate the next report after 13.5 minutes from last report.

Case 2

Time taken to calculate wave data	2 min
Time to get a GPS fix (fix good availability of GPS satellites)	1 min
Time to transmit data over WiFi (device available)	0.5 min
Time to transmit data over satellite (satellites available)	0.5 min
Total.....	4.5 min

Because our report period is 6 minutes, WCM-Sat will attempt to generate the next report after 10 minutes from the last report.

Safe Disposal

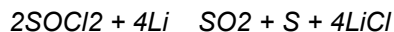
The Wave Characterization Modules consist of the electronics and the replaceable battery. The following are guidelines for safe disposal of WCMs.

- **Electronics** – The modules contain lead-free and Restriction of Hazardous Substances (RoHS)-compliant components. Their disposal follows the general small electronic items disposal best practices and regulatory guidelines.
- **Battery** – The devices use lithium/thionyl chloride battery cells.

The lithium/thionyl chloride battery cells do not contain malicious or hardly decomposable pollutants such as heavy metals or organic solvents, which have lasting toxic environmental effects. The batteries are free of mercury, lead, manganese, and cadmium.

Lithium thionyl chloride batteries are not listed or exempted from U.S. Environmental Protection Agency hazardous waste regulations, as conveyed by the Resources Conservation and Recovery Act. The only metal of possible concern in the cell is the lithium metal, which is not listed or characterized as a toxic hazardous waste. The battery is also small, reducing its waste. Still, recycling or properly disposing of the batteries is advised to be based on broad environment best practices and Federal, regional, and international (where applicable) regulations.

The discharge reaction of the lithium/thionyl chloride battery cells is described by the following formula:



where:

- SOCI₂ = thionyl chloride
- Li = lithium
- SO₂ = sulfur dioxide
- S = sulfur
- LiCl = lithium chloride

The thionyl chloride present in fresh cells is converted into lithium chloride during discharge. Some amounts of sulfur and sulfur dioxide are also formed. Generally, in fully discharged cells, 90 to 95 percent of the thionyl chloride reacts in accordance with the above formula.

When lithium/thionyl chloride cells are disposed of in an open landfill, they eventually discharge and may open from corrosion of the can. In this case, the residual thionyl chloride will react with moisture to form sulfur dioxide and hydrogen chloride.



where:

SOCl₂ = thionyl chloride

H₂O = water

SO₂ = sulfur dioxide

HCl = hydrogen chloride

The remaining cell components include the carbon cathode, lithium chloride, aluminum chloride, metallic can, cover, and current collector. Metallic lithium is almost completely consumed in a fully discharged cell.

There is no long-lasting contamination from the disposal of lithium/thionyl chloride cells. The only hazards are associated with the neutralization and disposal processes. Once batteries are neutralized, the end products of deactivated batteries are not toxic (Tadiran Batteries, 2008).

Appendix C: Local Application Dashboard User Guide

Setting Up

- iPad
 - An iPad is required to run the local application dashboard.
 - An iPad model iPad 2 or later is recommended.
 - An iPad operating system version of 10.3.1 or later is recommended.
 - If you wish to export your data via a comma-separated values (CSV) file in the application, you are **required** to set up an email account in the Apple Mail application on your iPad. This account in the Mail application will be the default sender when exporting a CSV of the wave data.
- Disconnecting from all WiFi
 - It is required that you disconnect from all reachable and previously accessed WiFi before running this application.
 - According to the Apple Documentation on iPad WiFi, “known networks will be joined automatically. If no known networks are available, you will have to manually select a network.”
 - Your iPad will automatically connect to known (previously accessed) WiFi networks.
 1. Go to the Settings application on your iPad.
 2. In the settings application, select the “WiFi” option on the left-oriented vertical settings panel (Figure C-1).
 3. Your iPad will automatically connect to known and nearby WiFi networks. You can see whether you are connected to WiFi and identify the WiFi you are connected to by looking for a blue checkmark next to the name of a WiFi on the right-oriented panel (Figure C-1).
 - a. If there are no known networks nearby and your iPad does not automatically connect to a network, skip the following instructions and move to the “Connect to Module WiFi” section.
 - b. If your iPad connects to a WiFi network, select the blue information button next to the connected WiFi.

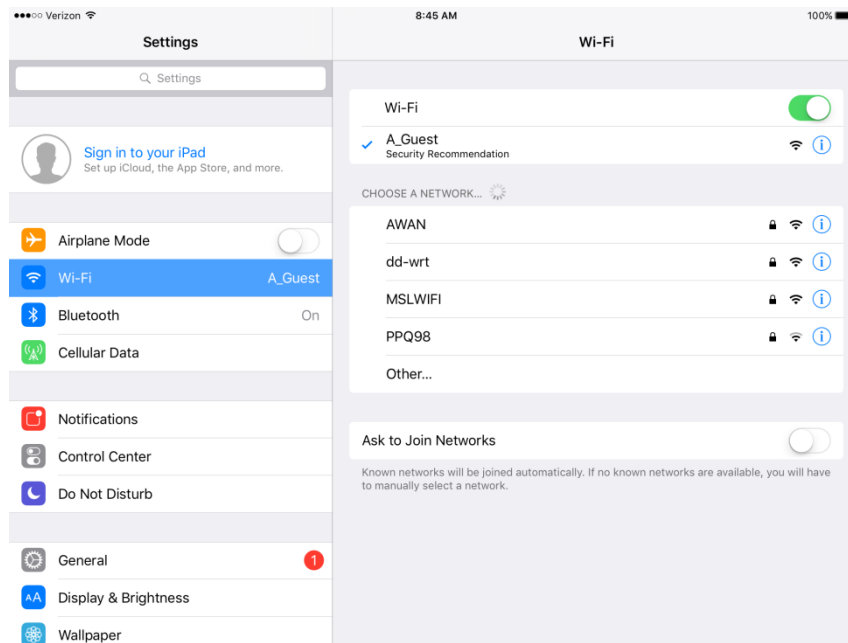


Figure C-1

4. You will be brought to the WiFi information screen pertaining to the WiFi you selected (Figure C-2).

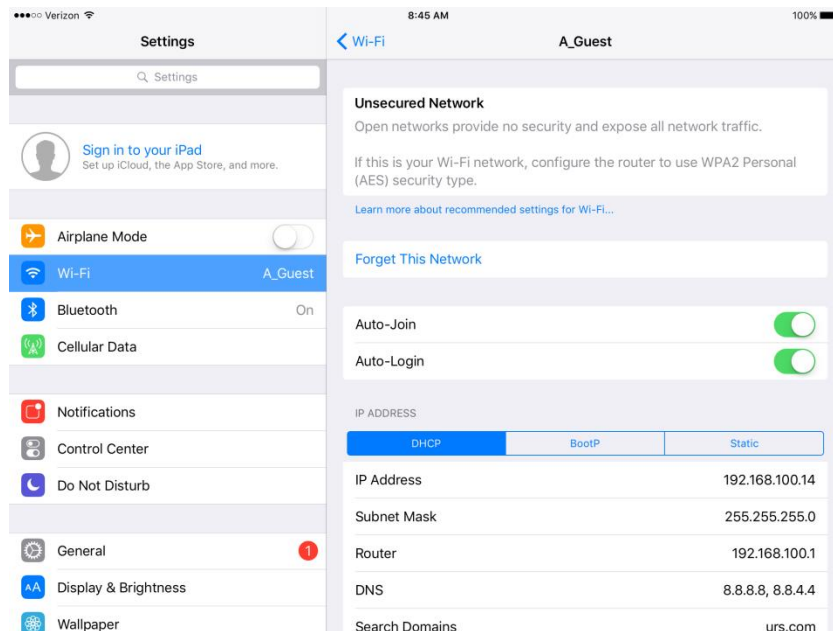


Figure C-2

5. Select the button “Forget This Network.” You will be prompted to confirm whether or not you want to forget the WiFi network. Select “Forget” (Figure C-3).

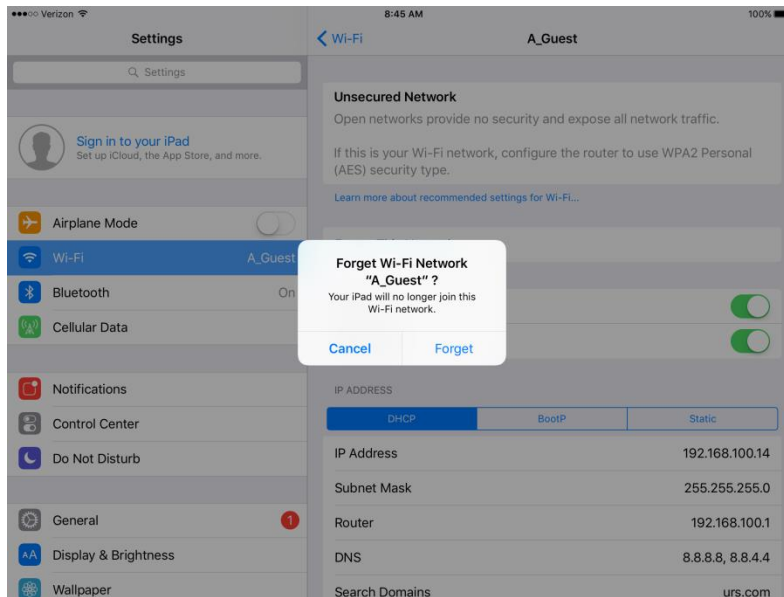


Figure C-3

6. You will be taken back to the WiFi page of the Settings application. Wait 15 seconds to allow your iPad to try to connect to other known networks.
7. Continue Steps 3-6 until your iPad no longer connects to any nearby and known WiFi networks (Figure C-4).

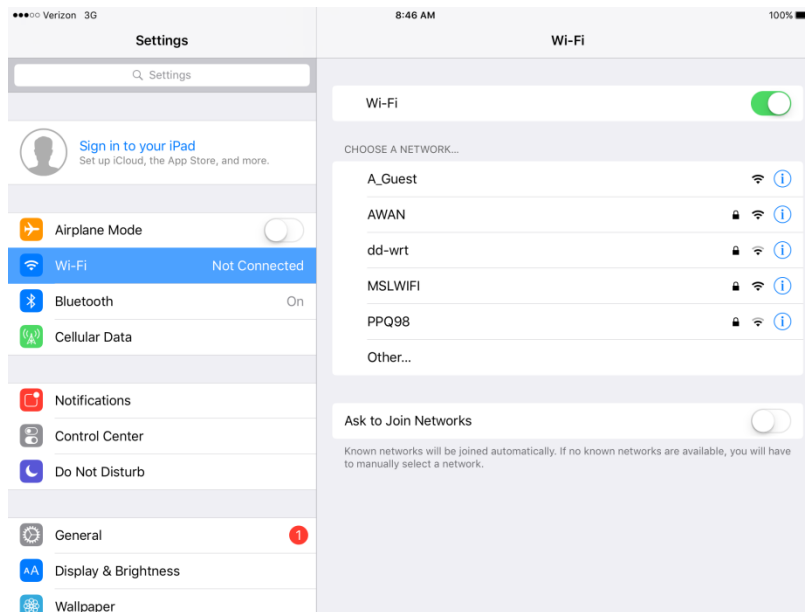


Figure C-4

- Connect to Module WiFi
 1. Go to the Settings application on your iPad.
 2. In the settings application, select the "WiFi" option on the left-oriented vertical settings panel (Figure C-5).

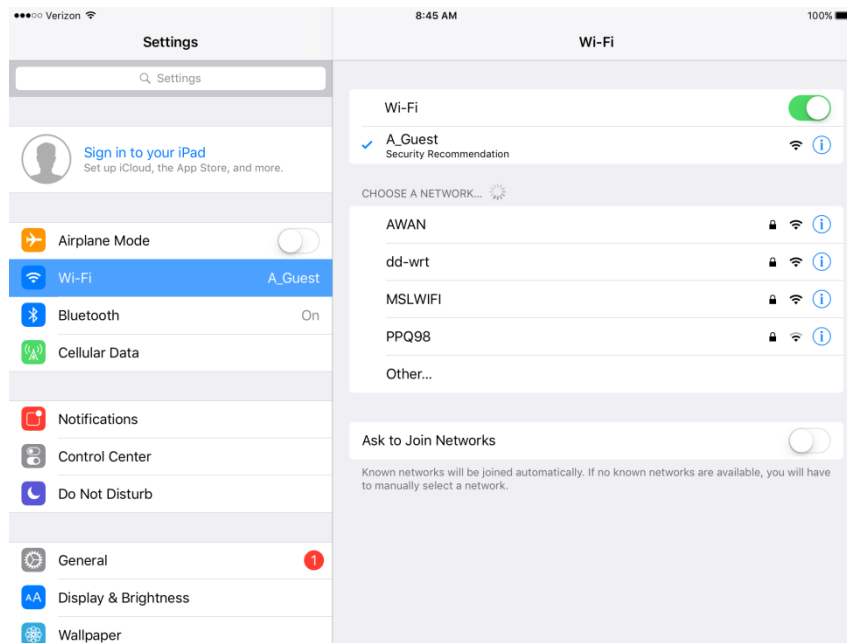


Figure C-5

3. Select the WCM Module WiFi from the listed available WiFi networks.
 - a. Note: WCM Module WiFi networks cycle on and off to preserve power in the Module. You may wait between 2 and 10 minutes, based on WCM WiFi configuration, on the settings screen before seeing a signal from the module. Since the WiFi page of the Settings application automatically refreshes the list of available WiFi networks, it is required that you stay on the WiFi page of the Settings Application during this process.
4. You will be prompted to enter the password for the WiFi network. Enter the password and select “Enter.”
5. You can confirm that you are connected to a WiFi network by looking for a blue checkmark next to the name of a WiFi on the right-oriented panel (Figure C-6).

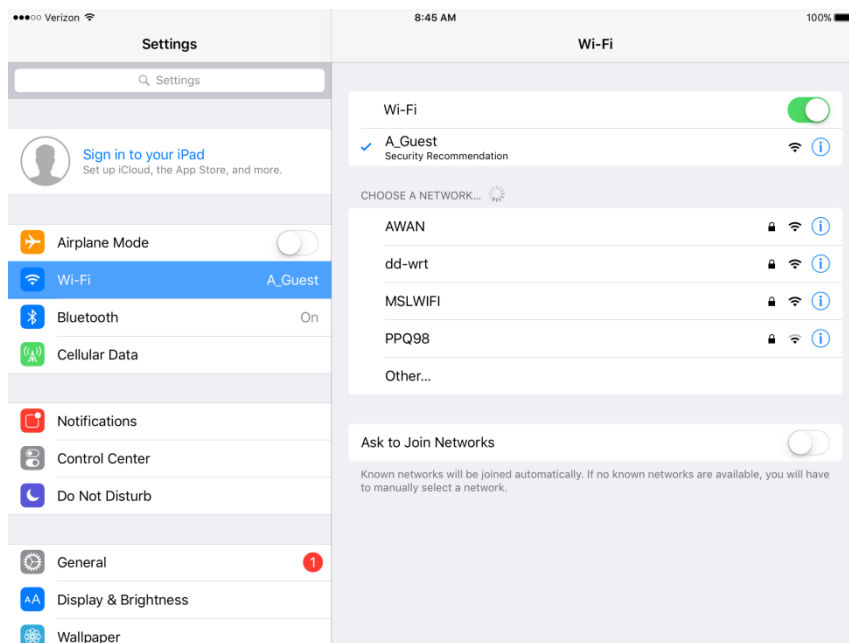


Figure C-6

- Using the application
 1. Once you are connected to the WCM WiFi on the Settings screen, launch the application by tapping the WCM mobile application icon (Figure C-7).



Figure C-7

2. Once you are inside the application, the application will automatically update when the WiFi is connected and a message is received.
 - When the WiFi signal is active, you can expect to receive data from the module within 2 minutes of the iPad connecting to the WiFi.
 - If the iPad is connected to the WCM WiFi but is not receiving applications, do the following:
 - Close the application.
 - Go to the Settings application.
 - Confirm that you are connected to the WCM WiFi.
 - Once you are connected to the WiFi on the Settings application, you may reopen the WCM mobile application.

3. After a message is successfully sent from the WCM to the iPad, the WCM WiFi component will shut down as the WCM records data. At this point, your iPad will disconnect from the WiFi network.
4. The WCM WiFi will cycle back on within 2 to 10 minutes based on the WCM's configuration.
5. Since iPads automatically connect to known networks, the iPad will automatically reconnect to the WCM WiFi.
 - If you think the iPad is taking too long to reconnect or is not reconnecting:
 - Close the application.
 - Go to the Settings application.
 - Wait until the WiFi signal is active.
 - Confirm that you are connected the WCM WiFi.
 - Once you are connected to the WiFi on the Settings application, reopen the WCM mobile application.

About the Application

- The Bureau of Safety and Environmental Enforcement (BSEE) WCM Mobile Application serves a purpose of connecting to WCM WiFi networks that stream wave characteristics. The wave characteristics, as well as a report from the modules, are displayed for analysis.
- Functionality breakdown
 1. Top-Oriented Horizontal Navigation Bar (Figure C-8)

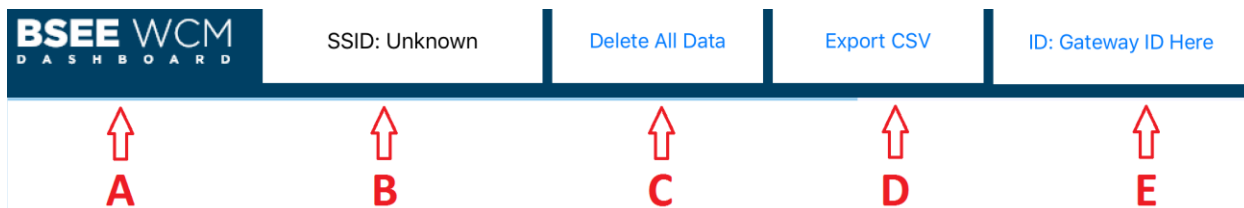


Figure C-8

- The top navigation bar presents information and menu options that affect the local application dashboard.
- BSEE WCM Dashboard Logo (“A” in Figure C)
- SSID (“B” in Figure C-8)
 - The SSID text shows the WiFi network name of the module from which the last WCM node report was sent.
- Delete All Data (“C” in Figure C-8)
 - Every WCM report that you receive is stored on your iPad, and its data are used to calculate characteristics.
 - This buttons function is to delete all of the WCM report data that are stored on the iPad.

- When the button is pressed, you will be prompted with a confirmation message asking if you are sure you want to delete all data. Press “Cancel” to cancel. Press “Yes” to delete all of the data stored on the iPad.
- Export CSV (“D” in Figure C-8)
 - Every WCM report that you receive is stored on your iPad, and its data are used to display wave characteristics within the application.
 - This button’s function is to package the WCM report data into a CSV file and attach that file in an email.
 - When this button is pressed, you will be taken to an Apple Email modal view over this application. The CSV file will be attached. Add the recipients to the email. Press “Send” to send the CSV file to the entered email addresses. Press “Cancel” to cancel the sending of the file.
 - You will have no Internet connection when connected to the WCM WiFi network. In order to export the CSV, you need to connect to a WiFi that offers an Internet connection.
 - Important: After connecting to a different WiFi in order to export the CSV, you MUST disconnect from that WiFi and forget that network.
 - Also note that the emails can be queued until an Internet signal is available, so do not “Delete All Data” until you have confirmation that the email was sent.
- ID (“E” in Figure C-8)
 - This button displays the WCM ID of the WCM report you are viewing.
 - Pressing this button prompts the user with a menu displaying all of the WCM IDs contained in the most recent WCM report.
 - Selecting one of these IDs will display the information gathered from that WCM on the application.

2. Right-Oriented Vertical Information Panel

- The information panel on the right side displays information and characteristics from the most recent report from the WCM selected on the ID field (“E” in Figure C-8) of the right side of the navigation bar. The Right-Oriented Vertical Information Panel changes based on whether you are viewing a Gateway Report or a Node Report.

- Gateway Report (Figure C-9)

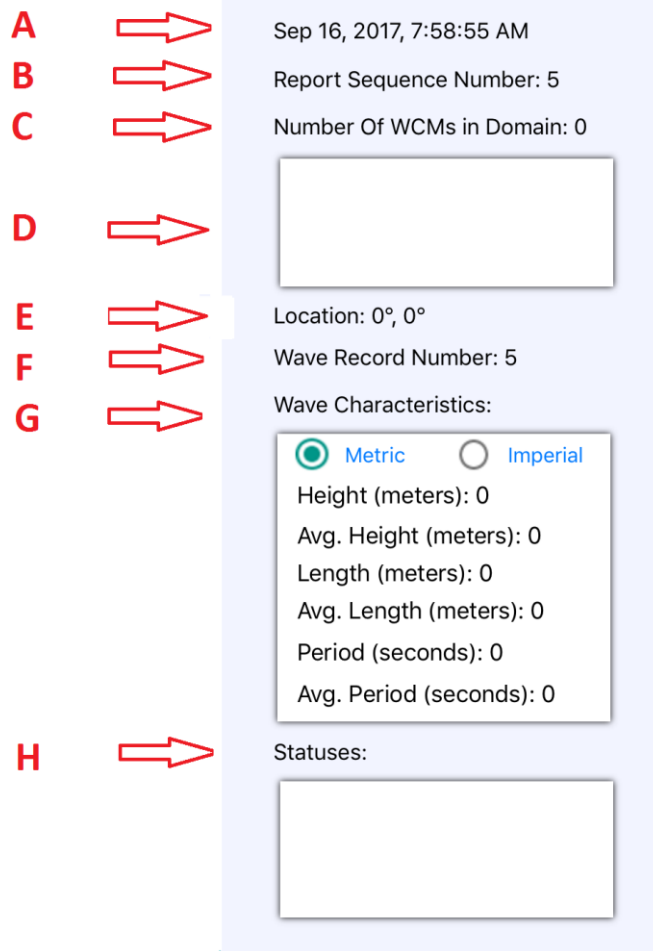


Figure C-9

- Timestamp (“A” in Figure C-9)
 - Displays the time the WCM message was received.
- Report Sequence Number (“B” in Figure C-9)
 - Displays the sequence number of the selected report.
- Number of WCMs in Domain (“C” in Figure C-9)
 - A count of the WCMs in the most recent Gateway Report.
 - Number of WCMs in Domain Text Area (“D” in Figure C-9)
 - Displays the WCM IDs in the most recent Gateway Report.
- Location (“E” in Figure C-9)
 - Latitude and longitude of the most recent Gateway Report
- Wave Record Number (“F” in Figure C-9)
- Wave Characteristics (“G” in Figure C-9)

- The text area for Wave Characteristics displays measurements in both metric and imperial units. To switch between measurement systems, select the desired system in the text area (“A+B” in Figure C-11).
- Characteristics
 - Height (“C” in Figure C-11): Height sent from the most recent report from the selected ID.
 - Average Height (“D” in Figure C-11): Average height of the 10 most recent reports from the selected ID.
 - Length (“E” in Figure C-11): Length sent from the most recent report from the selected ID.
 - Average Length (“F” in Figure C-11): Average length of the 10 most recent reports from the selected ID.
 - Period (“G” in Figure C-11): Period sent from the most recent report from the selected ID.
 - Average Period (“H” in Figure C-11): Average period of the 10 most recent reports from the selected ID.
- Statuses (“H” in Figure C-9)
 - The Status text area displays the statuses received from the selected report.
 - Status types
 - Status OK
 - Battery Low
 - GPS Fault
 - No GPS Fix
 - RF Module
 - WiFi Comm Fault
 - WiFi Socket Connection Refused
 - WiFi Busy

- Node Reports (Figure C-10)

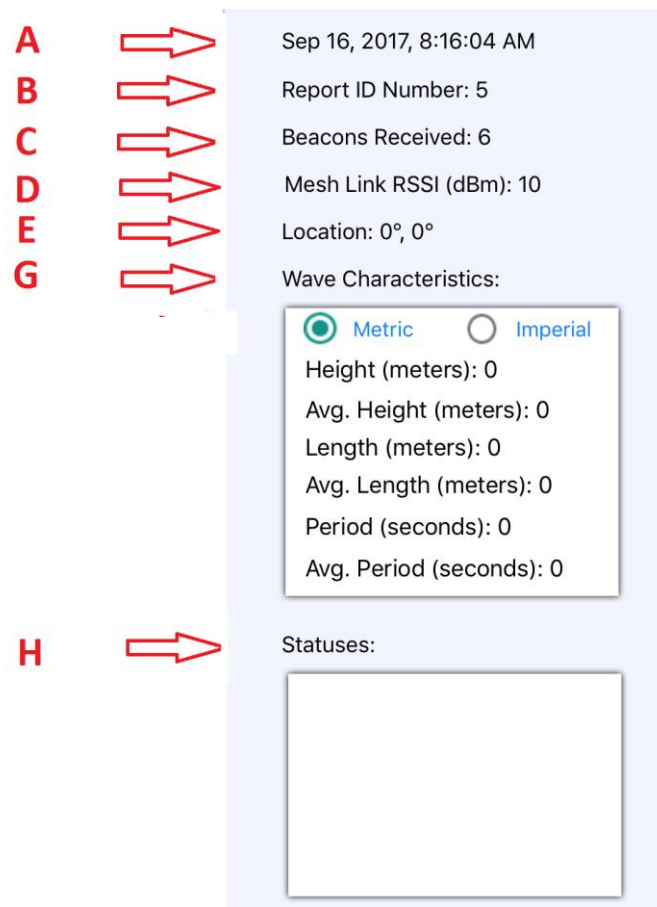


Figure C-10

- Timestamp (“A” in Figure C-10): Displays the time the WCM message was received.
- Report ID Number (“B” in Figure C-10): Displays the report ID of the selected report.
- Beacons Received (“C” in Figure C-10): Displays the number of beacons received.
- Mesh Link relative received signal strength (RSSI) (dBm) (“D” in Figure C-10): Displays the measured RSSI of the mesh network in dBm.
- Location (“E” in Figure C-10): Latitude and longitude of the most recent Node Report
- Wave Characteristics (“G” in Figure C-10): The text area for Wave Characteristics displays measurements in both metric and imperial units. To switch between measurement systems, select the desired system in the text area (“A” in Figure C-11 and “B” in Figure C-11).
- Statuses (“H” in Figure C-10)
 - The Status text area displays the statuses received from the selected report.
 - Status types
 - Status OK
 - Battery Low

- GPS Fault
- No GPS Fix
- RF Module

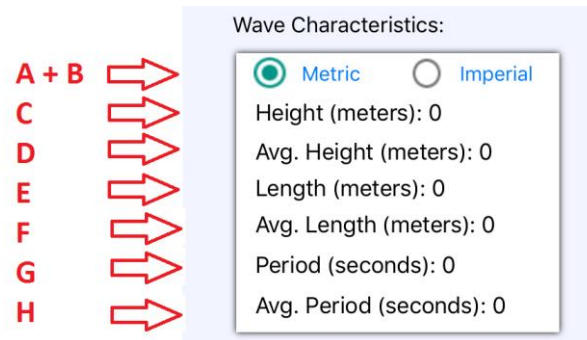


Figure C-11

- Characteristics
 - Height (“C” in Figure C-11)
 - Height sent from the most recent report from the selected ID.
 - Average Height (“D” in Figure C-11)
 - Average height of the 10 most recent reports from the selected ID.
 - Length (“E” in Figure C-11)
 - Length sent from the most recent report from the selected ID.
 - Average Length (“F” in Figure C-11)
 - Average length of the 10 most recent reports from the selected ID.
 - Period (“G” in Figure C-11)
 - Period sent from the most recent report from the selected ID.
 - Average Period (“H” in Figure C-11)
 - Average period of the 10 most recent reports from the selected ID.

- Statuses (“H” in Figure C-12)

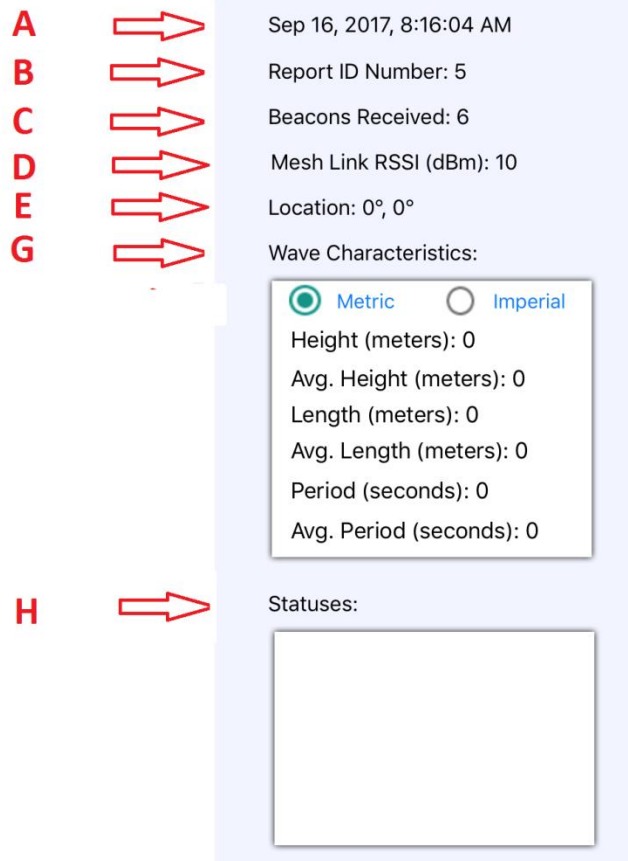


Figure C-12

- o The Statuses text area displays the statuses received from the selected report.
- o Status types
 - Status OK
 - Battery Low
 - GPS Fault
 - No GPS Fix
 - RF Module
 - WiFi Comm Fault
 - WiFi Socket Connection Refused
 - WiFi Busy

3. Sky and Wave Backdrop (Figure C-13)

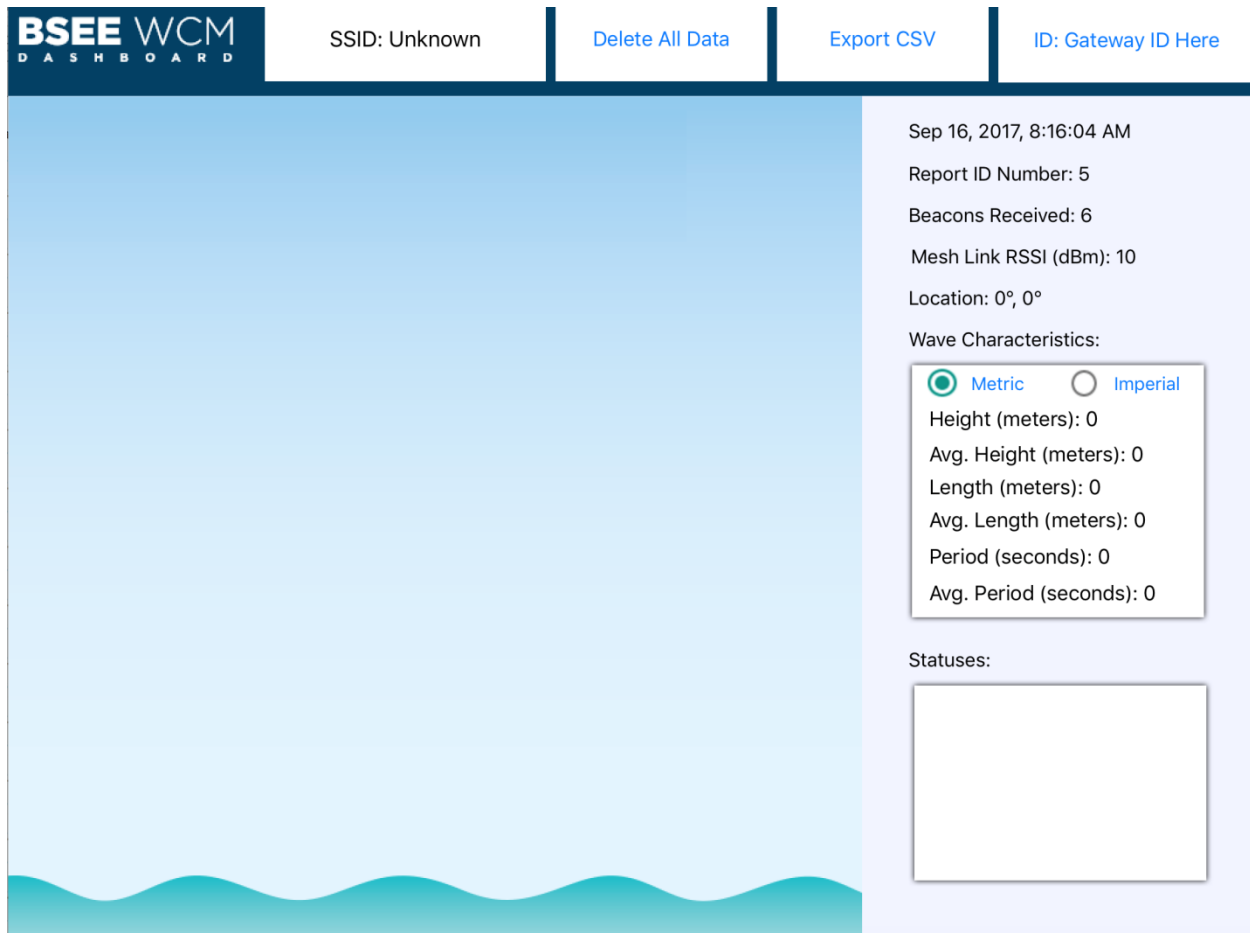


Figure C-13

- The wave animation changes when a message is received or when switching between IDs in a report.
- The wave animation change is generated based on a combination of the height, length, and period of the selected ID.

Appendix D: Remote GIS User Interface User Guide – BSEE Sensor Application

1. Application overview

- a. The Bureau of Safety and Environmental Enforcement (BSEE) Sensor Application enables remote stakeholders to view local wave characterization data from Wave Characterization Modules (WCMS) via a satellite network and web-accessible geographical information system (GIS) user interface.

2. Accessing the application

- a. The BSEE Sensor Application requires users to be signed into the application to access any and all parts of the program. To sign into the BSEE Sensor Application, the user needs to enter an email address and password. If you do not have an account, click the Register Now link below the sign-in button.

BSEE

Sensor Application

test@test.com

Sign In

New here? Register now!

- b. The registration process requires an email address, user name, and password.
 - i. The passwords must have at least eight characters and use three of the following: uppercase, lowercase, number, special character (e.g., !@#\$).



Sensor Application

 Email Address
 User Name
 Enter Password
 Confirm Password

[Register](#)

[Already Have An Account? Sign In](#)

3. Common terms

- a. Tag ID – Unique ID for WCM-Sat Tags, WCM-Buoy Tags, and WCM Node Tags. Administrators use Tag IDs to add WCM-Sat Tags and WCM-Buoy Tags to the BSEE Sensor Application and distinguish unique IDs for associated WCM Node Tags.
- b. Tag – Physical device used to characterize surface water waves. WCM-Sat, WCM-Buoy and WCM Node are defined as tags.
 - i. WCM-Sat Tag – WCM-Sat tag is a GPS, WiFi, and satellite-modem-enabled RF device that can act as a gateway for all WCM Node tags to communicate tag identification, time, location, wave characteristics, and status information to the BSEE Sensor Application. The WCM-Sat tag is represented by the symbol below.



- ii. WCM-Buoy Tag – Wave Characterization Module Buoy (WCM-Buoy) tag is a free floating GPS, WiFi, and satellite-modem-enabled RF device that can act as a gateway for all WCM Node tags to communicate tag identification, time, location, wave characteristics, and status information to the BSEE Sensor Application. The WCM-Buoy tag is represented by the symbol below.



- iii. WCM Node Tags – Wave Characterization Module Node (WCM Node) tag is a GPS, WiFi, and RF-enabled device that communicates through a local mesh network to a gateway tag

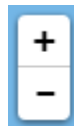
(WCM-Sat or WCM-Buoy) the WCM Node Tag identification, time, wave characteristics, and sequence number information to the BSEE Sensor Application.

4. Startup Navigation

- a. Upon logging into the application, you will see a map similar to the image below with the following features:

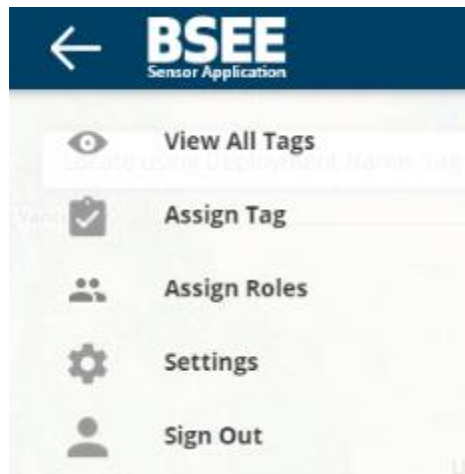


- i. User Name (#1 in the above image)
 - 1) The top right hand corner of the navigation bar will display the name of the current user logged into the application.
- ii. Notification (#2)
 - 1) The BSEE Sensor Application will notify the user when WCM-Sat or WCM-Buoy Tags have been assigned to the user. Notifications will persist in the top navigation bar and will reset after the user views the All Tags page.
- iii. Search (#3)
 - 1) The search box allows users to search the BSEE Sensor Application using Longitude and Latitude, Places of Interest, Tag ID, or Tag Name.
- iv. Map Navigation
 - 1) The user can click and hold/drag to move the map
- v. The map can be zoomed in or out using the buttons at the bottom left or the mouse scroll wheel.



vi. Main Menu (#4)

- 1) The main menu of the BSEE Sensor Application is accessible using the menu icon (three horizontal lines). The user can access the following actions from the menu:
 - a) View All Tags
 - b) Assign Tag
 - c) Assign Roles
 - d) Settings
 - e) Sign Out



5. View All Tags

- a. View all tags allows the user to see all of the WCM-Sat Tags and WCM-Buoy Tags assigned to a user. Clicking "View All Tags" in the menu opens up a panel to the right with two sections: Assigned Tags and Unassigned Tags.

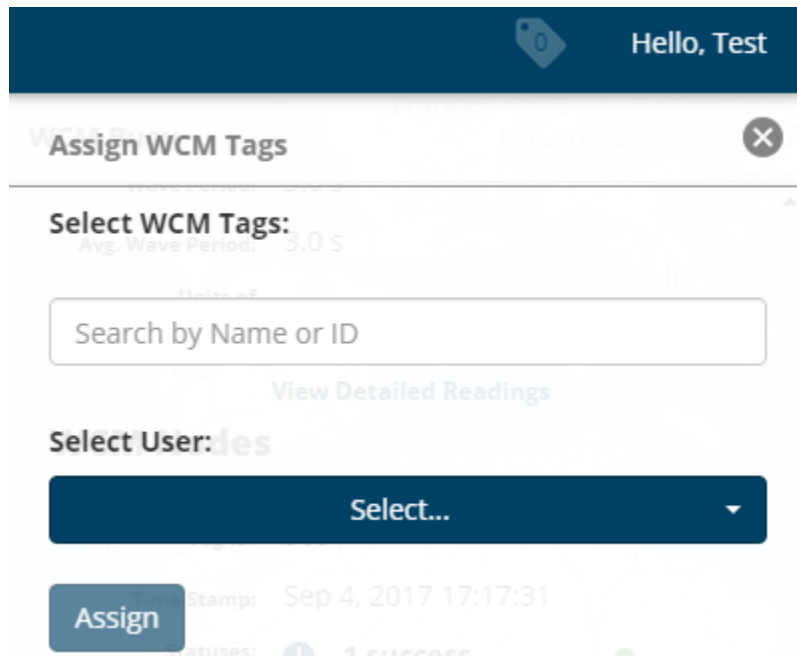
- i. Unassigned Tags: Any tag that has not been associated with a user.

- 1) There will also be an indicator to show which unassigned WCM-Sat Tags and WCM-Buoy Tags have been assigned to the user by an Administrator or Super User.



6. Assign Tag

- a. Clicking this option from the Main Menu opens a panel to the right where Tags can be assigned to users.



- i. Administrators and Super Users can assign WCM-Sat Tags or WCM-Buoy Tags to users. Once assigned, a Notification will be displayed to the user.



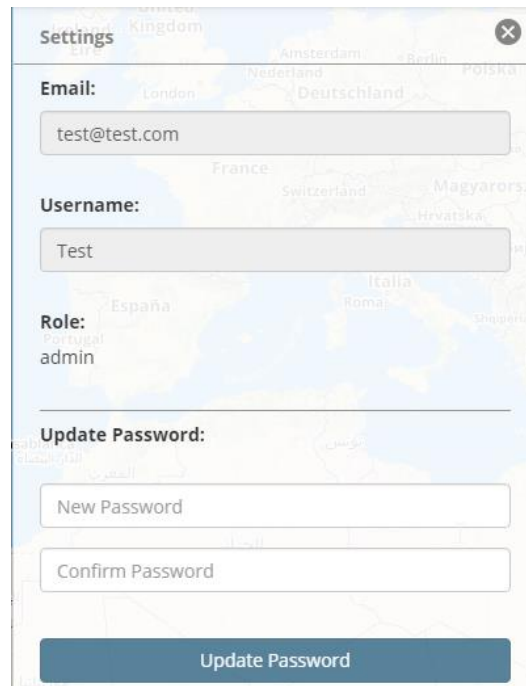
7. Assign Role

- a. There are three roles with three permission levels within the BSEE Sensor Application. The three roles are Administrator, Super User, and Regular User.
 - i. Administrator – Highest user setting in the BSEE Sensor Application. An administrator can see all Tags, add WCM-Sat Tags and WCM-Buoy Tags to the system, change a user’s role, and assign WCM-Sat Tags and WCM-Buoy Tags to users.
 - ii. Super User – Middle user setting in the BSEE Sensor Application. A Super User can see all Tags and assign WCM-Sat Tags and WCM-Buoy Tags to users. The only operations a Super User cannot perform is adding Tags to the system and modifying a user’s role.
 - iii. Regular User – Lowest user setting in the BSEE Sensor Application. A Regular User can only see the Tags an Administrator or Super User has assigned to the user.

The screenshot shows a mobile application interface for assigning a role to a user. The top navigation bar is dark blue with a tag icon and the text "Hello, Test". Below this, a white modal window titled "Assign Role" is displayed over a map background. The modal contains two dropdown menus: "Select User:" with the selected value "test@test.com" and "Select Permission Level:" with the selected value "Select...". A blue "Assign" button is located at the bottom left of the modal.

8. Settings

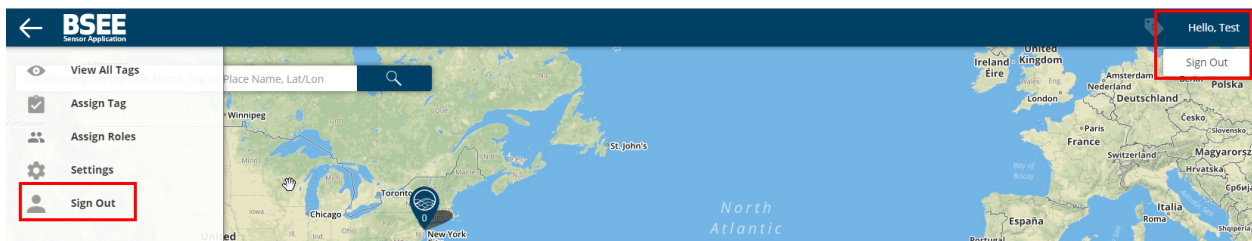
- a. Clicking on Settings in the Main Menu displays a panel to the right containing the following:
Email, Username, Update Password, and Role.
 - i. Update Password: Type a new password and re-enter the password to confirm the password. When you are done, click the update password button.
 - 1) Passwords for the BSEE Sensor Application must have at least eight characters and use three of the following: uppercase, lowercase, number, special character (e.g., !@#%).



The screenshot shows a 'Settings' modal window. At the top left is a back arrow and the title 'Settings'. At the top right is a close button (X). Below the title are four sections: 'Email:' with a text input containing 'test@test.com'; 'Username:' with a text input containing 'Test'; 'Role:' with the text 'admin'; and 'Update Password:' which includes two text inputs labeled 'New Password' and 'Confirm Password', and a blue button labeled 'Update Password' at the bottom.

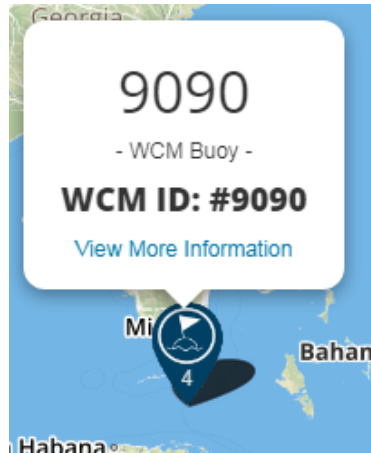
9. Sign Out

- a. Two ways to sign out of the application:
 - i) Find the Sign Out link at the bottom of the main menu.
 - ii) Click your user name in the upper right corner of the navigation bar.



10. Accessing Tag Information

- a. Clicking on a WCM-Sat or WCM-Buoy Tag displays a pop-up with the Tag ID:



- b. Clicking on View More Information opens a panel to the right of the screen:

WCM Buoy Tag

9090

WCM ID: 9090

Time Stamp: Sep 4, 2017 17:17:31

Statuses: **1 success**

Report Sequence Number: 18

Number of WCMs in Domain: 4

Location: 24.000000, -80.642300

Wave Record Number: 5

Wave Height: 1.5 m

Avg. Wave Height: 1.8 m

Wave Length: 18.0 m

Avg. Wave Length: 18.0 m

Wave Period: 3.0 s

Avg. Wave Period: 3.0 s

Units of Measurement: Metric Imperial

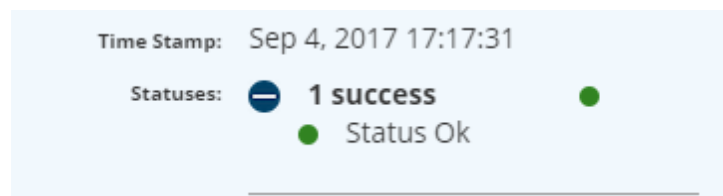
[View Detailed Readings](#)

WCM Nodes

Node - 9091

i) Definitions for terms in the above panel:

- 1) Timestamp – When the WCM-Sat Tag, WCM-Buoy Tag, or WCM Node Tag last collected or transmitted data.
 - 2) Report Sequence Number – Number of consecutive reports transmitted to the BSEE Sensor Application from a WCM-Sat Tag or WCM-Buoy Tag since powering on.
 - 3) Number of WCMs in Domain – Number of WCM Node Tags associated with a given WCM-Sat Tag or WCM-Buoy Tag.
 - 4) Location – Latitude and longitude of the tag.
 - 5) Wave Record Number – Count of wave characterization reports since the WCM unit was powered on.
 - 6) Wave Height – Vertical peak to trough measurement in meters or feet from the last report.
 - 7) Avg. Wave Height – Average of the last 10 reported wave height measurements.
 - 8) Wave Length – Horizontal peak-to-peak measurement in meters or feet from the last report.
 - 9) Avg. Wave Length – Average of the last 10 reported wave length measurements.
 - 10) Wave Period – Time in seconds between peaks measured from a fixed position from the last report.
 - 11) Average Wave Period – Average of the last 10 reported wave period measurements.
- a. Status – Clicking the plus sign next to Statuses displays the current status message. Messages displayed include Status OK, Battery Low, GPS Fault, No GPS Fix, RF Module Fault, WiFi Comm Fault, WiFi Socket Connection Refused, WiFi Busy, and Reserved.



- b. Nodes – Clicking the plus sign in the panel next to a node expands the details for that node.



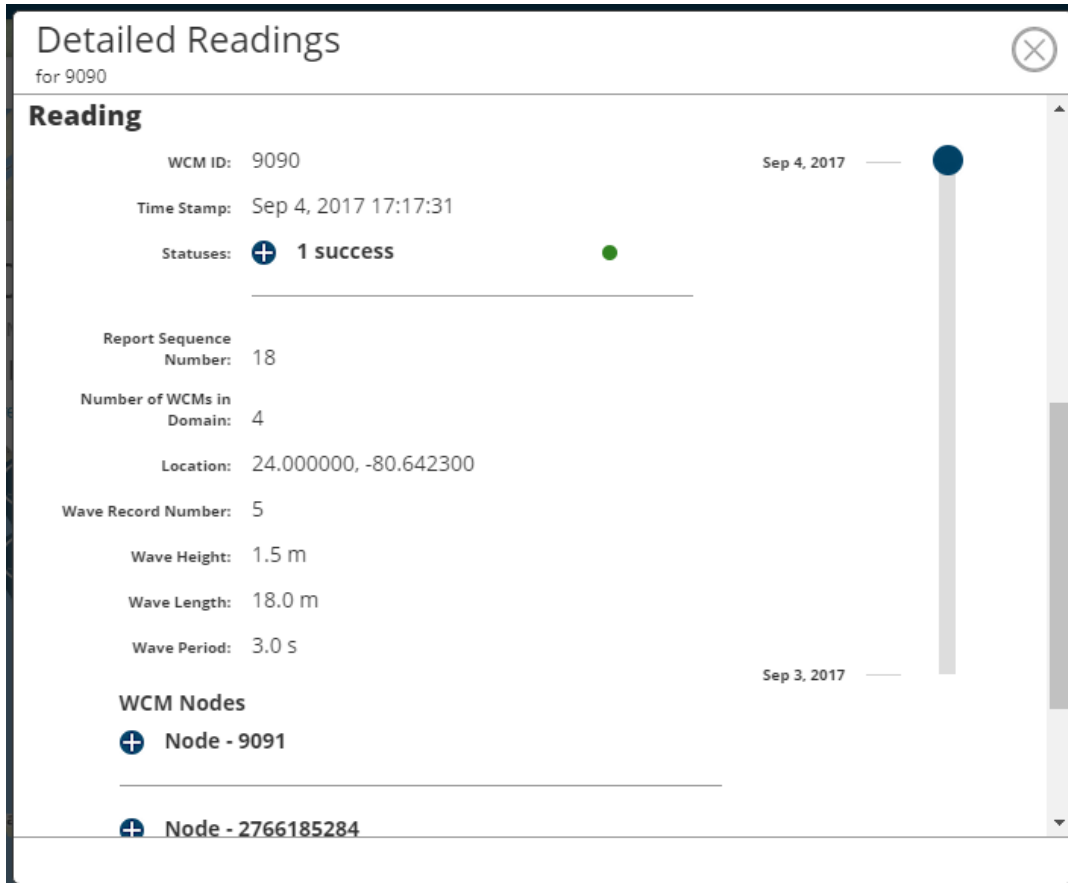
- i) Definitions for terms in Node details

- 1) Timestamp – When the WCM-Sat Tag, WCM-Buoy Tag, or WCM Node Tag last collected or transmitted data.
- 2) Mesh link RSSI – Relative received signal strength of the last received message at the Gateway from WCM Nodes in decibels.
- 3) # of Beacons – Number of beacons received from a WCM Node between reports sent to the WCM Gateway (either a WCM-Sat or WCM-Buoy).
- 4) Wave Record Number – Number of wave characterization reports since the WCM unit was powered on.
- 5) Wave Height – Vertical peak to trough measurement in meters or feet from the last report.
- 6) Wave Length – Horizontal peak-to-peak measurement in meters or feet from the last report.
- 7) Wave Period – Time in seconds between peaks measured from a fix position from the last report.

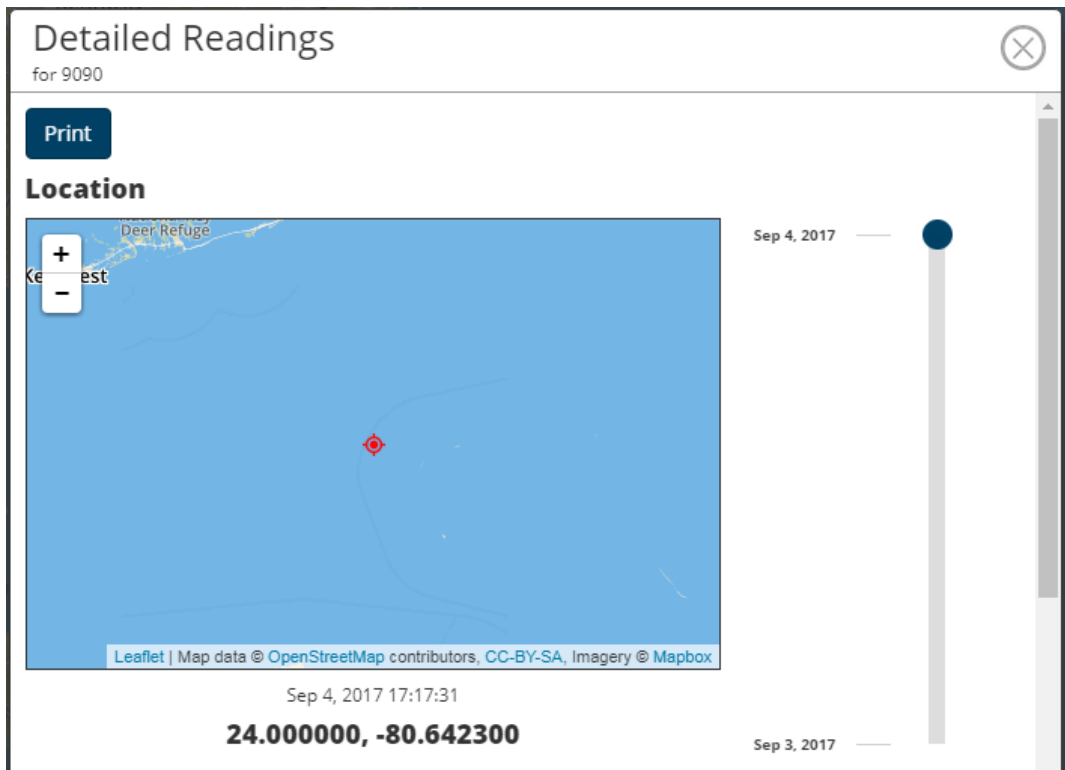
- a. Detailed Readings

- i) Clicking on View Detailed Readings in the View More Information Panel opens a pop-up window. Detail Readings contains two categories: Readings and Location.

- 1) The Readings section shows the following readings: Tag ID, Timestamp, Status, Report Sequence Number, Number of Tags in Domain, and Location, along with Wave Record Number, Wave Height, Wave Length, and Wave Period. There is a scrub slider that allows the user to see all of the aforementioned readings at different times over the life of the WCM-Sat Tag or WCM-Buoy Tag. The Readings section also includes details for each WCM Node report associated with the currently displayed Sat or Buoy Tag.



- 2) The Location section shows the position (visually and numerically) over time. There is a scrub slider that allows the user to select a particular point in time and thus the position of the WCM-Sat Tag or WCM-Buoy Tag.



Appendix E: Radio Frequency Attenuation Analysis of Crude Oil

Signal strength, ping, and packet loss are important factors to consider as they relate to the maximum physical distance tolerated between the WCM and iPad, which will impact the usability of the system in the field. Signal strength is commonly measured as a unit of power in dBm where ping is in milliseconds and packet loss is a percentage loss of total packets set.

Given a fixed distance between the WCM and iPad, fixed transmission frequency, preset transmit and receive power of the components, fixed antenna gain, and internal transmission losses, the radio waves will encounter objects such as the enclosure and oil that may be on the surface of the enclosure, which will cause antenna detuning and signal attenuation, reducing the power of the signal being received by the iPad.

Detuning

Antenna detuning shifts the frequency of where the transmitted power is concentrated, the center frequency, and what is expected by the receiver. Detuning decreases the power and usable range.

Permittivity (ϵ) is a complex number used to describe the dielectric properties of materials that influence reflection and attenuation of electromagnetic waves.

$$\epsilon = \epsilon_r \epsilon_0 = \epsilon' - j\epsilon''$$

Where:

ϵ_r = relative permittivity

ϵ_0 = vacuum permittivity (a constant)

ϵ' = dielectric constant

ϵ'' = dielectric loss factor influencing energy absorption and attenuation

The real part of the equation is ϵ' , the dielectric constant, which represents the stored energy when the material is exposed to an electric field such as our WiFi radio signal. The imaginary part is ϵ'' , the dielectric loss factor influencing energy absorption and attenuation. These components are also dependent on frequency and temperature (Bishop, 2001).

While the dielectric properties of the substrate behind an antenna are well known and accounted for by the manufacturer, other objects such as a coat of oil in close proximity to the antenna with a dielectric constant higher than air (air is approximately 1) will result in the antenna's seeing a higher effective dielectric constant. This higher effective dielectric constant effectively increases the electrical length of the antenna trace and reduces the resonant frequency (Pattayak and Thanikachalam, n.d.).

The shorter the distance to the object in terms of wavelength at the center frequency for which the antenna is designed, the larger this effect. Therefore, as discussed in Section 4.2.2, any coating on the enclosure has the potential to affect the RF signals that are transmitted and received by the WCM. Transmitted and received signals via WiFi and Bluetooth are centered at 2.45 GHz, Iridium messages are transmitted near 1.618 GHz, and GPS signals are received near 1.575 GHz. Non-electrically conductive substances (dielectrics) such as oil have a smaller impact on signal degradation if separated from the antennas by a few inches in our frequency domain of 1 to 3 GHz. This is why we chose a slightly larger enclosure in our WCM design compared to the baseline to assist RF communication quality.

Attenuation

Derived from Maxwell's equations defining electromagnetism, the loss tangent ($\tan\delta_e$) is composed of two terms.

1. The first term is based on static conductivity and describes the loss due to the collision of electrons. The static conductivity is high for metals (conductors), and this term dominates the loss tangent value for these types of materials.
2. The second term, a ratio of the dielectric loss factor (ϵ'') over the dielectric constant (ϵ'), describes how much energy supplied by an external electric field is dissipated as motion and heat. In other words, it can be defined as the loss current divided by the charging current or energy lost per cycle divided by the energy stored per cycle. For dielectric materials (insulators), the first term primarily influences the loss tangent (Chaplin, 2017).

$$\tan\delta_e = \frac{\epsilon''}{\epsilon'} + \frac{\sigma_s}{\omega\epsilon'}$$

In dielectric materials, the power can be represented by:

$$P = P_0 e^{-2\alpha z}$$

The power is based on initial power radiated (P_0), distance (z), and attenuation factor (α). The power from our antenna to the surface of the enclosure, oil, or another object is P . At that material interface, P becomes P_0 and the distance can be considered the thickness of the material the electromagnetic wave is passing through. The attenuation factor depends on the dielectric properties of the material and is directly influenced by the loss tangent of the dielectric material (Komar et al., 2005).

$$\alpha = \frac{2\pi}{\lambda_0} \left[\frac{1}{2} \epsilon' \left(\sqrt{1 + \left(\frac{\epsilon''}{\epsilon'} \right)^2} - 1 \right) \right]^{1/2}$$

Therefore, the larger the loss tangent and dielectric loss factor, the greater the attenuation factor is for a given thickness of material and the lower the power and signal strength.

Crude Oil Properties and Simulants

Now that the most critical material properties that will affect our signal have been determined, we need to determine the range of values of these electrical properties for a variety of crude oils and consider suitable simulants for testing purposes.

Most literature related to spill recovery options and operating conditions are concerned with the physical properties of oil, such as viscosity, density, flash point, and chemical composition and how they impact the resultant behavior of the spill, as shown in Table E-1.

While viscosity and emulsification will contribute to how the oil may adhere to the enclosure, and we may need to be concerned about a larger concentration of oil and varying water content if the oil emulsifies, we are primarily concerned with quantifying the components of permittivity.

Heavy crude oils were measured to have a dielectric constant (ϵ') from 2.8 to 2.4 at a range of frequencies between 1 kHz and 0.1 GHz, respectively. Their dielectric loss (ϵ'') ranged from 0.15 to 0.03 over the same frequency range (Park, 2014).

Table E-1. Physical Properties of Materials of Interest

Material	Viscosity (cP or mPa*sec)	Density (g/mL)
Light oil (Diesel)	1 – 10	0.820 – 0.870
Medium oil (Light crude)	200 – 400	0.860 – 0.970
Heavy oil (Bunker C)	1,500 – 2,500	0.930 – 1.000
Weathered (Emulsified)	8,000 – 10,000	0.930 – 1.000
Canola	56 (at 25°C)	0.9135 (at 25°C)
Castor	608 (at 25°C)	0.9565 (at 25°C)
Sources: Federici and Mintz (2014) Fingas (n.d.) SAIC Canada (2008)	°C = degrees Celsius cP = centiPoise g/mL = grams per milliliter mPa*sec = megaPascal second	

Another study of bitumen from oil sand deposits in Alberta, Canada, measured at 23°C and at 2.49 GHz found a dielectric constant range from 2.8 to 3.2 and dielectric loss from 0.0569 to 0.0152 (Erdogan, 2011).

Table E-2 shows the value of these electrical material properties. Variations in the literature can be attributed to material composition differences and measurements at different temperatures, voltages, or frequencies. Using these electrical properties and the equations above, we calculated the percentage in power reduction due to the attenuation of 1 inch of each material.

Table E-2. Electrical Properties of Materials of Interest

Material	Dielectric Constant (ϵ')	Dielectric Loss (ϵ'')	Loss Tangent ($\tan\delta_o$)	Power Reduction for 1 inch (%)
Air	1.0005	~0	~0	0.00
Water	80 (2.45 GHz, 20°C)	10 (2.45 GHz, 20°C)	0.125	76.71
Salt water (20 ppt)	72 (2.45 GHz, 20°C)	30 (2.45 GHz, 20°C)	0.416	98.92
Nylon	2.4	0.0199	0.0083	1.66
Polycarbonate	3.0	0.03	0.01	2.24
Parylene C	2.7	0.27	0.10	19.29
Heavy oil	2.4	.03	0.0125	2.50
Very low-grade bitumen	2.84	0.0569	0.020	4.31
High-grade bitumen	3.21	.0152	0.0047	1.10
Canola	5.5 (2.45 GHz, 20°C)	0.15 (2.45 GHz, 20°C)	0.03	8.01
Castor	3.7 – 4.7	0.1 (1 kHz)	0.03	6.32
Sources: Agilent (2017) Chaplin (2017) Clarke (2015)	IEEE (2017) Kabusa (n.d.) McGill University (n.d.) RF Café (n.d.)	°C = degrees Celsius GHz = gigahertz ppt = parts per thousand		

The various crude oils that have been studied and that are in the literature have low dielectric losses compared to water (on the order of common plastics such the materials we use for the enclosures). The thickness of a coating of oil should also be similar to or less than our enclosure so the effective signal attenuation will remain low. The significant effect of water compared to other common materials for a given thickness is clear from the percent power reduction. A 1/8-inch layer of salt water surrounding the enclosure is approximately the same as a 1-foot layer of crude oil in terms of signal attenuation. Also,

although a hydrophobic coating such as Parylene C has a much higher attenuation than our plastic enclosure, because the applied layer is so thin, the positive effects of repelling water may more than offset the attenuation caused by the coating itself.

We do not anticipate significant detuning or attenuation from the crude oil at moderate thickness and low water content, similar to what is expected from an operational environment and as observed during our testing of the WCM system at Ohmsett in terms of signal strength, attenuation, and the distance of reliable communication between the WCM and iPad.

Appendix F: WCM-Mounted Skimmer Significant Wave Heights

This appendix contains plots of the significant wave heights. The plus signs indicate the significant wave height (H_{m0}) calculated statistically using the raw data from the WCM mounted to the skimmer. The triangles represent the significant wave height (H_{m0}) calculated statistically using a segment of time corresponding to the WCM data from the raw Banner data. The dots represent the wave heights calculated using the average of the top third wave height from the same segments ($H_{1/3}$). Each data point represents a calculation of the significant wave height from approximately 60 seconds of raw data.

Figure F-1: Plots of the significant wave heights for Test 1 of the WCM mounted to the skimmer and the raw data from the main bridge Banner. The plus signs indicate the significant wave height (H_{m0}) calculated statistically using the raw data from the WCM mounted to the skimmer. The triangles represent the significant wave height (H_{m0}) calculated statistically using a segment of time corresponding to the WCM data from the raw Banner data. The dots represent the wave heights calculated using the average of the top third wave height from the same segments ($H_{1/3}$). Each data point represents a calculation of the significant wave height from approximately 60 seconds of raw data.

Here it can be seen that the $H_{1/3}$ calculation is lower than the H_{m0} value for each time segment. The H_{m0} calculated using the WCM data is higher than the bridge data. This test is one where the waves were created by the 18-inch stroke and 18 CPM setting of the wave generator, which creates a large sinusoidal wave. We believe the discrepancies between the WCM and Banner measurement are due to lateral motion from the large elliptical motion of the wave not being considered by the algorithms. This is because we trained them on real, complex wave motion where most of the movement is in the heave.

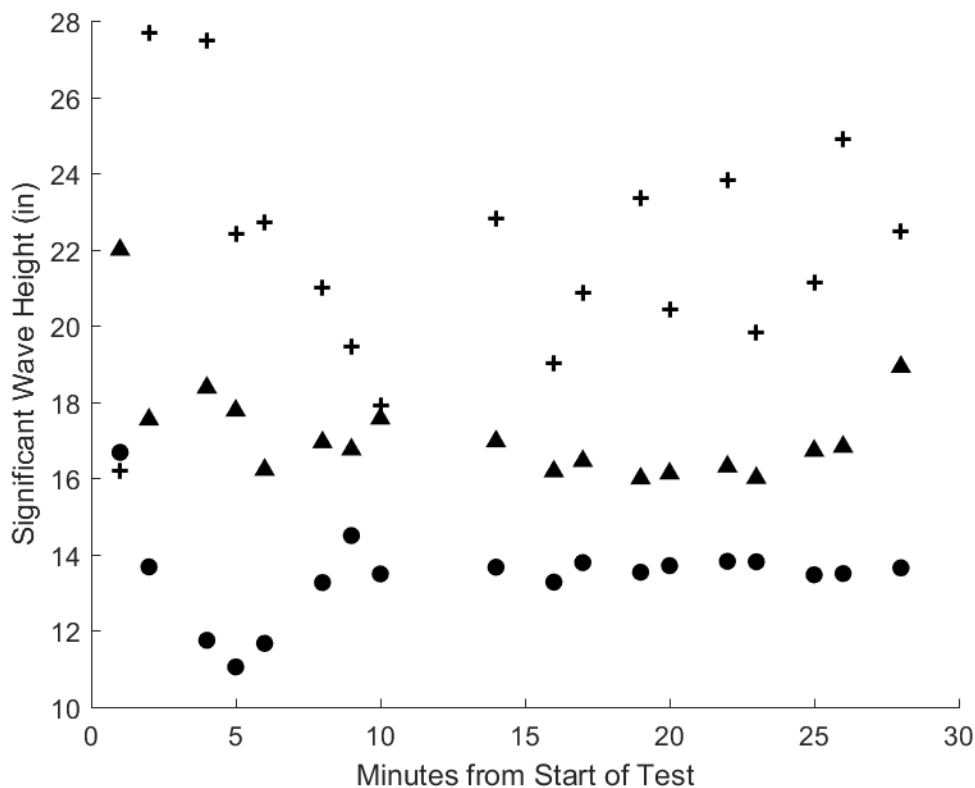


Figure F-1

Figure F-2: Plots of the significant wave heights for Test 1 of the WCM mounted to the skimmer and the raw data from the west auxiliary bridge Banner. The plus signs indicate the significant wave height (H_{m0}) calculated statistically using the raw data from the WCM mounted to the skimmer. The triangles represent the significant wave height (H_{m0}) calculated statistically using a segment of time corresponding to the WCM data from the raw Banner data. The dots represent the wave heights calculated using the average of the top third wave height from the same segments ($H_{1/3}$). Each data point represents a calculation of the significant wave height from approximately 60 seconds of raw data.

Here it can be seen that the $H_{1/3}$ calculation is lower than the H_{m0} value for each time segment. The H_{m0} calculated using the WCM data is higher than the bridge data. This test is one where the waves were created by the 18-inch stroke and 18 CPM setting of the wave generator, which creates a large sinusoidal wave. We believe the discrepancies between the WCM and Banner measurement are due to lateral motion from the large elliptical motion of the wave not being considered by the algorithms. This is because we trained them on real, complex wave motion where most of the movement is in the heave.

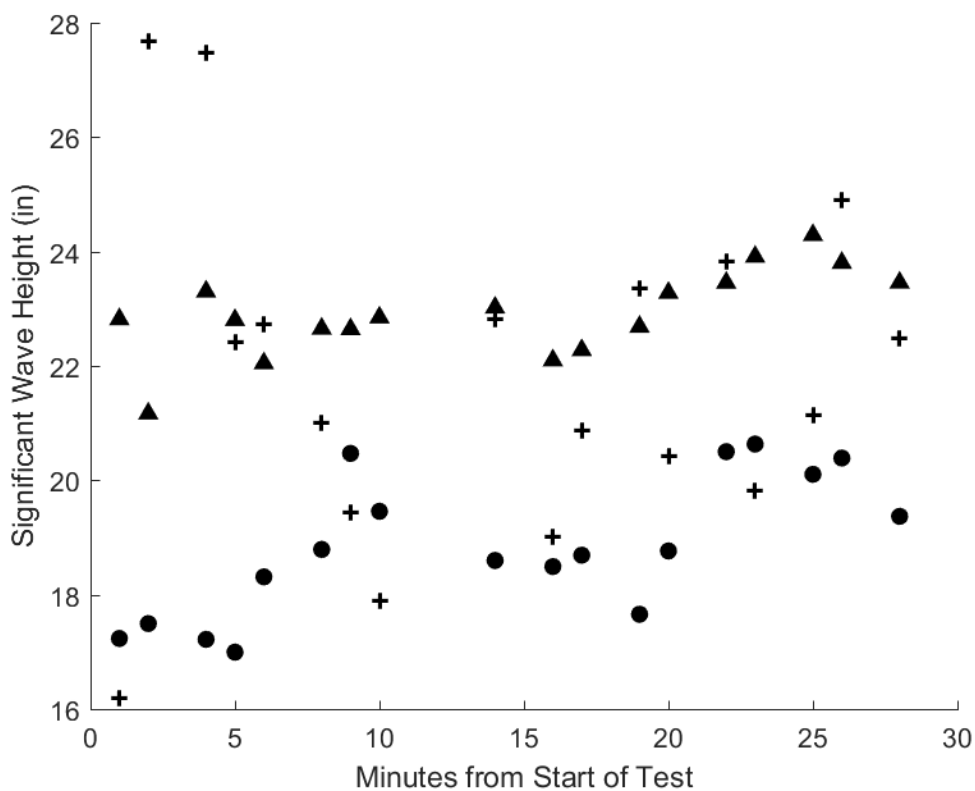


Figure F-2

Figure F-3: Plots of the significant wave heights for Test 1 of the WCM mounted to the skimmer and the raw data from the east auxiliary bridge Banner. The plus signs indicate the significant wave height (H_{m0}) calculated statistically using the raw data from the WCM mounted to the skimmer. The triangles represent the significant wave height (H_{m0}) calculated statistically using a segment of time corresponding to the WCM data from the raw Banner data. The dots represent the wave heights calculated using the average of the top third wave height from the same segments ($H_{1/3}$). Each data point represents a calculation of the significant wave height from approximately 60 seconds of raw data.

Here it can be seen that the $H_{1/3}$ calculation is lower than the H_{m0} value for each time segment. The H_{m0} calculated using the WCM data is higher than the bridge data. This test is one where the waves were created by the 18-inch stroke and 18 cycles per minute (CPM) setting of the wave generator, which creates a large sinusoidal wave. We believe the discrepancies between the WCM and Banner measurement are due to lateral motion from the large elliptical motion of the wave not being considered by the algorithms. This is because we trained them on real, complex wave motion where most of the movement is in the heave.

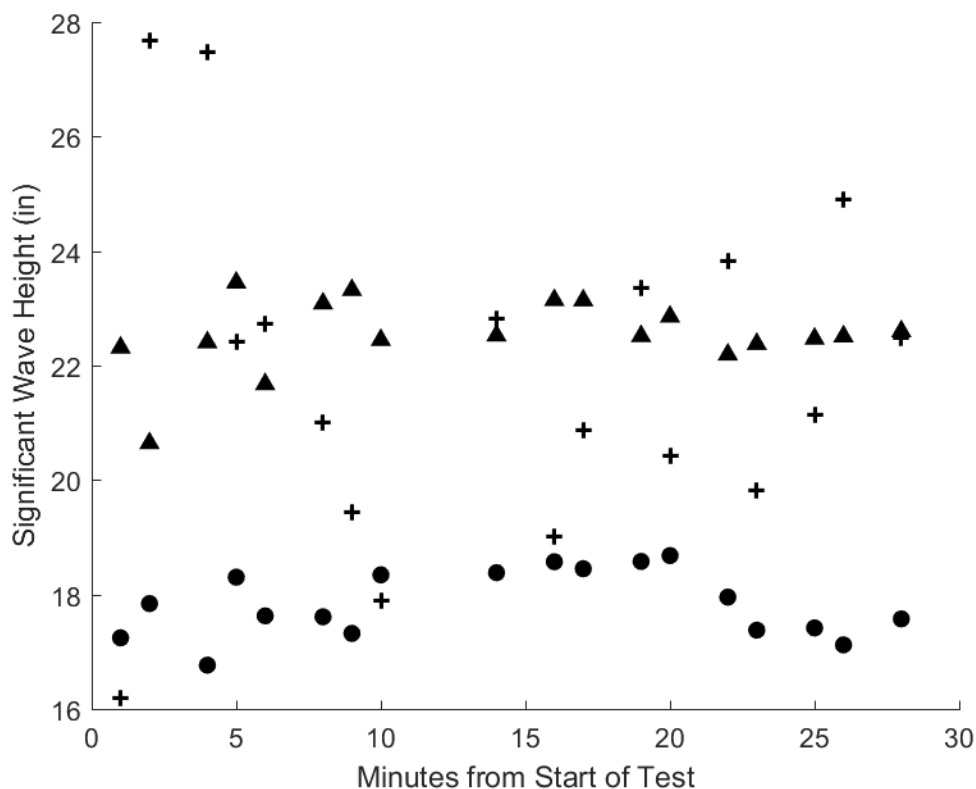


Figure F-3

Figure F-4: Plots of the significant wave heights for Test 2 of the WCM mounted to the skimmer and the raw data from the main bridge Banner. The plus signs indicate the significant wave height (H_{m0}) calculated statistically using the raw data from the WCM mounted to the skimmer. The triangles represent the significant wave height (H_{m0}) calculated statistically using a segment of time corresponding to the WCM data from the raw Banner data. The dots represent the wave heights calculated using the average of the top third wave height from the same segments ($H_{1/3}$). Each data point represents a calculation of the significant wave height from approximately 60 seconds of raw data.

Here it can be seen that the $H_{1/3}$ calculation is lower than the H_{m0} value calculated using the Banner data for each time segment. The H_{m0} calculated using the WCM data is generally within the 4-inch performance objective with the H_{m0} from the bridge data.

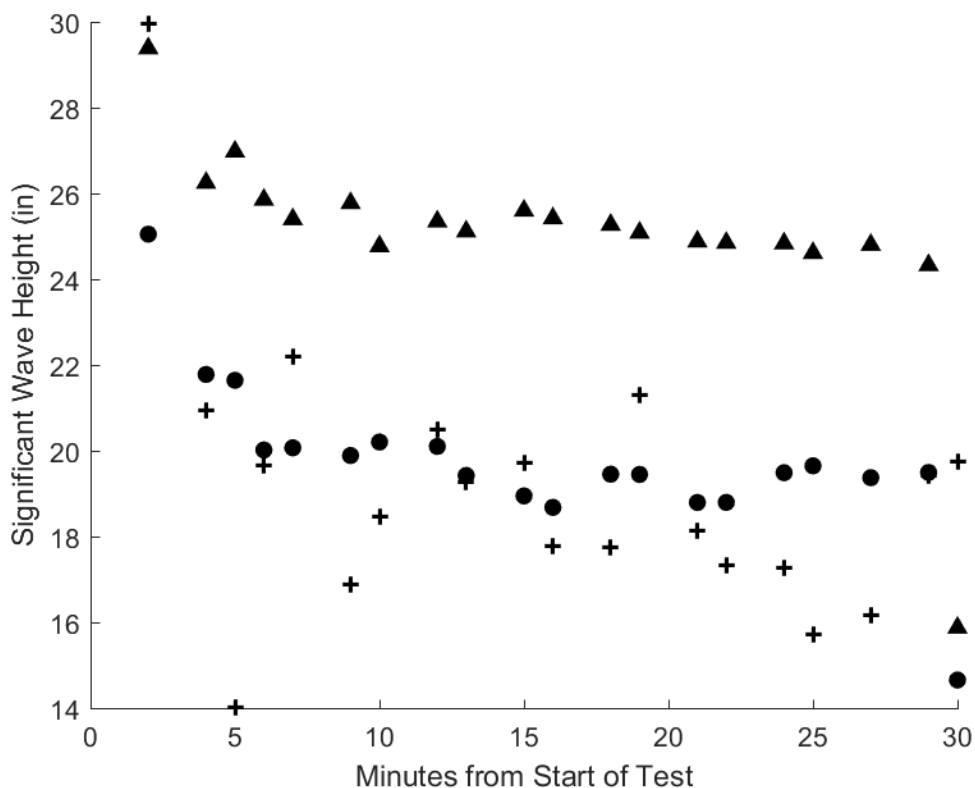


Figure F-4

Figure F-5: Plots of the significant wave heights for Test 2 of the WCM mounted to the skimmer and the raw data from the west auxiliary bridge Banner. The plus signs indicate the significant wave height (H_{m0}) calculated statistically using the raw data from the WCM mounted to the skimmer. The triangles represent the significant wave height (H_{m0}) calculated statistically using a segment of time corresponding to the WCM data from the raw Banner data. The dots represent the wave heights calculated using the average of the top third wave height from the same segments ($H_{1/3}$). Each data point represents a calculation of the significant wave height from approximately 60 seconds of raw data.

Here it can be seen that the $H_{1/3}$ calculation is lower than the H_{m0} value calculated using the Banner data for each time segment. The H_{m0} calculated using the WCM data is generally within the 4-inch performance objective with the H_{m0} from the bridge data.

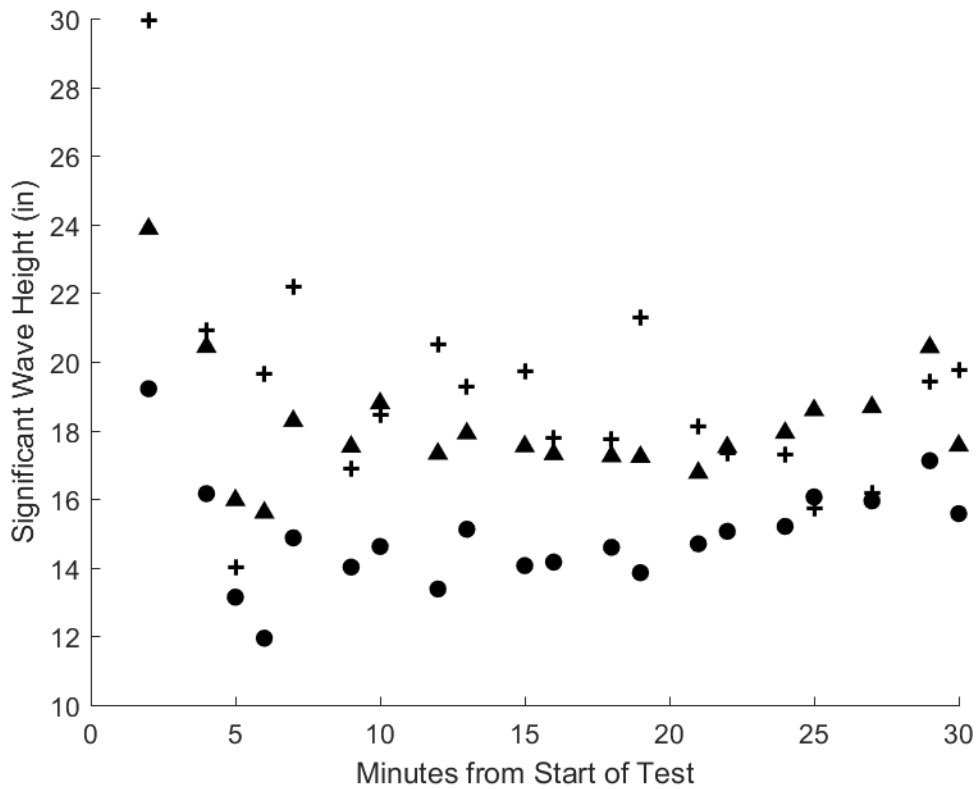


Figure F-5

Figure F-6: Plots of the significant wave heights for Test 2 of the WCM mounted to the skimmer and the raw data from the east auxiliary bridge Banner. The plus signs indicate the significant wave height (H_{m0}) calculated statistically using the raw data from the WCM mounted to the skimmer. The triangles represent the significant wave height (H_{m0}) calculated statistically using a segment of time corresponding to the WCM data from the raw Banner data. The dots represent the wave heights calculated using the average of the top third wave height from the same segments ($H_{1/3}$). Each data point represents a calculation of the significant wave height from approximately 60 seconds of raw data.

Here it can be seen that the $H_{1/3}$ calculation is lower than the H_{m0} value calculated using the Banner data for each time segment. The H_{m0} calculated using the WCM data is generally within the 4-inch performance objective with the H_{m0} from the bridge data.

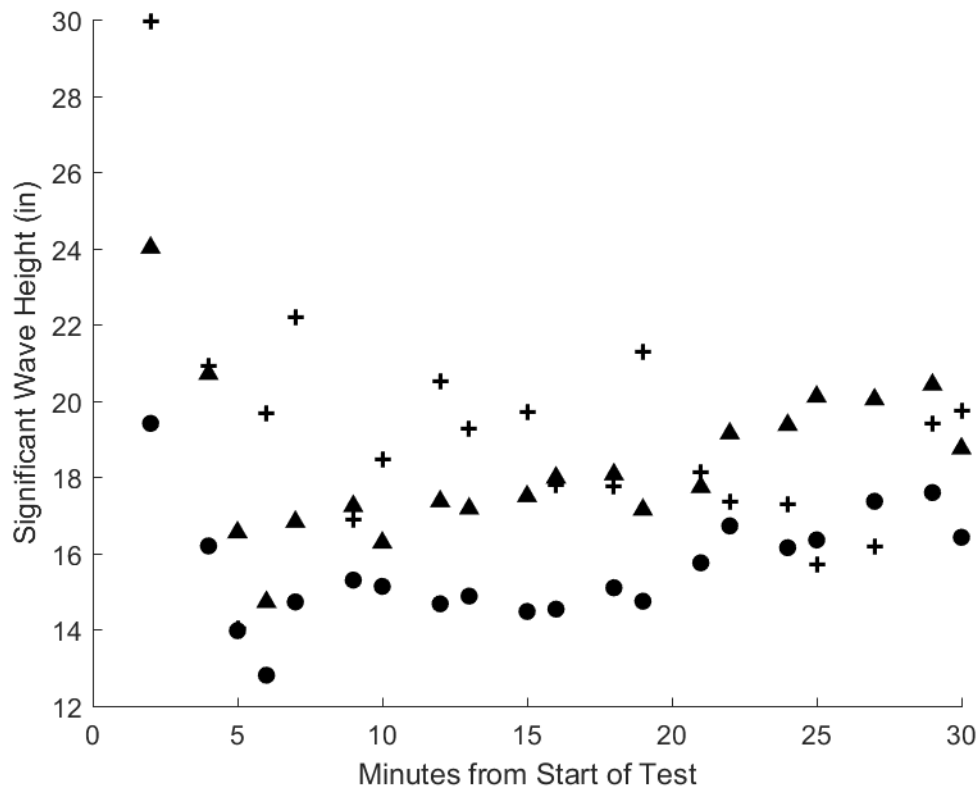


Figure F-6

Figure F-7: Plots of the significant wave heights for Test 3 of the WCM mounted to the skimmer and the raw data from the main bridge Banner. The plus signs indicate the significant wave height (H_{m0}) calculated statistically using the raw data from the WCM mounted to the skimmer. The triangles represent the significant wave height (H_{m0}) calculated statistically using a segment of time corresponding to the WCM data from the raw Banner data. The dots represent the wave heights calculated using the average of the top third wave height from the same segments ($H_{1/3}$). Each data point represents a calculation of the significant wave height from approximately 60 seconds of raw data.

Here it can be seen that the $H_{1/3}$ calculation is lower than the H_{m0} value calculated using the Banner data for each time segment. The H_{m0} calculated using the WCM data is generally within the 4-inch performance objective with the H_{m0} from the bridge data.

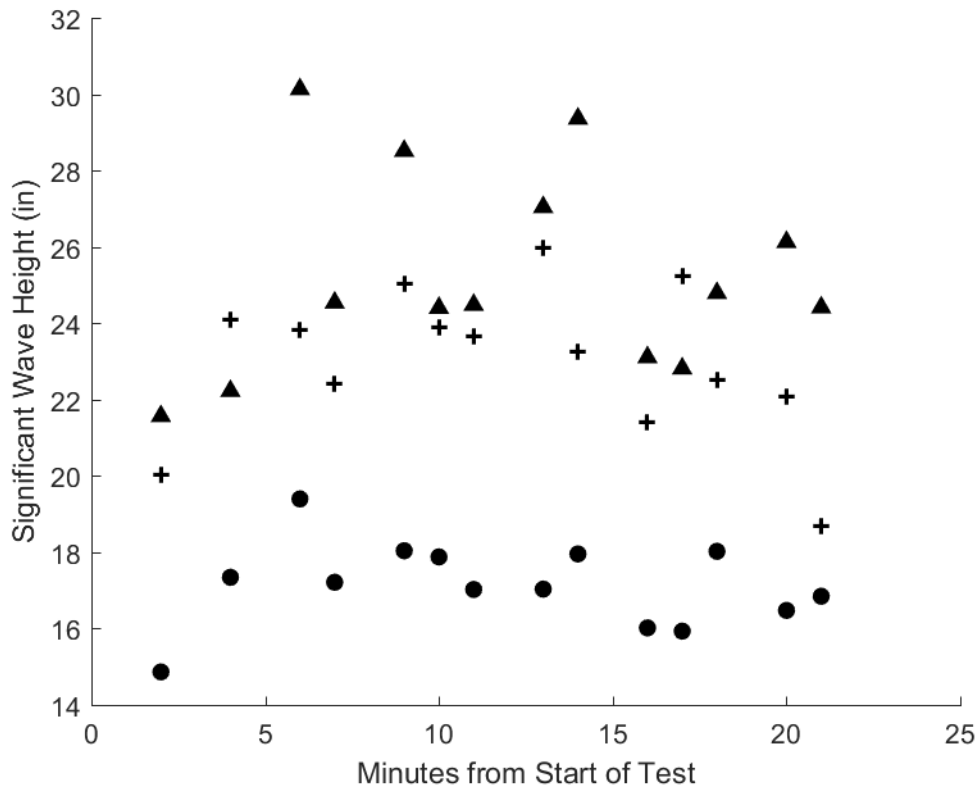


Figure F-7

Figure F-8: Plots of the significant wave heights for Test 3 of the WCM mounted to the skimmer and the raw data from the west auxiliary bridge Banner. The plus signs indicate the significant wave height (H_{m0}) calculated statistically using the raw data from the WCM mounted to the skimmer. The triangles represent the significant wave height (H_{m0}) calculated statistically using a segment of time corresponding to the WCM data from the raw Banner data. The dots represent the wave heights calculated using the average of the top third wave height from the same segments ($H_{1/3}$). Each data point represents a calculation of the significant wave height from approximately 60 seconds of raw data.

Here it can be seen that the $H_{1/3}$ calculation is lower than the H_{m0} value calculated using the Banner data for each time segment. The H_{m0} calculated using the WCM data is generally within the 4-inch performance objective with the H_{m0} from the bridge data.

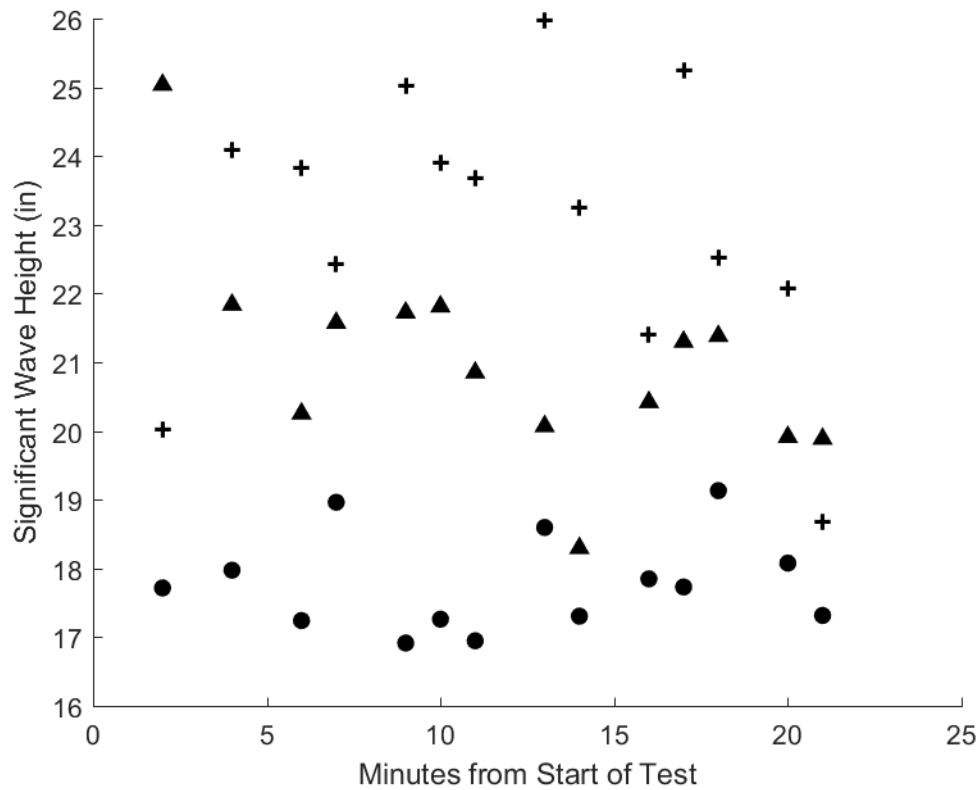


Figure F-8

Figure F-9: Plots of the significant wave heights for Test 3 of the WCM mounted to the skimmer and the raw data from the east auxiliary bridge Banner. The plus signs indicate the significant wave height (H_{m0}) calculated statistically using the raw data from the WCM mounted to the skimmer. The triangles represent the significant wave height (H_{m0}) calculated statistically using a segment of time corresponding to the WCM data from the raw Banner data. The dots represent the wave heights calculated using the average of the top third wave height from the same segments ($H_{1/3}$). Each data point represents a calculation of the significant wave height from approximately 60 seconds of raw data.

Here it can be seen that the $H_{1/3}$ calculation is lower than the H_{m0} value calculated using the Banner data for each time segment. The H_{m0} calculated using the WCM data is generally within the 4-inch performance objective with the H_{m0} from the bridge data.

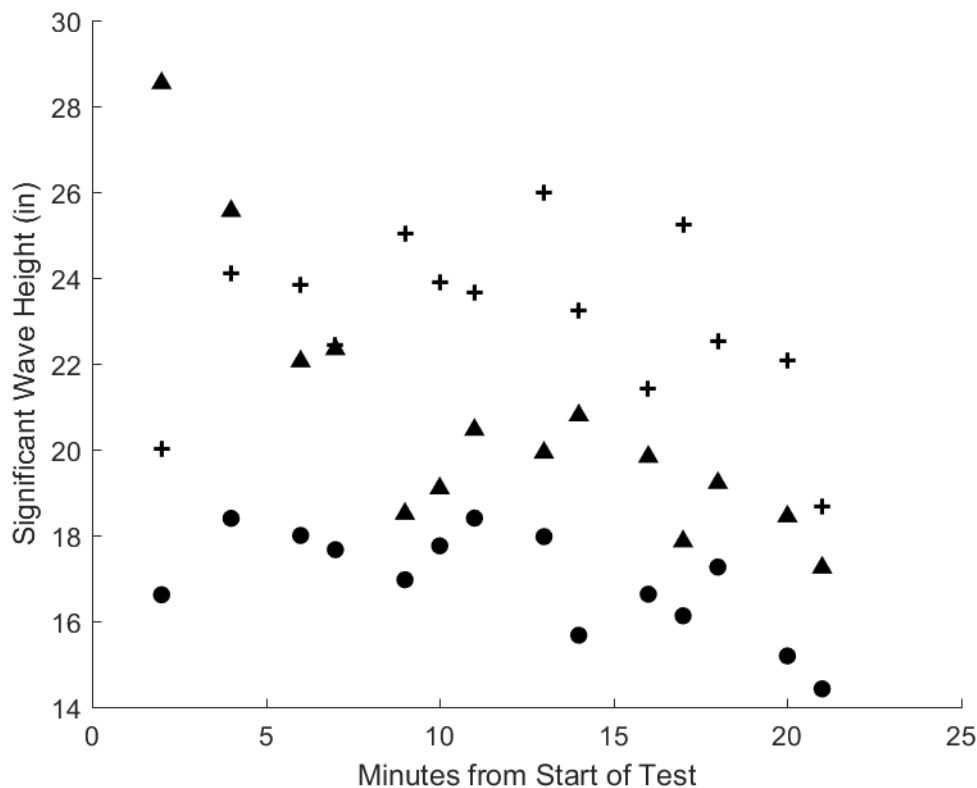


Figure F-9

Figure F-10: Plots of the significant wave heights for Test 4 of the WCM mounted to the skimmer and the raw data from the main bridge Banner. The plus signs indicate the significant wave height (H_{m0}) calculated statistically using the raw data from the WCM mounted to the skimmer. The triangles represent the significant wave height (H_{m0}) calculated statistically using a segment of time corresponding to the WCM data from the raw Banner data. The dots represent the wave heights calculated using the average of the top third wave height from the same segments ($H_{1/3}$). Each data point represents a calculation of the significant wave height from approximately 60 seconds of raw data.

Here it can be seen that the $H_{1/3}$ calculation is lower than the H_{m0} value calculated using the Banner data for each time segment. The H_{m0} calculated using the WCM data is generally within the 4-inch performance objective with the H_{m0} from the bridge data.

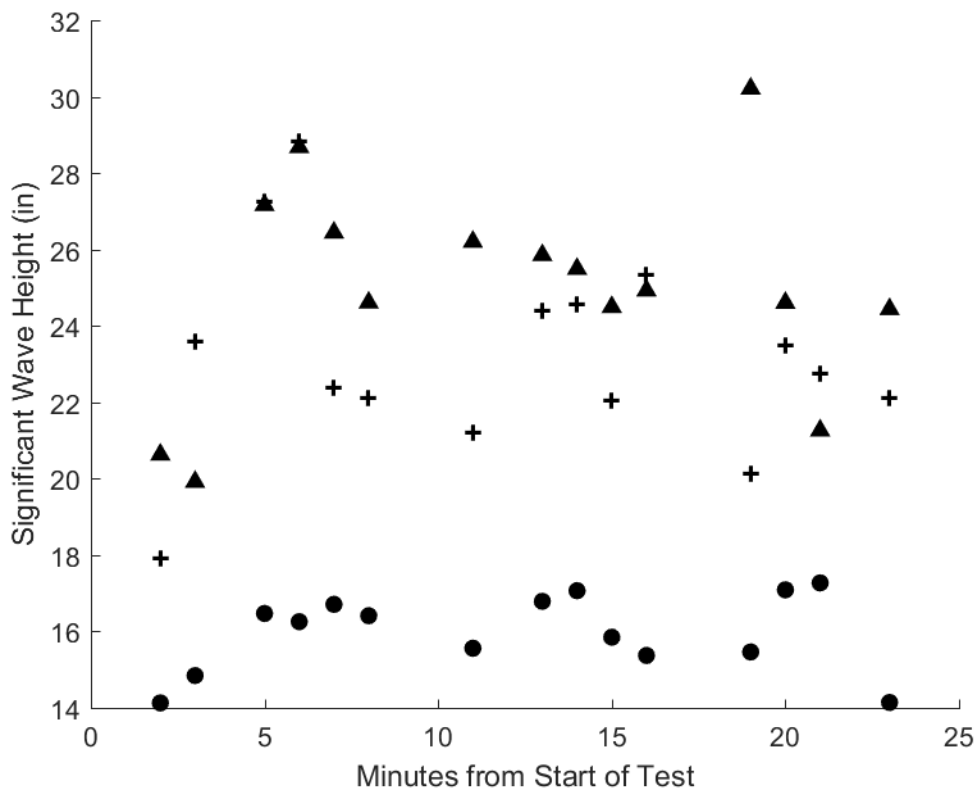


Figure F-10

Figure F-11: Plots of the significant wave heights for Test 4 of the WCM mounted to the skimmer and the raw data from the west auxiliary bridge Banner. The plus signs indicate the significant wave height (H_{m0}) calculated statistically using the raw data from the WCM mounted to the skimmer. The triangles represent the significant wave height (H_{m0}) calculated statistically using a segment of time corresponding to the WCM data from the raw Banner data. The dots represent the wave heights calculated using the average of the top third wave height from the same segments ($H_{1/3}$). Each data point represents a calculation of the significant wave height from approximately 60 seconds of raw data.

Here it can be seen that the $H_{1/3}$ calculation is lower than the H_{m0} value calculated using the Banner data for each time segment. The H_{m0} calculated using the WCM data is generally within the 4-inch performance objective with the H_{m0} from the bridge data.

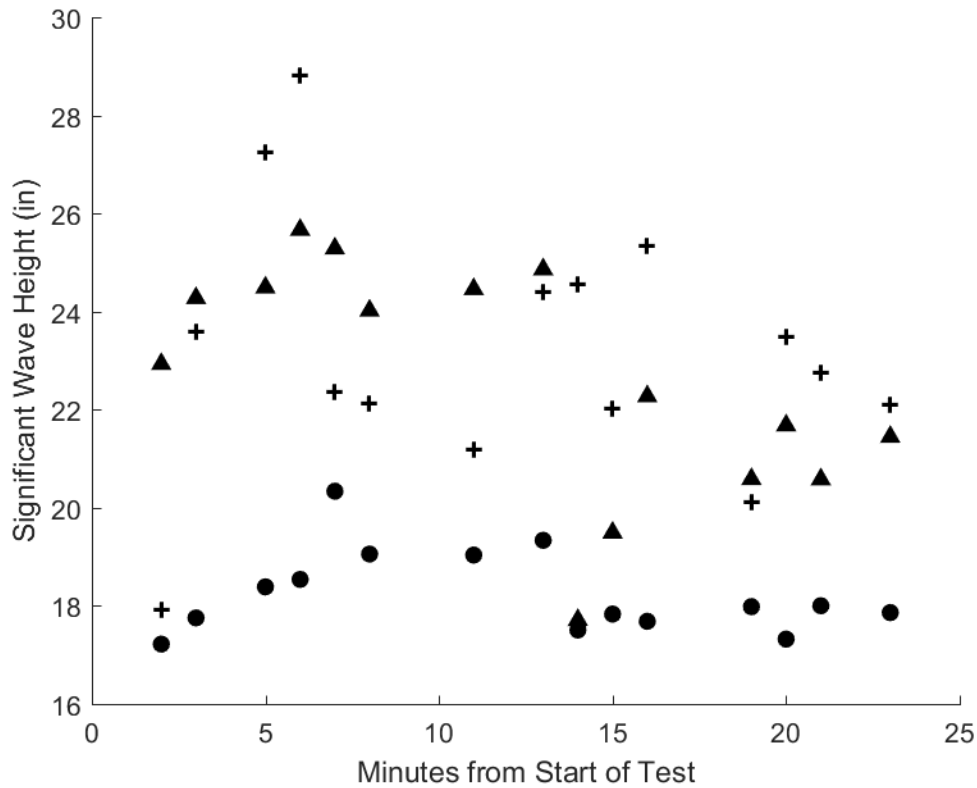


Figure F-11

Figure F-12: Plots of the significant wave heights for Test 4 of the WCM mounted to the skimmer and the raw data from the east auxiliary bridge Banner. The plus signs indicate the significant wave height (H_{m0}) calculated statistically using the raw data from the WCM mounted to the skimmer. The triangles represent the significant wave height (H_{m0}) calculated statistically using a segment of time corresponding to the WCM data from the raw Banner data. The dots represent the wave heights calculated using the average of the top third wave height from the same segments ($H_{1/3}$). Each data point represents a calculation of the significant wave height from approximately 60 seconds of raw data.

Here it can be seen that the $H_{1/3}$ calculation is lower than the H_{m0} value calculated using the Banner data for each time segment. The H_{m0} calculated using the WCM data is generally within the 4-inch performance objective with the H_{m0} from the bridge data.

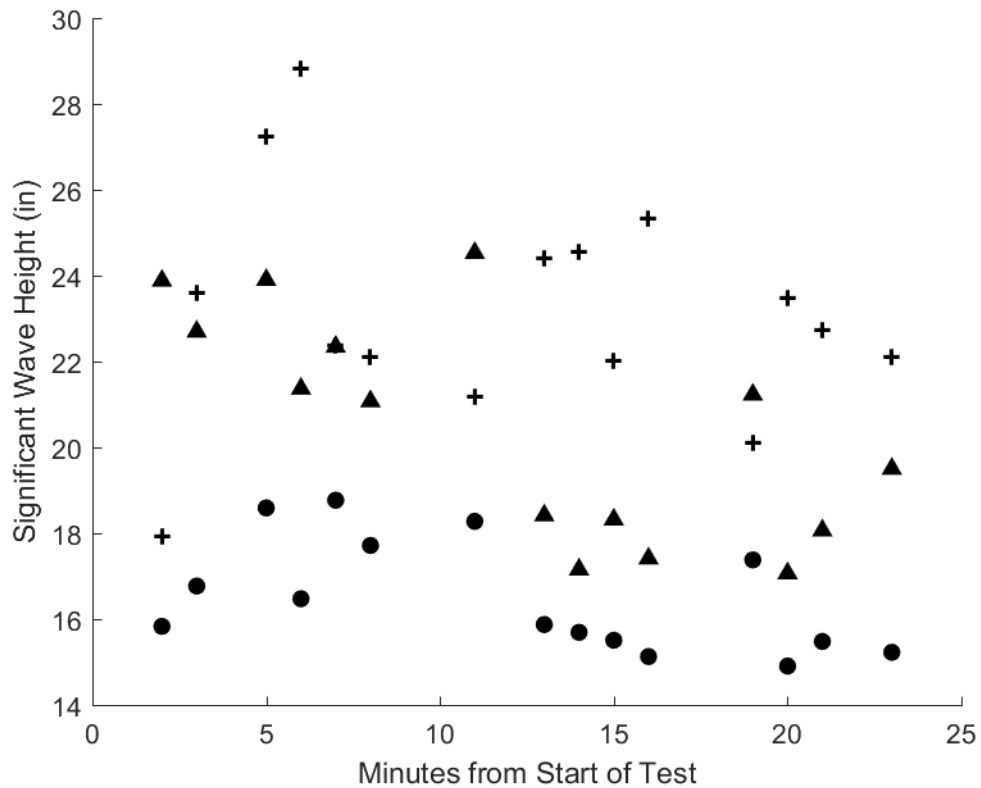


Figure F-12

Figure F-13: Plots of the significant wave heights for Test 5 of the WCM mounted to the skimmer and the raw data from the main bridge Banner. The plus signs indicate the significant wave height (H_{m0}) calculated statistically using the raw data from the WCM mounted to the skimmer. The triangles represent the significant wave height (H_{m0}) calculated statistically using a segment of time corresponding to the WCM data from the raw Banner data. The dots represent the wave heights calculated using the average of the top third wave height from the same segments ($H_{1/3}$). Each data point represents a calculation of the significant wave height from approximately 60 seconds of raw data.

Here it can be seen that the $H_{1/3}$ calculation is lower than the H_{m0} value for each time segment. The H_{m0} calculated using the WCM data is higher than the bridge data. This test is one where the waves were created by the 18-inch stroke and 18 CPM setting of the wave generator, which creates a large sinusoidal wave. We believe the discrepancies between the WCM and Banner measurement are due to lateral motion from the large elliptical motion of the wave not being considered by the algorithms. This is because we trained them on real, complex wave motion where most of the movement is in the heave.

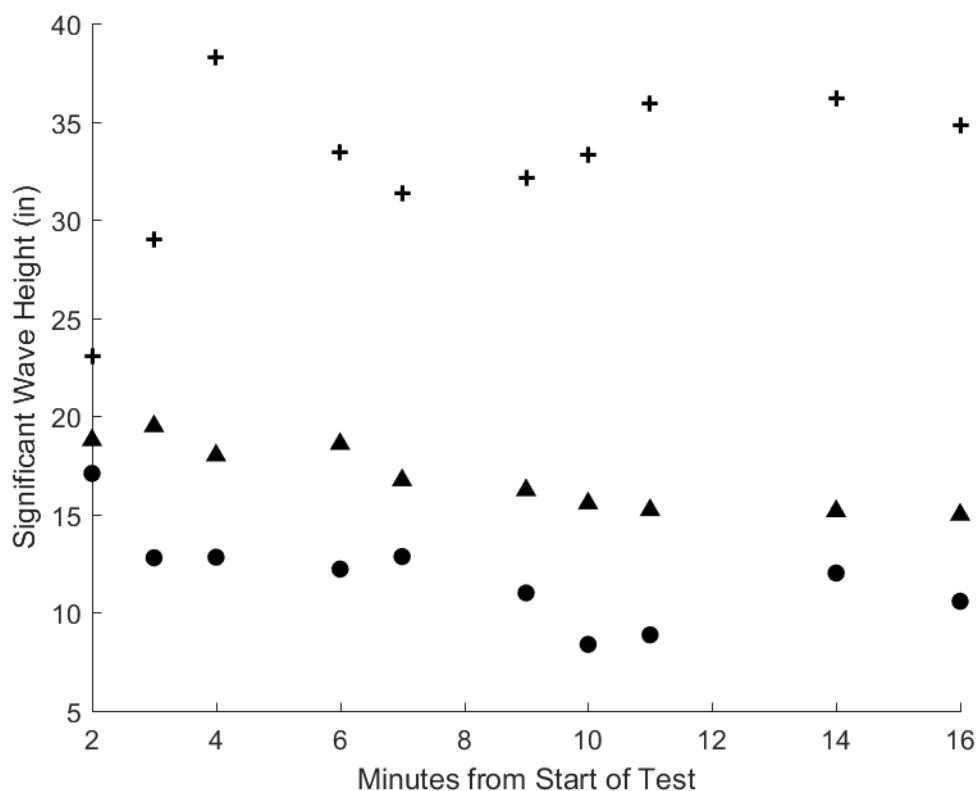


Figure F-13

Figure F-14: Plots of the significant wave heights for Test 5 of the WCM mounted to the skimmer and the raw data from the west auxiliary bridge Banner. The plus signs indicate the significant wave height (H_{m0}) calculated statistically using the raw data from the WCM mounted to the skimmer. The triangles represent the significant wave height (H_{m0}) calculated statistically using a segment of time corresponding to the WCM data from the raw Banner data. The dots represent the wave heights calculated using the average of the top third wave height from the same segments ($H_{1/3}$). Each data point represents a calculation of the significant wave height from approximately 60 seconds of raw data.

Here it can be seen that the $H_{1/3}$ calculation is lower than the H_{m0} value for each time segment. The H_{m0} calculated using the WCM data is higher than the bridge data. This test is one where the waves were created by the 18-inch stroke and 18 CPM setting of the wave generator, which creates a large sinusoidal wave. We believe the discrepancies between the WCM and Banner measurement are due to lateral motion from the large elliptical motion of the wave not being considered by the algorithms. This is because we trained them on real, complex wave motion where most of the movement is in the heave.

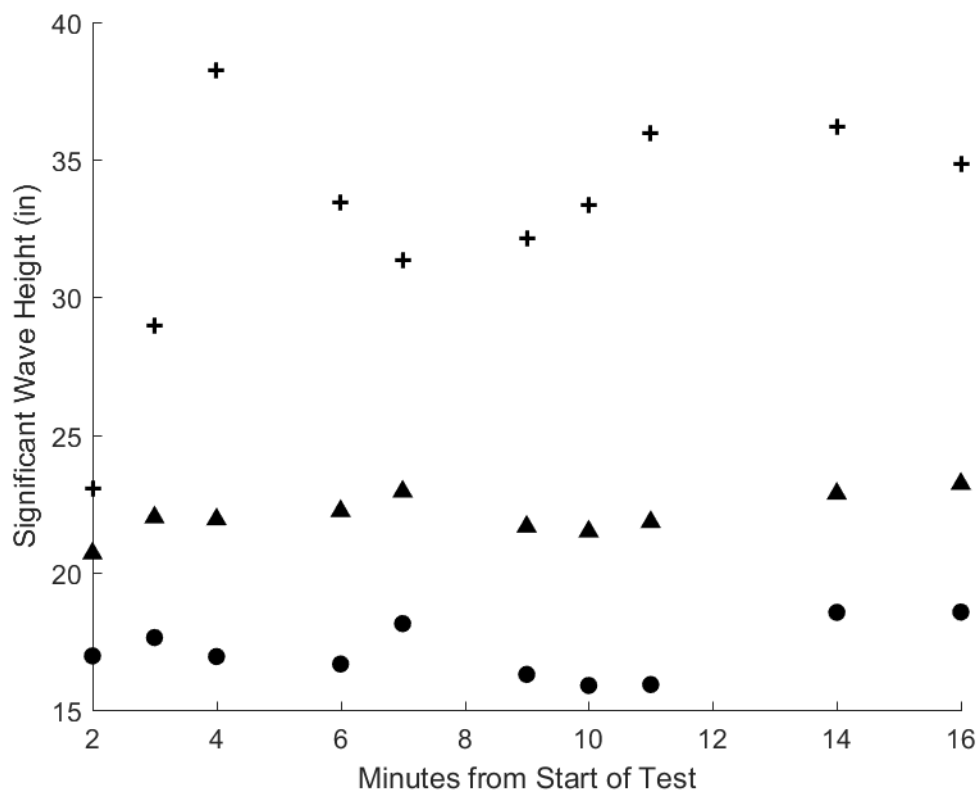


Figure F-14

Figure F-15: Plots of the significant wave heights for Test 5 of the WCM mounted to the skimmer and the raw data from the east auxiliary bridge Banner. The plus signs indicate the significant wave height (H_{m0}) calculated statistically using the raw data from the WCM mounted to the skimmer. The triangles represent the significant wave height (H_{m0}) calculated statistically using a segment of time corresponding to the WCM data from the raw Banner data. The dots represent the wave heights calculated using the average of the top third wave height from the same segments ($H_{1/3}$). Each data point represents a calculation of the significant wave height from approximately 60 seconds of raw data.

Here it can be seen that the $H_{1/3}$ calculation is lower than the H_{m0} value for each time segment. The H_{m0} calculated using the WCM data is higher than the bridge data. This test is one where the waves were created by the 18-inch stroke and 18 CPM setting of the wave generator, which creates a large sinusoidal wave. We believe the discrepancies between the WCM and Banner measurement are due to lateral motion from the large elliptical motion of the wave not being considered by the algorithms. This is because we trained them on real, complex wave motion where most of the movement is in the heave.

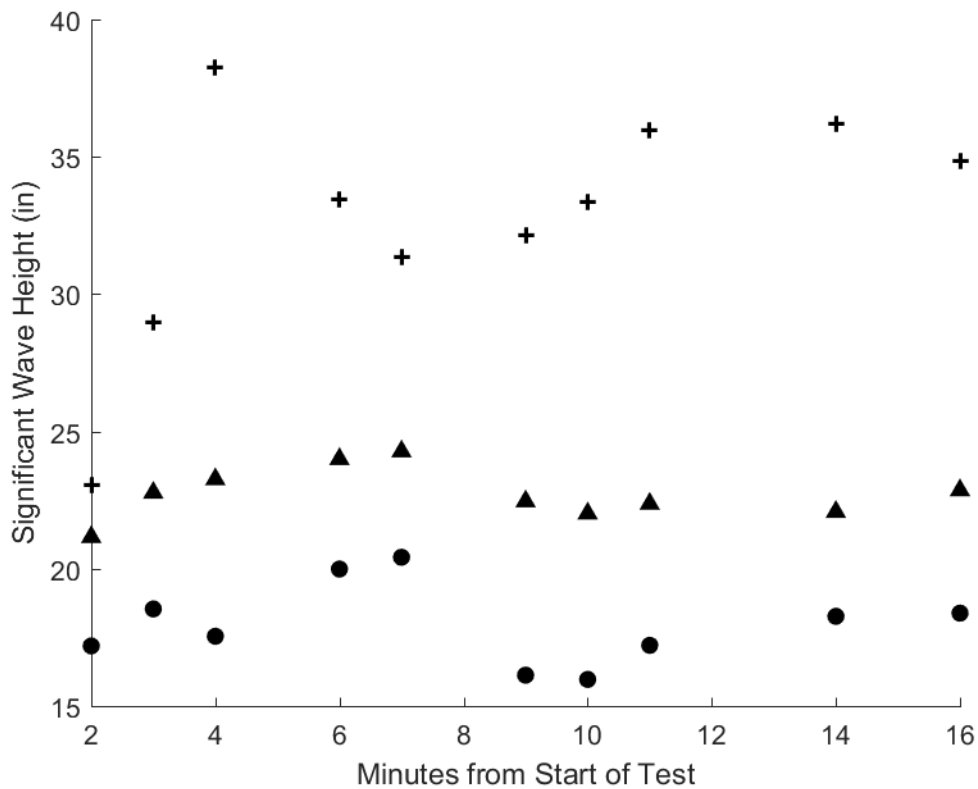


Figure F-15

Figure F-16: Plots of the significant wave heights for Test 6 of the WCM mounted to the skimmer and the raw data from the main bridge Banner. The plus signs indicate the significant wave height (H_{m0}) calculated statistically using the raw data from the WCM mounted to the skimmer. The triangles represent the significant wave height (H_{m0}) calculated statistically using a segment of time corresponding to the WCM data from the raw Banner data. The dots represent the wave heights calculated using the average of the top third wave height from the same segments ($H_{1/3}$). Each data point represents a calculation of the significant wave height from approximately 60 seconds of raw data.

Here it can be seen that the $H_{1/3}$ calculation is lower than the H_{m0} value for each time segment. The H_{m0} calculated using the WCM data is higher than the bridge data. This test is one where the waves were created by the 18-inch stroke and 18 CPM setting of the wave generator, which creates a large sinusoidal wave. We believe the discrepancies between the WCM and Banner measurement are due to lateral motion from the large elliptical motion of the wave not being considered by the algorithms. This is because we trained them on real, complex wave motion where most of the movement is in the heave.

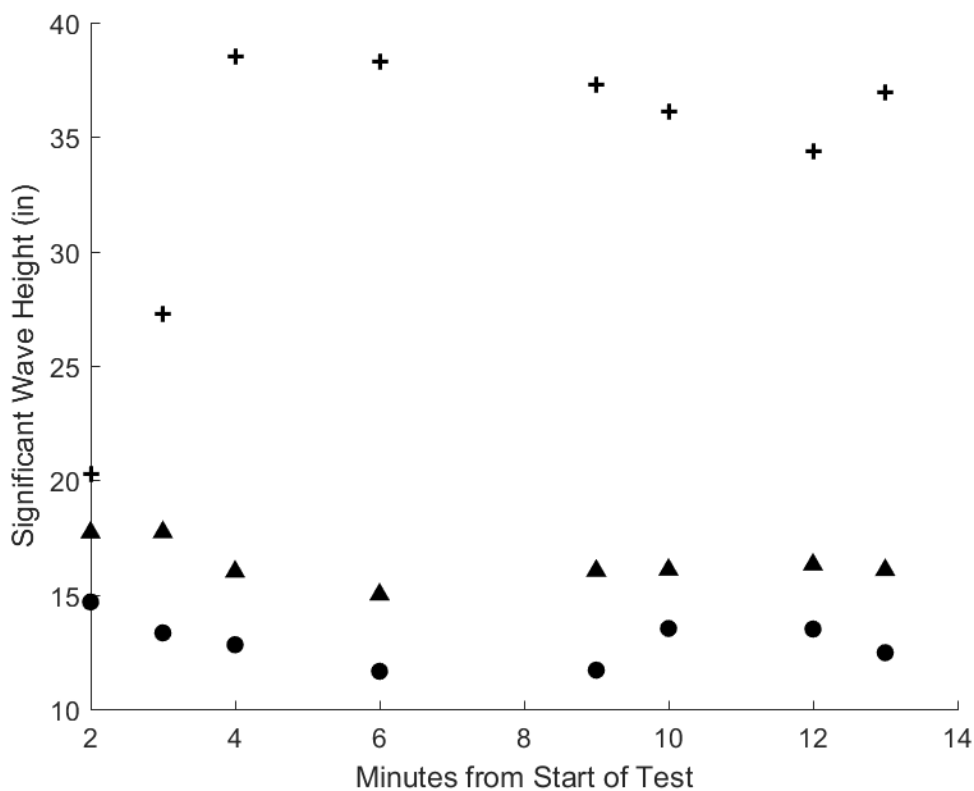


Figure F-16

Figure F-17: Plots of the significant wave heights for Test 6 of the WCM mounted to the skimmer and the raw data from the west auxiliary bridge Banner. The plus signs indicate the significant wave height (H_{m0}) calculated statistically using the raw data from the WCM mounted to the skimmer. The triangles represent the significant wave height (H_{m0}) calculated statistically using a segment of time corresponding to the WCM data from the raw Banner data. The dots represent the wave heights calculated using the average of the top third wave height from the same segments ($H_{1/3}$). Each data point represents a calculation of the significant wave height from approximately 60 seconds of raw data.

Here it can be seen that the $H_{1/3}$ calculation is lower than the H_{m0} value for each time segment. The H_{m0} calculated using the WCM data is higher than the bridge data. This test is one where the waves were created by the 18-inch stroke and 18 CPM setting of the wave generator, which creates a large sinusoidal wave. We believe the discrepancies between the WCM and Banner measurement are due to lateral motion from the large elliptical motion of the wave not being considered by the algorithms. This is because we trained them on real, complex wave motion where most of the movement is in the heave.

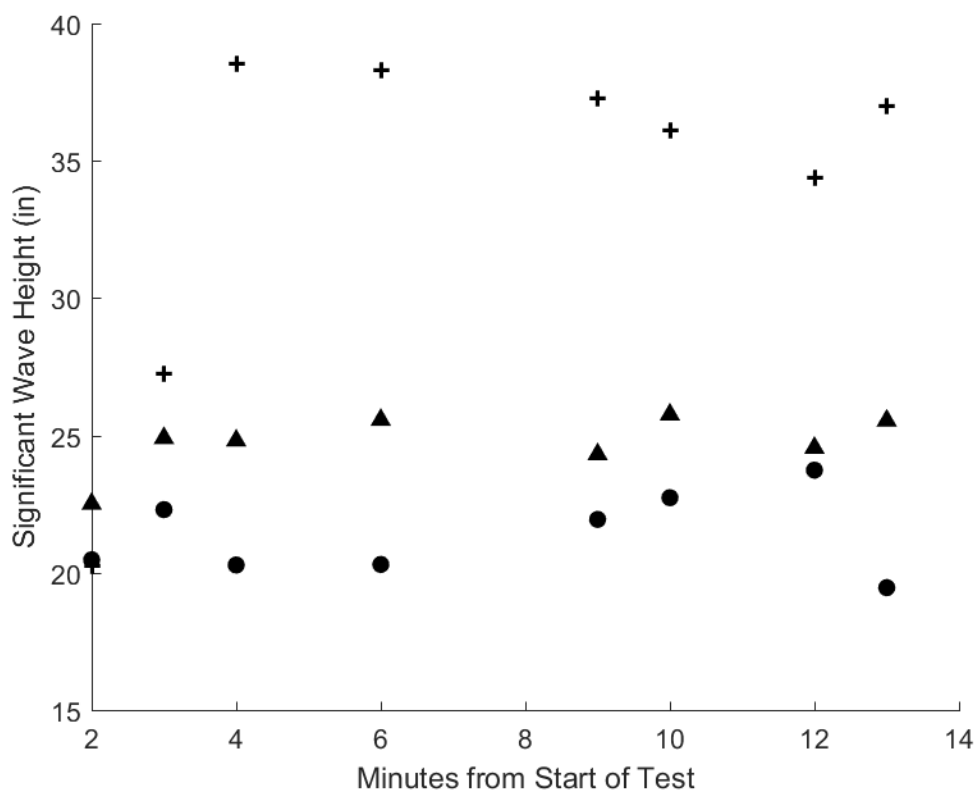


Figure F-17

Figure F-18: Plots of the significant wave heights for Test 6 of the WCM mounted to the skimmer and the raw data from the east auxiliary bridge Banner. The plus signs indicate the significant wave height (H_{m0}) calculated statistically using the raw data from the WCM mounted to the skimmer. The triangles represent the significant wave height (H_{m0}) calculated statistically using a segment of time corresponding to the WCM data from the raw Banner data. The dots represent the wave heights calculated using the average of the top third wave height from the same segments ($H_{1/3}$). Each data point represents a calculation of the significant wave height from approximately 60 seconds of raw data.

Here it can be seen that the $H_{1/3}$ calculation is lower than the H_{m0} value for each time segment. The H_{m0} calculated using the WCM data is higher than the bridge data. This test is one where the waves were created by the 18-inch stroke and 18 CPM setting of the wave generator, which creates a large sinusoidal wave. We believe the discrepancies between the WCM and Banner measurement are due to lateral motion from the large elliptical motion of the wave not being considered by the algorithms. This is because we trained them on real, complex wave motion where most of the movement is in the heave.

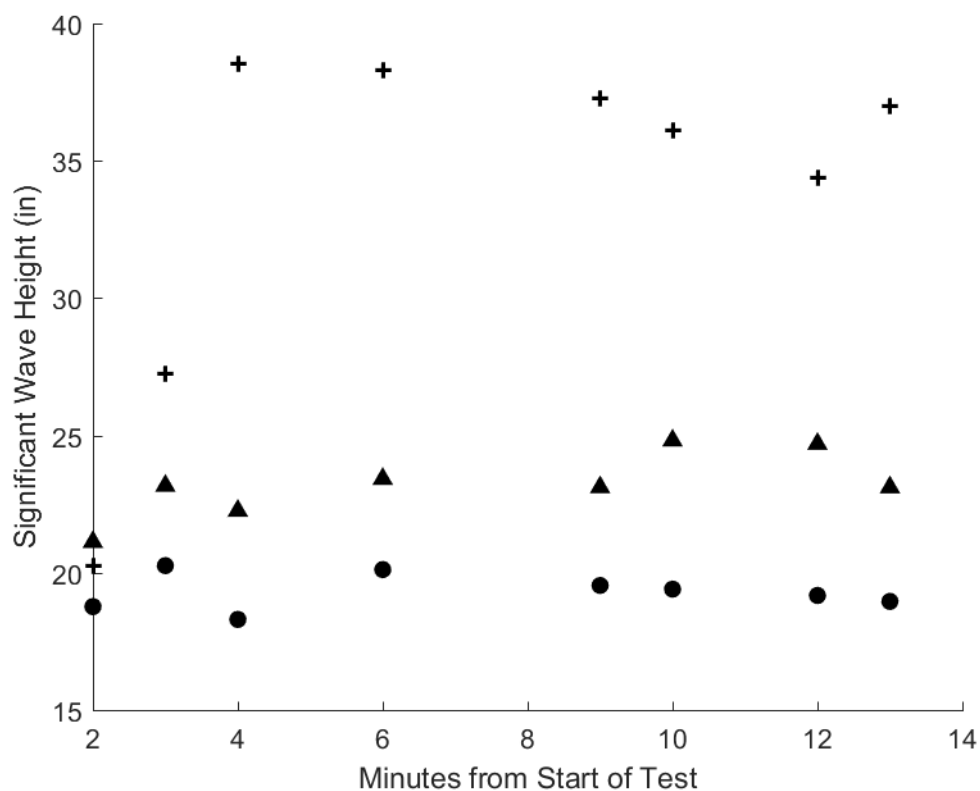


Figure F-18

Figure F-19: Plots of the significant wave heights for Test 7 of the WCM mounted to the skimmer and the raw data from the main bridge Banner. The plus signs indicate the significant wave height (H_{m0}) calculated statistically using the raw data from the WCM mounted to the skimmer. The triangles represent the significant wave height (H_{m0}) calculated statistically using a segment of time corresponding to the WCM data from the raw Banner data. The dots represent the wave heights calculated using the average of the top third wave height from the same segments ($H_{1/3}$). Each data point represents a calculation of the significant wave height from approximately 60 seconds of raw data.

Here it can be seen that the $H_{1/3}$ calculation is lower than the H_{m0} value calculated using the Banner data for each time segment. The H_{m0} calculated using the WCM data is generally within the 4-inch performance objective with the H_{m0} from the bridge data.

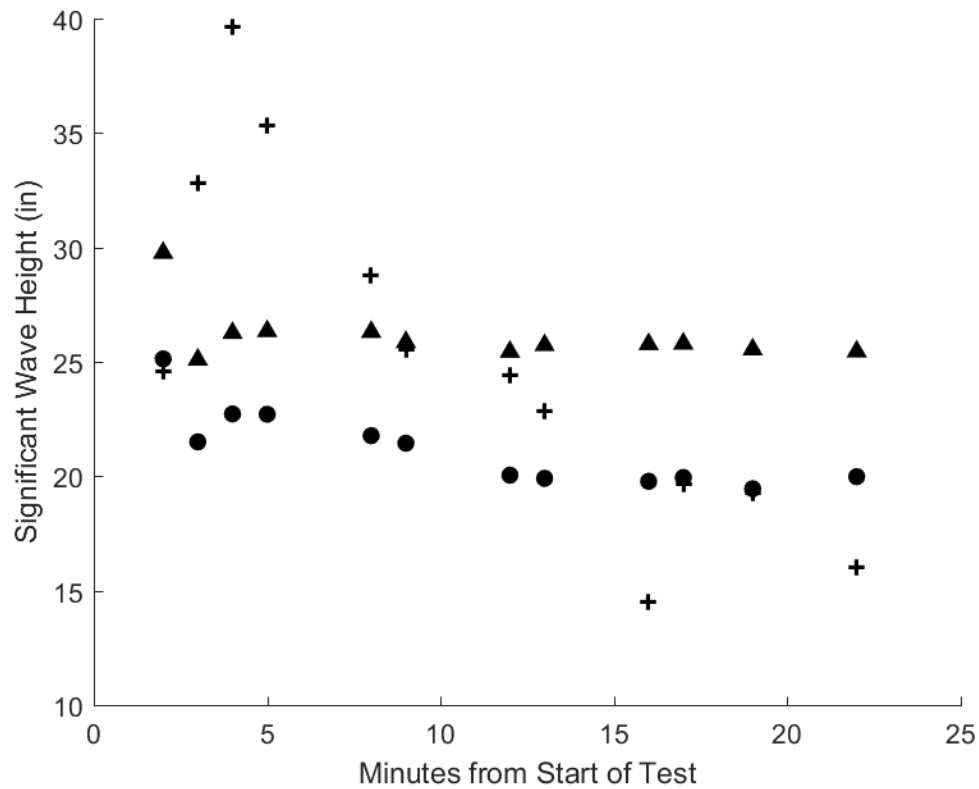


Figure F-19

Figure F-20: Plots of the significant wave heights for Test 7 of the WCM mounted to the skimmer and the raw data from the west auxiliary bridge Banner. The plus signs indicate the significant wave height (H_{m0}) calculated statistically using the raw data from the WCM mounted to the skimmer. The triangles represent the significant wave height (H_{m0}) calculated statistically using a segment of time corresponding to the WCM data from the raw Banner data. The dots represent the wave heights calculated using the average of the top third wave height from the same segments ($H_{1/3}$). Each data point represents a calculation of the significant wave height from approximately 60 seconds of raw data.

Here it can be seen that the $H_{1/3}$ calculation is lower than the H_{m0} value calculated using the Banner data for each time segment. The H_{m0} calculated using the WCM data is generally within the 4-inch performance objective with the H_{m0} from the bridge data.

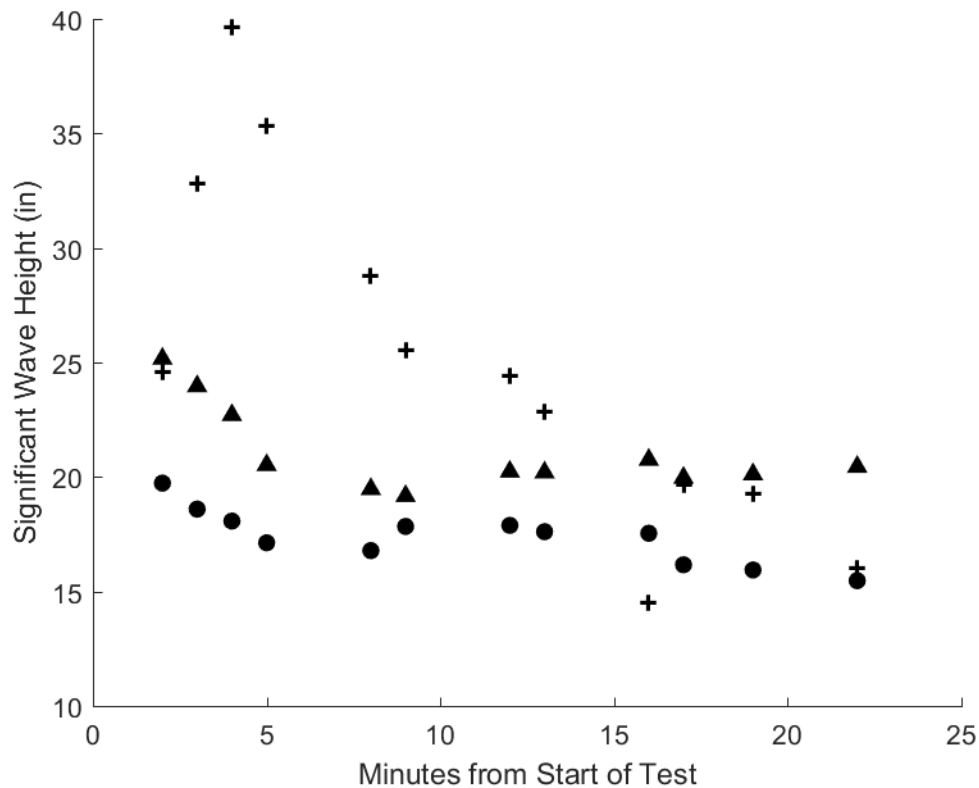


Figure F-20

Figure F-21: Plots of the significant wave heights for Test 7 of the WCM mounted to the skimmer and the raw data from the east auxiliary bridge Banner. The plus signs indicate the significant wave height (H_{m0}) calculated statistically using the raw data from the WCM mounted to the skimmer. The triangles represent the significant wave height (H_{m0}) calculated statistically using a segment of time corresponding to the WCM data from the raw Banner data. The dots represent the wave heights calculated using the average of the top third wave height from the same segments ($H_{1/3}$). Each data point represents a calculation of the significant wave height from approximately 60 seconds of raw data.

Here it can be seen that the $H_{1/3}$ calculation is lower than the H_{m0} value calculated using the Banner data for each time segment. The H_{m0} calculated using the WCM data is generally within the 4-inch performance objective with the H_{m0} from the bridge data.

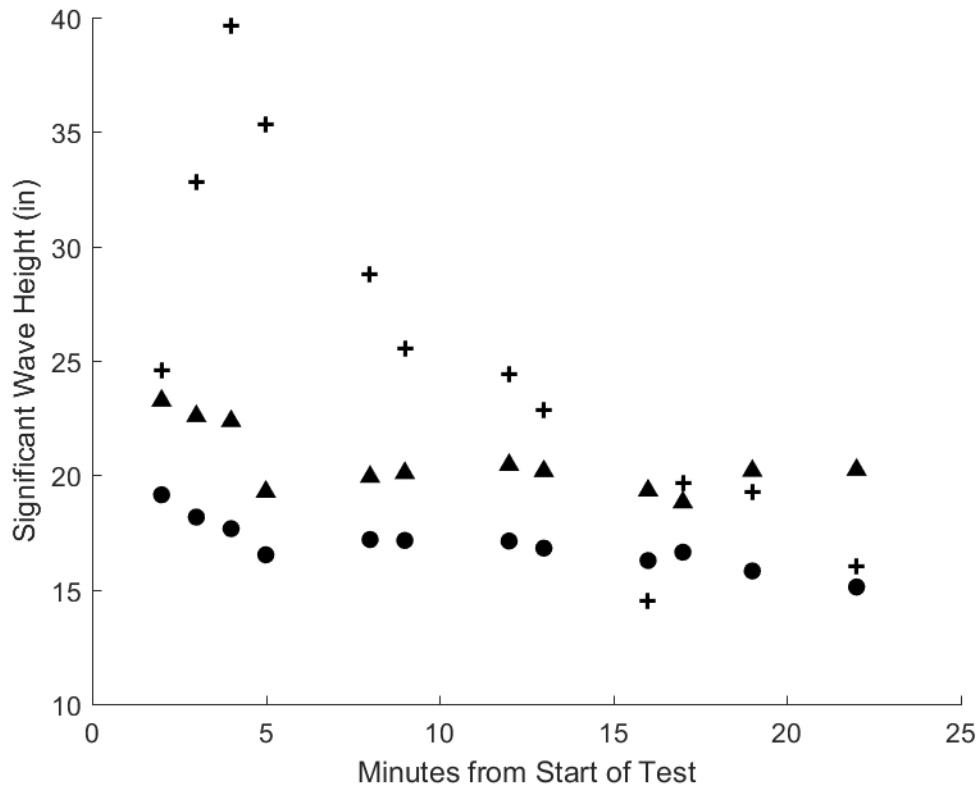


Figure F-21

Figure F-22: Plots of the significant wave heights for Test 8 of the WCM mounted to the skimmer and the raw data from the main bridge Banner. The plus signs indicate the significant wave height (H_{m0}) calculated statistically using the raw data from the WCM mounted to the skimmer. The triangles represent the significant wave height (H_{m0}) calculated statistically using a segment of time corresponding to the WCM data from the raw Banner data. The dots represent the wave heights calculated using the average of the top third wave height from the same segments ($H_{1/3}$). Each data point represents a calculation of the significant wave height from approximately 60 seconds of raw data.

Here it can be seen that the $H_{1/3}$ calculation is lower than the H_{m0} value calculated using the Banner data for each time segment. The H_{m0} calculated using the WCM data is generally within the 4-inch performance objective with the H_{m0} from the bridge data.

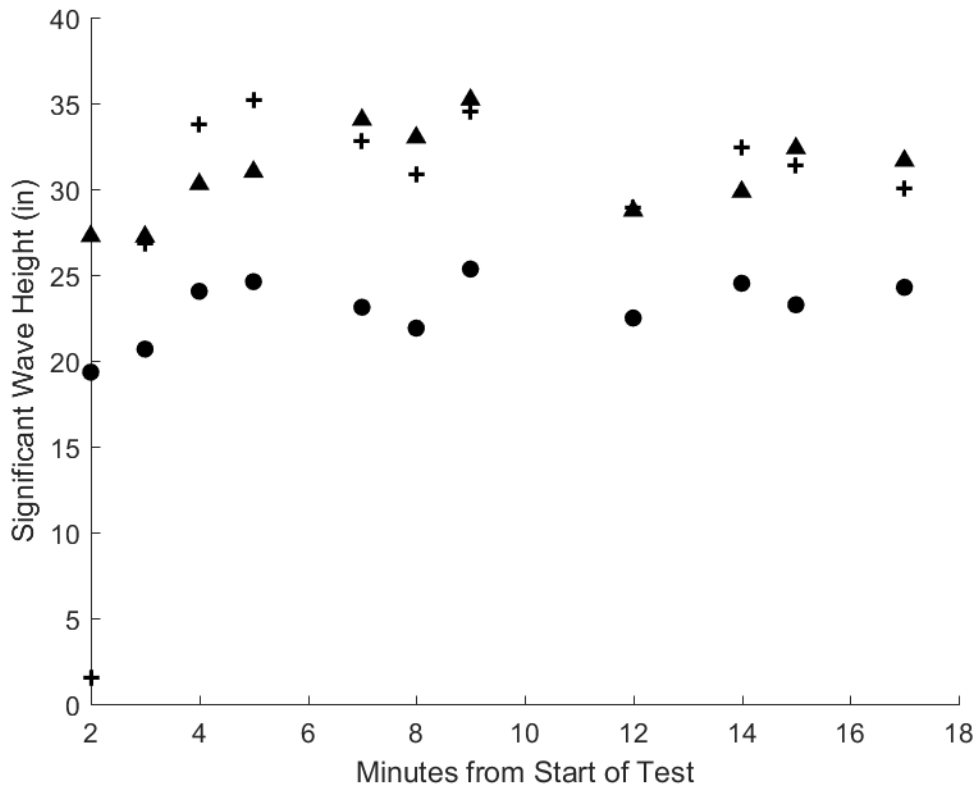


Figure F-22

Figure F-23: Plots of the significant wave heights for Test 8 of the WCM mounted to the skimmer and the raw data from the west auxiliary bridge Banner. The plus signs indicate the significant wave height (H_{m0}) calculated statistically using the raw data from the WCM mounted to the skimmer. The triangles represent the significant wave height (H_{m0}) calculated statistically using a segment of time corresponding to the WCM data from the raw Banner data. The dots represent the wave heights calculated using the average of the top third wave height from the same segments ($H_{1/3}$). Each data point represents a calculation of the significant wave height from approximately 60 seconds of raw data.

Here it can be seen that the $H_{1/3}$ calculation is lower than the H_{m0} value calculated using the Banner data for each time segment. The H_{m0} calculated using the WCM data is generally within the 4-inch performance objective with the H_{m0} from the bridge data.

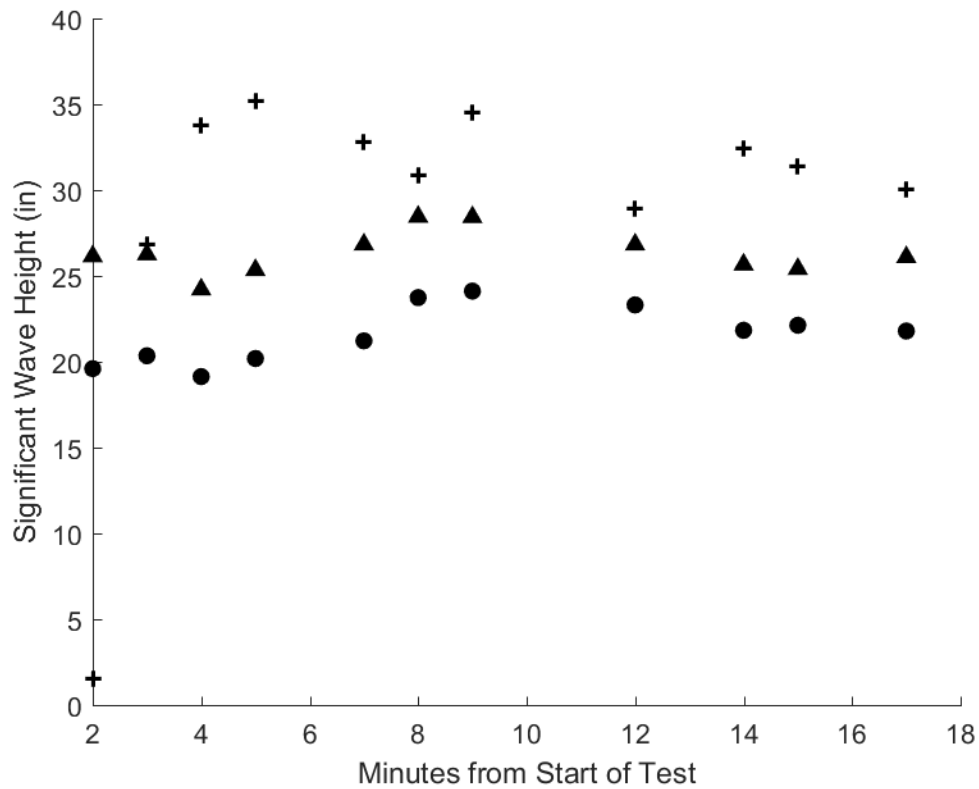


Figure F-23

Figure F-24: Plots of the significant wave heights for Test 8 of the WCM mounted to the skimmer and the raw data from the east auxiliary bridge Banner. The plus signs indicate the significant wave height (H_{m0}) calculated statistically using the raw data from the WCM mounted to the skimmer. The triangles represent the significant wave height (H_{m0}) calculated statistically using a segment of time corresponding to the WCM data from the raw Banner data. The dots represent the wave heights calculated using the average of the top third wave height from the same segments ($H_{1/3}$). Each data point represents a calculation of the significant wave height from approximately 60 seconds of raw data.

Here it can be seen that the $H_{1/3}$ calculation is lower than the H_{m0} value calculated using the Banner data for each time segment. The H_{m0} calculated using the WCM data is generally within the 4-inch performance objective with the H_{m0} from the bridge data.

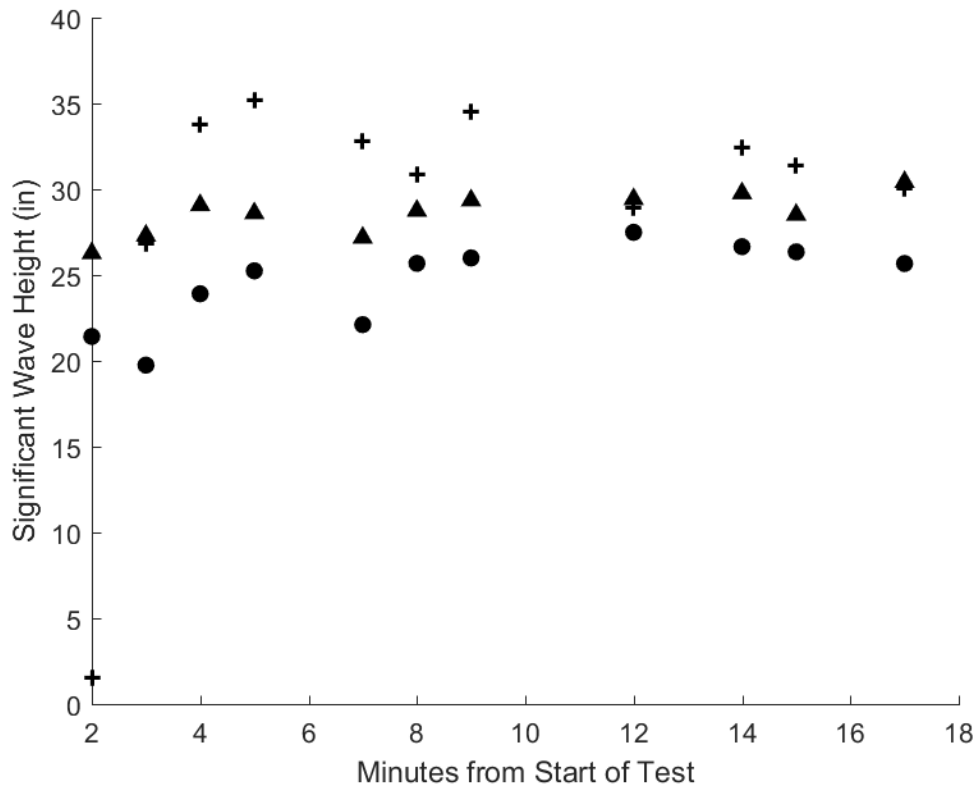


Figure F-24

Figure F-25: Plots of the significant wave heights for Test 9 of the WCM mounted to the skimmer and the raw data from the main bridge Banner. The plus signs indicate the significant wave height (H_{m0}) calculated statistically using the raw data from the WCM mounted to the skimmer. The triangles represent the significant wave height (H_{m0}) calculated statistically using a segment of time corresponding to the WCM data from the raw Banner data. The dots represent the wave heights calculated using the average of the top third wave height from the same segments ($H_{1/3}$). Each data point represents a calculation of the significant wave height from approximately 60 seconds of raw data.

Here it can be seen that the $H_{1/3}$ calculation is lower than the H_{m0} value calculated using the Banner data for each time segment. The H_{m0} calculated using the WCM data is generally within the 4-inch performance objective with the H_{m0} from the bridge data.

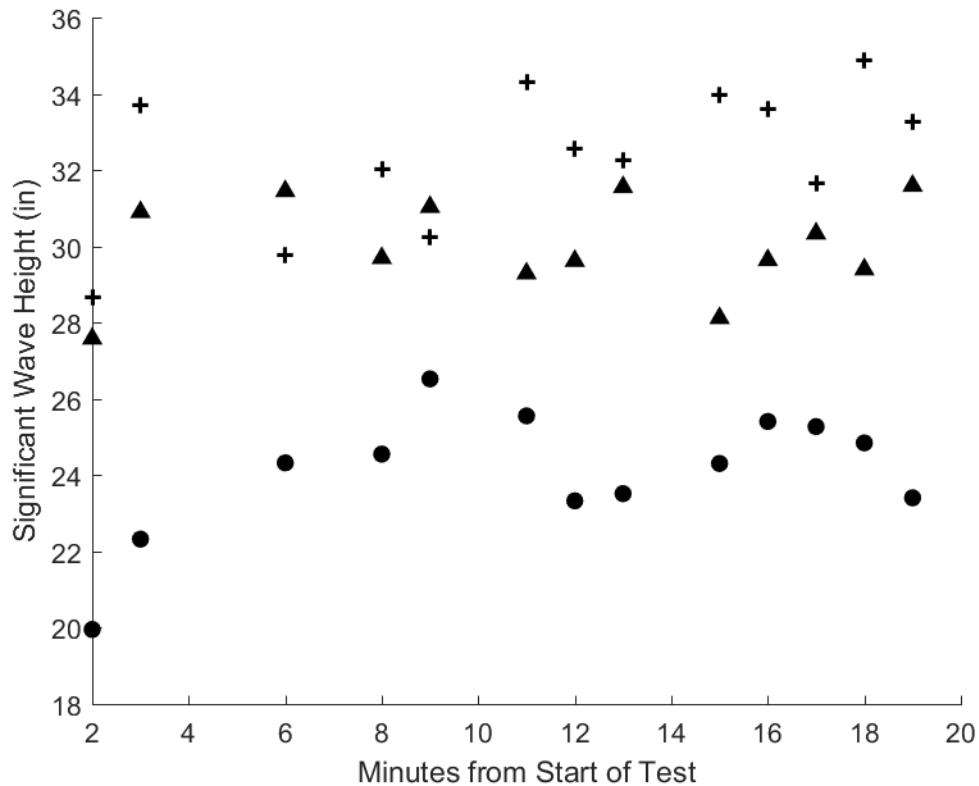


Figure F-25

Figure F-26: Plots of the significant wave heights for Test 9 of the WCM mounted to the skimmer and the raw data from the west auxiliary bridge Banner. The plus signs indicate the significant wave height (H_{m0}) calculated statistically using the raw data from the WCM mounted to the skimmer. The triangles represent the significant wave height (H_{m0}) calculated statistically using a segment of time corresponding to the WCM data from the raw Banner data. The dots represent the wave heights calculated using the average of the top third wave height from the same segments ($H_{1/3}$). Each data point represents a calculation of the significant wave height from approximately 60 seconds of raw data.

Here it can be seen that the $H_{1/3}$ calculation is lower than the H_{m0} value calculated using the Banner data for each time segment. The H_{m0} calculated using the WCM data is generally within the 4-inch performance objective with the H_{m0} from the bridge data.

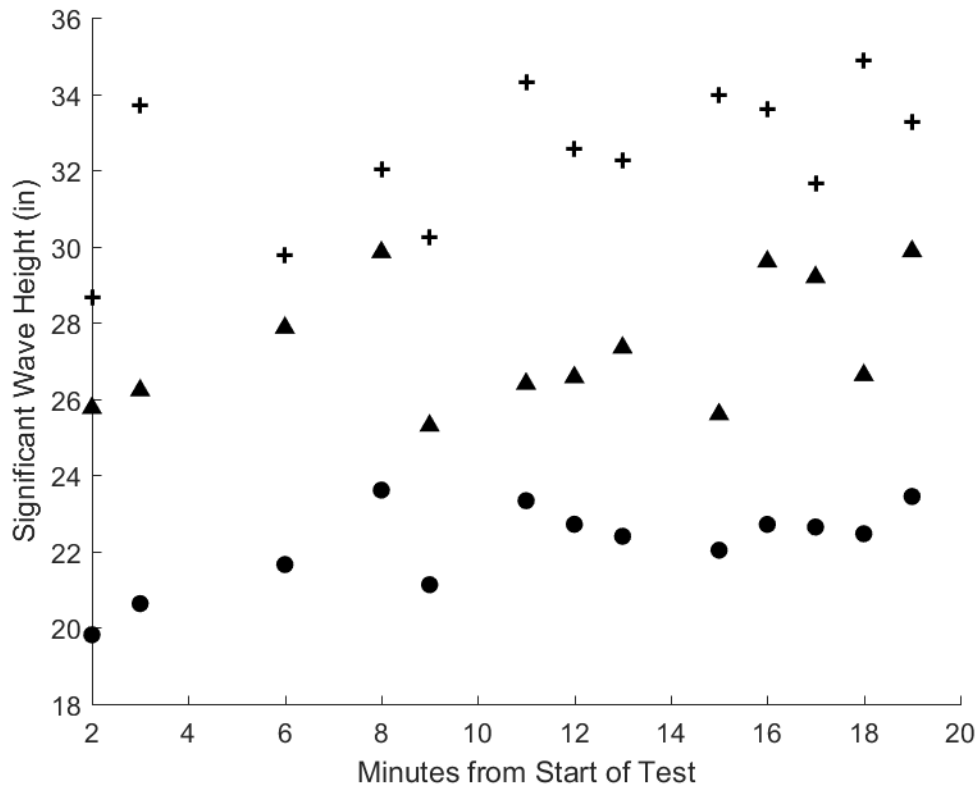


Figure F-26

Figure F-27: Plots of the significant wave heights for Test 9 of the WCM mounted to the skimmer and the raw data from the east auxiliary bridge Banner. The plus signs indicate the significant wave height (H_{m0}) calculated statistically using the raw data from the WCM mounted to the skimmer. The triangles represent the significant wave height (H_{m0}) calculated statistically using a segment of time corresponding to the WCM data from the raw Banner data. The dots represent the wave heights calculated using the average of the top third wave height from the same segments ($H_{1/3}$). Each data point represents a calculation of the significant wave height from approximately 60 seconds of raw data.

Here it can be seen that the $H_{1/3}$ calculation is lower than the H_{m0} value calculated using the Banner data for each time segment. The H_{m0} calculated using the WCM data is generally within the 4-inch performance objective with the H_{m0} from the bridge data.

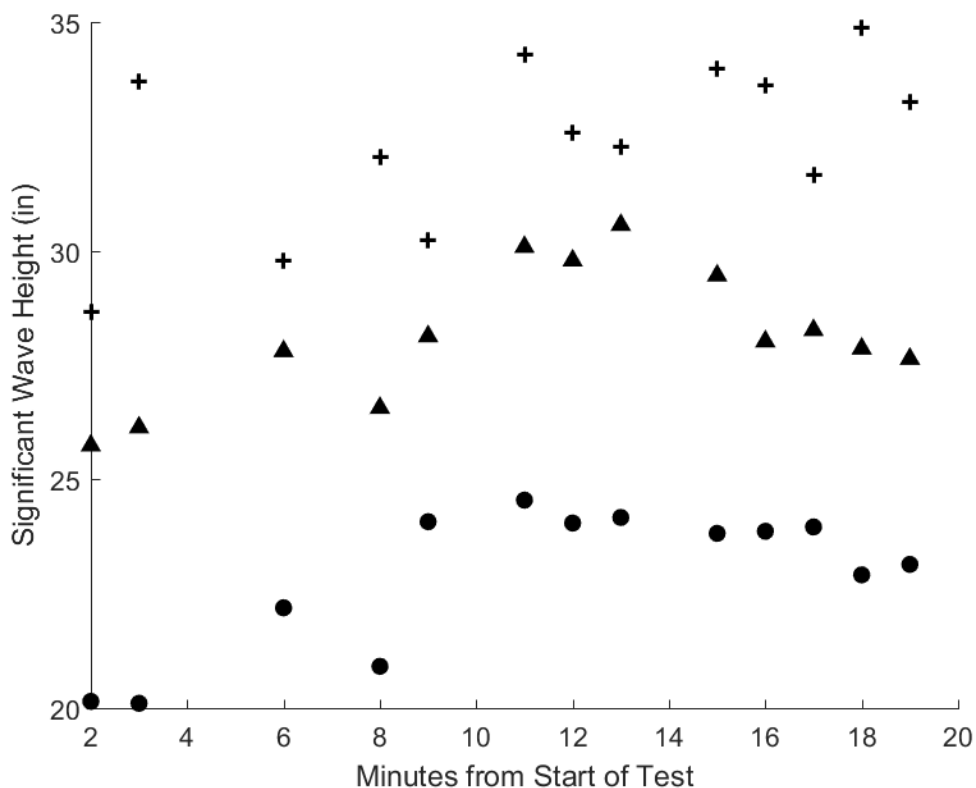


Figure F-27

Figure F-28: Plots of the significant wave heights for Test 10 of the WCM mounted to the skimmer and the raw data from the main bridge Banner. The plus signs indicate the significant wave height (H_{m0}) calculated statistically using the raw data from the WCM mounted to the skimmer. The triangles represent the significant wave height (H_{m0}) calculated statistically using a segment of time corresponding to the WCM data from the raw Banner data. The dots represent the wave heights calculated using the average of the top third wave height from the same segments ($H_{1/3}$). Each data point represents a calculation of the significant wave height from approximately 60 seconds of raw data.

Here it can be seen that the $H_{1/3}$ calculation is lower than the H_{m0} value calculated using the Banner data for each time segment. The H_{m0} calculated using the WCM data is generally within the 4-inch performance objective with the H_{m0} from the bridge data.

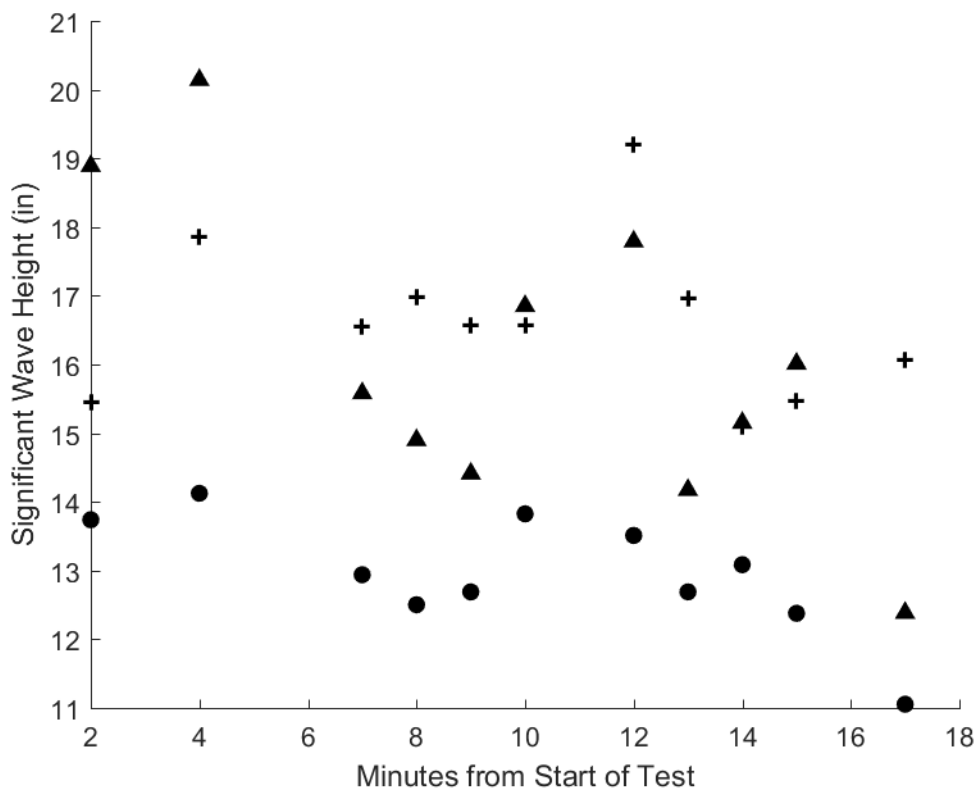


Figure F-28

Figure F-29: Plots of the significant wave heights for Test 10 of the WCM mounted to the skimmer and the raw data from the west auxiliary bridge Banner. The plus signs indicate the significant wave height (H_{m0}) calculated statistically using the raw data from the WCM mounted to the skimmer. The triangles represent the significant wave height (H_{m0}) calculated statistically using a segment of time corresponding to the WCM data from the raw Banner data. The dots represent the wave heights calculated using the average of the top third wave height from the same segments ($H_{1/3}$). Each data point represents a calculation of the significant wave height from approximately 60 seconds of raw data.

Here it can be seen that the $H_{1/3}$ calculation is lower than the H_{m0} value calculated using the Banner data for each time segment. The H_{m0} calculated using the WCM data is generally within the 4-inch performance objective with the H_{m0} from the bridge data.

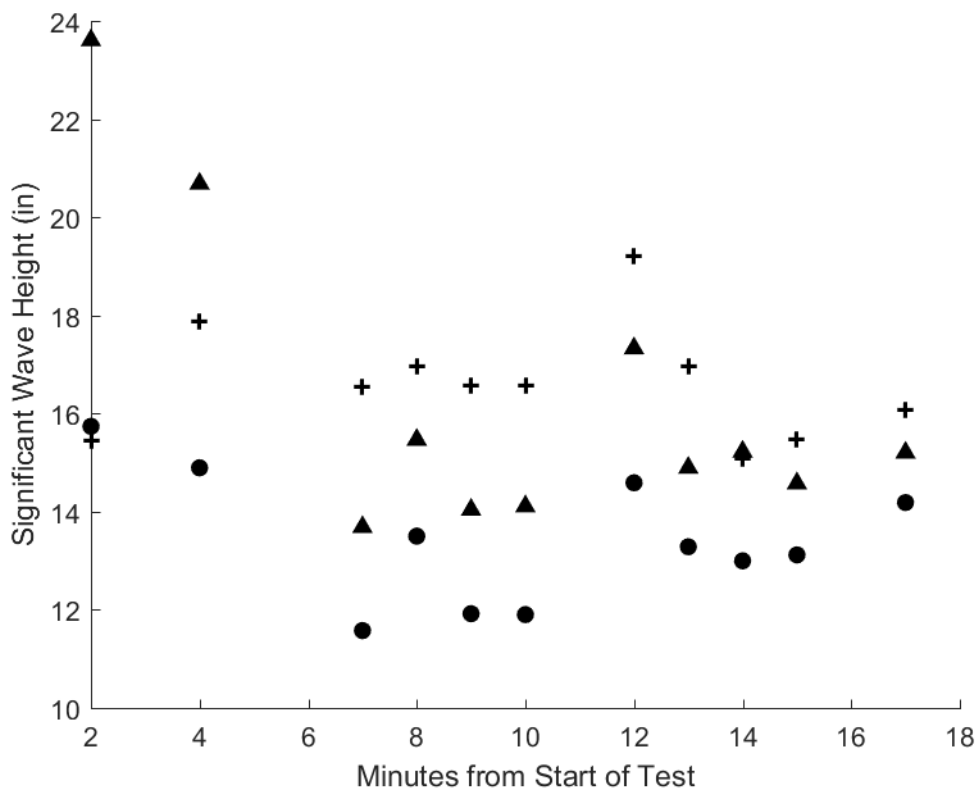


Figure F-29

Figure F-30: Plots of the significant wave heights for Test 10 of the WCM mounted to the skimmer and the raw data from the east auxiliary bridge Banner. The plus signs indicate the significant wave height (H_{m0}) calculated statistically using the raw data from the WCM mounted to the skimmer. The triangles represent the significant wave height (H_{m0}) calculated statistically using a segment of time corresponding to the WCM data from the raw Banner data. The dots represent the wave heights calculated using the average of the top third wave height from the same segments ($H_{1/3}$). Each data point represents a calculation of the significant wave height from approximately 60 seconds of raw data.

Here it can be seen that the $H_{1/3}$ calculation is lower than the H_{m0} value calculated using the Banner data for each time segment. The H_{m0} calculated using the WCM data is generally within the 4-inch performance objective with the H_{m0} from the bridge data.

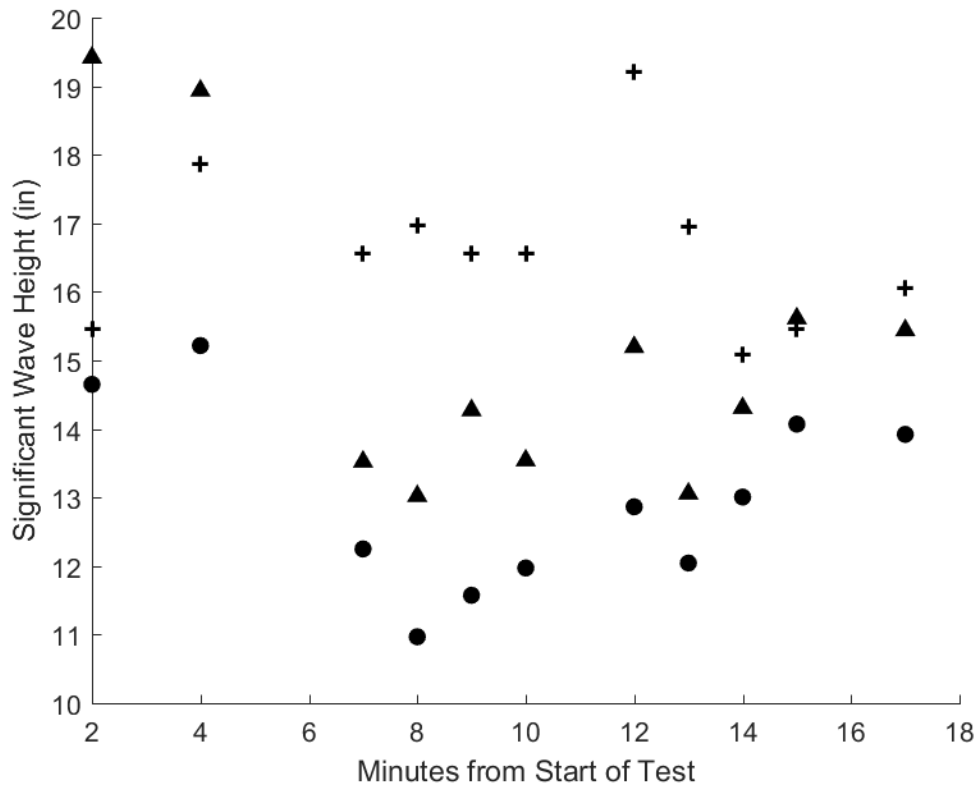


Figure F-30

Figure F-31: Plots of the significant wave heights for Test 11 of the WCM mounted to the skimmer and the raw data from the main bridge Banner. The plus signs indicate the significant wave height (H_{m0}) calculated statistically using the raw data from the WCM mounted to the skimmer. The triangles represent the significant wave height (H_{m0}) calculated statistically using a segment of time corresponding to the WCM data from the raw Banner data. The dots represent the wave heights calculated using the average of the top third wave height from the same segments ($H_{1/3}$). Each data point represents a calculation of the significant wave height from approximately 60 seconds of raw data.

Here it can be seen that the $H_{1/3}$ calculation is lower than the H_{m0} value calculated using the Banner data for each time segment. The H_{m0} calculated using the WCM data is generally within the 4-inch performance objective with the H_{m0} from the bridge data.

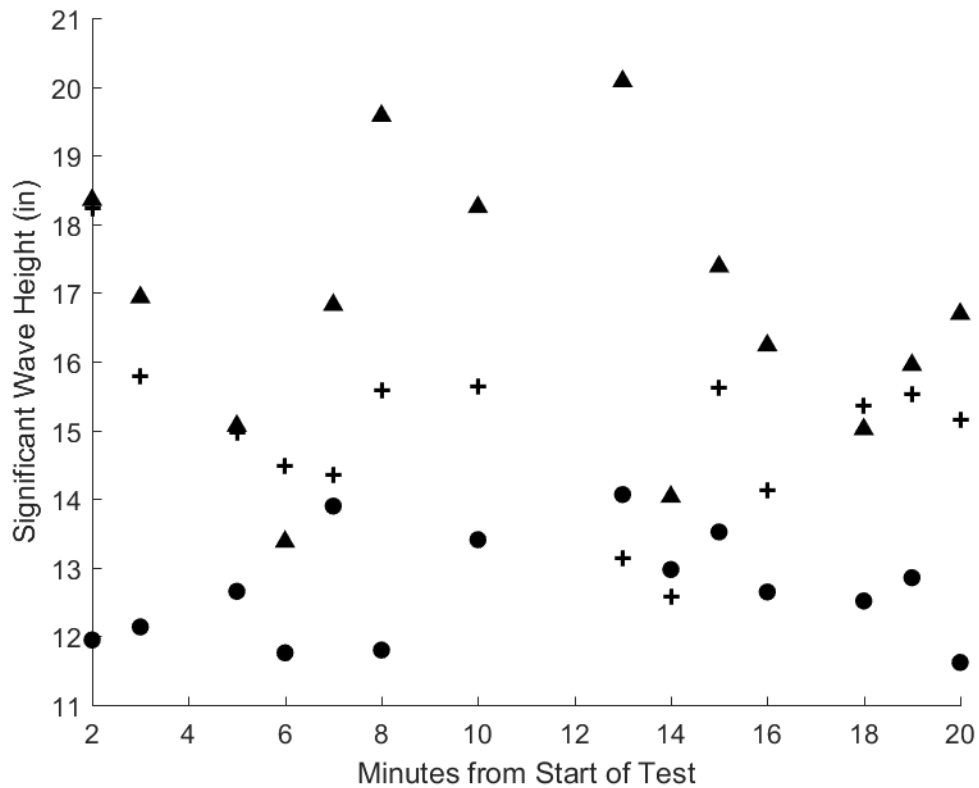


Figure F-31

Figure F-32: Plots of the significant wave heights for Test 11 of the WCM mounted to the skimmer and the raw data from the west auxiliary bridge Banner. The plus signs indicate the significant wave height (H_{m0}) calculated statistically using the raw data from the WCM mounted to the skimmer. The triangles represent the significant wave height (H_{m0}) calculated statistically using a segment of time corresponding to the WCM data from the raw Banner data. The dots represent the wave heights calculated using the average of the top third wave height from the same segments ($H_{1/3}$). Each data point represents a calculation of the significant wave height from approximately 60 seconds of raw data.

Here it can be seen that the $H_{1/3}$ calculation is lower than the H_{m0} value calculated using the Banner data for each time segment. The H_{m0} calculated using the WCM data is generally within the 4-inch performance objective with the H_{m0} from the bridge data.

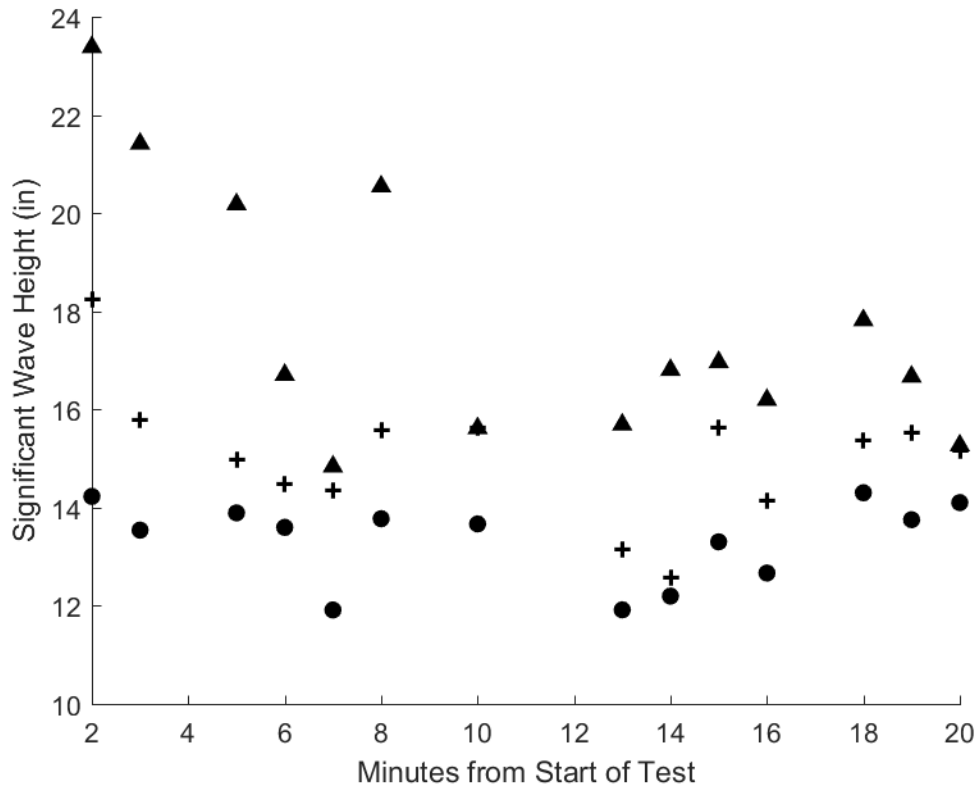


Figure F-32

Figure F-33: Plots of the significant wave heights for Test 11 of the WCM mounted to the skimmer and the raw data from the east auxiliary bridge Banner. The plus signs indicate the significant wave height (H_{m0}) calculated statistically using the raw data from the WCM mounted to the skimmer. The triangles represent the significant wave height (H_{m0}) calculated statistically using a segment of time corresponding to the WCM data from the raw Banner data. The dots represent the wave heights calculated using the average of the top third wave height from the same segments ($H_{1/3}$). Each data point represents a calculation of the significant wave height from approximately 60 seconds of raw data.

Here it can be seen that the $H_{1/3}$ calculation is lower than the H_{m0} value calculated using the Banner data for each time segment. The H_{m0} calculated using the WCM data is generally within the 4-inch performance objective with the H_{m0} from the bridge data.

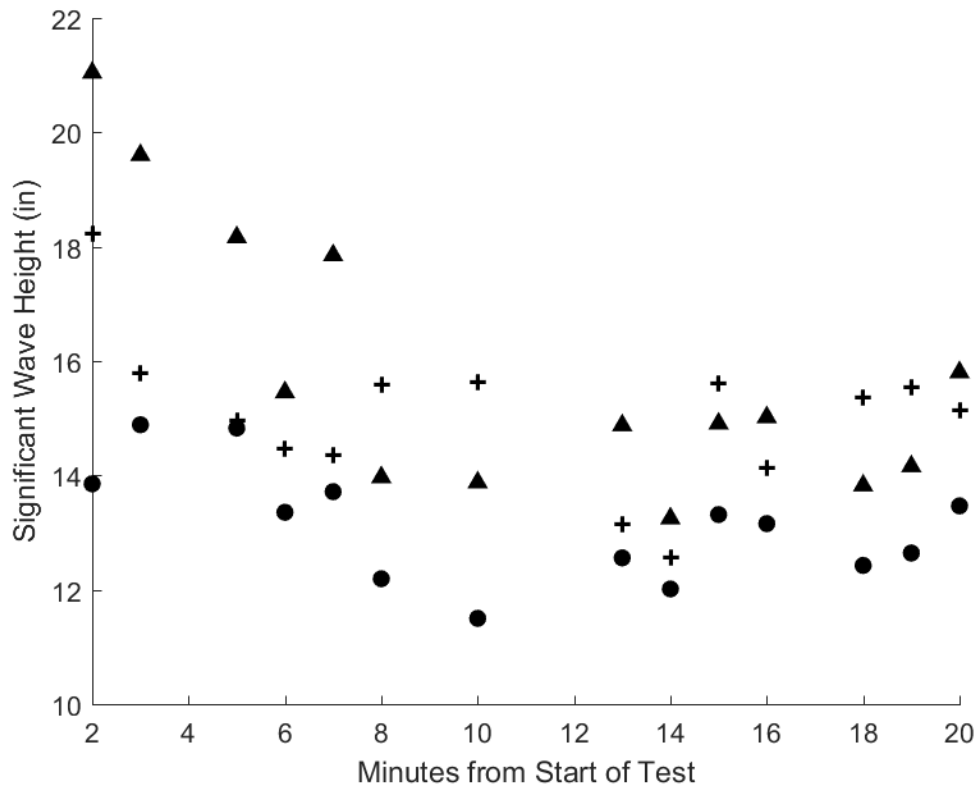


Figure F-33

Figure F-34: Plots of the significant wave heights for Test 12 of the WCM mounted to the skimmer and the raw data from the main bridge Banner. The plus signs indicate the significant wave height (H_{m0}) calculated statistically using the raw data from the WCM mounted to the skimmer. The triangles represent the significant wave height (H_{m0}) calculated statistically using a segment of time corresponding to the WCM data from the raw Banner data. The dots represent the wave heights calculated using the average of the top third wave height from the same segments ($H_{1/3}$). Each data point represents a calculation of the significant wave height from approximately 60 seconds of raw data.

Here it can be seen that the $H_{1/3}$ calculation is lower than the H_{m0} value calculated using the Banner data for each time segment. The H_{m0} calculated using the WCM data is generally within the 4-inch performance objective with the H_{m0} from the bridge data.

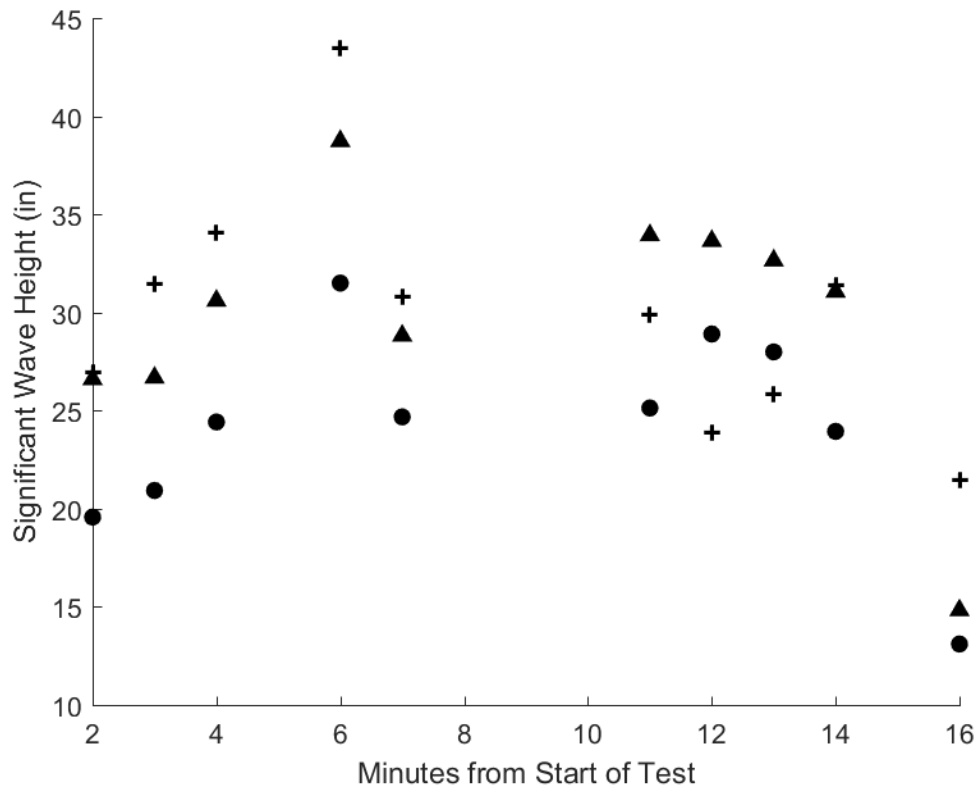


Figure F-34

Figure F-35: Plots of the significant wave heights for Test 12 of the WCM mounted to the skimmer and the raw data from the west auxiliary bridge Banner. The plus signs indicate the significant wave height (H_{m0}) calculated statistically using the raw data from the WCM mounted to the skimmer. The triangles represent the significant wave height (H_{m0}) calculated statistically using a segment of time corresponding to the WCM data from the raw Banner data. The dots represent the wave heights calculated using the average of the top third wave height from the same segments ($H_{1/3}$). Each data point represents a calculation of the significant wave height from approximately 60 seconds of raw data.

Here it can be seen that the $H_{1/3}$ calculation is lower than the H_{m0} value calculated using the Banner data for each time segment. The H_{m0} calculated using the WCM data is generally within the 4-inch performance objective with the H_{m0} from the bridge data.

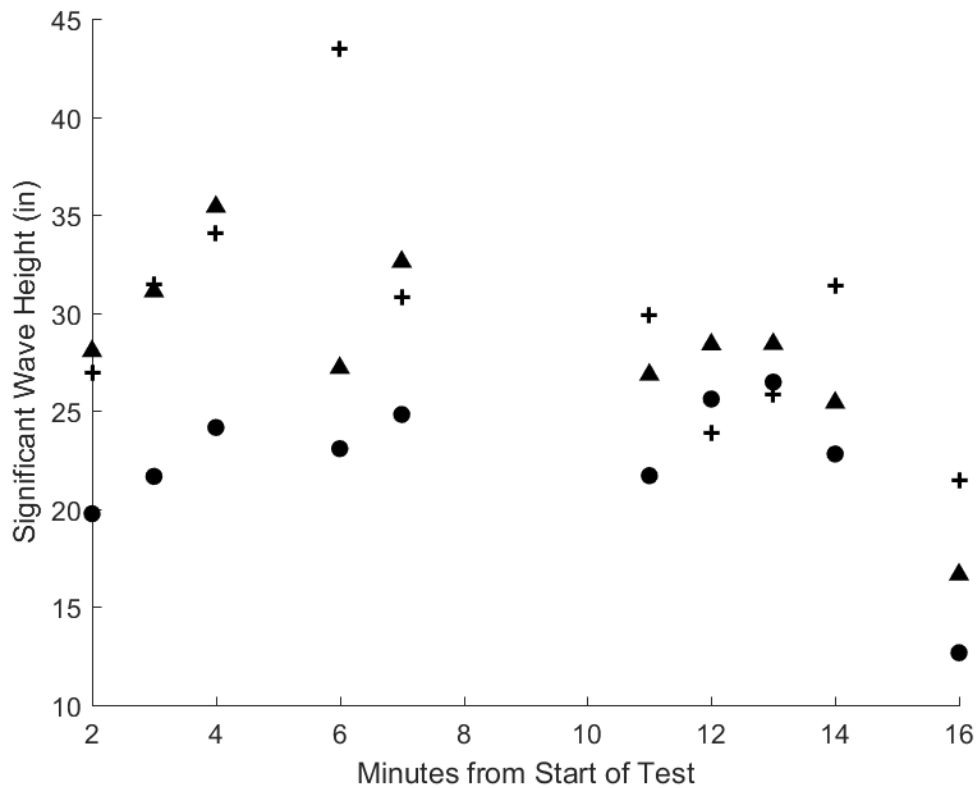


Figure F-35

Figure F-36: Plots of the significant wave heights for Test 12 of the WCM mounted to the skimmer and the raw data from the east auxiliary bridge Banner. The plus signs indicate the significant wave height (H_{m0}) calculated statistically using the raw data from the WCM mounted to the skimmer. The triangles represent the significant wave height (H_{m0}) calculated statistically using a segment of time corresponding to the WCM data from the raw Banner data. The dots represent the wave heights calculated using the average of the top third wave height from the same segments ($H_{1/3}$). Each data point represents a calculation of the significant wave height from approximately 60 seconds of raw data.

Here it can be seen that the $H_{1/3}$ calculation is lower than the H_{m0} value calculated using the Banner data for each time segment. The H_{m0} calculated using the WCM data is generally within the 4-inch performance objective with the H_{m0} from the bridge data.

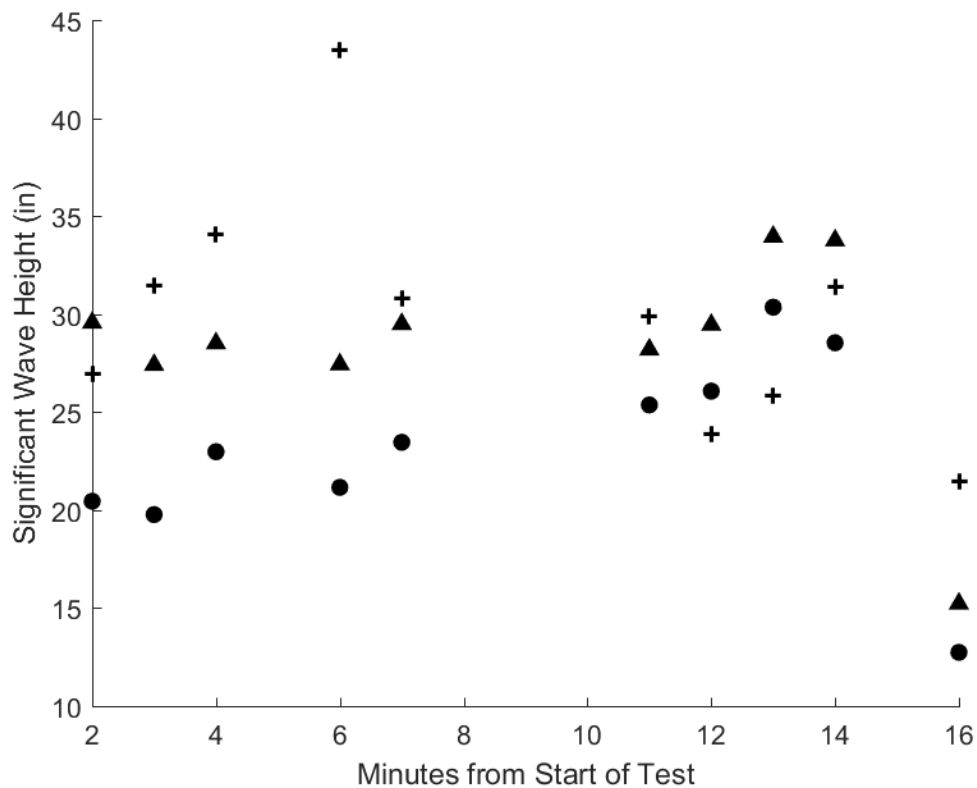


Figure F-36

Figure F-37: Plots of the significant wave heights for Test 13 of the WCM mounted to the skimmer and the raw data from the main bridge Banner. The plus signs indicate the significant wave height (H_{m0}) calculated statistically using the raw data from the WCM mounted to the skimmer. The triangles represent the significant wave height (H_{m0}) calculated statistically using a segment of time corresponding to the WCM data from the raw Banner data. The dots represent the wave heights calculated using the average of the top third wave height from the same segments ($H_{1/3}$). Each data point represents a calculation of the significant wave height from approximately 60 seconds of raw data.

Here it can be seen that the $H_{1/3}$ calculation is lower than the H_{m0} value calculated using the Banner data for each time segment. The H_{m0} calculated using the WCM data is generally within the 4-inch performance objective with the H_{m0} from the bridge data.

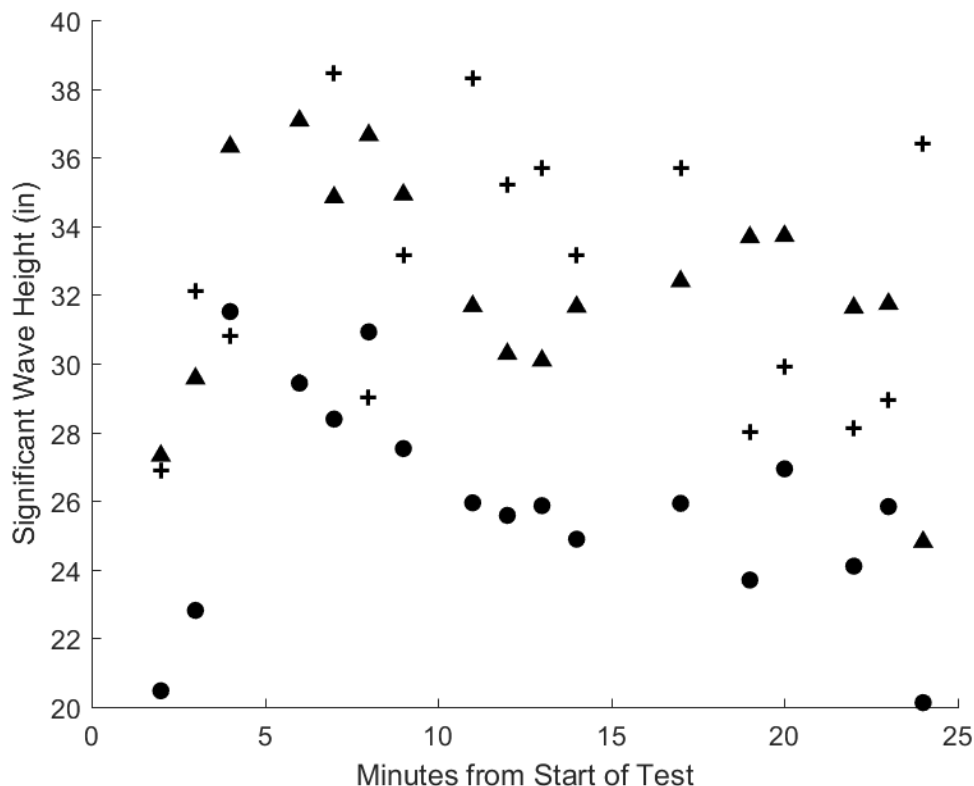


Figure F-37

Figure F-38: Plots of the significant wave heights for Test 13 of the WCM mounted to the skimmer and the raw data from the west auxiliary bridge Banner. The plus signs indicate the significant wave height (H_{m0}) calculated statistically using the raw data from the WCM mounted to the skimmer. The triangles represent the significant wave height (H_{m0}) calculated statistically using a segment of time corresponding to the WCM data from the raw Banner data. The dots represent the wave heights calculated using the average of the top third wave height from the same segments ($H_{1/3}$). Each data point represents a calculation of the significant wave height from approximately 60 seconds of raw data.

Here it can be seen that the $H_{1/3}$ calculation is lower than the H_{m0} value calculated using the Banner data for each time segment. The H_{m0} calculated using the WCM data is generally within the 4-inch performance objective with the H_{m0} from the bridge data.

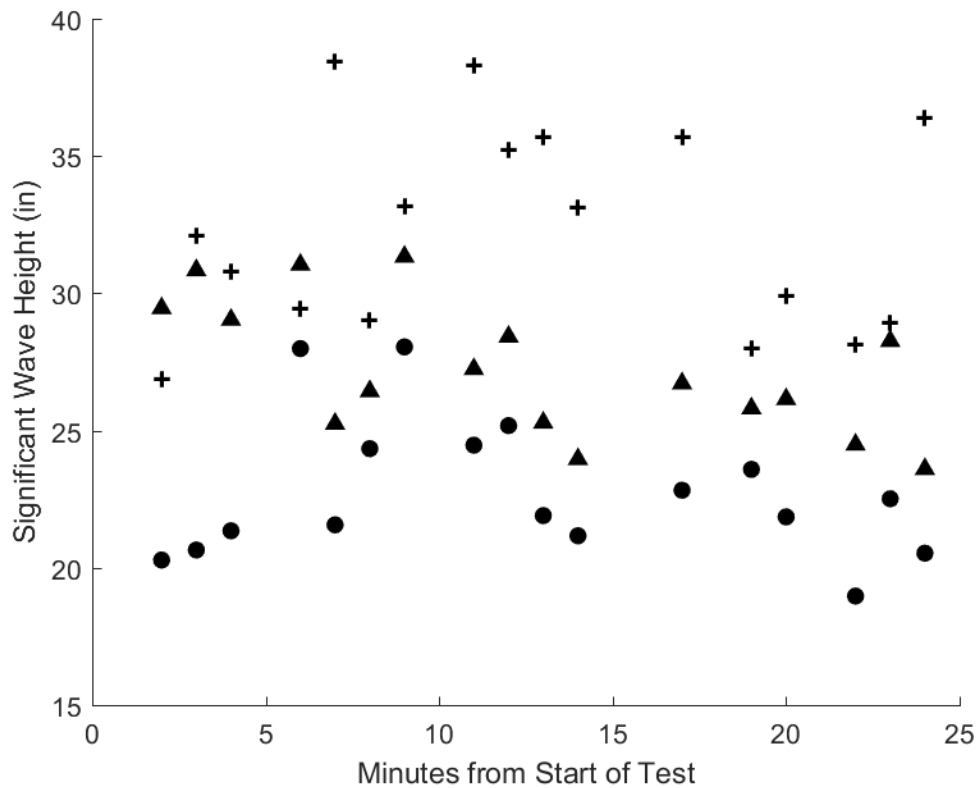


Figure F-38

Figure F-39: Plots of the significant wave heights for Test 13 of the WCM mounted to the skimmer and the raw data from the east auxiliary bridge Banner. The plus signs indicate the significant wave height (H_{m0}) calculated statistically using the raw data from the WCM mounted to the skimmer. The triangles represent the significant wave height (H_{m0}) calculated statistically using a segment of time corresponding to the WCM data from the raw Banner data. The dots represent the wave heights calculated using the average of the top third wave height from the same segments ($H_{1/3}$). Each data point represents a calculation of the significant wave height from approximately 60 seconds of raw data.

Here it can be seen that the $H_{1/3}$ calculation is lower than the H_{m0} value calculated using the Banner data for each time segment. The H_{m0} calculated using the WCM data is generally within the 4-inch performance objective with the H_{m0} from the bridge data.

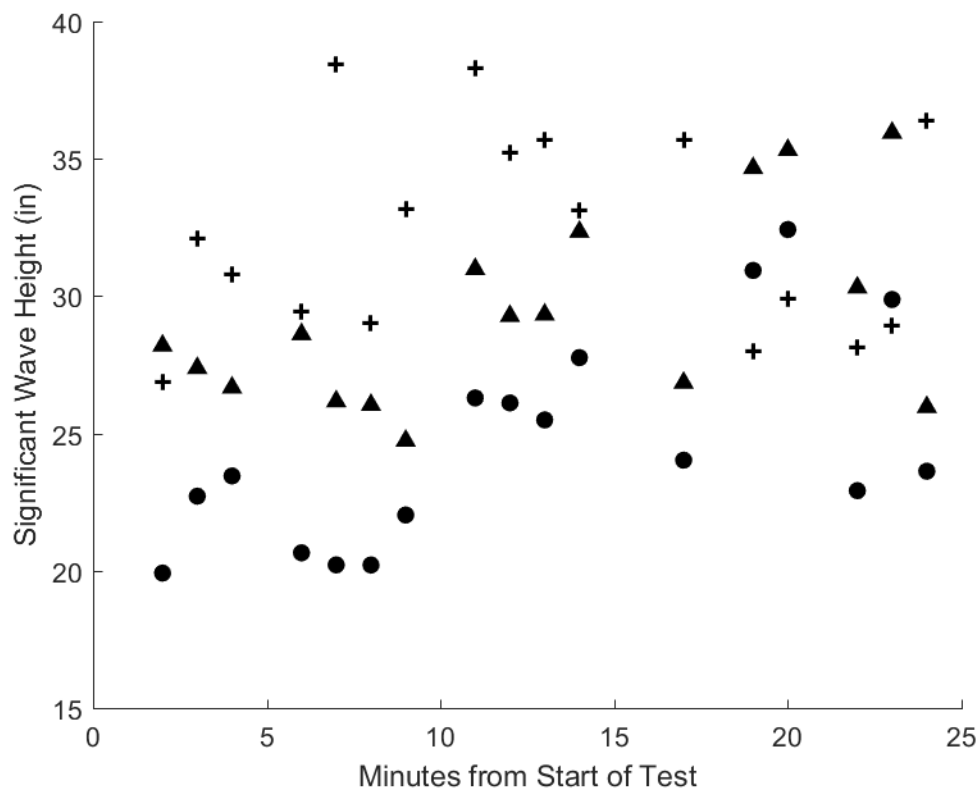


Figure F-39

Figure F-40: Plots of the significant wave heights for Test 14 of the WCM mounted to the skimmer and the raw data from the main bridge Banner. The plus signs indicate the significant wave height (H_{m0}) calculated statistically using the raw data from the WCM mounted to the skimmer. The triangles represent the significant wave height (H_{m0}) calculated statistically using a segment of time corresponding to the WCM data from the raw Banner data. The dots represent the wave heights calculated using the average of the top third wave height from the same segments ($H_{1/3}$). Each data point represents a calculation of the significant wave height from approximately 60 seconds of raw data.

Here it can be seen that the $H_{1/3}$ calculation is lower than the H_{m0} value calculated using the Banner data for each time segment. The H_{m0} calculated using the WCM data is generally within the 4-inch performance objective with the H_{m0} from the bridge data.

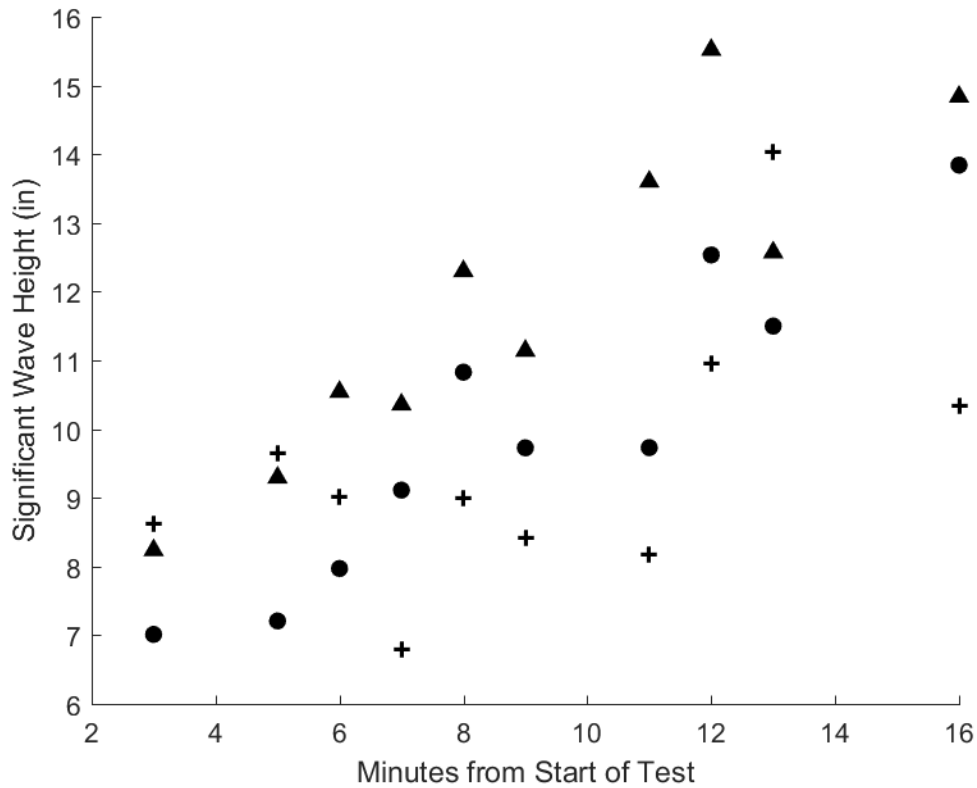


Figure F-40

Figure F-41: Plots of the significant wave heights for Test 14 of the WCM mounted to the skimmer and the raw data from the west auxiliary bridge Banner. The plus signs indicate the significant wave height (H_{m0}) calculated statistically using the raw data from the WCM mounted to the skimmer. The triangles represent the significant wave height (H_{m0}) calculated statistically using a segment of time corresponding to the WCM data from the raw Banner data. The dots represent the wave heights calculated using the average of the top third wave height from the same segments ($H_{1/3}$). Each data point represents a calculation of the significant wave height from approximately 60 seconds of raw data.

Here it can be seen that the $H_{1/3}$ calculation is lower than the H_{m0} value calculated using the Banner data for each time segment. The H_{m0} calculated using the WCM data is generally within the 4-inch performance objective with the H_{m0} from the bridge data.

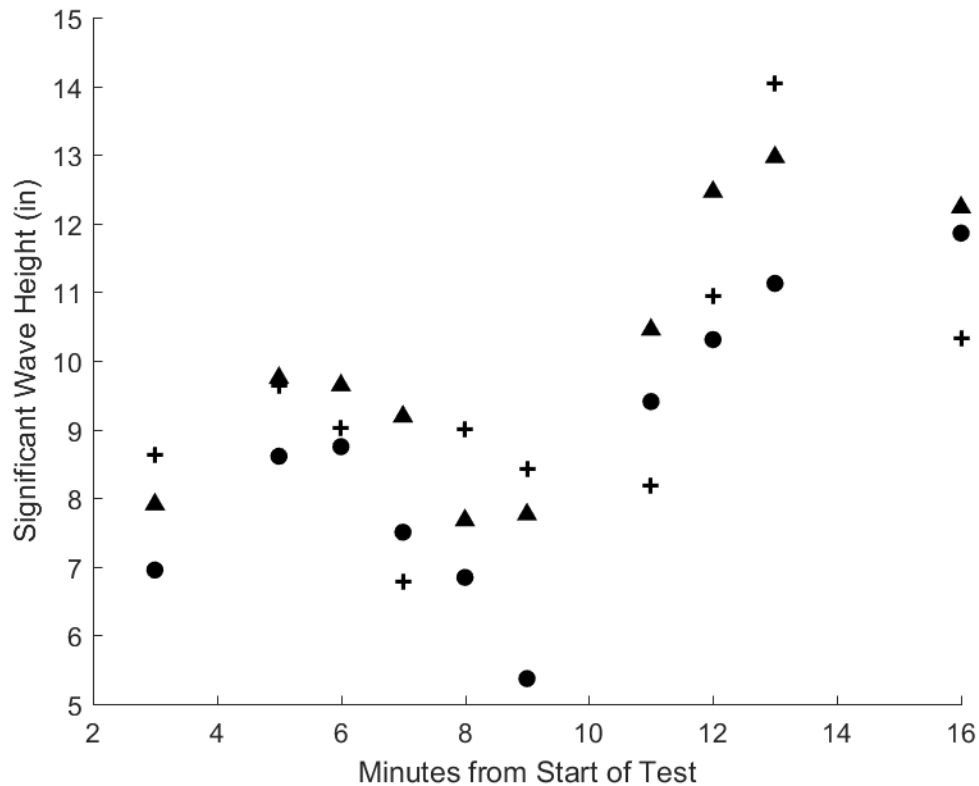


Figure F-41

Figure F-42: Plots of the significant wave heights for Test 14 of the WCM mounted to the skimmer and the raw data from the east auxiliary bridge Banner. The plus signs indicate the significant wave height (H_{m0}) calculated statistically using the raw data from the WCM mounted to the skimmer. The triangles represent the significant wave height (H_{m0}) calculated statistically using a segment of time corresponding to the WCM data from the raw Banner data. The dots represent the wave heights calculated using the average of the top third wave height from the same segments ($H_{1/3}$). Each data point represents a calculation of the significant wave height from approximately 60 seconds of raw data.

Here it can be seen that the $H_{1/3}$ calculation is lower than the H_{m0} value calculated using the Banner data for each time segment. The H_{m0} calculated using the WCM data is generally within the 4-inch performance objective with the H_{m0} from the bridge data.

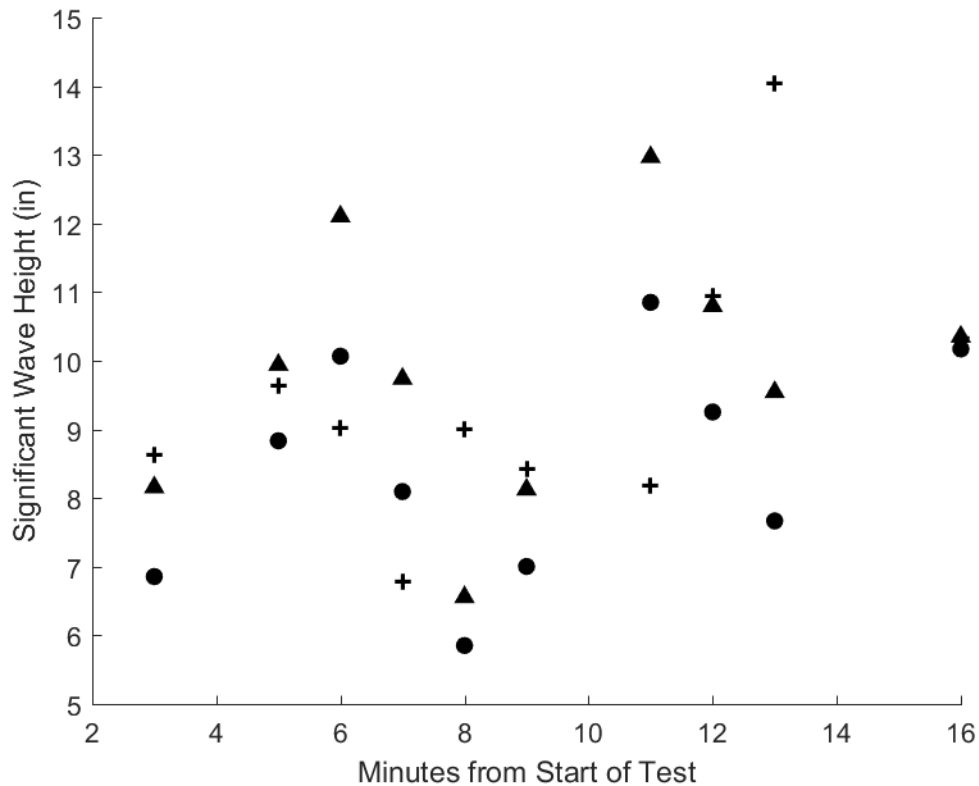


Figure F-42

Figure F-43: Plots of the significant wave heights for Test 15 of the WCM mounted to the skimmer and the raw data from the main bridge Banner. The plus signs indicate the significant wave height (H_{m0}) calculated statistically using the raw data from the WCM mounted to the skimmer. The triangles represent the significant wave height (H_{m0}) calculated statistically using a segment of time corresponding to the WCM data from the raw Banner data. The dots represent the wave heights calculated using the average of the top third wave height from the same segments ($H_{1/3}$). Each data point represents a calculation of the significant wave height from approximately 60 seconds of raw data.

Here it can be seen that the $H_{1/3}$ calculation is lower than the H_{m0} value calculated using the Banner data for each time segment. The H_{m0} calculated using the WCM data is generally within the 4-inch performance objective with the H_{m0} from the bridge data.

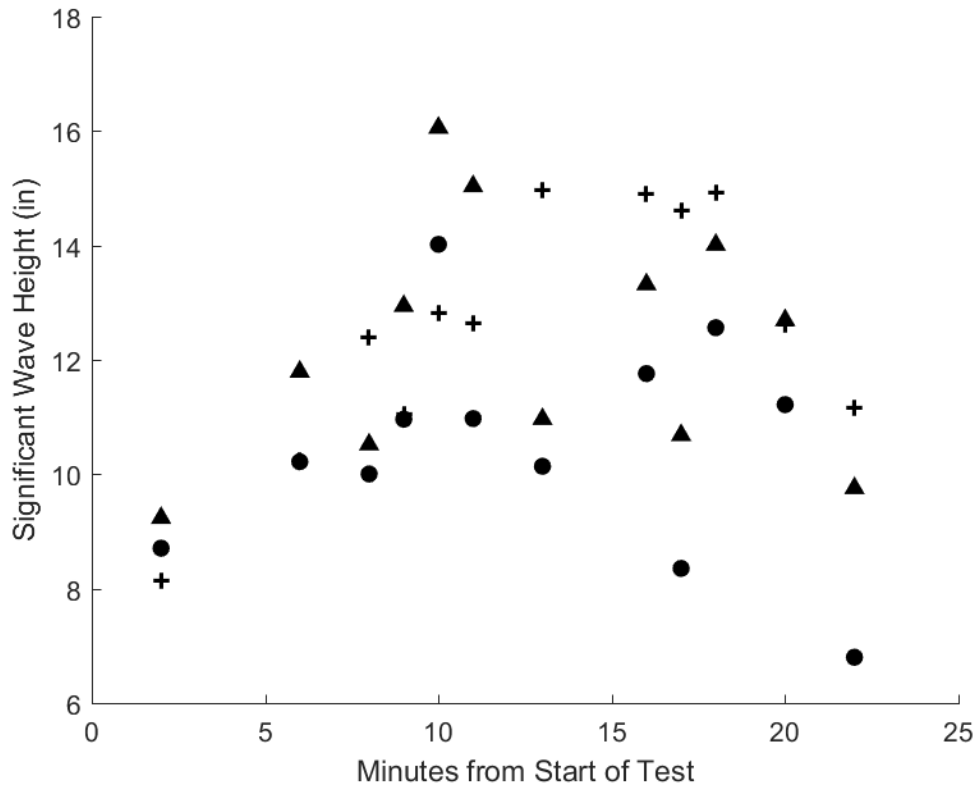


Figure F-43

Figure F-44: Plots of the significant wave heights for Test 15 of the WCM mounted to the skimmer and the raw data from the west auxiliary bridge Banner. The plus signs indicate the significant wave height (H_{m0}) calculated statistically using the raw data from the WCM mounted to the skimmer. The triangles represent the significant wave height (H_{m0}) calculated statistically using a segment of time corresponding to the WCM data from the raw Banner data. The dots represent the wave heights calculated using the average of the top third wave height from the same segments ($H_{1/3}$). Each data point represents a calculation of the significant wave height from approximately 60 seconds of raw data.

Here it can be seen that the $H_{1/3}$ calculation is lower than the H_{m0} value calculated using the Banner data for each time segment. The H_{m0} calculated using the WCM data is generally within the 4-inch performance objective with the H_{m0} from the bridge data.

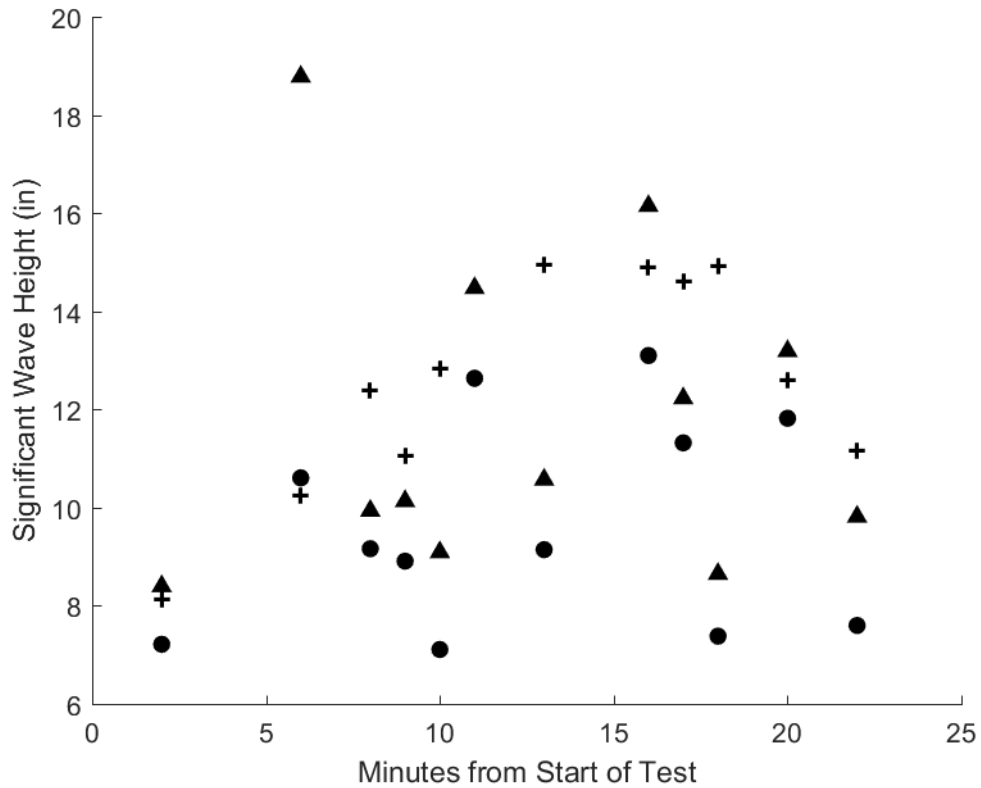


Figure F-44

Figure F-45: Plots of the significant wave heights for Test 15 of the WCM mounted to the skimmer and the raw data from the east auxiliary bridge Banner. The plus signs indicate the significant wave height (H_{m0}) calculated statistically using the raw data from the WCM mounted to the skimmer. The triangles represent the significant wave height (H_{m0}) calculated statistically using a segment of time corresponding to the WCM data from the raw Banner data. The dots represent the wave heights calculated using the average of the top third wave height from the same segments ($H_{1/3}$). Each data point represents a calculation of the significant wave height from approximately 60 seconds of raw data.

Here it can be seen that the $H_{1/3}$ calculation is lower than the H_{m0} value calculated using the Banner data for each time segment. The H_{m0} calculated using the WCM data is generally within the 4-inch performance objective with the H_{m0} from the bridge data.

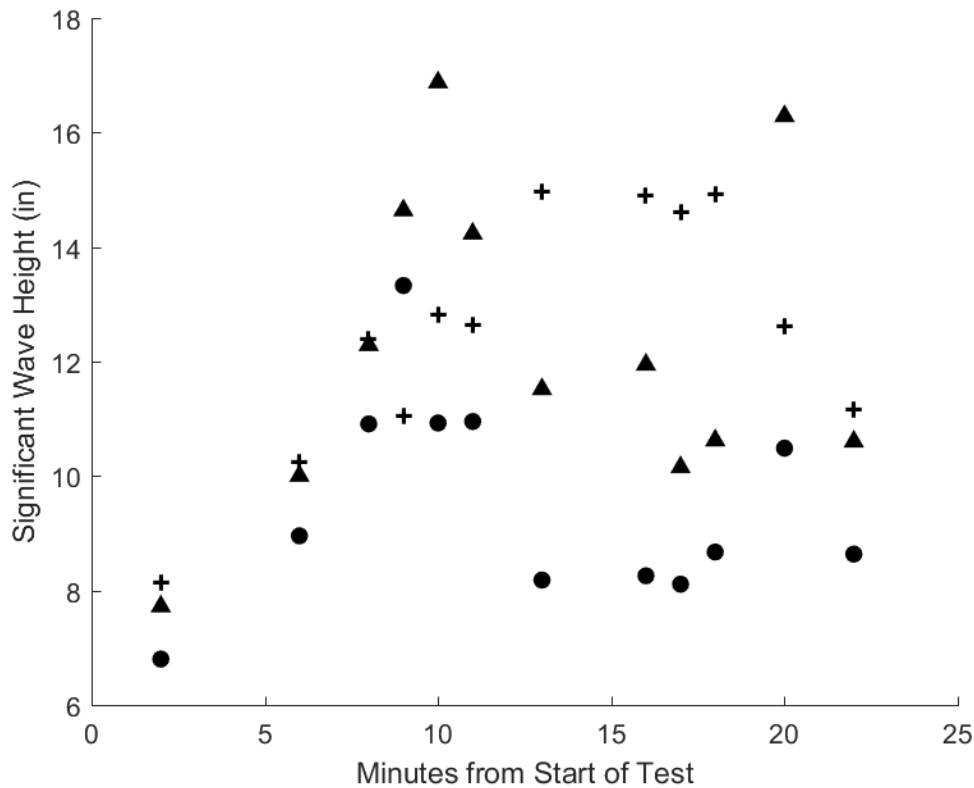


Figure F-45

Figure F-46: Plots of the significant wave heights for Test 16 of the WCM mounted to the skimmer and the raw data from the main bridge Banner. The plus signs indicate the significant wave height (H_{m0}) calculated statistically using the raw data from the WCM mounted to the skimmer. The triangles represent the significant wave height (H_{m0}) calculated statistically using a segment of time corresponding to the WCM data from the raw Banner data. The dots represent the wave heights calculated using the average of the top third wave height from the same segments ($H_{1/3}$). Each data point represents a calculation of the significant wave height from approximately 60 seconds of raw data.

Here it can be seen that the $H_{1/3}$ calculation is lower than the H_{m0} value calculated using the Banner data for each time segment. The H_{m0} calculated using the WCM data is generally within the 4-inch performance objective with the H_{m0} from the bridge data.

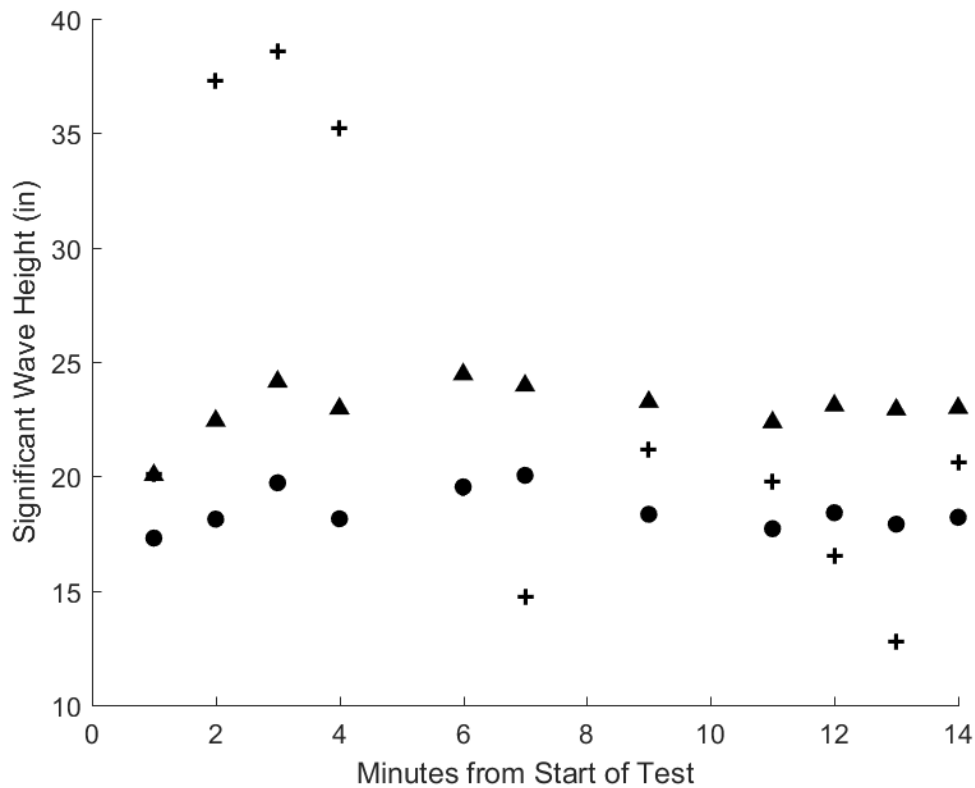


Figure F-46

Figure F-47: Plots of the significant wave heights for Test 16 of the WCM mounted to the skimmer and the raw data from the west auxiliary bridge Banner. The plus signs indicate the significant wave height (H_{m0}) calculated statistically using the raw data from the WCM mounted to the skimmer. The triangles represent the significant wave height (H_{m0}) calculated statistically using a segment of time corresponding to the WCM data from the raw Banner data. The dots represent the wave heights calculated using the average of the top third wave height from the same segments ($H_{1/3}$). Each data point represents a calculation of the significant wave height from approximately 60 seconds of raw data.

Here it can be seen that the $H_{1/3}$ calculation is lower than the H_{m0} value calculated using the Banner data for each time segment. The H_{m0} calculated using the WCM data is generally within the 4-inch performance objective with the H_{m0} from the bridge data.

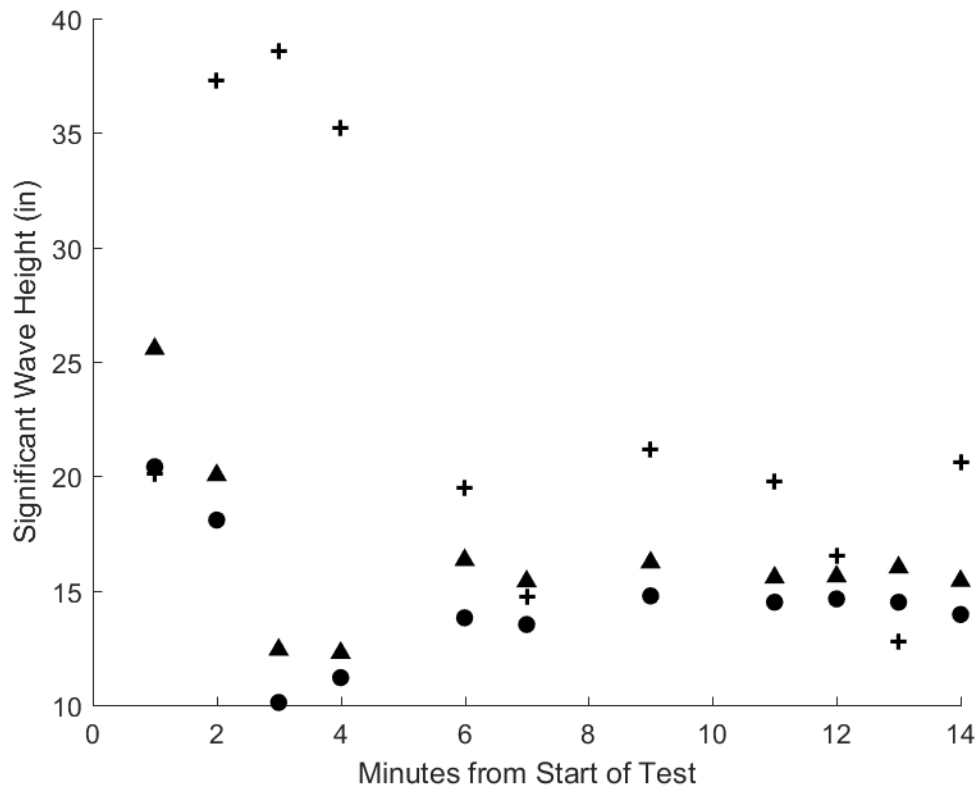


Figure F-47

Figure F-48: Plots of the significant wave heights for Test 16 of the WCM mounted to the skimmer and the raw data from the east auxiliary bridge Banner. The plus signs indicate the significant wave height (H_{m0}) calculated statistically using the raw data from the WCM mounted to the skimmer. The triangles represent the significant wave height (H_{m0}) calculated statistically using a segment of time corresponding to the WCM data from the raw Banner data. The dots represent the wave heights calculated using the average of the top third wave height from the same segments ($H_{1/3}$). Each data point represents a calculation of the significant wave height from approximately 60 seconds of raw data.

Here it can be seen that the $H_{1/3}$ calculation is lower than the H_{m0} value calculated using the Banner data for each time segment. The H_{m0} calculated using the WCM data is generally within the 4-inch performance objective with the H_{m0} from the bridge data.

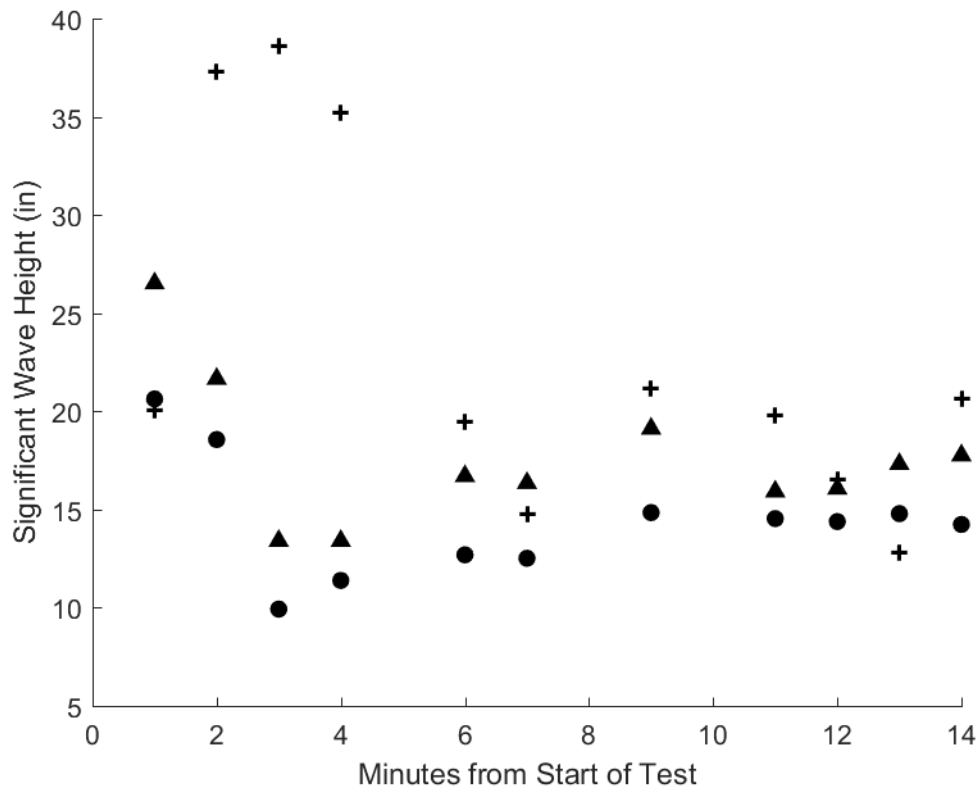


Figure F-48

Figure F-49: Plots of the significant wave heights for Test 17 of the WCM mounted to the skimmer and the raw data from the main bridge Banner. The plus signs indicate the significant wave height (H_{m0}) calculated statistically using the raw data from the WCM mounted to the skimmer. The triangles represent the significant wave height (H_{m0}) calculated statistically using a segment of time corresponding to the WCM data from the raw Banner data. The dots represent the wave heights calculated using the average of the top third wave height from the same segments ($H_{1/3}$). Each data point represents a calculation of the significant wave height from approximately 60 seconds of raw data.

Here it can be seen that the $H_{1/3}$ calculation is lower than the H_{m0} value calculated using the Banner data for each time segment. The H_{m0} calculated using the WCM data is generally within the 4-inch performance objective with the H_{m0} from the bridge data.

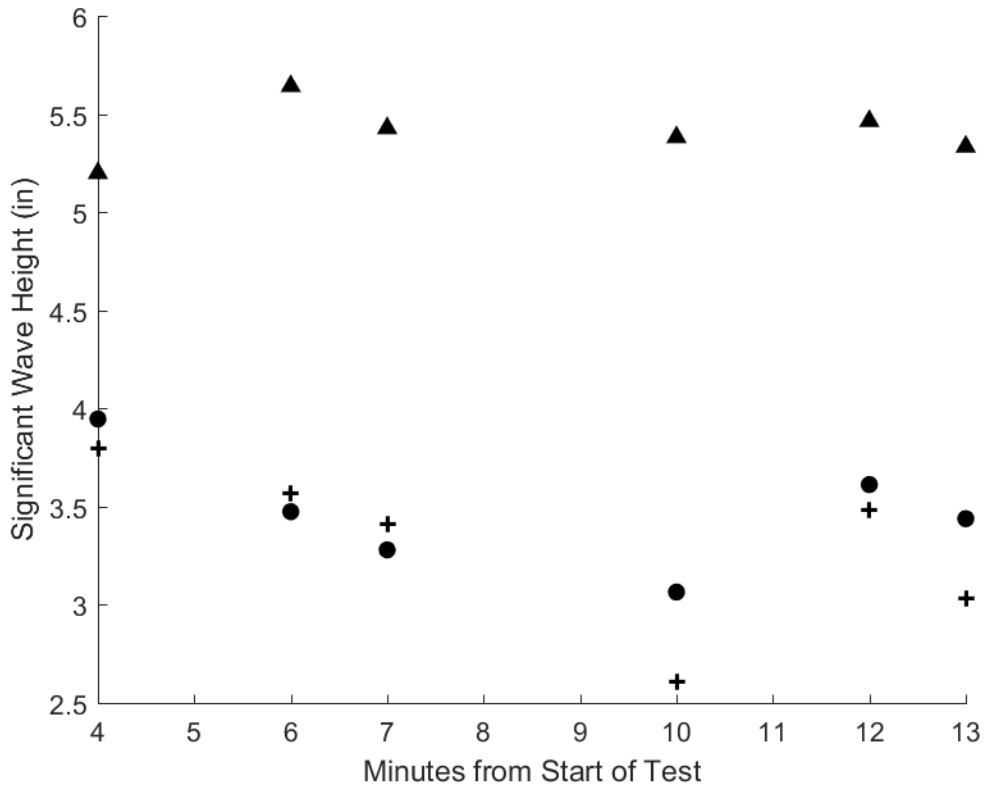


Figure F-49

Figure F-50: Plots of the significant wave heights for Test 17 of the WCM mounted to the skimmer and the raw data from the west auxiliary bridge Banner. The plus signs indicate the significant wave height (H_{m0}) calculated statistically using the raw data from the WCM mounted to the skimmer. The triangles represent the significant wave height (H_{m0}) calculated statistically using a segment of time corresponding to the WCM data from the raw Banner data. The dots represent the wave heights calculated using the average of the top third wave height from the same segments ($H_{1/3}$). Each data point represents a calculation of the significant wave height from approximately 60 seconds of raw data.

Here it can be seen that the $H_{1/3}$ calculation is lower than the H_{m0} value calculated using the Banner data for each time segment. The H_{m0} calculated using the WCM data is generally within the 4-inch performance objective with the H_{m0} from the bridge data.

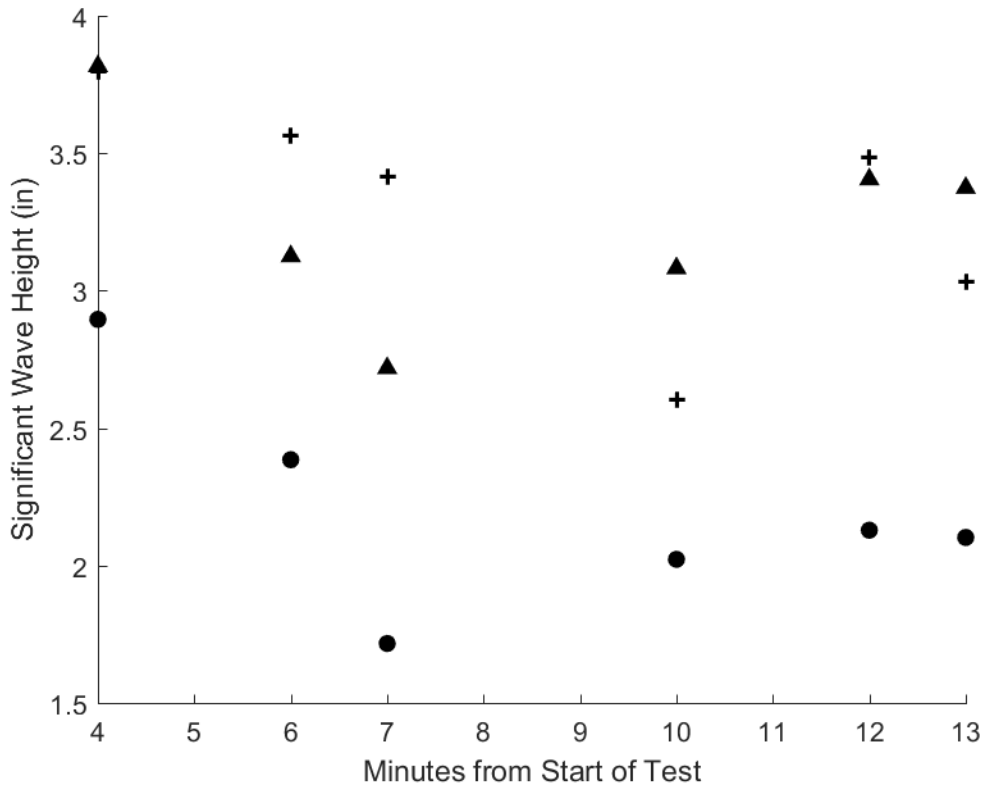


Figure F-50

Figure F-51: Plots of the significant wave heights for Test 17 of the WCM mounted to the skimmer and the raw data from the east auxiliary bridge Banner. The plus signs indicate the significant wave height (H_{m0}) calculated statistically using the raw data from the WCM mounted to the skimmer. The triangles represent the significant wave height (H_{m0}) calculated statistically using a segment of time corresponding to the WCM data from the raw Banner data. The dots represent the wave heights calculated using the average of the top third wave height from the same segments ($H_{1/3}$). Each data point represents a calculation of the significant wave height from approximately 60 seconds of raw data.

Here it can be seen that the $H_{1/3}$ calculation is lower than the H_{m0} value calculated using the Banner data for each time segment. The H_{m0} calculated using the WCM data is generally within the 4-inch performance objective with the H_{m0} from the bridge data.

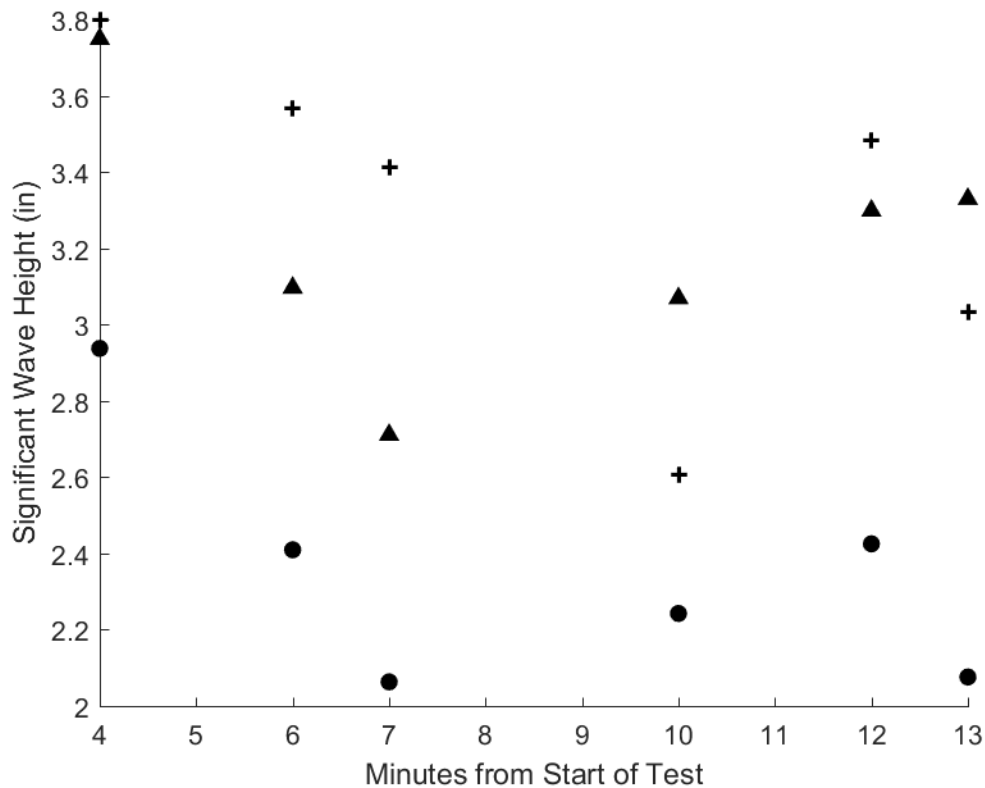


Figure F-51

Figure F-52: Plots of the significant wave heights for Test 18 of the WCM mounted to the skimmer and the raw data from the main bridge Banner. The plus signs indicate the significant wave height (H_{m0}) calculated statistically using the raw data from the WCM mounted to the skimmer. The triangles represent the significant wave height (H_{m0}) calculated statistically using a segment of time corresponding to the WCM data from the raw Banner data. The dots represent the wave heights calculated using the average of the top third wave height from the same segments ($H_{1/3}$). Each data point represents a calculation of the significant wave height from approximately 60 seconds of raw data.

Here it can be seen that the $H_{1/3}$ calculation is lower than the H_{m0} value calculated using the Banner data for each time segment. The H_{m0} calculated using the WCM data is generally within the 4-inch performance objective with the H_{m0} from the bridge data.

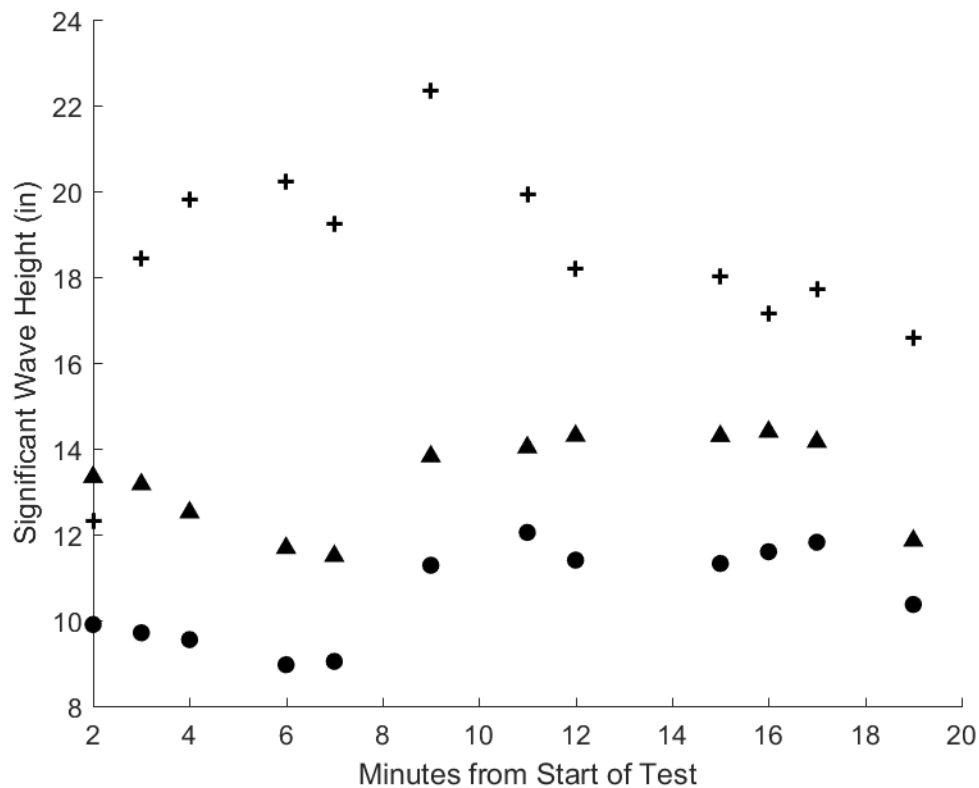


Figure F-52

Figure F-53: Plots of the significant wave heights for Test 18 of the WCM mounted to the skimmer and the raw data from the west auxiliary bridge Banner. The plus signs indicate the significant wave height (H_{m0}) calculated statistically using the raw data from the WCM mounted to the skimmer. The triangles represent the significant wave height (H_{m0}) calculated statistically using a segment of time corresponding to the WCM data from the raw Banner data. The dots represent the wave heights calculated using the average of the top third wave height from the same segments ($H_{1/3}$). Each data point represents a calculation of the significant wave height from approximately 60 seconds of raw data.

Here it can be seen that the $H_{1/3}$ calculation is lower than the H_{m0} value calculated using the Banner data for each time segment. The H_{m0} calculated using the WCM data is generally within the 4-inch performance objective with the H_{m0} from the bridge data.

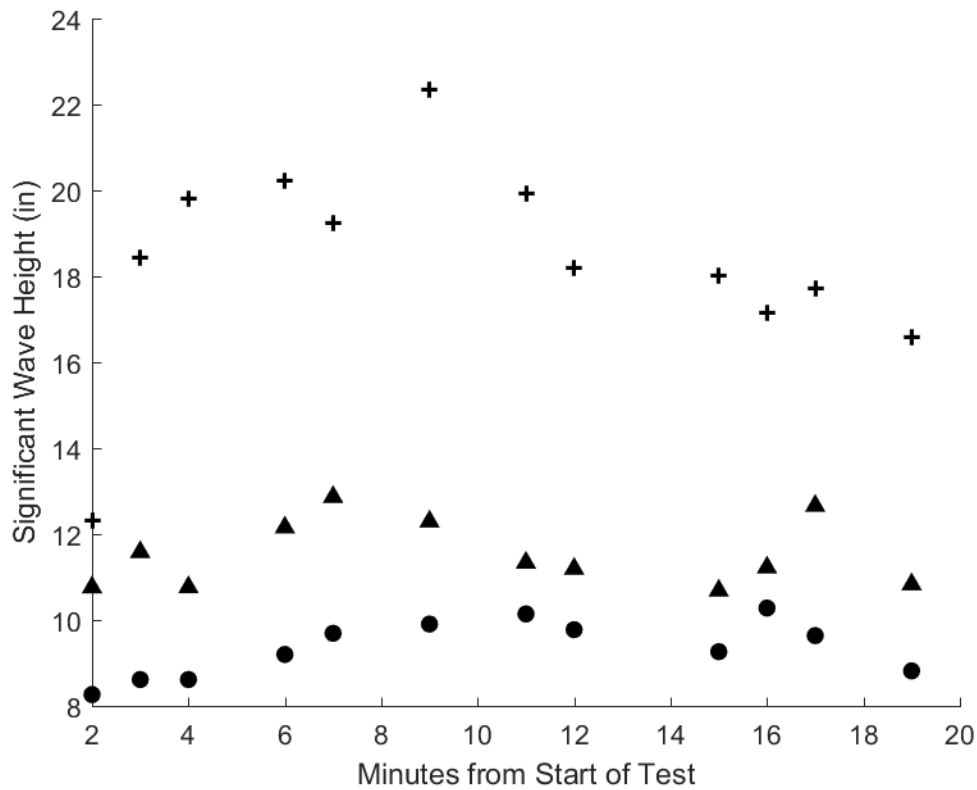


Figure F-53

Figure F-54: Plots of the significant wave heights for Test 18 of the WCM mounted to the skimmer and the raw data from the east auxiliary bridge Banner. The plus signs indicate the significant wave height (H_{m0}) calculated statistically using the raw data from the WCM mounted to the skimmer. The triangles represent the significant wave height (H_{m0}) calculated statistically using a segment of time corresponding to the WCM data from the raw Banner data. The dots represent the wave heights calculated using the average of the top third wave height from the same segments ($H_{1/3}$). Each data point represents a calculation of the significant wave height from approximately 60 seconds of raw data.

Here it can be seen that the $H_{1/3}$ calculation is lower than the H_{m0} value calculated using the Banner data for each time segment. The H_{m0} calculated using the WCM data is generally within the 4-inch performance objective with the H_{m0} from the bridge data.

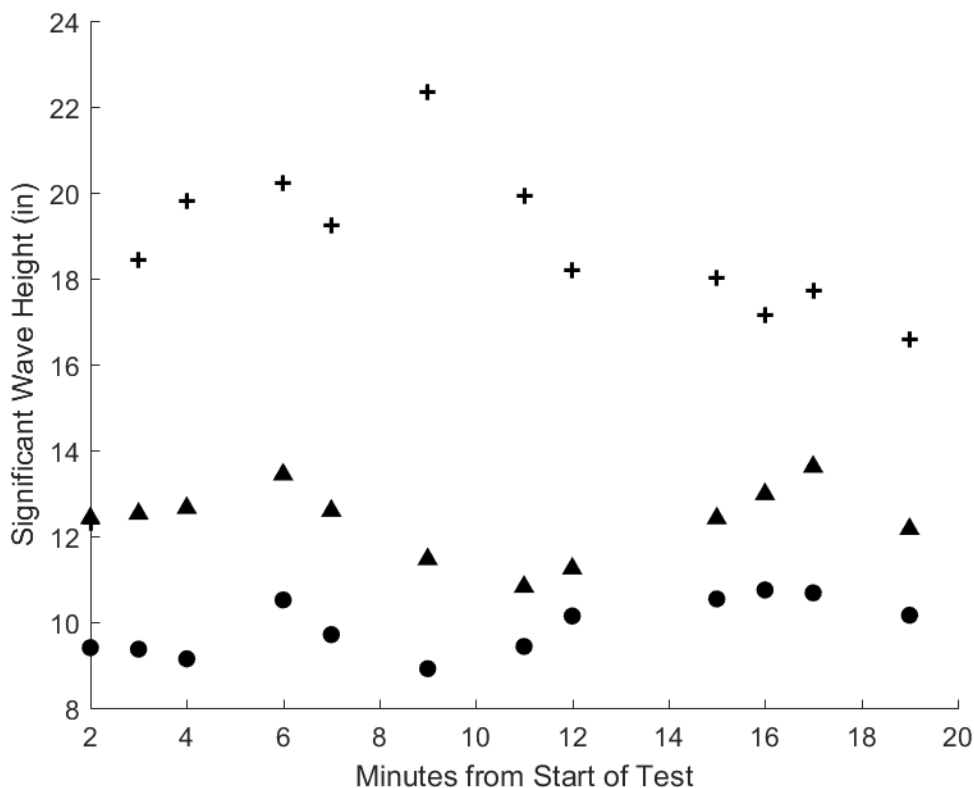


Figure F-54

Figure F-55: Plots of the significant wave heights for Test 19 of the WCM mounted to the skimmer and the raw data from the main bridge Banner. The plus signs indicate the significant wave height (H_{m0}) calculated statistically using the raw data from the WCM mounted to the skimmer. The triangles represent the significant wave height (H_{m0}) calculated statistically using a segment of time corresponding to the WCM data from the raw Banner data. The dots represent the wave heights calculated using the average of the top third wave height from the same segments ($H_{1/3}$). Each data point represents a calculation of the significant wave height from approximately 60 seconds of raw data.

Here it can be seen that the $H_{1/3}$ calculation is lower than the H_{m0} value calculated using the Banner data for each time segment. The H_{m0} calculated using the WCM data is generally within the 4-inch performance objective with the H_{m0} from the bridge data.

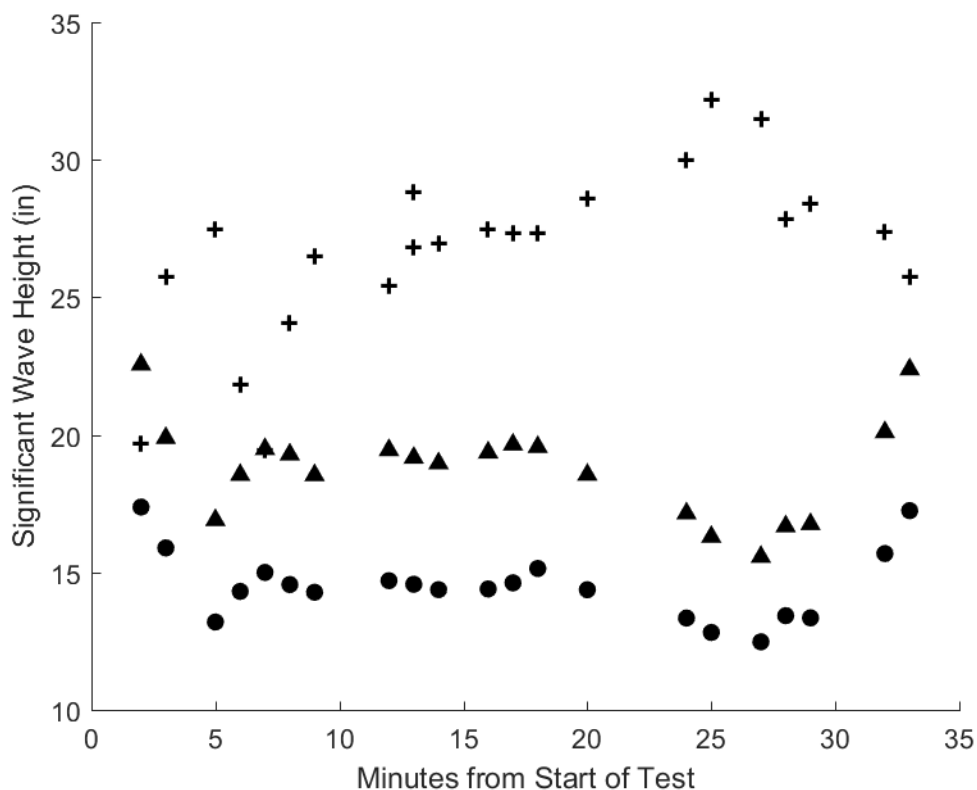


Figure F-55

Figure F-56: Plots of the significant wave heights for Test 19 of the WCM mounted to the skimmer and the raw data from the west auxiliary bridge Banner. The plus signs indicate the significant wave height (H_{m0}) calculated statistically using the raw data from the WCM mounted to the skimmer. The triangles represent the significant wave height (H_{m0}) calculated statistically using a segment of time corresponding to the WCM data from the raw Banner data. The dots represent the wave heights calculated using the average of the top third wave height from the same segments ($H_{1/3}$). Each data point represents a calculation of the significant wave height from approximately 60 seconds of raw data.

Here it can be seen that the $H_{1/3}$ calculation is lower than the H_{m0} value calculated using the Banner data for each time segment. The H_{m0} calculated using the WCM data is generally within the 4-inch performance objective with the H_{m0} from the bridge data.

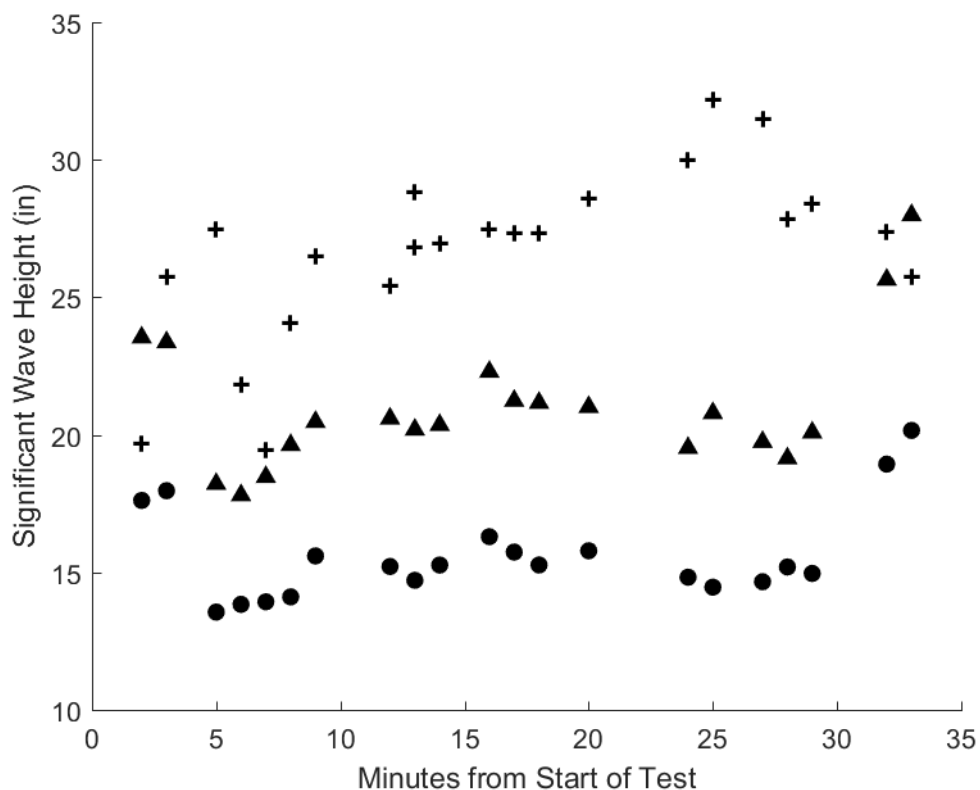


Figure F-56

Figure F-57: Plots of the significant wave heights for Test 19 of the WCM mounted to the skimmer and the raw data from the east auxiliary bridge Banner. The plus signs indicate the significant wave height (H_{m0}) calculated statistically using the raw data from the WCM mounted to the skimmer. The triangles represent the significant wave height (H_{m0}) calculated statistically using a segment of time corresponding to the WCM data from the raw Banner data. The dots represent the wave heights calculated using the average of the top third wave height from the same segments ($H_{1/3}$). Each data point represents a calculation of the significant wave height from approximately 60 seconds of raw data.

Here it can be seen that the $H_{1/3}$ calculation is lower than the H_{m0} value calculated using the Banner data for each time segment. The H_{m0} calculated using the WCM data is generally within the 4-inch performance objective with the H_{m0} from the bridge data.

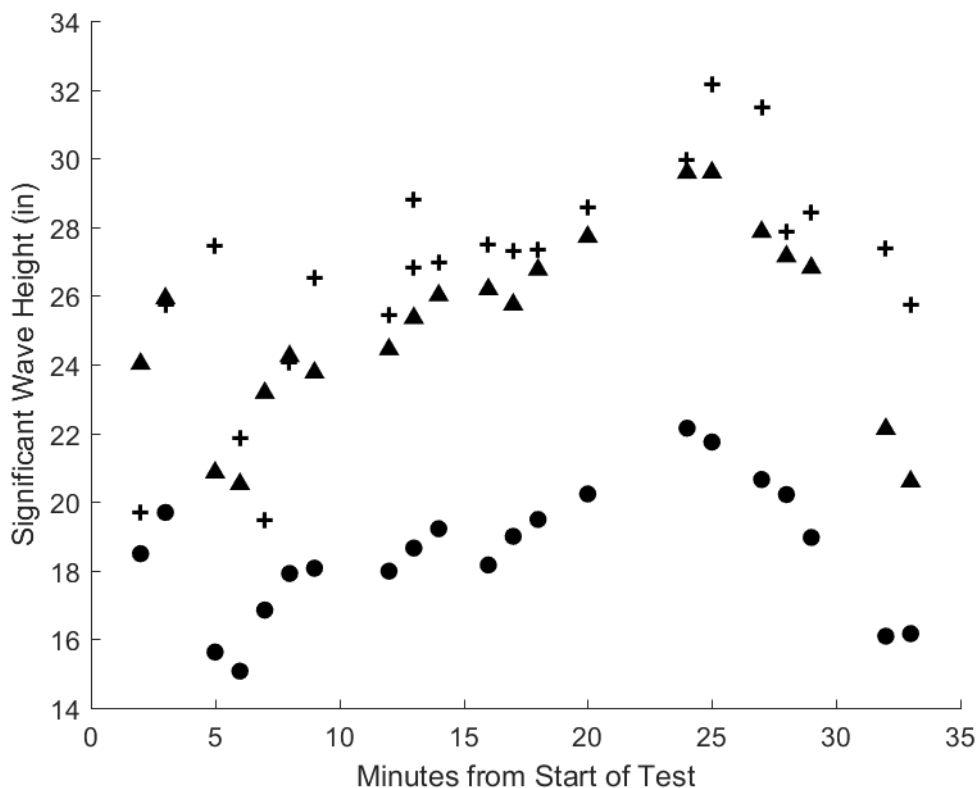


Figure F-57

Figure F-58: Plots of the significant wave heights for Test 20 of the WCM mounted to the skimmer and the raw data from the main bridge Banner. The plus signs indicate the significant wave height (H_{m0}) calculated statistically using the raw data from the WCM mounted to the skimmer. The triangles represent the significant wave height (H_{m0}) calculated statistically using a segment of time corresponding to the WCM data from the raw Banner data. The dots represent the wave heights calculated using the average of the top third wave height from the same segments ($H_{1/3}$). Each data point represents a calculation of the significant wave height from approximately 60 seconds of raw data.

Here it can be seen that the $H_{1/3}$ calculation is lower than the H_{m0} value calculated using the Banner data for each time segment. The H_{m0} calculated using the WCM data is generally within the 4-inch performance objective with the H_{m0} from the bridge data.

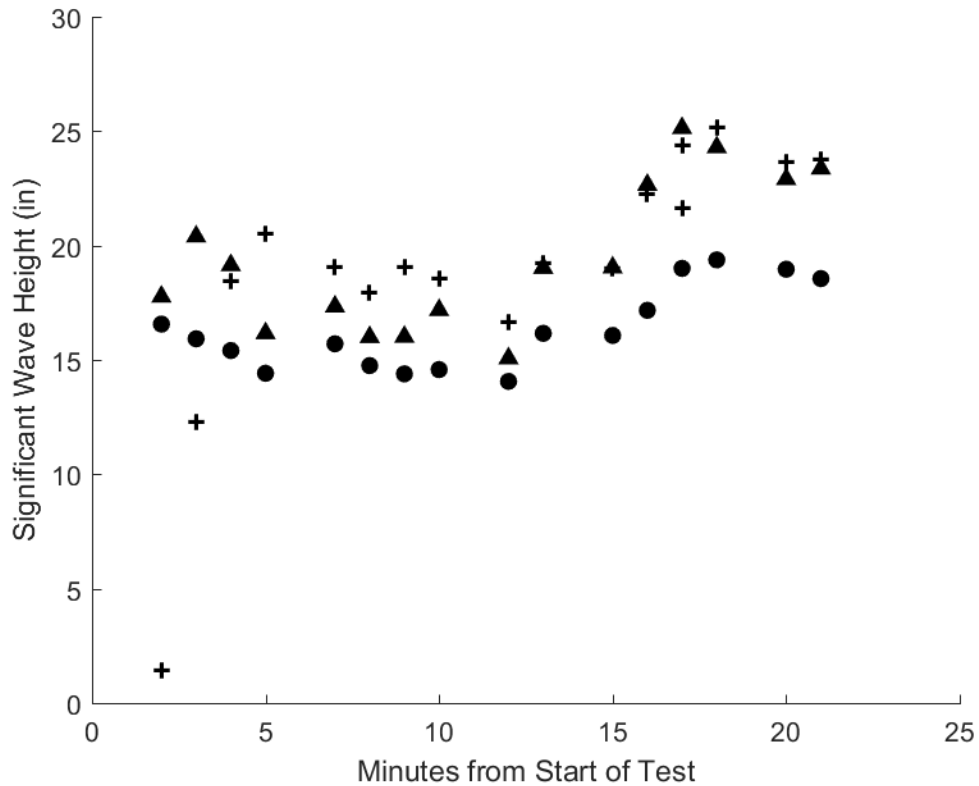


Figure F-58

Figure F-59: Plots of the significant wave heights for Test 20 of the WCM mounted to the skimmer and the raw data from the west auxiliary bridge Banner. The plus signs indicate the significant wave height (H_{m0}) calculated statistically using the raw data from the WCM mounted to the skimmer. The triangles represent the significant wave height (H_{m0}) calculated statistically using a segment of time corresponding to the WCM data from the raw Banner data. The dots represent the wave heights calculated using the average of the top third wave height from the same segments ($H_{1/3}$). Each data point represents a calculation of the significant wave height from approximately 60 seconds of raw data.

Here it can be seen that the $H_{1/3}$ calculation is lower than the H_{m0} value calculated using the Banner data for each time segment. The H_{m0} calculated using the WCM data is generally within the 4-inch performance objective with the H_{m0} from the bridge data.

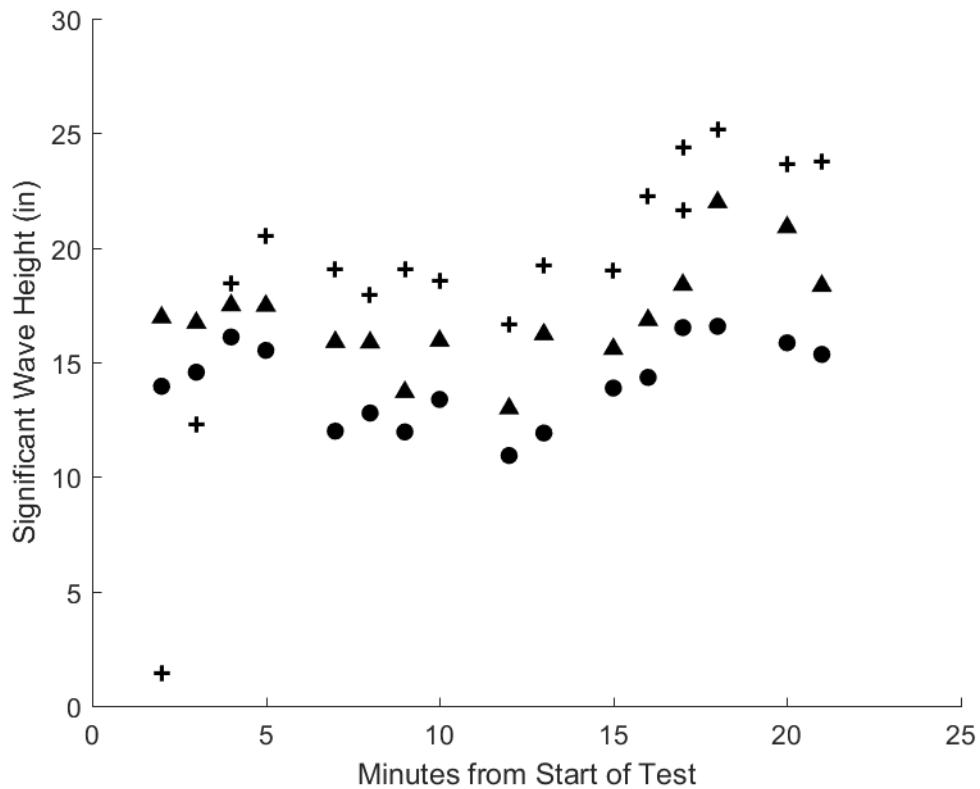


Figure F-59

Figure F-60: Plots of the significant wave heights for Test 20 of the WCM mounted to the skimmer and the raw data from the east auxiliary bridge Banner. The plus signs indicate the significant wave height (H_{m0}) calculated statistically using the raw data from the WCM mounted to the skimmer. The triangles represent the significant wave height (H_{m0}) calculated statistically using a segment of time corresponding to the WCM data from the raw Banner data. The dots represent the wave heights calculated using the average of the top third wave height from the same segments ($H_{1/3}$). Each data point represents a calculation of the significant wave height from approximately 60 seconds of raw data.

Here it can be seen that the $H_{1/3}$ calculation is lower than the H_{m0} value calculated using the Banner data for each time segment. The H_{m0} calculated using the WCM data is generally within the 4-inch performance objective with the H_{m0} from the bridge data.

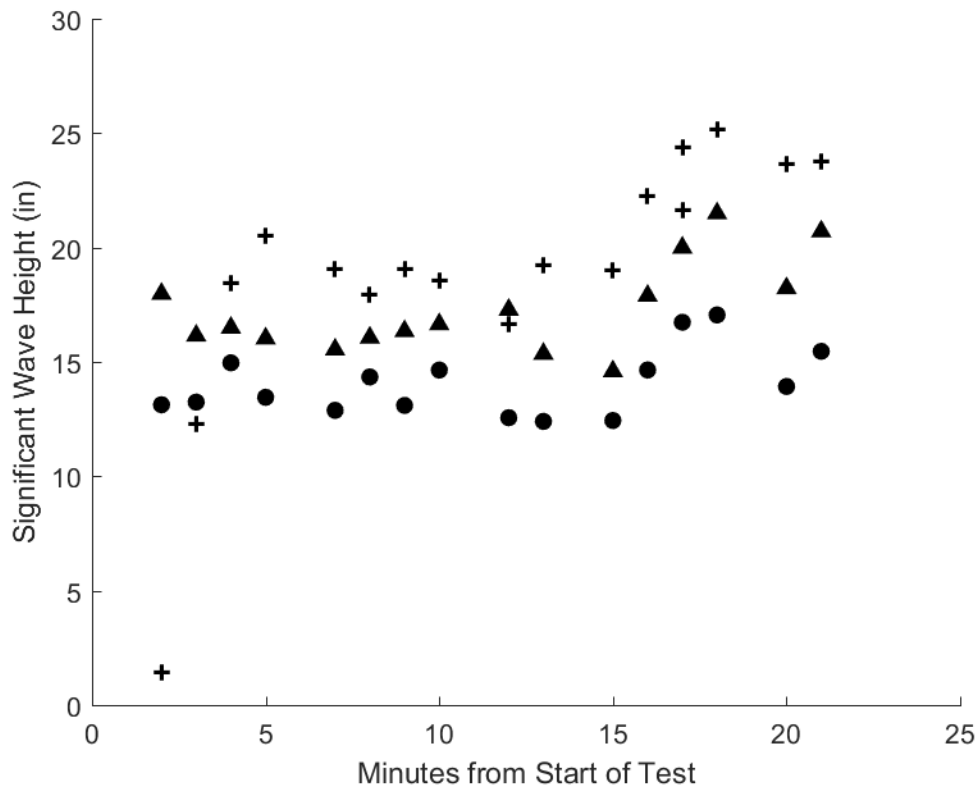


Figure F-60

Figure F-61: Plots of the significant wave heights for Test 21 of the WCM mounted to the skimmer and the raw data from the main bridge Banner. The plus signs indicate the significant wave height (H_{m0}) calculated statistically using the raw data from the WCM mounted to the skimmer. The triangles represent the significant wave height (H_{m0}) calculated statistically using a segment of time corresponding to the WCM data from the raw Banner data. The dots represent the wave heights calculated using the average of the top third wave height from the same segments ($H_{1/3}$). Each data point represents a calculation of the significant wave height from approximately 60 seconds of raw data.

Here it can be seen that the $H_{1/3}$ calculation is lower than the H_{m0} value calculated using the Banner data for each time segment. The H_{m0} calculated using the WCM data is generally within the 4-inch performance objective with the H_{m0} from the bridge data.

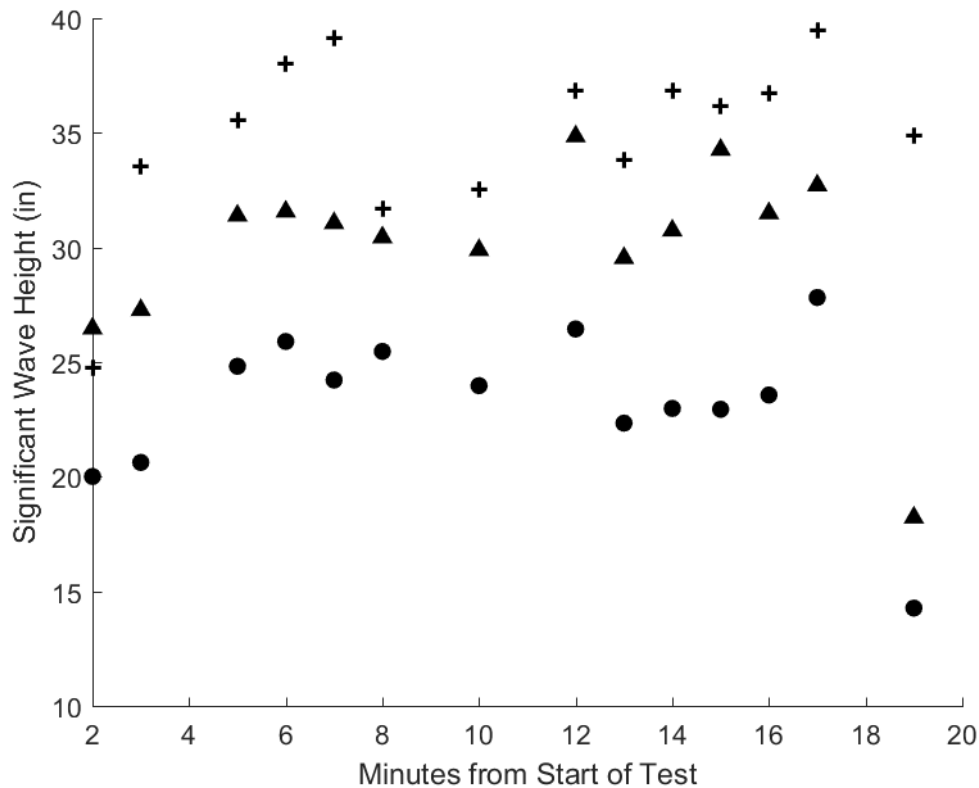


Figure F-61

Figure F-62: Plots of the significant wave heights for Test 21 of the WCM mounted to the skimmer and the raw data from the west auxiliary bridge Banner. The plus signs indicate the significant wave height (H_{m0}) calculated statistically using the raw data from the WCM mounted to the skimmer. The triangles represent the significant wave height (H_{m0}) calculated statistically using a segment of time corresponding to the WCM data from the raw Banner data. The dots represent the wave heights calculated using the average of the top third wave height from the same segments ($H_{1/3}$). Each data point represents a calculation of the significant wave height from approximately 60 seconds of raw data.

Here it can be seen that the $H_{1/3}$ calculation is lower than the H_{m0} value calculated using the Banner data for each time segment. The H_{m0} calculated using the WCM data is generally within the 4-inch performance objective with the H_{m0} from the bridge data.

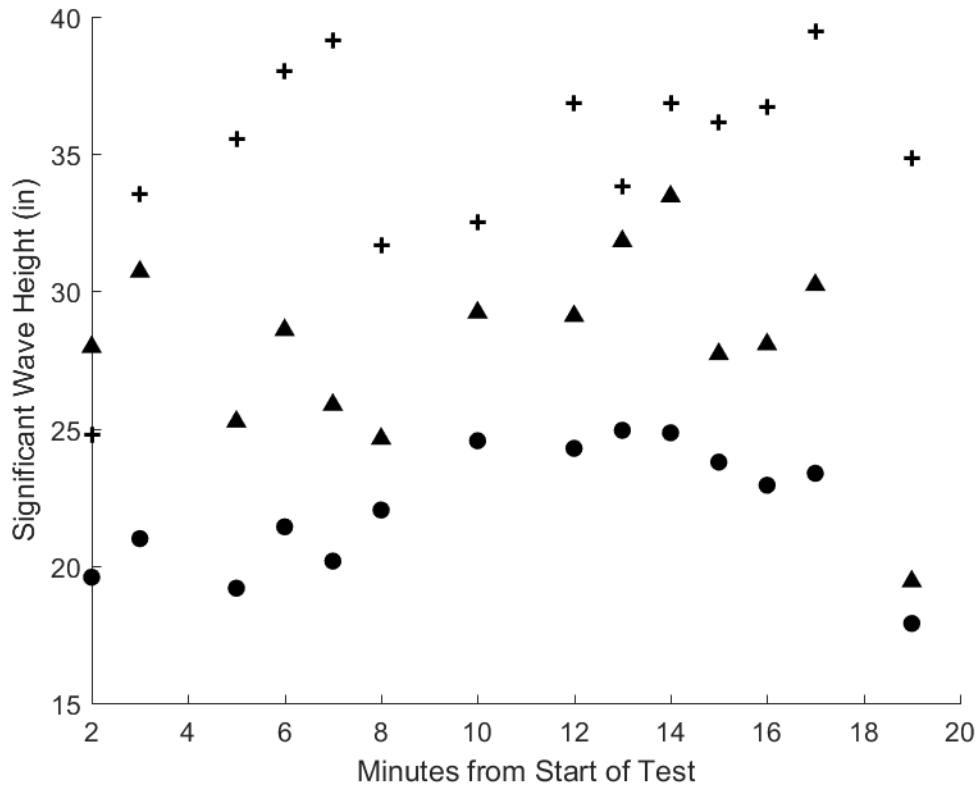


Figure F-62

Figure F-63: Plots of the significant wave heights for Test 21 of the WCM mounted to the skimmer and the raw data from the east auxiliary bridge Banner. The plus signs indicate the significant wave height (H_{m0}) calculated statistically using the raw data from the WCM mounted to the skimmer. The triangles represent the significant wave height (H_{m0}) calculated statistically using a segment of time corresponding to the WCM data from the raw Banner data. The dots represent the wave heights calculated using the average of the top third wave height from the same segments ($H_{1/3}$). Each data point represents a calculation of the significant wave height from approximately 60 seconds of raw data.

Here it can be seen that the $H_{1/3}$ calculation is lower than the H_{m0} value calculated using the Banner data for each time segment. The H_{m0} calculated using the WCM data is generally within the 4-inch performance objective with the H_{m0} from the bridge data.

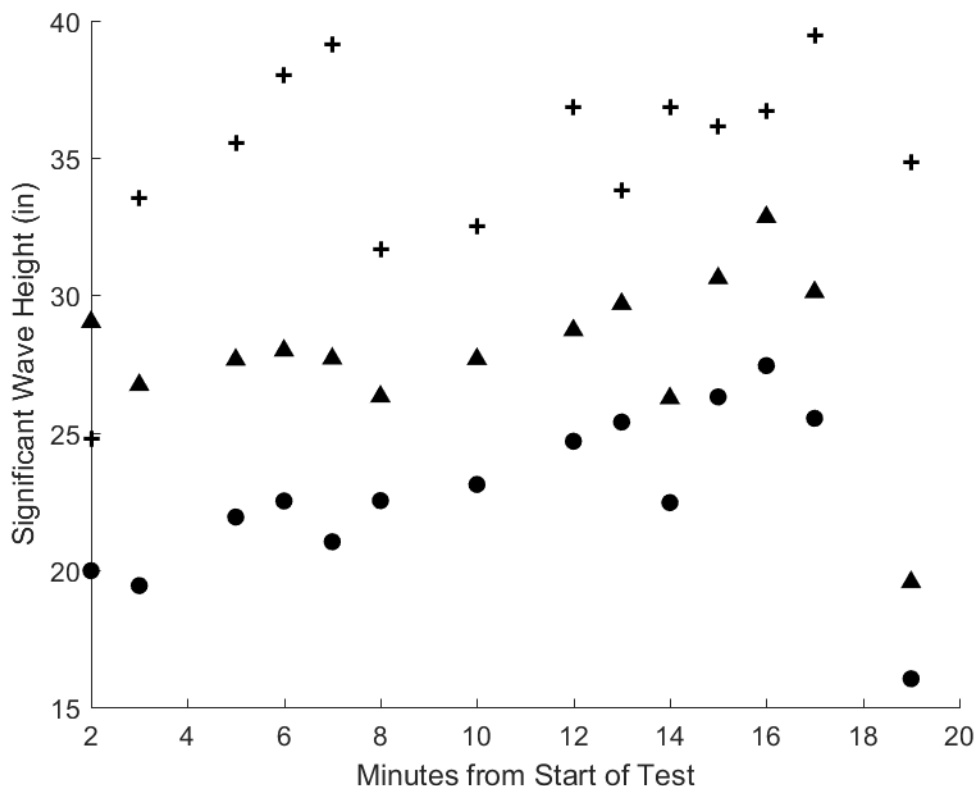


Figure F-63

Figure F-64: Plots of the significant wave heights for Test 22 of the WCM mounted to the skimmer and the raw data from the main bridge Banner. The plus signs indicate the significant wave height (H_{m0}) calculated statistically using the raw data from the WCM mounted to the skimmer. The triangles represent the significant wave height (H_{m0}) calculated statistically using a segment of time corresponding to the WCM data from the raw Banner data. The dots represent the wave heights calculated using the average of the top third wave height from the same segments ($H_{1/3}$). Each data point represents a calculation of the significant wave height from approximately 60 seconds of raw data.

Here it can be seen that the $H_{1/3}$ calculation is lower than the H_{m0} value for each time segment. The H_{m0} calculated using the WCM data is higher than the bridge data. This test is one where the waves were created by the 18-inch stroke and 18 CPM setting of the wave generator, which creates a large sinusoidal wave. We believe the discrepancies between the WCM and Banner measurement are due to lateral motion from the large elliptical motion of the wave not being considered by the algorithms. This is because we trained them on real, complex wave motion where most of the movement is in the heave.

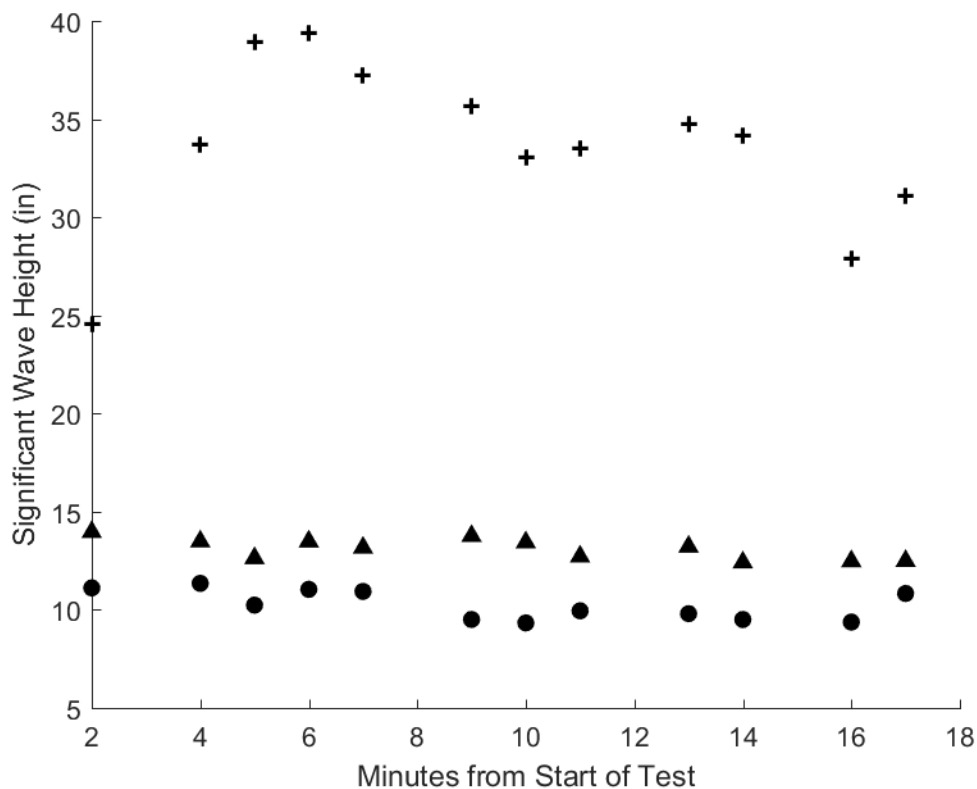


Figure F-64

Figure F-65: Plots of the significant wave heights for Test 22 of the WCM mounted to the skimmer and the raw data from the west auxiliary bridge Banner. The plus signs indicate the significant wave height (H_{m0}) calculated statistically using the raw data from the WCM mounted to the skimmer. The triangles represent the significant wave height (H_{m0}) calculated statistically using a segment of time corresponding to the WCM data from the raw Banner data. The dots represent the wave heights calculated using the average of the top third wave height from the same segments ($H_{1/3}$). Each data point represents a calculation of the significant wave height from approximately 60 seconds of raw data.

Here it can be seen that the $H_{1/3}$ calculation is lower than the H_{m0} value for each time segment. The H_{m0} calculated using the WCM data is higher than the bridge data. This test is one where the waves were created by the 18-inch stroke and 18 CPM setting of the wave generator, which creates a large sinusoidal wave. We believe the discrepancies between the WCM and Banner measurement are due to lateral motion from the large elliptical motion of the wave not being considered by the algorithms. This is because we trained them on real, complex wave motion where most of the movement is in the heave.

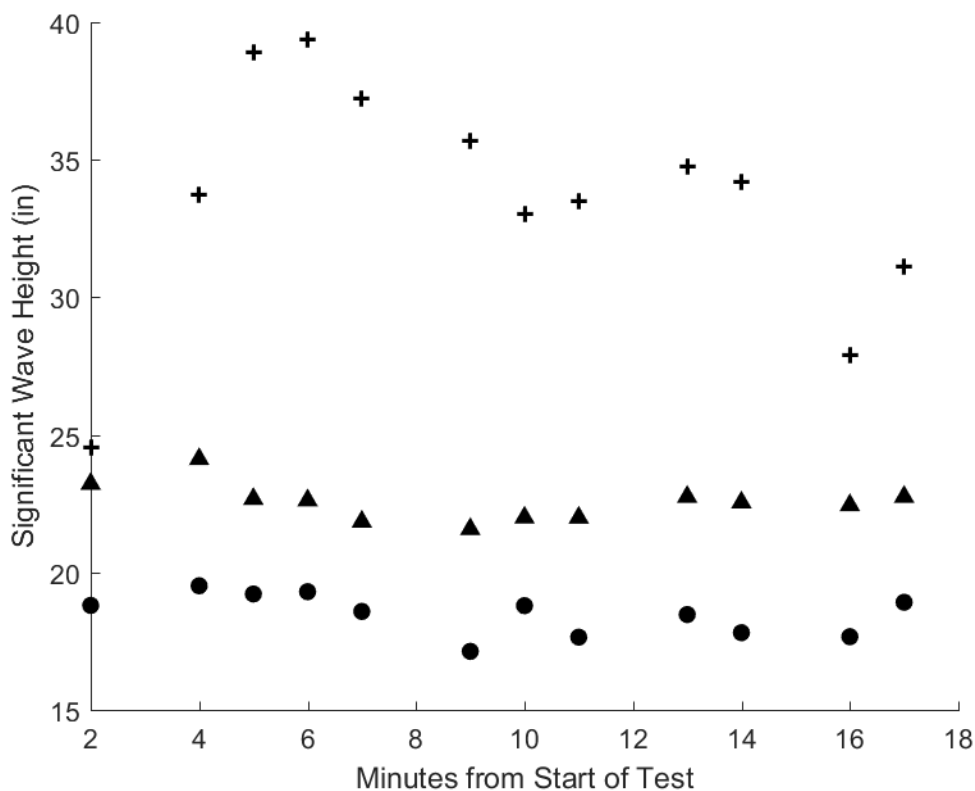


Figure F-65

Figure F-66: Plots of the significant wave heights for Test 22 of the WCM mounted to the skimmer and the raw data from the east auxiliary bridge Banner. The plus signs indicate the significant wave height (H_{m0}) calculated statistically using the raw data from the WCM mounted to the skimmer. The triangles represent the significant wave height (H_{m0}) calculated statistically using a segment of time corresponding to the WCM data from the raw Banner data. The dots represent the wave heights calculated using the average of the top third wave height from the same segments ($H_{1/3}$). Each data point represents a calculation of the significant wave height from approximately 60 seconds of raw data.

Here it can be seen that the $H_{1/3}$ calculation is lower than the H_{m0} value for each time segment. The H_{m0} calculated using the WCM data is higher than the bridge data. This test is one where the waves were created by the 18-inch stroke and 18 CPM setting of the wave generator, which creates a large sinusoidal wave. We believe the discrepancies between the WCM and Banner measurement are due to lateral motion from the large elliptical motion of the wave not being considered by the algorithms. This is because we trained them on real, complex wave motion where most of the movement is in the heave.

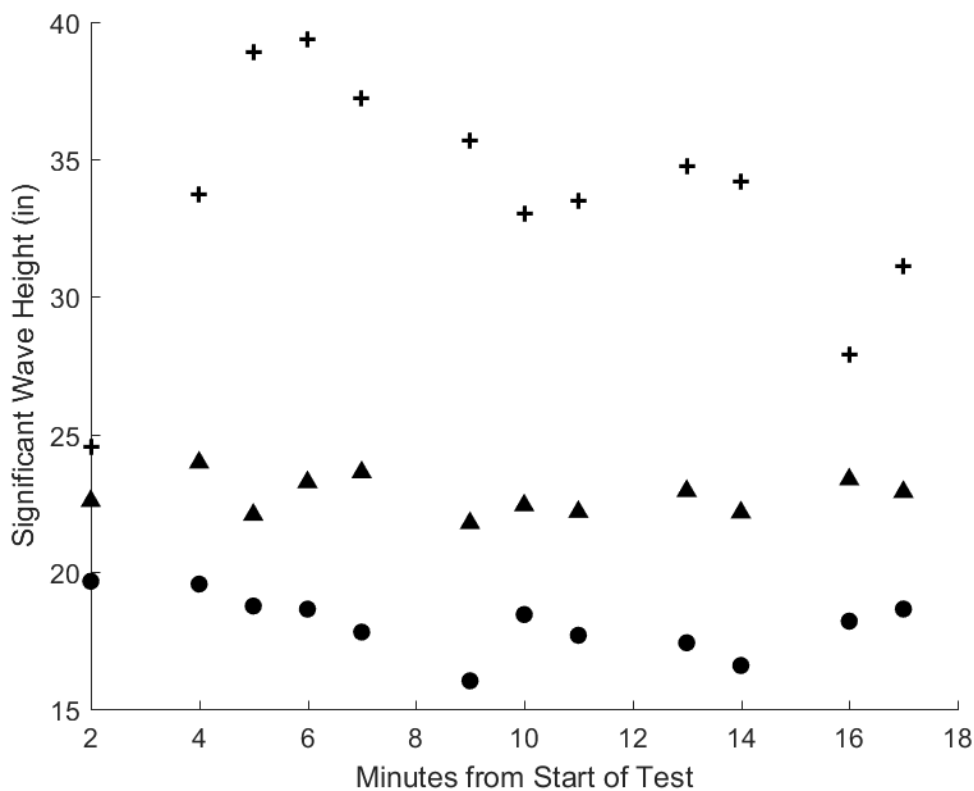


Figure F-66

Appendix G: WCM-Buoy Significant Wave Heights

This appendix contains plots of the significant wave heights. The plus signs indicate the significant wave height (H_{m0}) calculated statistically using the raw data from the WCM buoy. The triangles represent the significant wave height (H_{m0}) calculated statistically using a segment of time corresponding to the WCM data from the raw Banner data. The dots represent the wave heights calculated using the average of the top third wave height from the same segments ($H_{1/3}$). Each data point represents a calculation of the significant wave height from approximately 60 seconds of raw data.

Figure G-1: Plots of the significant wave heights for Test 1 of the WCM mounted to the skimmer and the raw data from the main bridge Banner. The plus signs indicate the significant wave height (H_{m0}) calculated statistically using the raw data from the WCM mounted to the skimmer. The triangles represent the significant wave height (H_{m0}) calculated statistically using a segment of time corresponding to the WCM data from the raw Banner data. The dots represent the wave heights calculated using the average of the top third wave height from the same segments ($H_{1/3}$). Each data point represents a calculation of the significant wave height from approximately 60 seconds of raw data.

Here it can be seen that the $H_{1/3}$ calculation is lower than the H_{m0} value for each time segment. The H_{m0} calculated using the WCM data is higher than the bridge data. This test is one where the waves were created by the 18-inch stroke and 18 cycles per minute (CPM) setting of the wave generator, which creates a large sinusoidal wave. We believe the discrepancies between the WCM and Banner measurement are due to lateral motion from the large elliptical motion of the wave not being considered by the algorithms. This is because we trained them on real, complex wave motion where most of the movement is in the heave.

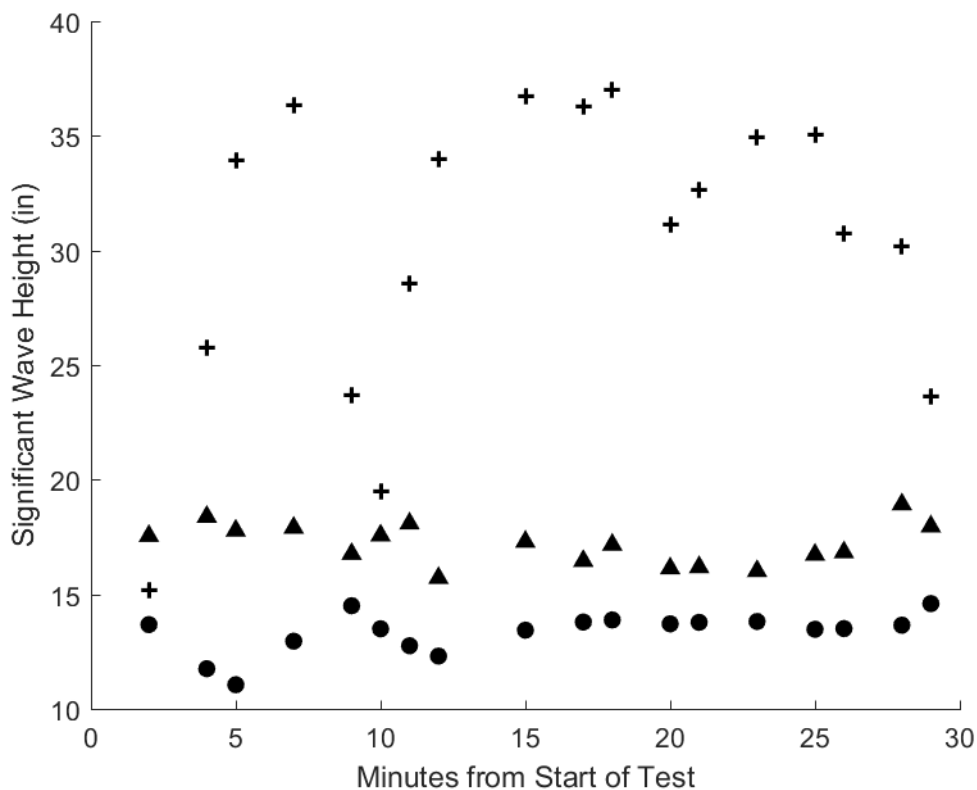


Figure G-1

Figure G-2: Plots of the significant wave heights for Test 1 of the WCM mounted to the skimmer and the raw data from the west auxiliary bridge Banner. The plus signs indicate the significant wave height (H_{m0}) calculated statistically using the raw data from the WCM mounted to the skimmer. The triangles represent the significant wave height (H_{m0}) calculated statistically using a segment of time corresponding to the WCM data from the raw Banner data. The dots represent the wave heights calculated using the average of the top third wave height from the same segments ($H_{1/3}$). Each data point represents a calculation of the significant wave height from approximately 60 seconds of raw data.

Here it can be seen that the $H_{1/3}$ calculation is lower than the H_{m0} value for each time segment. The H_{m0} calculated using the WCM data is higher than the bridge data. This test is one where the waves were created by the 18-inch stroke and 18 CPM setting of the wave generator, which creates a large sinusoidal wave. We believe the discrepancies between the WCM and Banner measurement are due to lateral motion from the large elliptical motion of the wave not being considered by the algorithms. This is because we trained them on real, complex wave motion where most of the movement is in the heave.

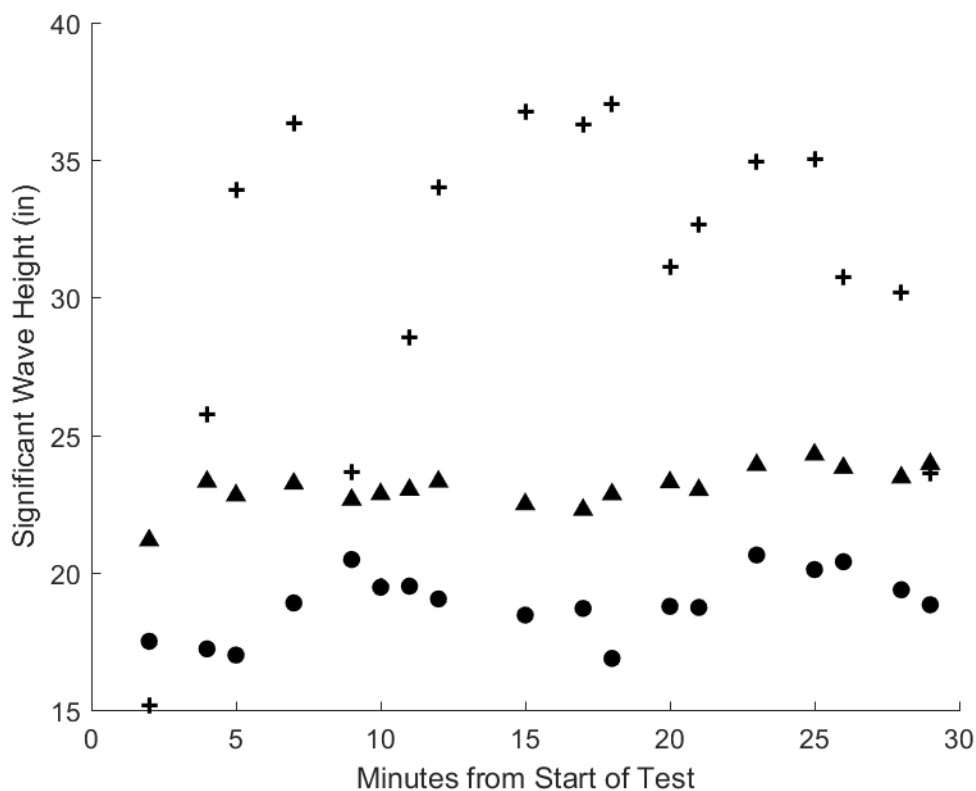


Figure G-2

Figure G-3: Plots of the significant wave heights for Test 1 of the WCM mounted to the skimmer and the raw data from the east auxiliary bridge Banner. The plus signs indicate the significant wave height (H_{m0}) calculated statistically using the raw data from the WCM mounted to the skimmer. The triangles represent the significant wave height (H_{m0}) calculated statistically using a segment of time corresponding to the WCM data from the raw Banner data. The dots represent the wave heights calculated using the average of the top third wave height from the same segments ($H_{1/3}$). Each data point represents a calculation of the significant wave height from approximately 60 seconds of raw data.

Here it can be seen that the $H_{1/3}$ calculation is lower than the H_{m0} value for each time segment. The H_{m0} calculated using the WCM data is higher than the bridge data. This test is one where the waves were created by the 18-inch stroke and 18 CPM setting of the wave generator, which creates a large sinusoidal wave. We believe the discrepancies between the WCM and Banner measurement are due to lateral motion from the large elliptical motion of the wave not being considered by the algorithms. This is because we trained them on real, complex wave motion where most of the movement is in the heave.

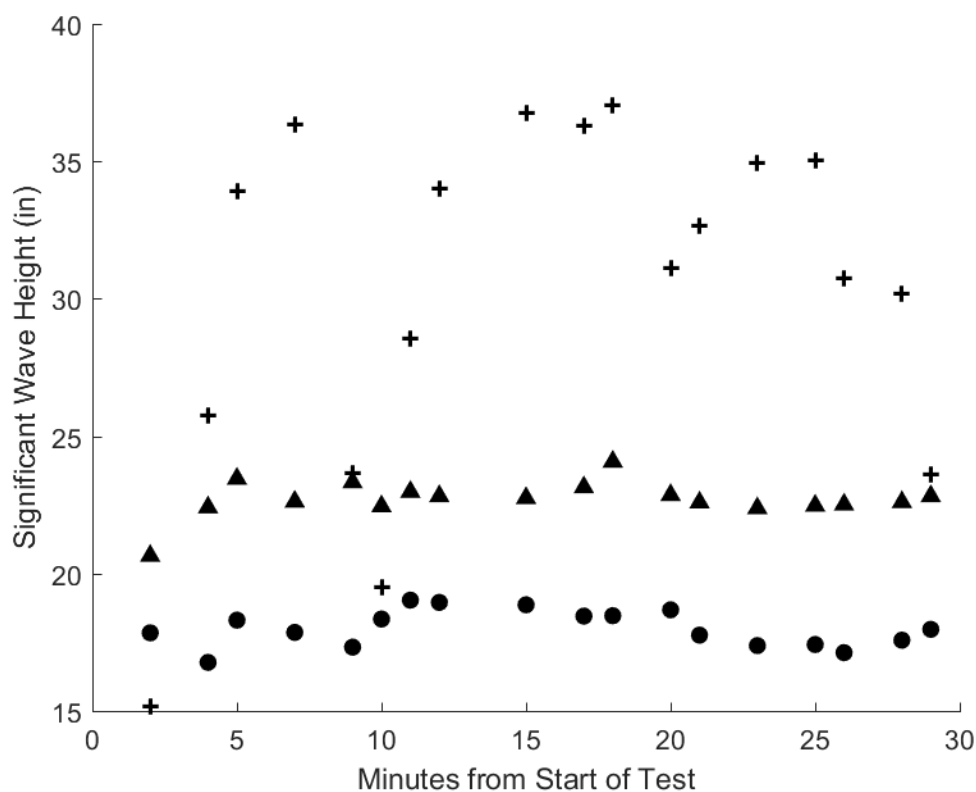


Figure G-3

Figure G-4: Plots of the significant wave heights for Test 2 of the WCM mounted to the skimmer and the raw data from the main bridge Banner. The plus signs indicate the significant wave height (H_{m0}) calculated statistically using the raw data from the WCM mounted to the skimmer. The triangles represent the significant wave height (H_{m0}) calculated statistically using a segment of time corresponding to the WCM data from the raw Banner data. The dots represent the wave heights calculated using the average of the top third wave height from the same segments ($H_{1/3}$). Each data point represents a calculation of the significant wave height from approximately 60 seconds of raw data.

Here it can be seen that the $H_{1/3}$ calculation is lower than the H_{m0} value calculated using the Banner data for each time segment. The H_{m0} calculated using the WCM data is generally within the 4-inch performance objective with the H_{m0} from the bridge data.

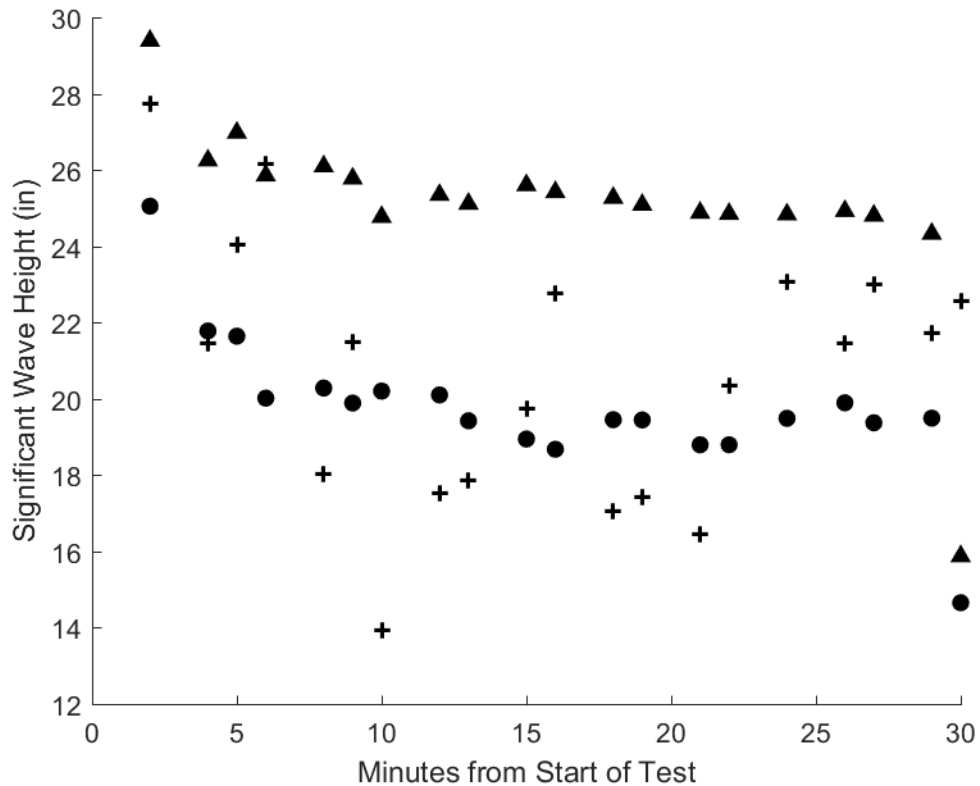


Figure G-4

Figure G-5: Plots of the significant wave heights for Test 2 of the WCM mounted to the skimmer and the raw data from the west auxiliary bridge Banner. The plus signs indicate the significant wave height (H_{m0}) calculated statistically using the raw data from the WCM mounted to the skimmer. The triangles represent the significant wave height (H_{m0}) calculated statistically using a segment of time corresponding to the WCM data from the raw Banner data. The dots represent the wave heights calculated using the average of the top third wave height from the same segments ($H_{1/3}$). Each data point represents a calculation of the significant wave height from approximately 60 seconds of raw data.

Here it can be seen that the $H_{1/3}$ calculation is lower than the H_{m0} value calculated using the Banner data for each time segment. The H_{m0} calculated using the WCM data is generally within the 4-inch performance objective with the H_{m0} from the bridge data.

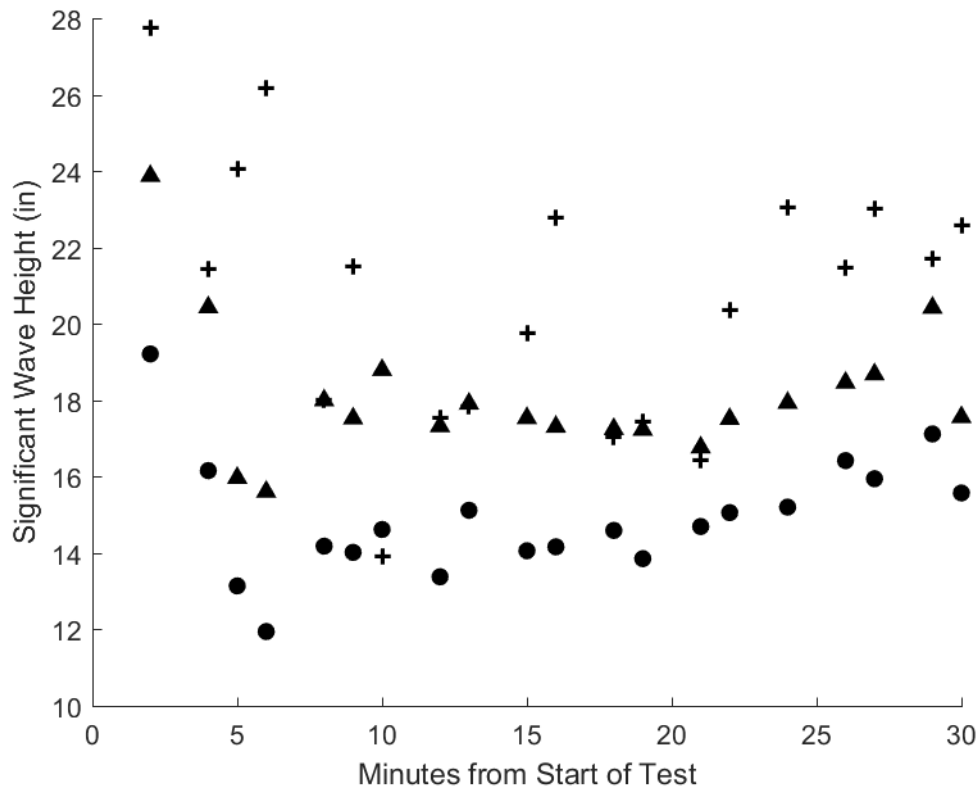


Figure G-5

Figure G-6: Plots of the significant wave heights for Test 2 of the WCM mounted to the skimmer and the raw data from the east auxiliary bridge Banner. The plus signs indicate the significant wave height (H_{m0}) calculated statistically using the raw data from the WCM mounted to the skimmer. The triangles represent the significant wave height (H_{m0}) calculated statistically using a segment of time corresponding to the WCM data from the raw Banner data. The dots represent the wave heights calculated using the average of the top third wave height from the same segments ($H_{1/3}$). Each data point represents a calculation of the significant wave height from approximately 60 seconds of raw data.

Here it can be seen that the $H_{1/3}$ calculation is lower than the H_{m0} value calculated using the Banner data for each time segment. The H_{m0} calculated using the WCM data is generally within the 4-inch performance objective with the H_{m0} from the bridge data.

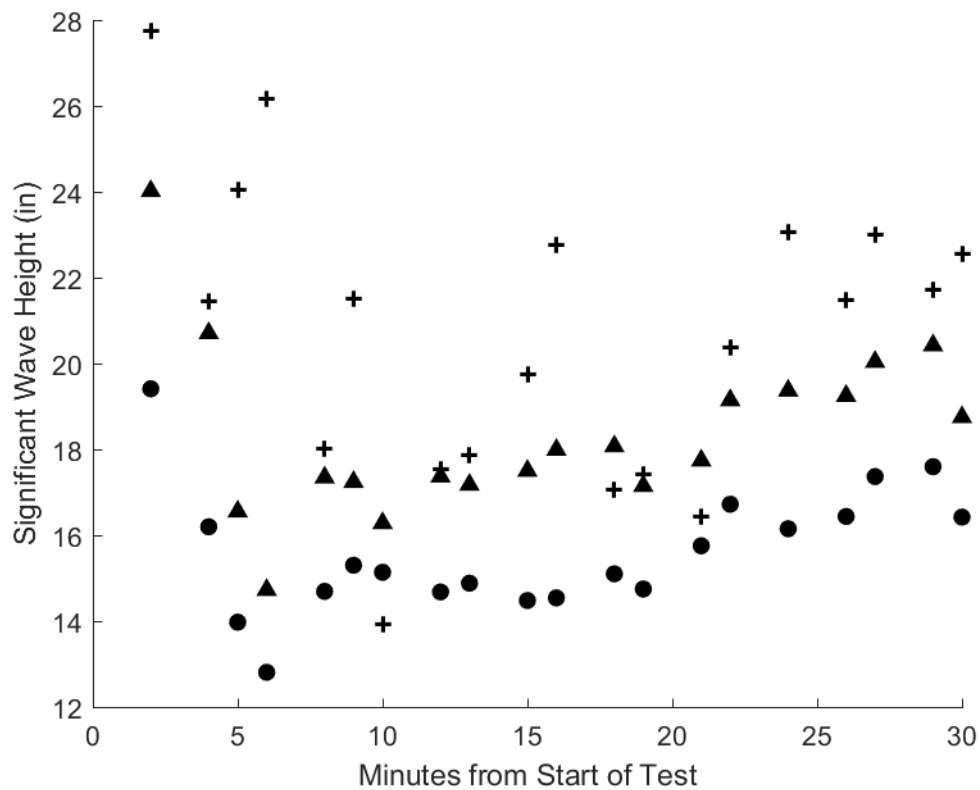


Figure G-6

Figure G-7: Plots of the significant wave heights for Test 3 of the WCM mounted to the skimmer and the raw data from the main bridge Banner. The plus signs indicate the significant wave height (H_{m0}) calculated statistically using the raw data from the WCM mounted to the skimmer. The triangles represent the significant wave height (H_{m0}) calculated statistically using a segment of time corresponding to the WCM data from the raw Banner data. The dots represent the wave heights calculated using the average of the top third wave height from the same segments ($H_{1/3}$). Each data point represents a calculation of the significant wave height from approximately 60 seconds of raw data.

Here it can be seen that the $H_{1/3}$ calculation is lower than the H_{m0} value calculated using the Banner data for each time segment. The H_{m0} calculated using the WCM data is generally within the 4-inch performance objective with the H_{m0} from the bridge data.

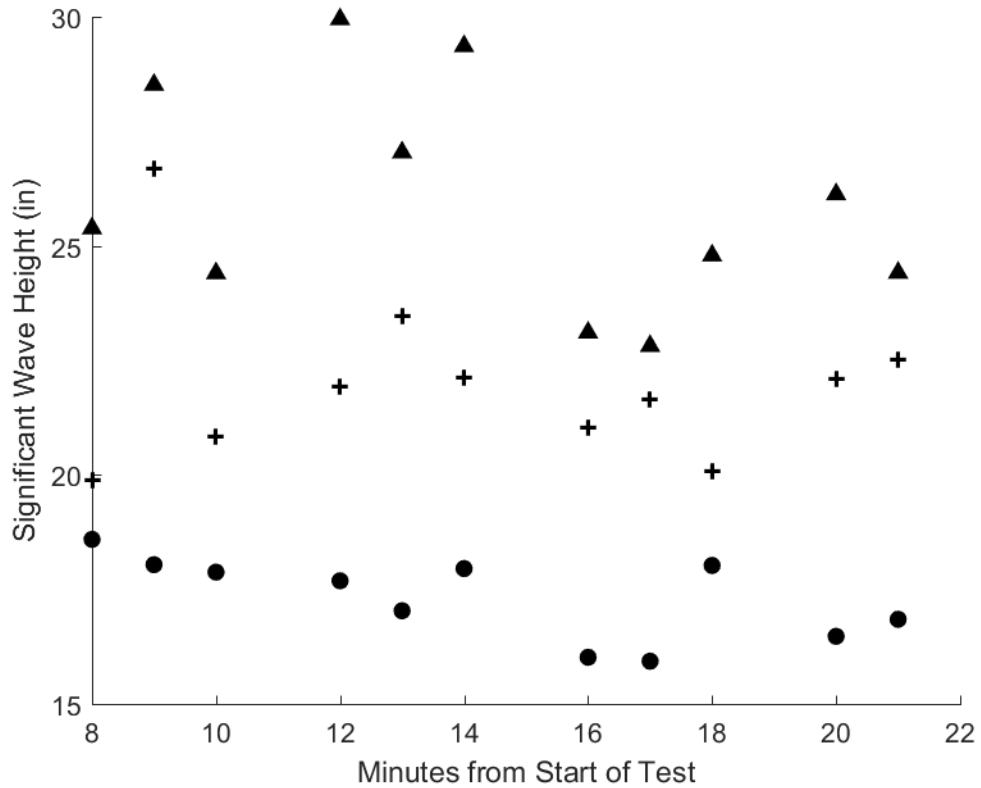


Figure G-7

Figure G-8: Plots of the significant wave heights for Test 3 of the WCM mounted to the skimmer and the raw data from the west auxiliary bridge Banner. The plus signs indicate the significant wave height (H_{m0}) calculated statistically using the raw data from the WCM mounted to the skimmer. The triangles represent the significant wave height (H_{m0}) calculated statistically using a segment of time corresponding to the WCM data from the raw Banner data. The dots represent the wave heights calculated using the average of the top third wave height from the same segments ($H_{1/3}$). Each data point represents a calculation of the significant wave height from approximately 60 seconds of raw data.

Here it can be seen that the $H_{1/3}$ calculation is lower than the H_{m0} value calculated using the Banner data for each time segment. The H_{m0} calculated using the WCM data is generally within the 4-inch performance objective with the H_{m0} from the bridge data.

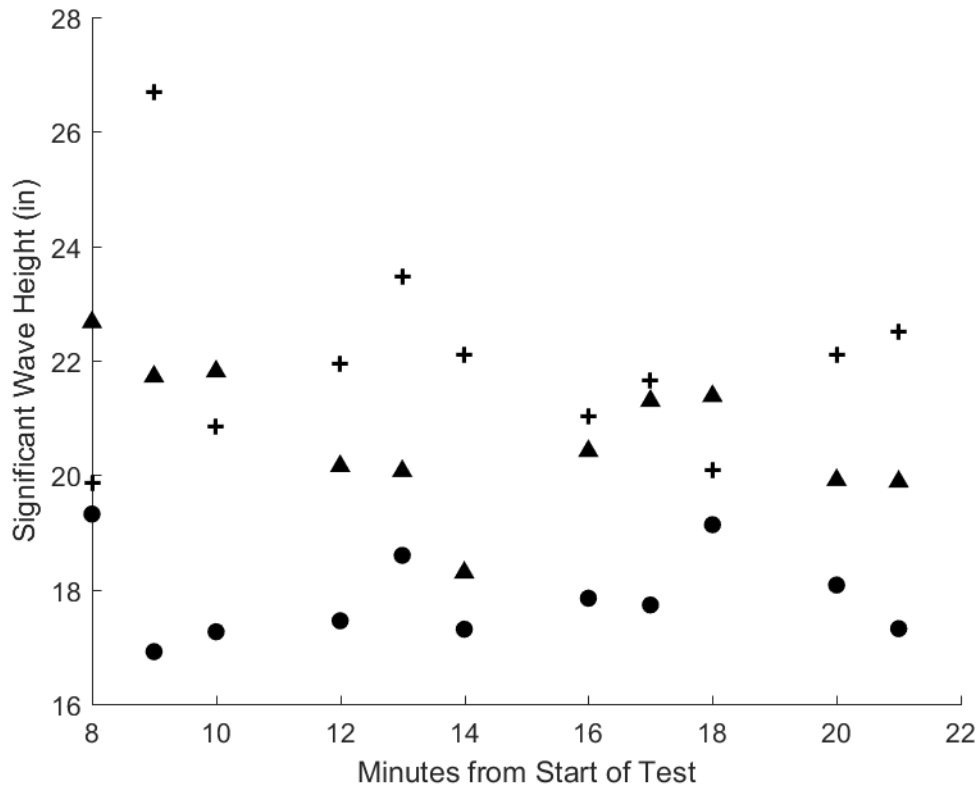


Figure G-8

Figure G-9: Plots of the significant wave heights for Test 3 of the WCM mounted to the skimmer and the raw data from the east auxiliary bridge Banner. The plus signs indicate the significant wave height (H_{m0}) calculated statistically using the raw data from the WCM mounted to the skimmer. The triangles represent the significant wave height (H_{m0}) calculated statistically using a segment of time corresponding to the WCM data from the raw Banner data. The dots represent the wave heights calculated using the average of the top third wave height from the same segments ($H_{1/3}$). Each data point represents a calculation of the significant wave height from approximately 60 seconds of raw data.

Here it can be seen that the $H_{1/3}$ calculation is lower than the H_{m0} value calculated using the Banner data for each time segment. The H_{m0} calculated using the WCM data is generally within the 4-inch performance objective with the H_{m0} from the bridge data.

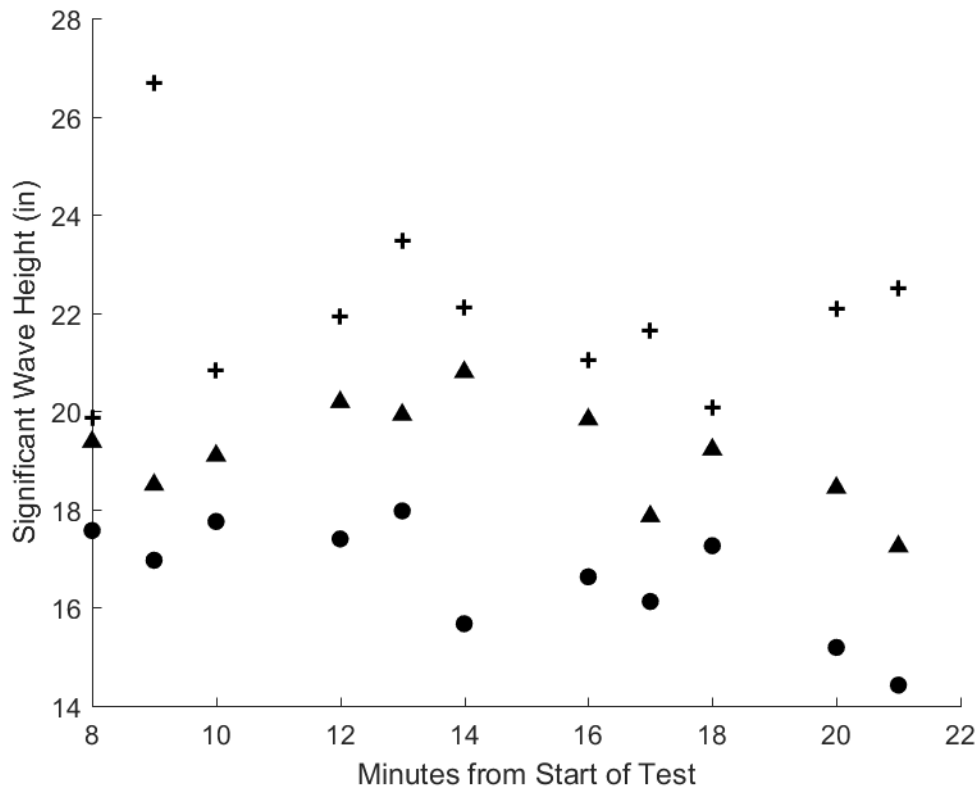


Figure G-9

Figure G-10: Plots of the significant wave heights for Test 4 of the WCM mounted to the skimmer and the raw data from the main bridge Banner. The plus signs indicate the significant wave height (H_{m0}) calculated statistically using the raw data from the WCM mounted to the skimmer. The triangles represent the significant wave height (H_{m0}) calculated statistically using a segment of time corresponding to the WCM data from the raw Banner data. The dots represent the wave heights calculated using the average of the top third wave height from the same segments ($H_{1/3}$). Each data point represents a calculation of the significant wave height from approximately 60 seconds of raw data.

Here it can be seen that the $H_{1/3}$ calculation is lower than the H_{m0} value calculated using the Banner data for each time segment. The H_{m0} calculated using the WCM data is generally within the 4-inch performance objective with the H_{m0} from the bridge data.

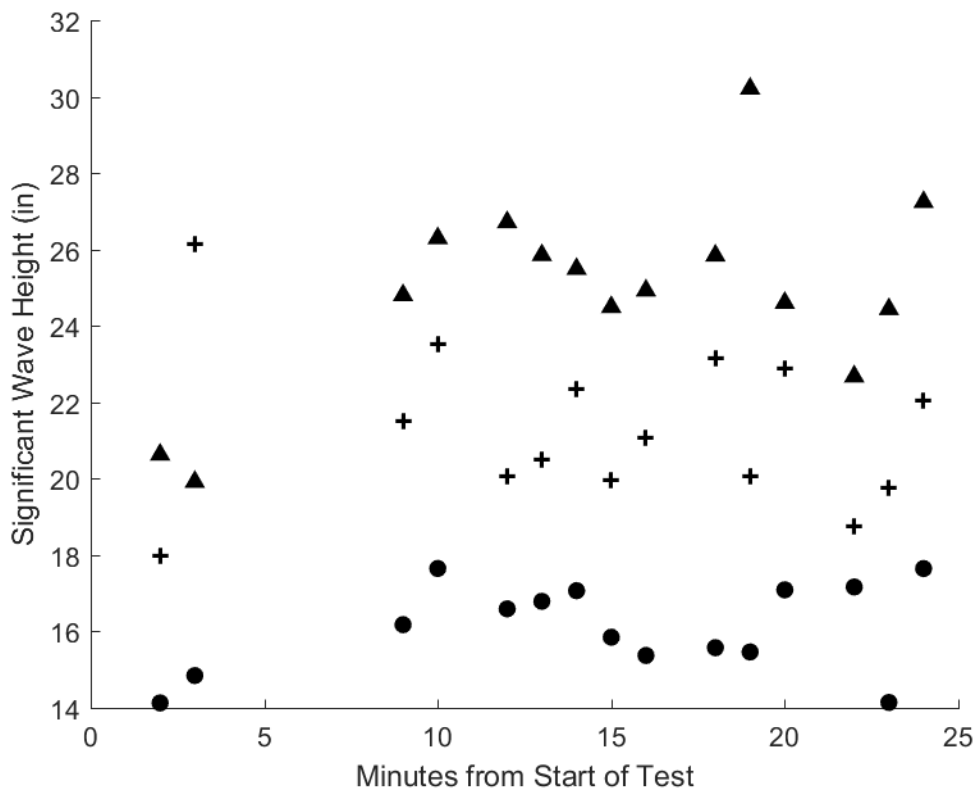


Figure G-10

Figure G-11: Plots of the significant wave heights for Test 4 of the WCM mounted to the skimmer and the raw data from the west auxiliary bridge Banner. The plus signs indicate the significant wave height (H_{m0}) calculated statistically using the raw data from the WCM mounted to the skimmer. The triangles represent the significant wave height (H_{m0}) calculated statistically using a segment of time corresponding to the WCM data from the raw Banner data. The dots represent the wave heights calculated using the average of the top third wave height from the same segments ($H_{1/3}$). Each data point represents a calculation of the significant wave height from approximately 60 seconds of raw data.

Here it can be seen that the $H_{1/3}$ calculation is lower than the H_{m0} value calculated using the Banner data for each time segment. The H_{m0} calculated using the WCM data is generally within the 4-inch performance objective with the H_{m0} from the bridge data.

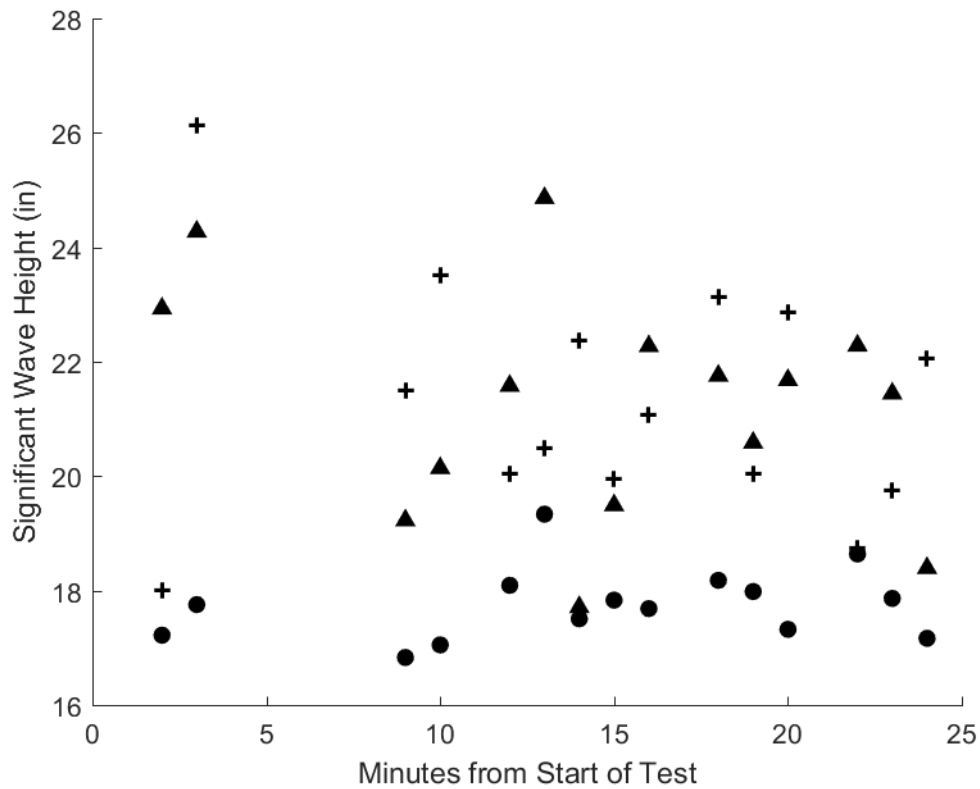


Figure G-11

Figure G-12: Plots of the significant wave heights for Test 4 of the WCM mounted to the skimmer and the raw data from the east auxiliary bridge Banner. The plus signs indicate the significant wave height (H_{m0}) calculated statistically using the raw data from the WCM mounted to the skimmer. The triangles represent the significant wave height (H_{m0}) calculated statistically using a segment of time corresponding to the WCM data from the raw Banner data. The dots represent the wave heights calculated using the average of the top third wave height from the same segments ($H_{1/3}$). Each data point represents a calculation of the significant wave height from approximately 60 seconds of raw data.

Here it can be seen that the $H_{1/3}$ calculation is lower than the H_{m0} value calculated using the Banner data for each time segment. The H_{m0} calculated using the WCM data is generally within the 4-inch performance objective with the H_{m0} from the bridge data.

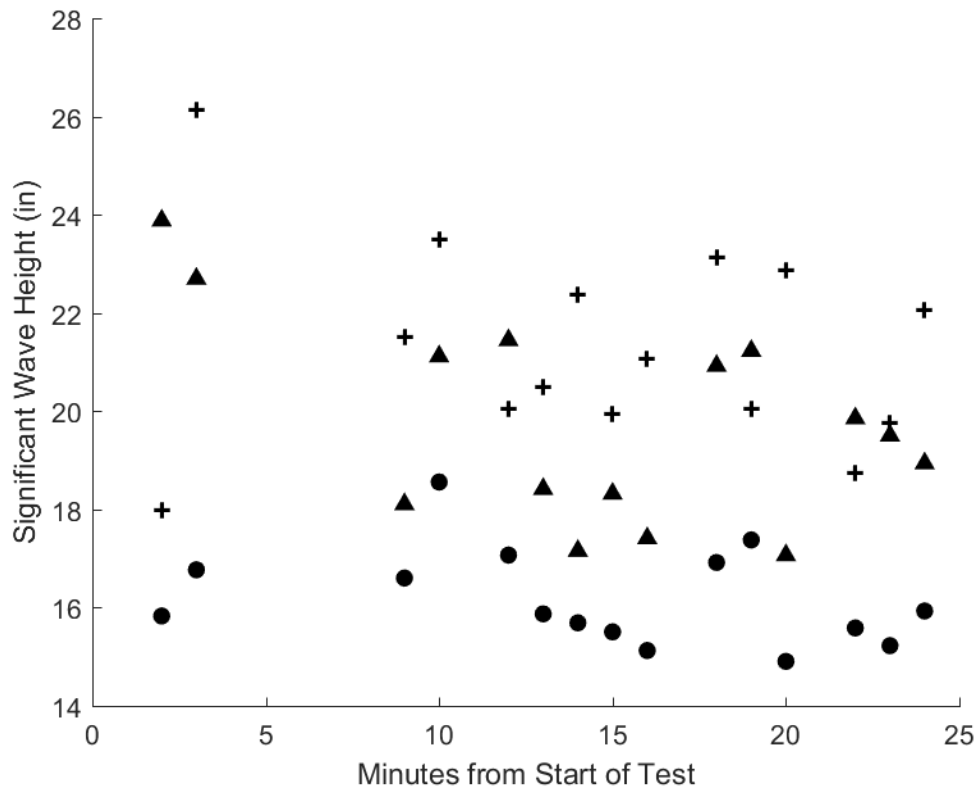


Figure G-12

Figure G-13: Plots of the significant wave heights for Test 5 of the WCM mounted to the skimmer and the raw data from the main bridge Banner. The plus signs indicate the significant wave height (H_{m0}) calculated statistically using the raw data from the WCM mounted to the skimmer. The triangles represent the significant wave height (H_{m0}) calculated statistically using a segment of time corresponding to the WCM data from the raw Banner data. The dots represent the wave heights calculated using the average of the top third wave height from the same segments ($H_{1/3}$). Each data point represents a calculation of the significant wave height from approximately 60 seconds of raw data.

Here it can be seen that the $H_{1/3}$ calculation is lower than the H_{m0} value for each time segment. The H_{m0} calculated using the WCM data is higher than the bridge data. This test is one where the waves were created by the 18-inch stroke and 18 CPM setting of the wave generator, which creates a large sinusoidal wave. We believe the discrepancies between the WCM and Banner measurement are due to lateral motion from the large elliptical motion of the wave not being considered by the algorithms. This is because we trained them on real, complex wave motion where most of the movement is in the heave.

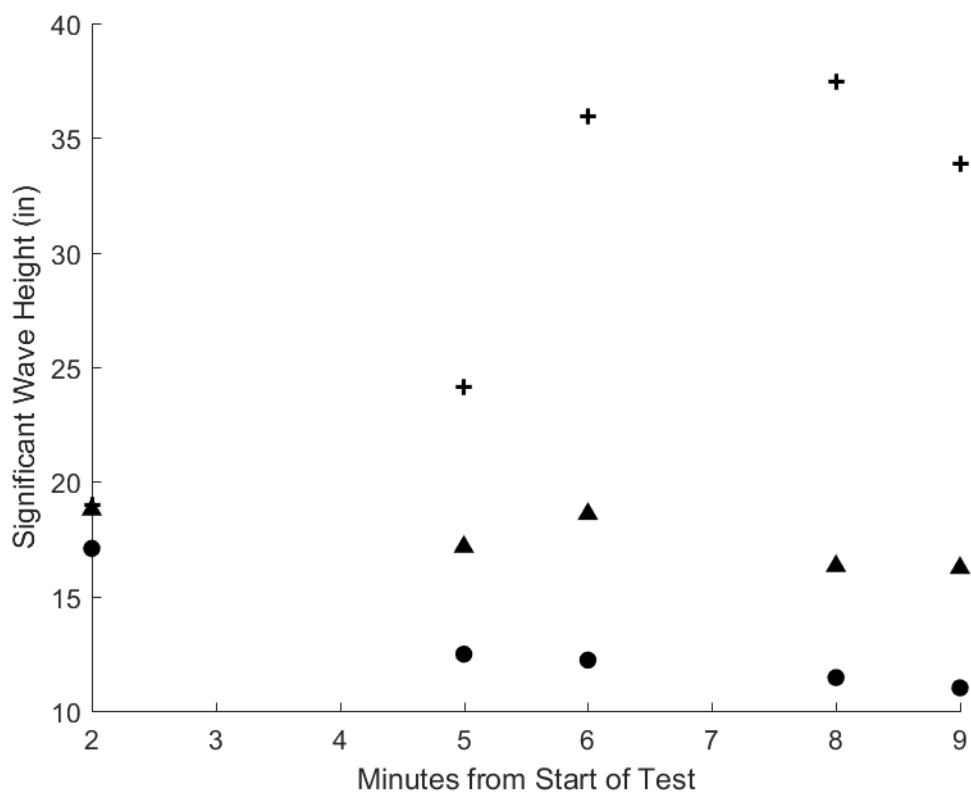


Figure G-13

Figure G-14: Plots of the significant wave heights for Test 5 of the WCM mounted to the skimmer and the raw data from the west auxiliary bridge Banner. The plus signs indicate the significant wave height (H_{m0}) calculated statistically using the raw data from the WCM mounted to the skimmer. The triangles represent the significant wave height (H_{m0}) calculated statistically using a segment of time corresponding to the WCM data from the raw Banner data. The dots represent the wave heights calculated using the average of the top third wave height from the same segments ($H_{1/3}$). Each data point represents a calculation of the significant wave height from approximately 60 seconds of raw data.

Here it can be seen that the $H_{1/3}$ calculation is lower than the H_{m0} value for each time segment. The H_{m0} calculated using the WCM data is higher than the bridge data. This test is one where the waves were created by the 18-inch stroke and 18 CPM setting of the wave generator, which creates a large sinusoidal wave. We believe the discrepancies between the WCM and Banner measurement are due to lateral motion from the large elliptical motion of the wave not being considered by the algorithms. This is because we trained them on real, complex wave motion where most of the movement is in the heave.

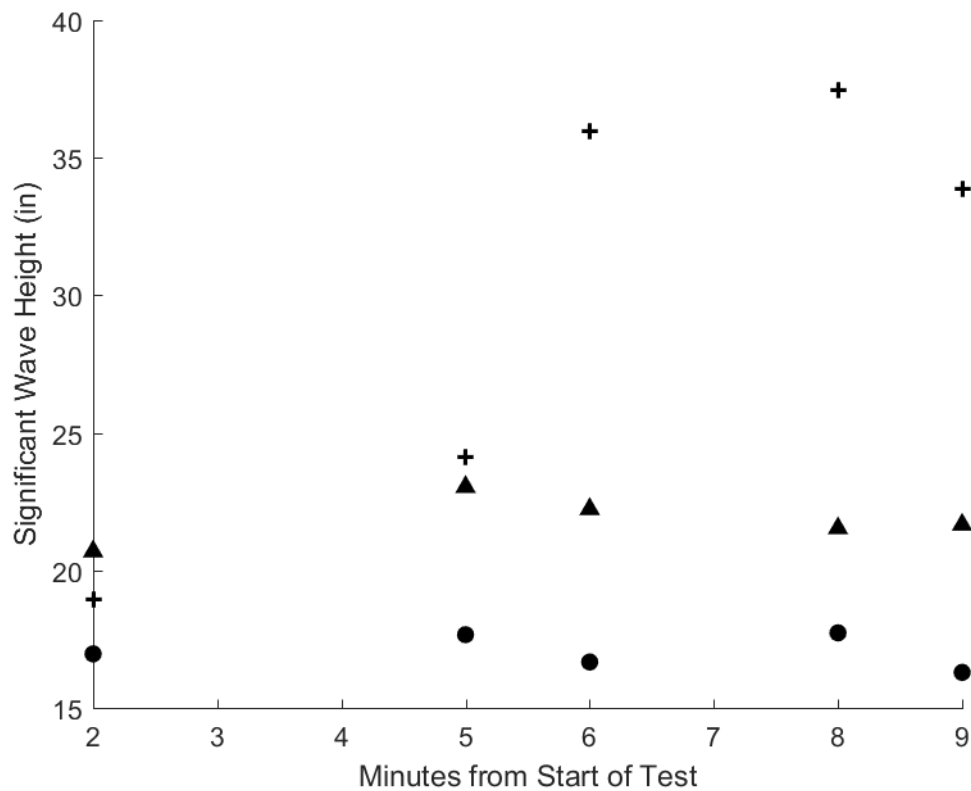


Figure G-14

Figure G-15: Plots of the significant wave heights for Test 5 of the WCM mounted to the skimmer and the raw data from the east auxiliary bridge Banner. The plus signs indicate the significant wave height (H_{m0}) calculated statistically using the raw data from the WCM mounted to the skimmer. The triangles represent the significant wave height (H_{m0}) calculated statistically using a segment of time corresponding to the WCM data from the raw Banner data. The dots represent the wave heights calculated using the average of the top third wave height from the same segments ($H_{1/3}$). Each data point represents a calculation of the significant wave height from approximately 60 seconds of raw data.

Here it can be seen that the $H_{1/3}$ calculation is lower than the H_{m0} value for each time segment. The H_{m0} calculated using the WCM data is higher than the bridge data. This test is one where the waves were created by the 18-inch stroke and 18 CPM setting of the wave generator, which creates a large sinusoidal wave. We believe the discrepancies between the WCM and Banner measurement are due to lateral motion from the large elliptical motion of the wave not being considered by the algorithms. This is because we trained them on real, complex wave motion where most of the movement is in the heave.

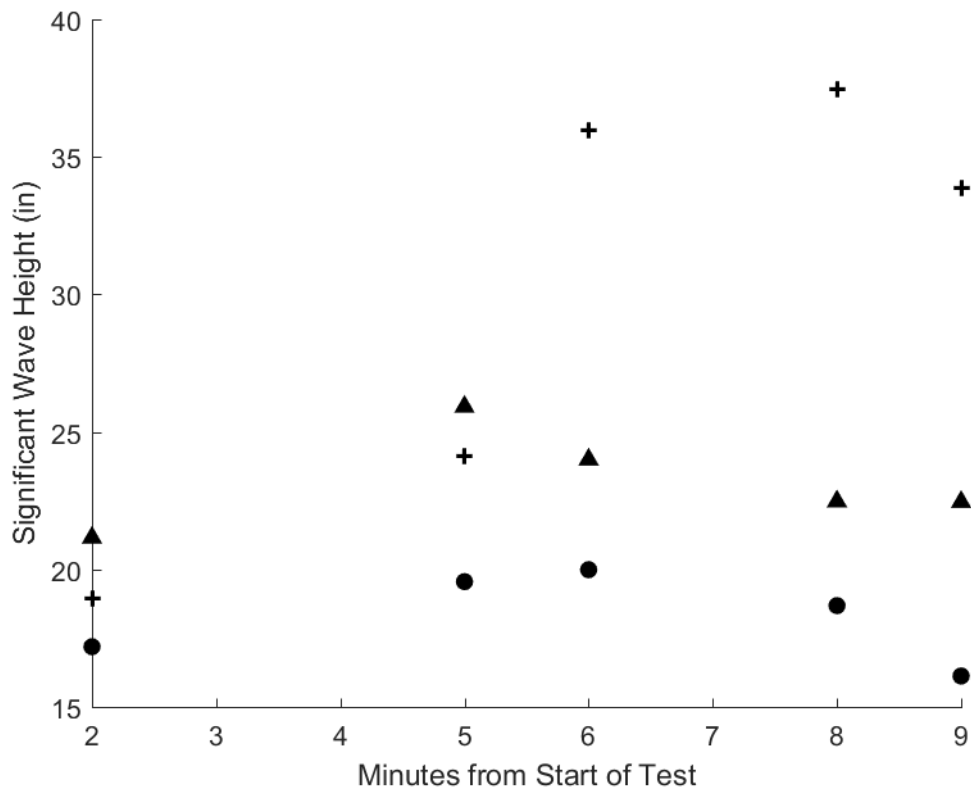


Figure G-15

Figure G-16: Plots of the significant wave heights for Test 6 of the WCM mounted to the skimmer and the raw data from the main bridge Banner. The plus signs indicate the significant wave height (H_{m0}) calculated statistically using the raw data from the WCM mounted to the skimmer. The triangles represent the significant wave height (H_{m0}) calculated statistically using a segment of time corresponding to the WCM data from the raw Banner data. The dots represent the wave heights calculated using the average of the top third wave height from the same segments ($H_{1/3}$). Each data point represents a calculation of the significant wave height from approximately 60 seconds of raw data.

Here it can be seen that the $H_{1/3}$ calculation is lower than the H_{m0} value for each time segment. The H_{m0} calculated using the WCM data is higher than the bridge data. This test is one where the waves were created by the 18-inch stroke and 18 CPM setting of the wave generator, which creates a large sinusoidal wave. We believe the discrepancies between the WCM and Banner measurement are due to lateral motion from the large elliptical motion of the wave not being considered by the algorithms. This is because we trained them on real, complex wave motion where most of the movement is in the heave.

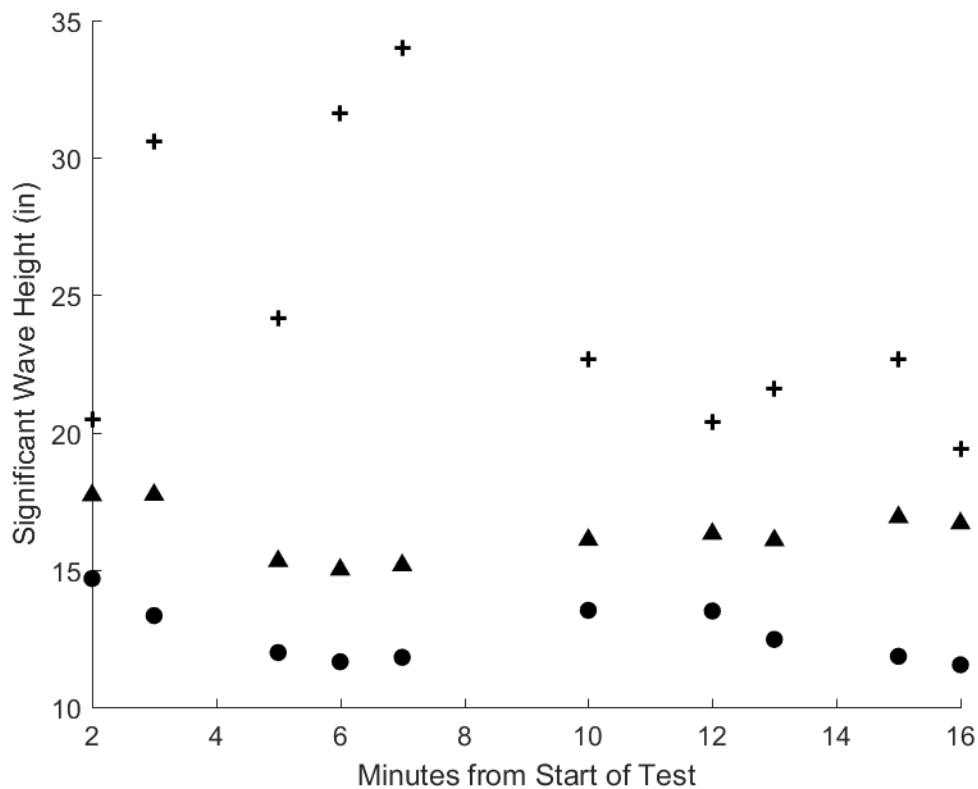


Figure G-16

Figure G-17: Plots of the significant wave heights for Test 6 of the WCM mounted to the skimmer and the raw data from the west auxiliary bridge Banner. The plus signs indicate the significant wave height (H_{m0}) calculated statistically using the raw data from the WCM mounted to the skimmer. The triangles represent the significant wave height (H_{m0}) calculated statistically using a segment of time corresponding to the WCM data from the raw Banner data. The dots represent the wave heights calculated using the average of the top third wave height from the same segments ($H_{1/3}$). Each data point represents a calculation of the significant wave height from approximately 60 seconds of raw data.

Here it can be seen that the $H_{1/3}$ calculation is lower than the H_{m0} value for each time segment. The H_{m0} calculated using the WCM data is higher than the bridge data. This test is one where the waves were created by the 18-inch stroke and 18 CPM setting of the wave generator, which creates a large sinusoidal wave. We believe the discrepancies between the WCM and Banner measurement are due to lateral motion from the large elliptical motion of the wave not being considered by the algorithms. This is because we trained them on real, complex wave motion where most of the movement is in the heave.

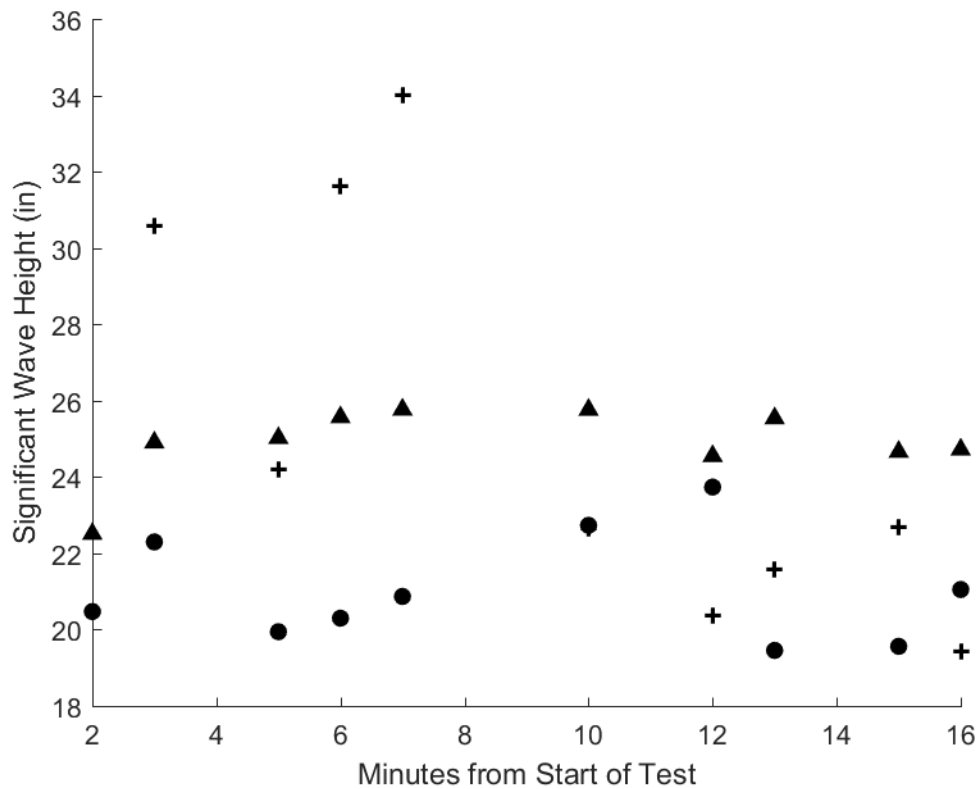


Figure G-17

Figure G-18: Plots of the significant wave heights for Test 6 of the WCM mounted to the skimmer and the raw data from the east auxiliary bridge Banner. The plus signs indicate the significant wave height (H_{m0}) calculated statistically using the raw data from the WCM mounted to the skimmer. The triangles represent the significant wave height (H_{m0}) calculated statistically using a segment of time corresponding to the WCM data from the raw Banner data. The dots represent the wave heights calculated using the average of the top third wave height from the same segments ($H_{1/3}$). Each data point represents a calculation of the significant wave height from approximately 60 seconds of raw data.

Here it can be seen that the $H_{1/3}$ calculation is lower than the H_{m0} value for each time segment. The H_{m0} calculated using the WCM data is higher than the bridge data. This test is one where the waves were created by the 18-inch stroke and 18 CPM setting of the wave generator, which creates a large sinusoidal wave. We believe the discrepancies between the WCM and Banner measurement are due to lateral motion from the large elliptical motion of the wave not being considered by the algorithms. This is because we trained them on real, complex wave motion where most of the movement is in the heave.

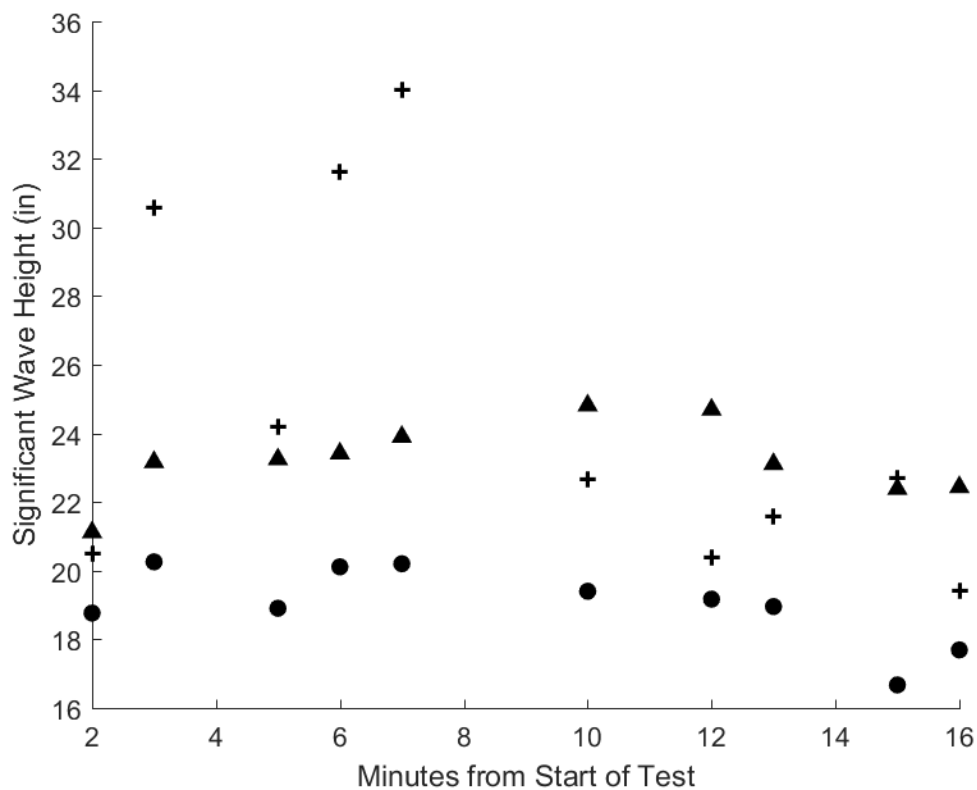


Figure G-18

Figure G-19: Plots of the significant wave heights for Test 7 of the WCM mounted to the skimmer and the raw data from the main bridge Banner. The plus signs indicate the significant wave height (H_{m0}) calculated statistically using the raw data from the WCM mounted to the skimmer. The triangles represent the significant wave height (H_{m0}) calculated statistically using a segment of time corresponding to the WCM data from the raw Banner data. The dots represent the wave heights calculated using the average of the top third wave height from the same segments ($H_{1/3}$). Each data point represents a calculation of the significant wave height from approximately 60 seconds of raw data.

Here it can be seen that the $H_{1/3}$ calculation is lower than the H_{m0} value calculated using the Banner data for each time segment. The H_{m0} calculated using the WCM data is generally within the 4-inch performance objective with the H_{m0} from the bridge data.

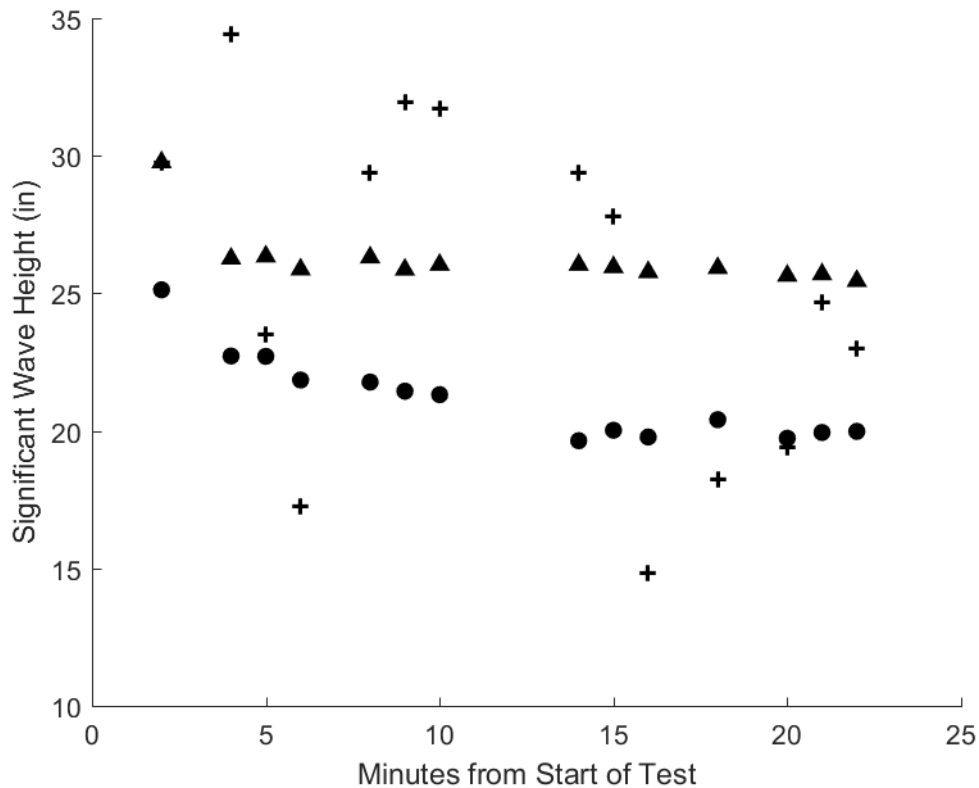


Figure G-19

Figure G-20: Plots of the significant wave heights for Test 7 of the WCM mounted to the skimmer and the raw data from the west auxiliary bridge Banner. The plus signs indicate the significant wave height (H_{m0}) calculated statistically using the raw data from the WCM mounted to the skimmer. The triangles represent the significant wave height (H_{m0}) calculated statistically using a segment of time corresponding to the WCM data from the raw Banner data. The dots represent the wave heights calculated using the average of the top third wave height from the same segments ($H_{1/3}$). Each data point represents a calculation of the significant wave height from approximately 60 seconds of raw data.

Here it can be seen that the $H_{1/3}$ calculation is lower than the H_{m0} value calculated using the Banner data for each time segment. The H_{m0} calculated using the WCM data is generally within the 4-inch performance objective with the H_{m0} from the bridge data.

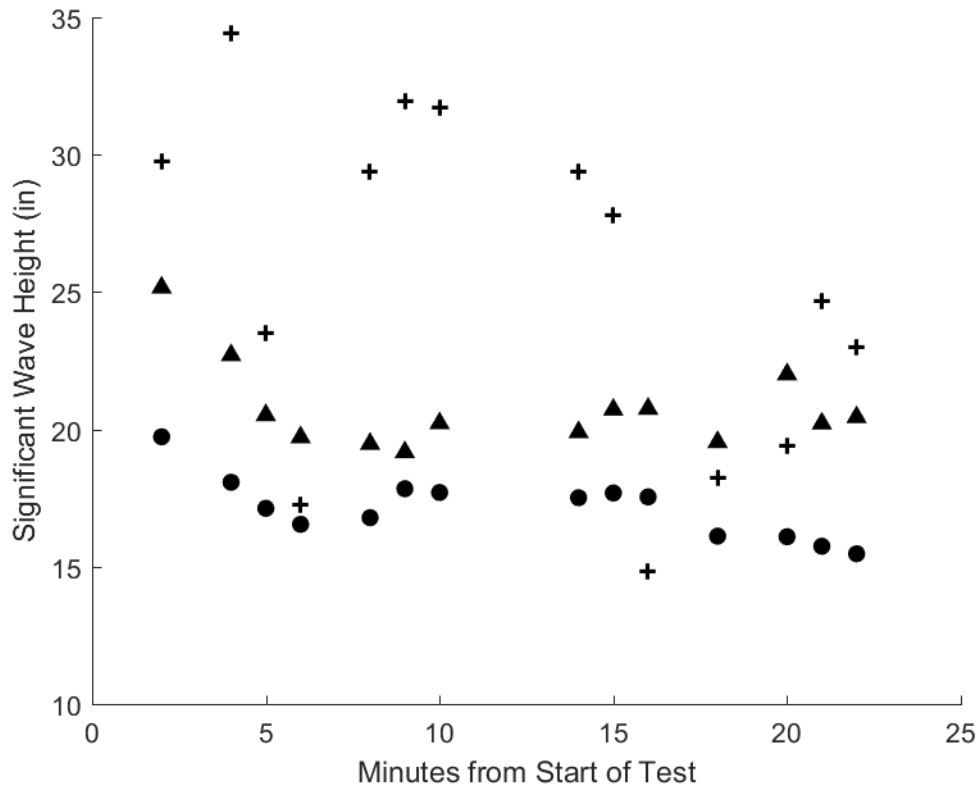


Figure G-20

Figure G-21: Plots of the significant wave heights for Test 7 of the WCM mounted to the skimmer and the raw data from the east auxiliary bridge Banner. The plus signs indicate the significant wave height (H_{m0}) calculated statistically using the raw data from the WCM mounted to the skimmer. The triangles represent the significant wave height (H_{m0}) calculated statistically using a segment of time corresponding to the WCM data from the raw Banner data. The dots represent the wave heights calculated using the average of the top third wave height from the same segments ($H_{1/3}$). Each data point represents a calculation of the significant wave height from approximately 60 seconds of raw data.

Here it can be seen that the $H_{1/3}$ calculation is lower than the H_{m0} value calculated using the Banner data for each time segment. The H_{m0} calculated using the WCM data is generally within the 4-inch performance objective with the H_{m0} from the bridge data.

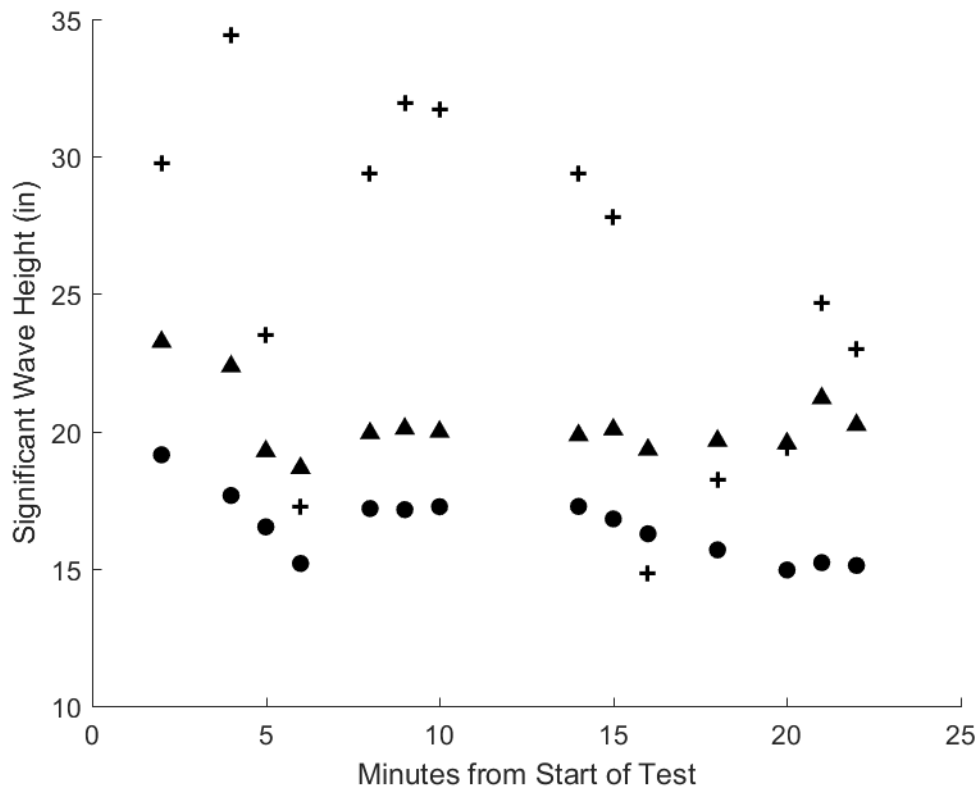


Figure G-21

Figure G-22: Plots of the significant wave heights for Test 8 of the WCM mounted to the skimmer and the raw data from the main bridge Banner. The plus signs indicate the significant wave height (H_{m0}) calculated statistically using the raw data from the WCM mounted to the skimmer. The triangles represent the significant wave height (H_{m0}) calculated statistically using a segment of time corresponding to the WCM data from the raw Banner data. The dots represent the wave heights calculated using the average of the top third wave height from the same segments ($H_{1/3}$). Each data point represents a calculation of the significant wave height from approximately 60 seconds of raw data.

Here it can be seen that the $H_{1/3}$ calculation is lower than the H_{m0} value calculated using the Banner data for each time segment. The H_{m0} calculated using the WCM data is generally within the 4-inch performance objective with the H_{m0} from the bridge data.

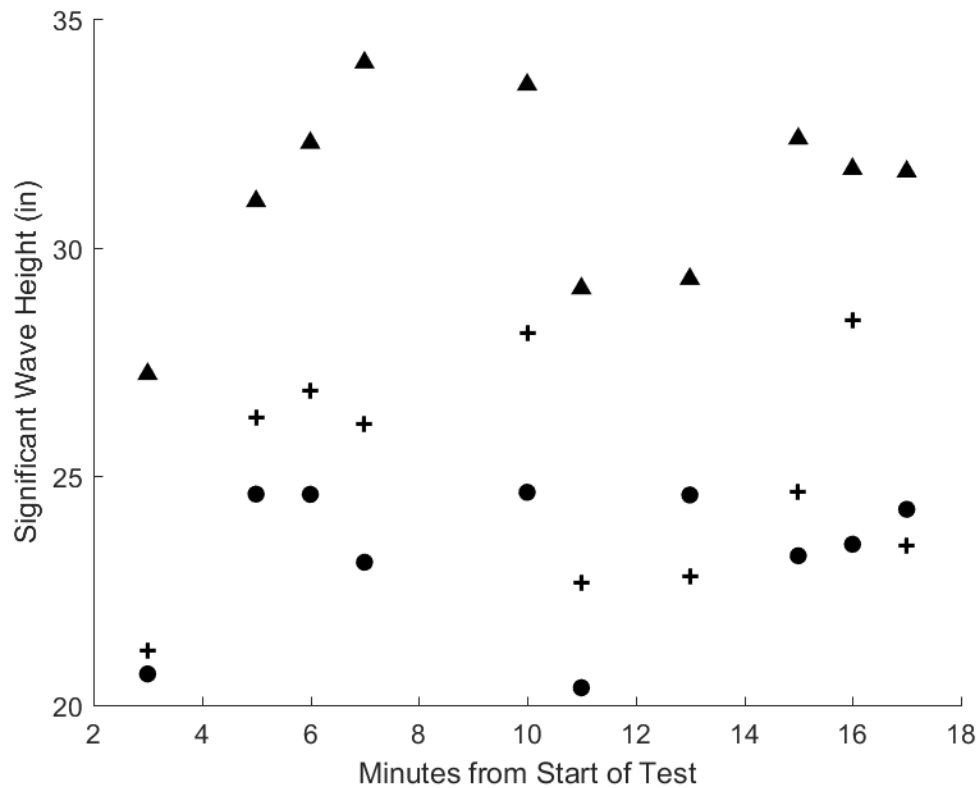


Figure G-22

Figure G-23: Plots of the significant wave heights for Test 8 of the WCM mounted to the skimmer and the raw data from the west auxiliary bridge Banner. The plus signs indicate the significant wave height (H_{m0}) calculated statistically using the raw data from the WCM mounted to the skimmer. The triangles represent the significant wave height (H_{m0}) calculated statistically using a segment of time corresponding to the WCM data from the raw Banner data. The dots represent the wave heights calculated using the average of the top third wave height from the same segments ($H_{1/3}$). Each data point represents a calculation of the significant wave height from approximately 60 seconds of raw data.

Here it can be seen that the $H_{1/3}$ calculation is lower than the H_{m0} value calculated using the Banner data for each time segment. The H_{m0} calculated using the WCM data is generally within the 4-inch performance objective with the H_{m0} from the bridge data.

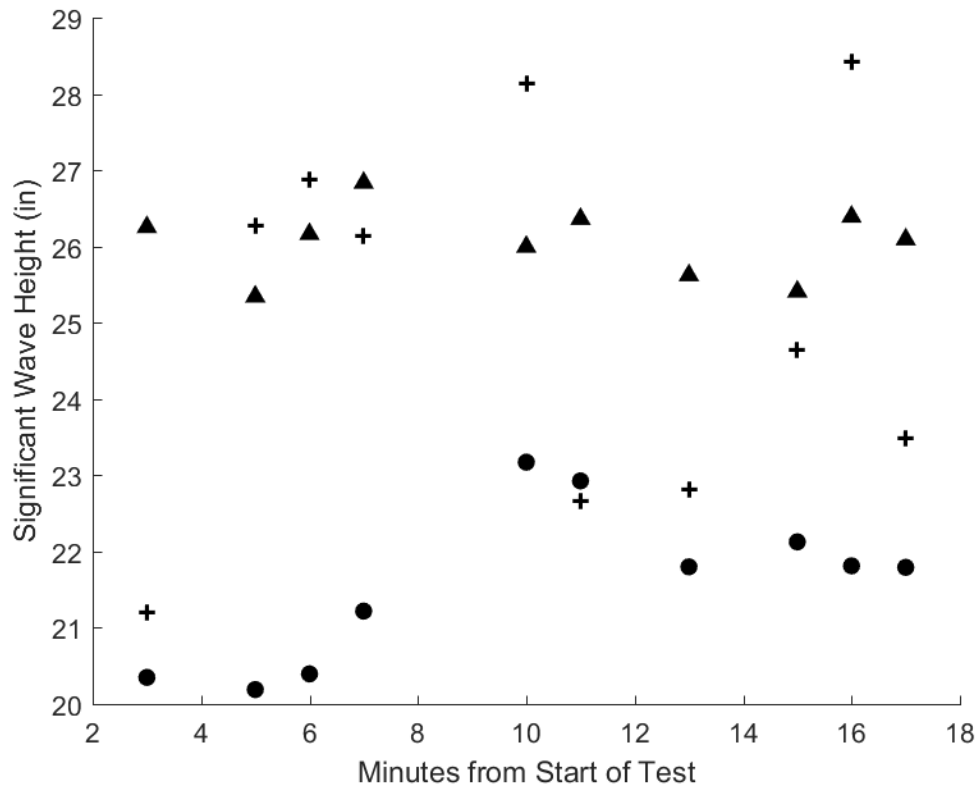


Figure G-23

Figure G-24: Plots of the significant wave heights for Test 8 of the WCM mounted to the skimmer and the raw data from the east auxiliary bridge Banner. The plus signs indicate the significant wave height (H_{m0}) calculated statistically using the raw data from the WCM mounted to the skimmer. The triangles represent the significant wave height (H_{m0}) calculated statistically using a segment of time corresponding to the WCM data from the raw Banner data. The dots represent the wave heights calculated using the average of the top third wave height from the same segments ($H_{1/3}$). Each data point represents a calculation of the significant wave height from approximately 60 seconds of raw data.

Here it can be seen that the $H_{1/3}$ calculation is lower than the H_{m0} value calculated using the Banner data for each time segment. The H_{m0} calculated using the WCM data is generally within the 4-inch performance objective with the H_{m0} from the bridge data.

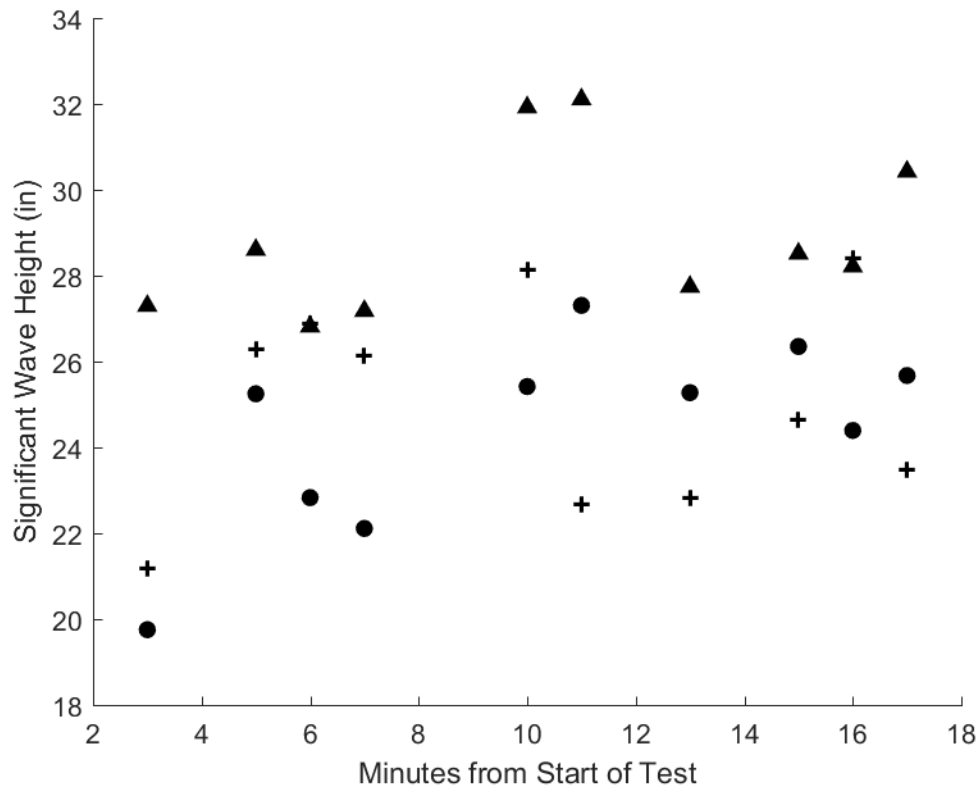


Figure G-24

Figure G-25: Plots of the significant wave heights for Test 9 of the WCM mounted to the skimmer and the raw data from the main bridge Banner. The plus signs indicate the significant wave height (H_{m0}) calculated statistically using the raw data from the WCM mounted to the skimmer. The triangles represent the significant wave height (H_{m0}) calculated statistically using a segment of time corresponding to the WCM data from the raw Banner data. The dots represent the wave heights calculated using the average of the top third wave height from the same segments ($H_{1/3}$). Each data point represents a calculation of the significant wave height from approximately 60 seconds of raw data.

Here it can be seen that the $H_{1/3}$ calculation is lower than the H_{m0} value calculated using the Banner data for each time segment. The H_{m0} calculated using the WCM data is generally within the 4-inch performance objective with the H_{m0} from the bridge data.

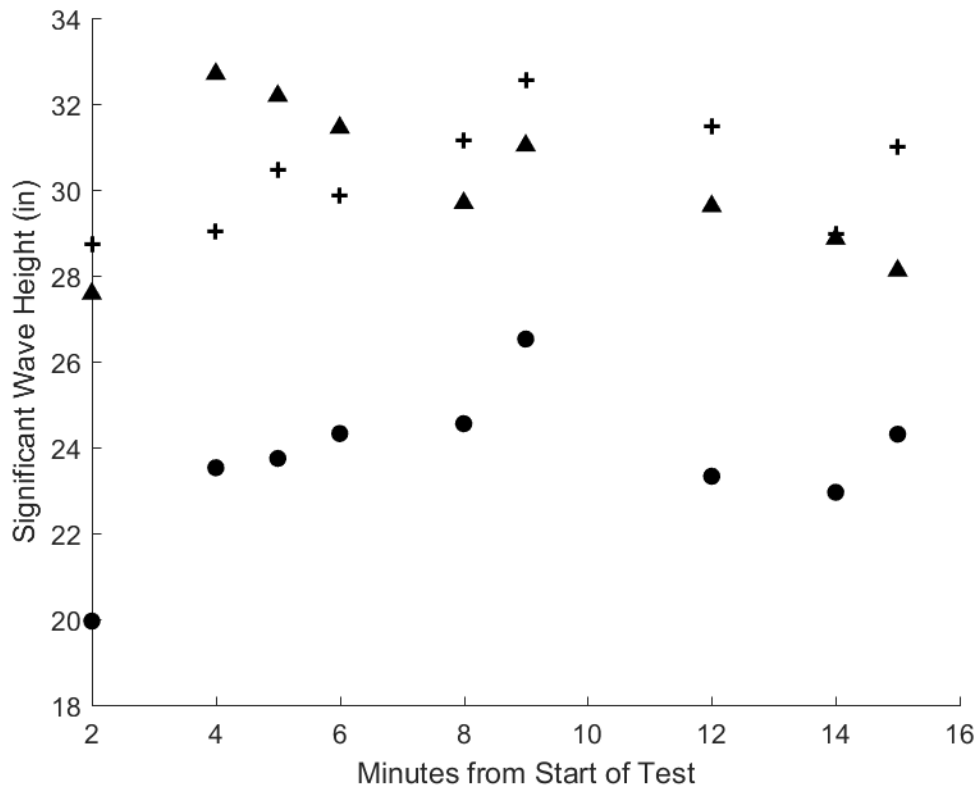


Figure G-25

Figure G-26: Plots of the significant wave heights for Test 9 of the WCM mounted to the skimmer and the raw data from the west auxiliary bridge Banner. The plus signs indicate the significant wave height (H_{m0}) calculated statistically using the raw data from the WCM mounted to the skimmer. The triangles represent the significant wave height (H_{m0}) calculated statistically using a segment of time corresponding to the WCM data from the raw Banner data. The dots represent the wave heights calculated using the average of the top third wave height from the same segments ($H_{1/3}$). Each data point represents a calculation of the significant wave height from approximately 60 seconds of raw data.

Here it can be seen that the $H_{1/3}$ calculation is lower than the H_{m0} value calculated using the Banner data for each time segment. The H_{m0} calculated using the WCM data is generally within the 4-inch performance objective with the H_{m0} from the bridge data.

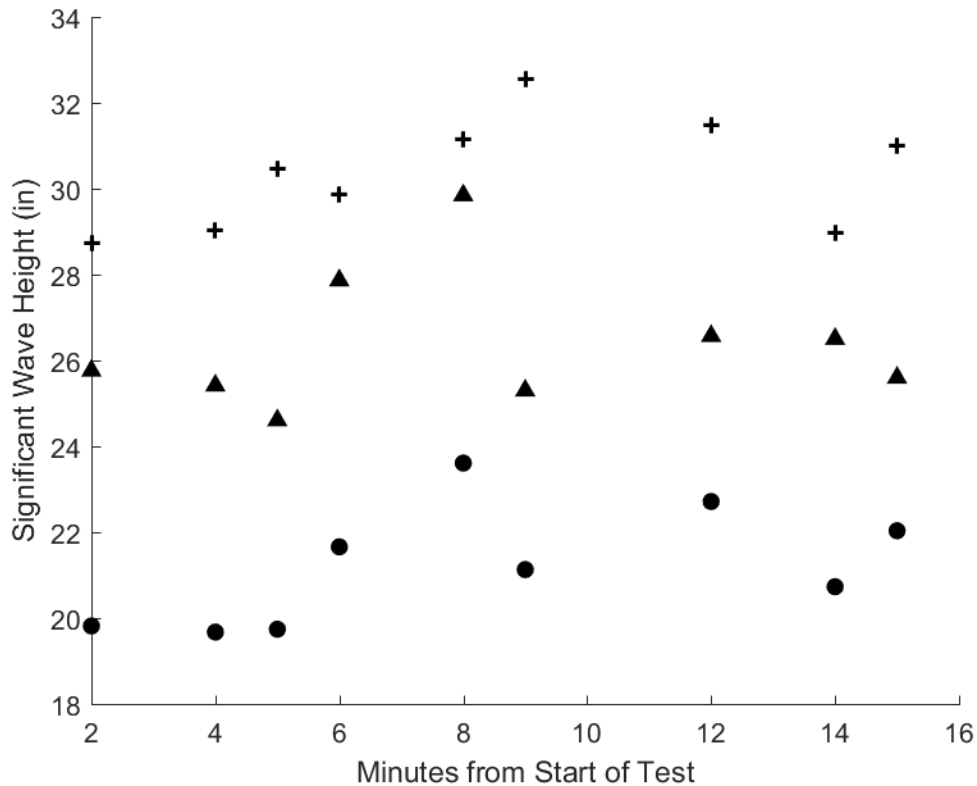


Figure G-26

Figure G-27: Plots of the significant wave heights for Test 9 of the WCM mounted to the skimmer and the raw data from the east auxiliary bridge Banner. The plus signs indicate the significant wave height (H_{m0}) calculated statistically using the raw data from the WCM mounted to the skimmer. The triangles represent the significant wave height (H_{m0}) calculated statistically using a segment of time corresponding to the WCM data from the raw Banner data. The dots represent the wave heights calculated using the average of the top third wave height from the same segments ($H_{1/3}$). Each data point represents a calculation of the significant wave height from approximately 60 seconds of raw data.

Here it can be seen that the $H_{1/3}$ calculation is lower than the H_{m0} value calculated using the Banner data for each time segment. The H_{m0} calculated using the WCM data is generally within the 4-inch performance objective with the H_{m0} from the bridge data.

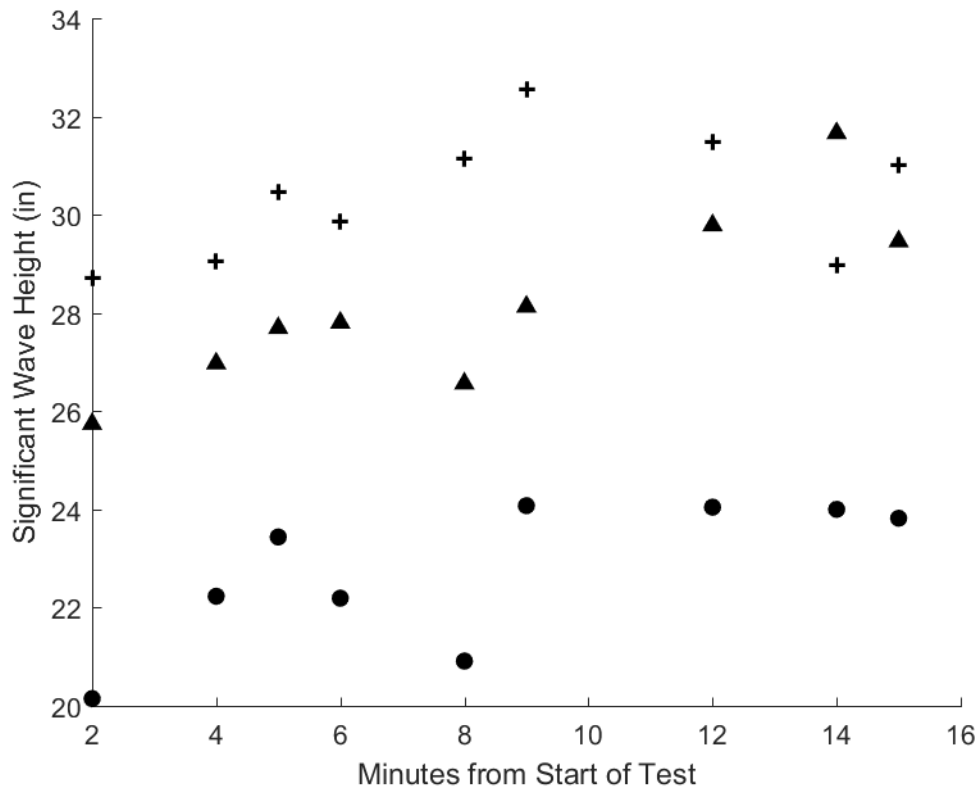


Figure G-27

Figure G-28: Plots of the significant wave heights for Test 10 of the WCM mounted to the skimmer and the raw data from the main bridge Banner. The plus signs indicate the significant wave height (H_{m0}) calculated statistically using the raw data from the WCM mounted to the skimmer. The triangles represent the significant wave height (H_{m0}) calculated statistically using a segment of time corresponding to the WCM data from the raw Banner data. The dots represent the wave heights calculated using the average of the top third wave height from the same segments ($H_{1/3}$). Each data point represents a calculation of the significant wave height from approximately 60 seconds of raw data.

Here it can be seen that the $H_{1/3}$ calculation is lower than the H_{m0} value calculated using the Banner data for each time segment. The H_{m0} calculated using the WCM data is generally within the 4-inch performance objective with the H_{m0} from the bridge data.

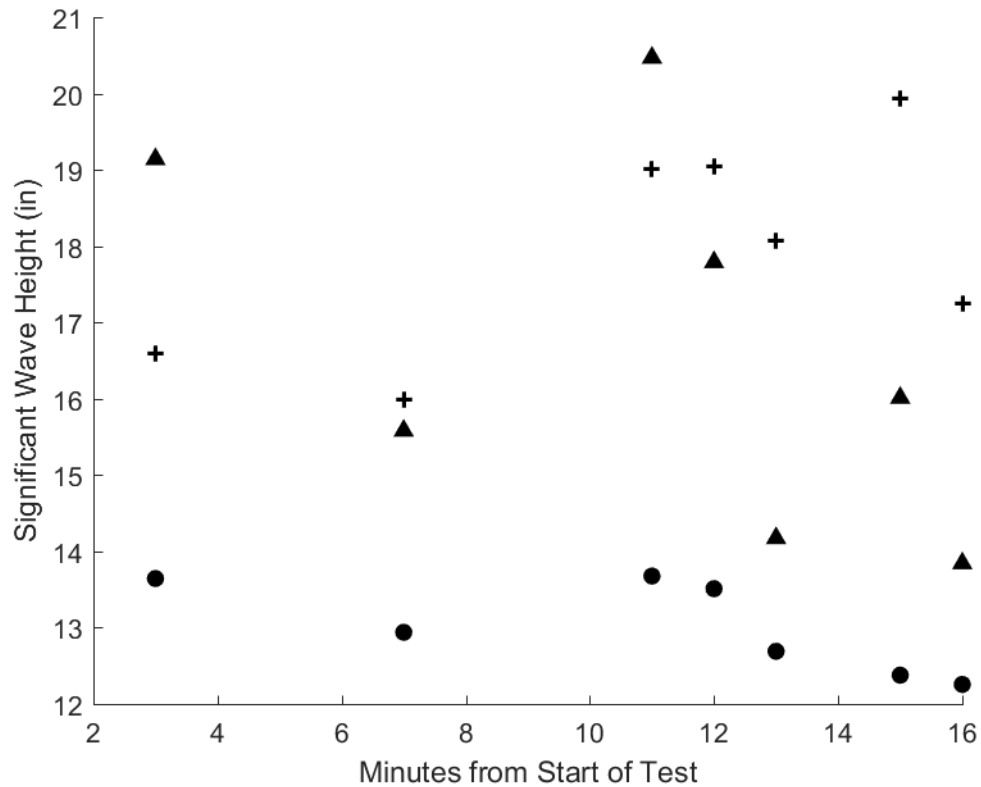


Figure G-28

Figure G-29: Plots of the significant wave heights for Test 10 of the WCM mounted to the skimmer and the raw data from the west auxiliary bridge Banner. The plus signs indicate the significant wave height (H_{m0}) calculated statistically using the raw data from the WCM mounted to the skimmer. The triangles represent the significant wave height (H_{m0}) calculated statistically using a segment of time corresponding to the WCM data from the raw Banner data. The dots represent the wave heights calculated using the average of the top third wave height from the same segments ($H_{1/3}$). Each data point represents a calculation of the significant wave height from approximately 60 seconds of raw data.

Here it can be seen that the $H_{1/3}$ calculation is lower than the H_{m0} value calculated using the Banner data for each time segment. The H_{m0} calculated using the WCM data is generally within the 4-inch performance objective with the H_{m0} from the bridge data.

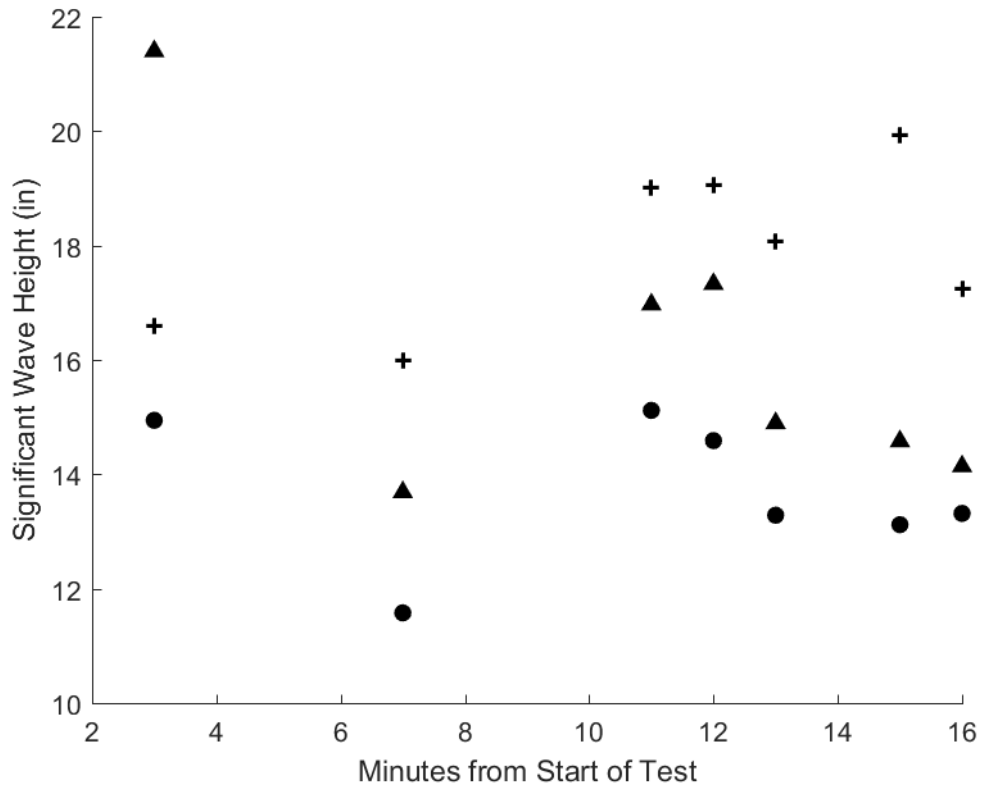


Figure G-29

Figure G-30: Plots of the significant wave heights for Test 10 of the WCM mounted to the skimmer and the raw data from the east auxiliary bridge Banner. The plus signs indicate the significant wave height (H_{m0}) calculated statistically using the raw data from the WCM mounted to the skimmer. The triangles represent the significant wave height (H_{m0}) calculated statistically using a segment of time corresponding to the WCM data from the raw Banner data. The dots represent the wave heights calculated using the average of the top third wave height from the same segments ($H_{1/3}$). Each data point represents a calculation of the significant wave height from approximately 60 seconds of raw data.

Here it can be seen that the $H_{1/3}$ calculation is lower than the H_{m0} value calculated using the Banner data for each time segment. The H_{m0} calculated using the WCM data is generally within the 4-inch performance objective with the H_{m0} from the bridge data.

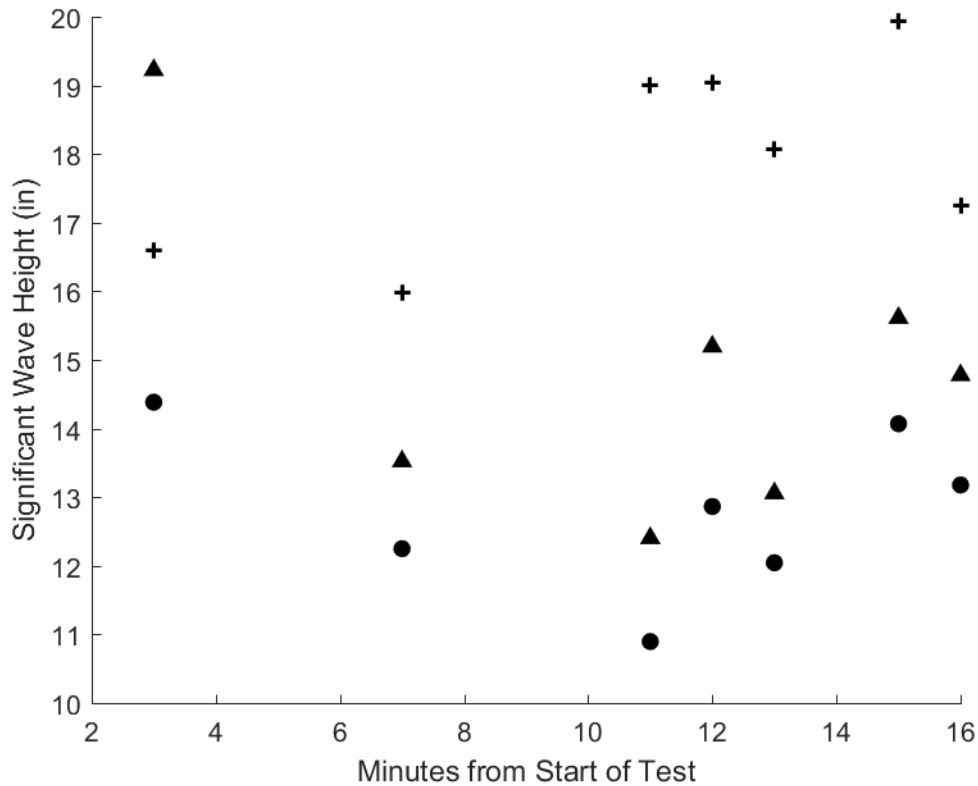


Figure G-30

Figure G-31: Plots of the significant wave heights for Test 11 of the WCM mounted to the skimmer and the raw data from the main bridge Banner. The plus signs indicate the significant wave height (H_{m0}) calculated statistically using the raw data from the WCM mounted to the skimmer. The triangles represent the significant wave height (H_{m0}) calculated statistically using a segment of time corresponding to the WCM data from the raw Banner data. The dots represent the wave heights calculated using the average of the top third wave height from the same segments ($H_{1/3}$). Each data point represents a calculation of the significant wave height from approximately 60 seconds of raw data.

Here it can be seen that the $H_{1/3}$ calculation is lower than the H_{m0} value calculated using the Banner data for each time segment. The H_{m0} calculated using the WCM data is generally within the 4-inch performance objective with the H_{m0} from the bridge data.

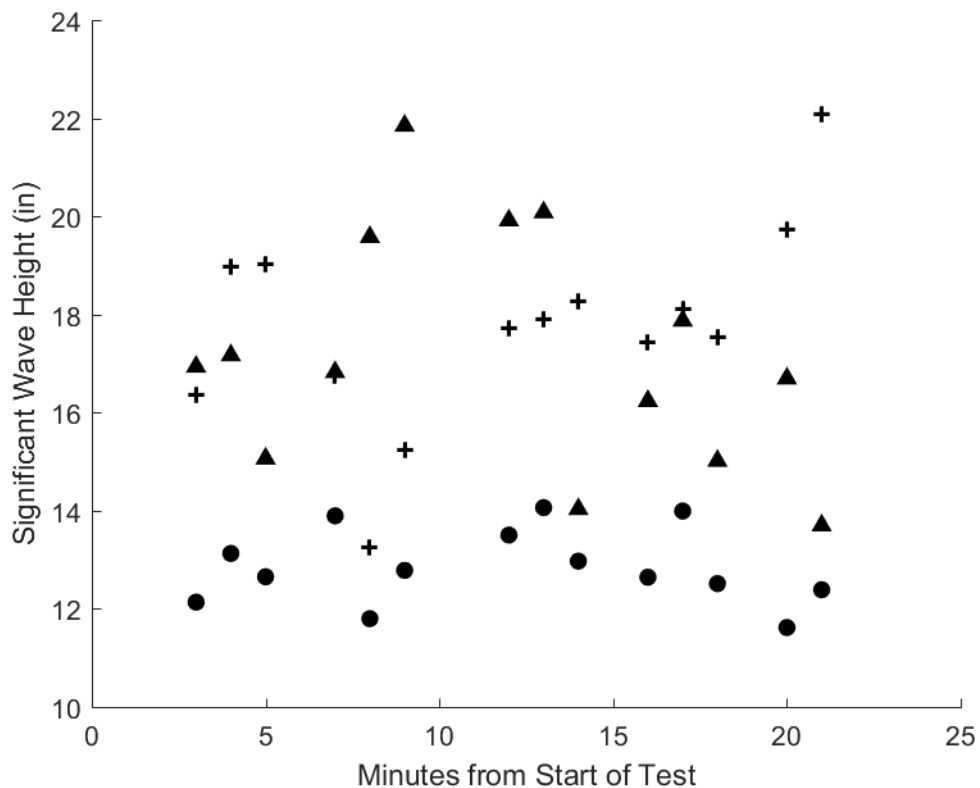


Figure G-31

Figure G-32: Plots of the significant wave heights for Test 11 of the WCM mounted to the skimmer and the raw data from the west auxiliary bridge Banner. The plus signs indicate the significant wave height (H_{m0}) calculated statistically using the raw data from the WCM mounted to the skimmer. The triangles represent the significant wave height (H_{m0}) calculated statistically using a segment of time corresponding to the WCM data from the raw Banner data. The dots represent the wave heights calculated using the average of the top third wave height from the same segments ($H_{1/3}$). Each data point represents a calculation of the significant wave height from approximately 60 seconds of raw data.

Here it can be seen that the $H_{1/3}$ calculation is lower than the H_{m0} value calculated using the Banner data for each time segment. The H_{m0} calculated using the WCM data is generally within the 4-inch performance objective with the H_{m0} from the bridge data.

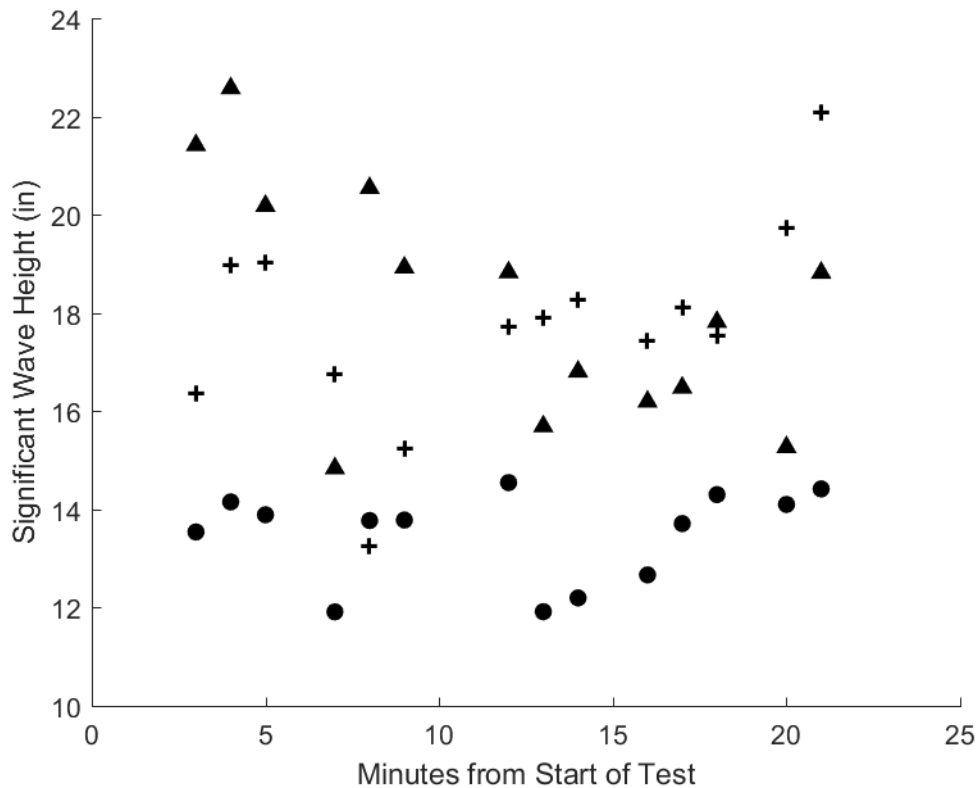


Figure G-32

Figure G-33: Plots of the significant wave heights for Test 11 of the WCM mounted to the skimmer and the raw data from the east auxiliary bridge Banner. The plus signs indicate the significant wave height (H_{m0}) calculated statistically using the raw data from the WCM mounted to the skimmer. The triangles represent the significant wave height (H_{m0}) calculated statistically using a segment of time corresponding to the WCM data from the raw Banner data. The dots represent the wave heights calculated using the average of the top third wave height from the same segments ($H_{1/3}$). Each data point represents a calculation of the significant wave height from approximately 60 seconds of raw data.

Here it can be seen that the $H_{1/3}$ calculation is lower than the H_{m0} value calculated using the Banner data for each time segment. The H_{m0} calculated using the WCM data is generally within the 4-inch performance objective with the H_{m0} from the bridge data.

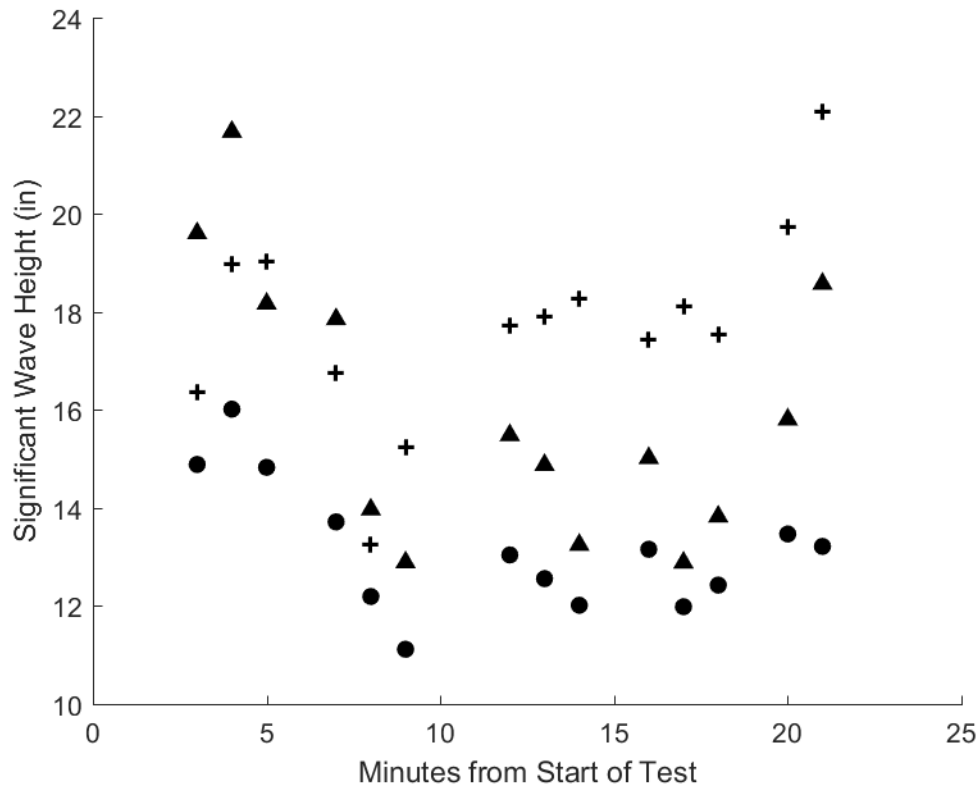


Figure G-33

Figure G-34: Plots of the significant wave heights for Test 12 of the WCM mounted to the skimmer and the raw data from the main bridge Banner. The plus signs indicate the significant wave height (H_{m0}) calculated statistically using the raw data from the WCM mounted to the skimmer. The triangles represent the significant wave height (H_{m0}) calculated statistically using a segment of time corresponding to the WCM data from the raw Banner data. The dots represent the wave heights calculated using the average of the top third wave height from the same segments ($H_{1/3}$). Each data point represents a calculation of the significant wave height from approximately 60 seconds of raw data.

Here it can be seen that the $H_{1/3}$ calculation is lower than the H_{m0} value calculated using the Banner data for each time segment. The H_{m0} calculated using the WCM data is generally within the 4-inch performance objective with the H_{m0} from the bridge data.

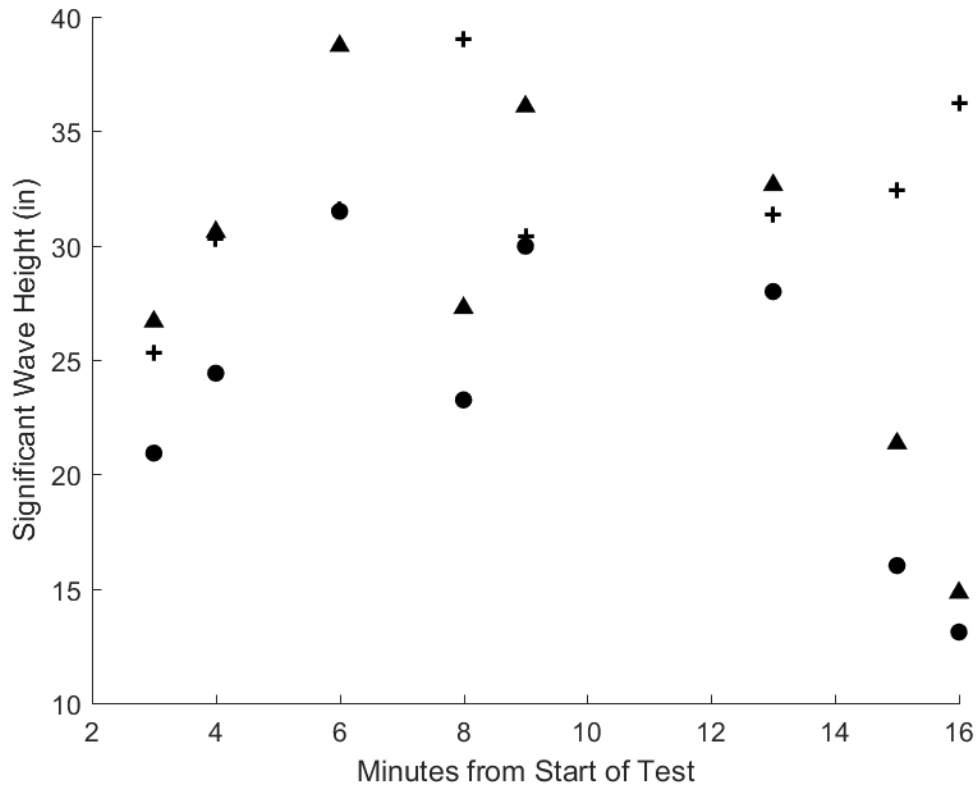


Figure G-34

Figure G-35: Plots of the significant wave heights for Test 12 of the WCM mounted to the skimmer and the raw data from the west auxiliary bridge Banner. The plus signs indicate the significant wave height (H_{m0}) calculated statistically using the raw data from the WCM mounted to the skimmer. The triangles represent the significant wave height (H_{m0}) calculated statistically using a segment of time corresponding to the WCM data from the raw Banner data. The dots represent the wave heights calculated using the average of the top third wave height from the same segments ($H_{1/3}$). Each data point represents a calculation of the significant wave height from approximately 60 seconds of raw data.

Here it can be seen that the $H_{1/3}$ calculation is lower than the H_{m0} value calculated using the Banner data for each time segment. The H_{m0} calculated using the WCM data is generally within the 4-inch performance objective with the H_{m0} from the bridge data.

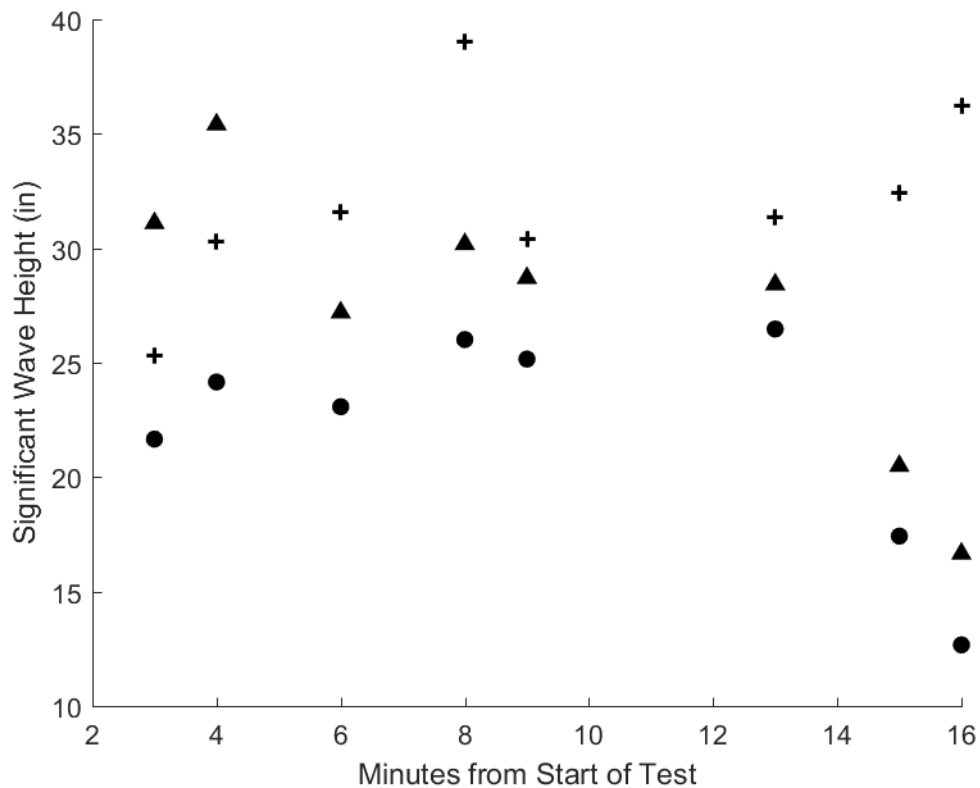


Figure G-35

Figure G-36: Plots of the significant wave heights for Test 12 of the WCM mounted to the skimmer and the raw data from the east auxiliary bridge Banner. The plus signs indicate the significant wave height (H_{m0}) calculated statistically using the raw data from the WCM mounted to the skimmer. The triangles represent the significant wave height (H_{m0}) calculated statistically using a segment of time corresponding to the WCM data from the raw Banner data. The dots represent the wave heights calculated using the average of the top third wave height from the same segments ($H_{1/3}$). Each data point represents a calculation of the significant wave height from approximately 60 seconds of raw data.

Here it can be seen that the $H_{1/3}$ calculation is lower than the H_{m0} value calculated using the Banner data for each time segment. The H_{m0} calculated using the WCM data is generally within the 4-inch performance objective with the H_{m0} from the bridge data.

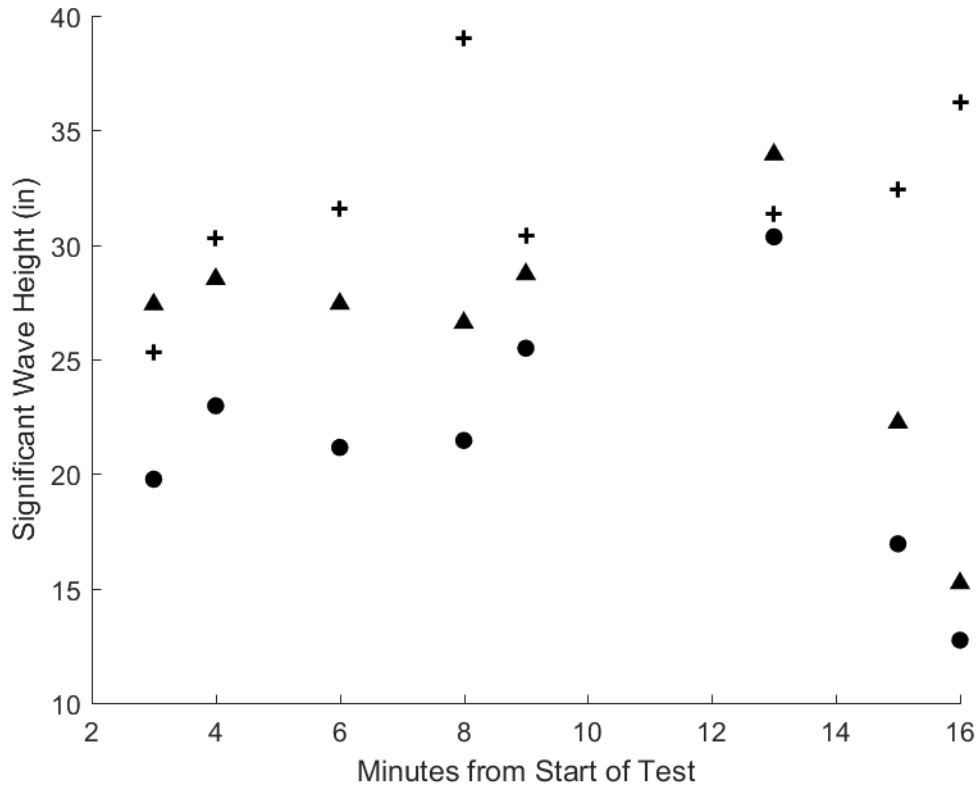


Figure G-36

Figure G-37: Plots of the significant wave heights for Test 13 of the WCM mounted to the skimmer and the raw data from the main bridge Banner. The plus signs indicate the significant wave height (H_{m0}) calculated statistically using the raw data from the WCM mounted to the skimmer. The triangles represent the significant wave height (H_{m0}) calculated statistically using a segment of time corresponding to the WCM data from the raw Banner data. The dots represent the wave heights calculated using the average of the top third wave height from the same segments ($H_{1/3}$). Each data point represents a calculation of the significant wave height from approximately 60 seconds of raw data.

Here it can be seen that the $H_{1/3}$ calculation is lower than the H_{m0} value calculated using the Banner data for each time segment. The H_{m0} calculated using the WCM data is generally within the 4-inch performance objective with the H_{m0} from the bridge data.

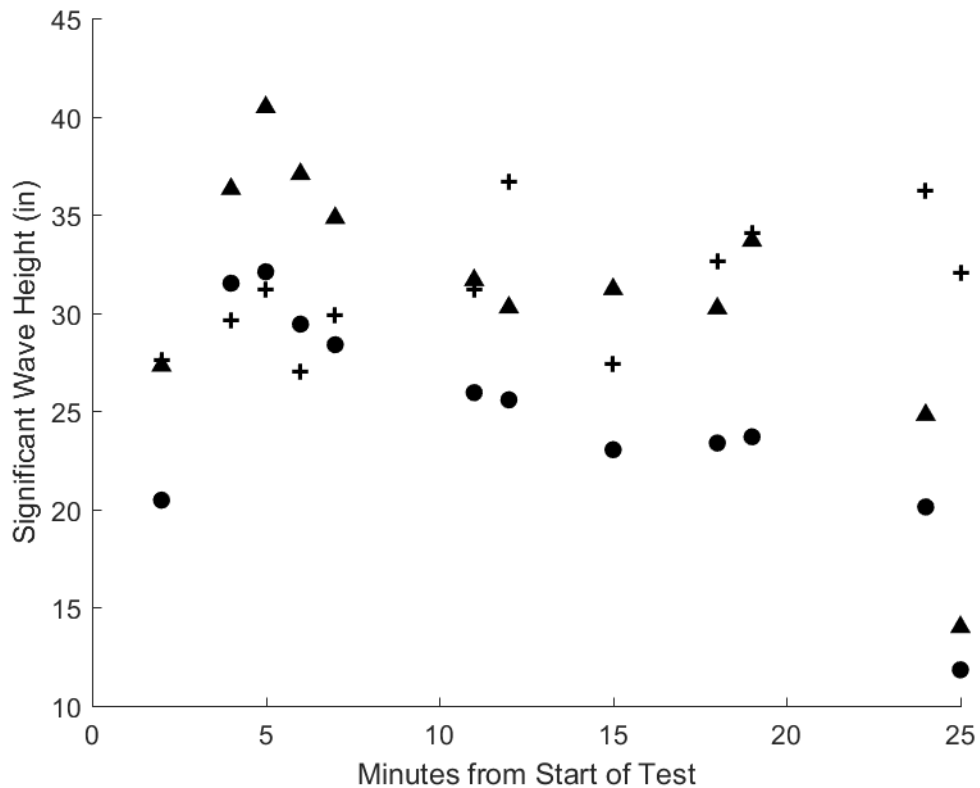


Figure G-37

Figure G-38: Plots of the significant wave heights for Test 13 of the WCM mounted to the skimmer and the raw data from the west auxiliary bridge Banner. The plus signs indicate the significant wave height (H_{m0}) calculated statistically using the raw data from the WCM mounted to the skimmer. The triangles represent the significant wave height (H_{m0}) calculated statistically using a segment of time corresponding to the WCM data from the raw Banner data. The dots represent the wave heights calculated using the average of the top third wave height from the same segments ($H_{1/3}$). Each data point represents a calculation of the significant wave height from approximately 60 seconds of raw data.

Here it can be seen that the $H_{1/3}$ calculation is lower than the H_{m0} value calculated using the Banner data for each time segment. The H_{m0} calculated using the WCM data is generally within the 4-inch performance objective with the H_{m0} from the bridge data.

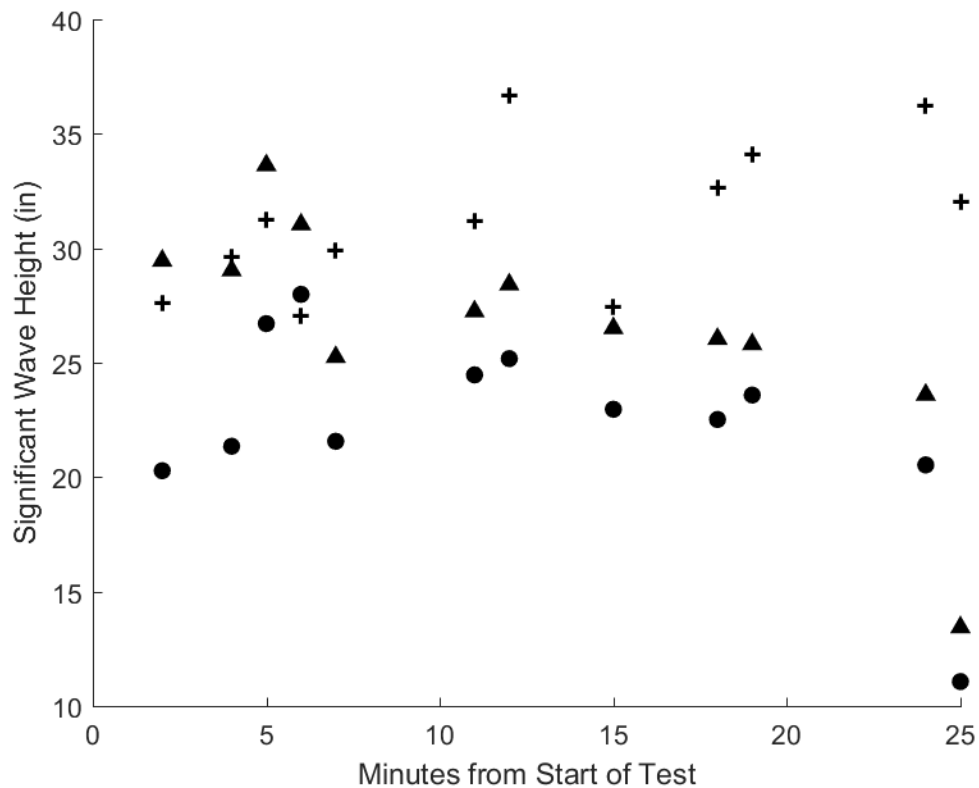


Figure G-38

Figure G-39: Plots of the significant wave heights for Test 13 of the WCM mounted to the skimmer and the raw data from the east auxiliary bridge Banner. The plus signs indicate the significant wave height (H_{m0}) calculated statistically using the raw data from the WCM mounted to the skimmer. The triangles represent the significant wave height (H_{m0}) calculated statistically using a segment of time corresponding to the WCM data from the raw Banner data. The dots represent the wave heights calculated using the average of the top third wave height from the same segments ($H_{1/3}$). Each data point represents a calculation of the significant wave height from approximately 60 seconds of raw data.

Here it can be seen that the $H_{1/3}$ calculation is lower than the H_{m0} value calculated using the Banner data for each time segment. The H_{m0} calculated using the WCM data is generally within the 4-inch performance objective with the H_{m0} from the bridge data.

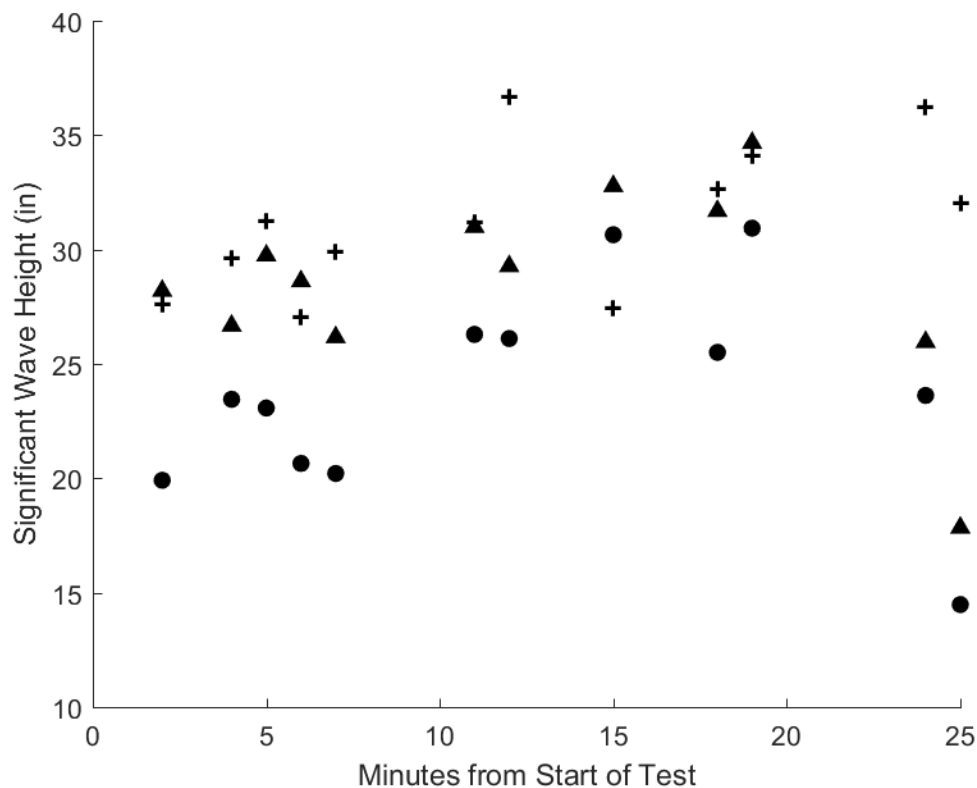


Figure G-39

Figure G-40: Plots of the significant wave heights for Test 14 of the WCM mounted to the skimmer and the raw data from the main bridge Banner. The plus signs indicate the significant wave height (H_{m0}) calculated statistically using the raw data from the WCM mounted to the skimmer. The triangles represent the significant wave height (H_{m0}) calculated statistically using a segment of time corresponding to the WCM data from the raw Banner data. The dots represent the wave heights calculated using the average of the top third wave height from the same segments ($H_{1/3}$). Each data point represents a calculation of the significant wave height from approximately 60 seconds of raw data.

Here it can be seen that the $H_{1/3}$ calculation is lower than the H_{m0} value calculated using the Banner data for each time segment. The H_{m0} calculated using the WCM data is generally within the 4-inch performance objective with the H_{m0} from the bridge data.

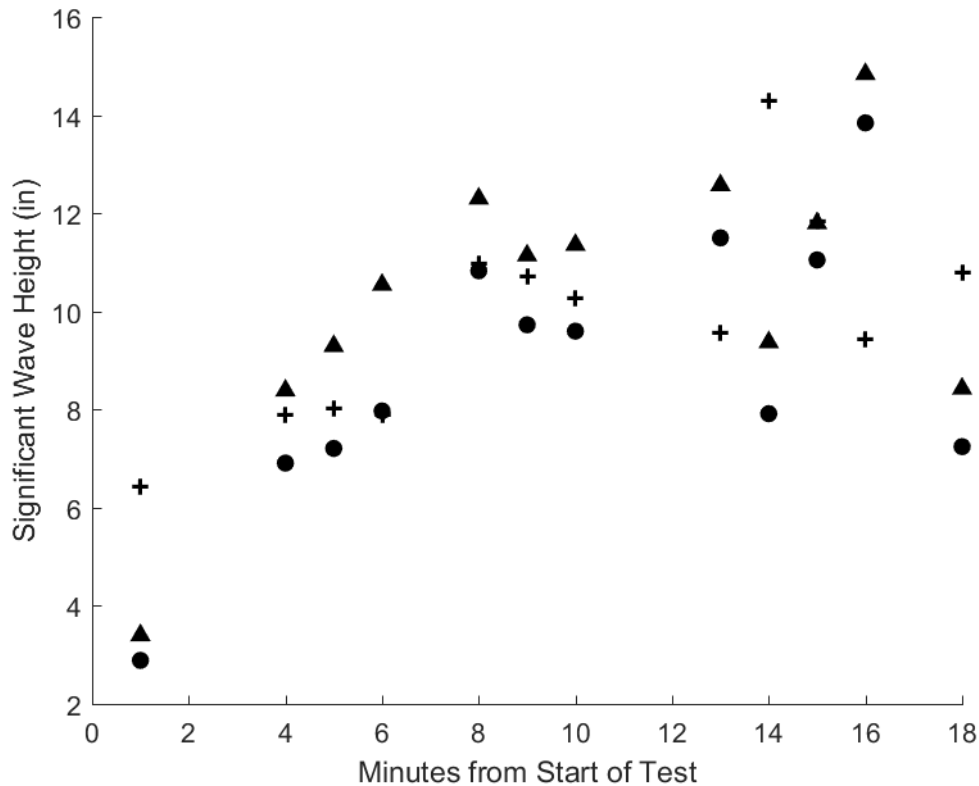


Figure G-40

Figure G-41: Plots of the significant wave heights for Test 14 of the WCM mounted to the skimmer and the raw data from the west auxiliary bridge Banner. The plus signs indicate the significant wave height (H_{m0}) calculated statistically using the raw data from the WCM mounted to the skimmer. The triangles represent the significant wave height (H_{m0}) calculated statistically using a segment of time corresponding to the WCM data from the raw Banner data. The dots represent the wave heights calculated using the average of the top third wave height from the same segments ($H_{1/3}$). Each data point represents a calculation of the significant wave height from approximately 60 seconds of raw data.

Here it can be seen that the $H_{1/3}$ calculation is lower than the H_{m0} value calculated using the Banner data for each time segment. The H_{m0} calculated using the WCM data is generally within the 4-inch performance objective with the H_{m0} from the bridge data.

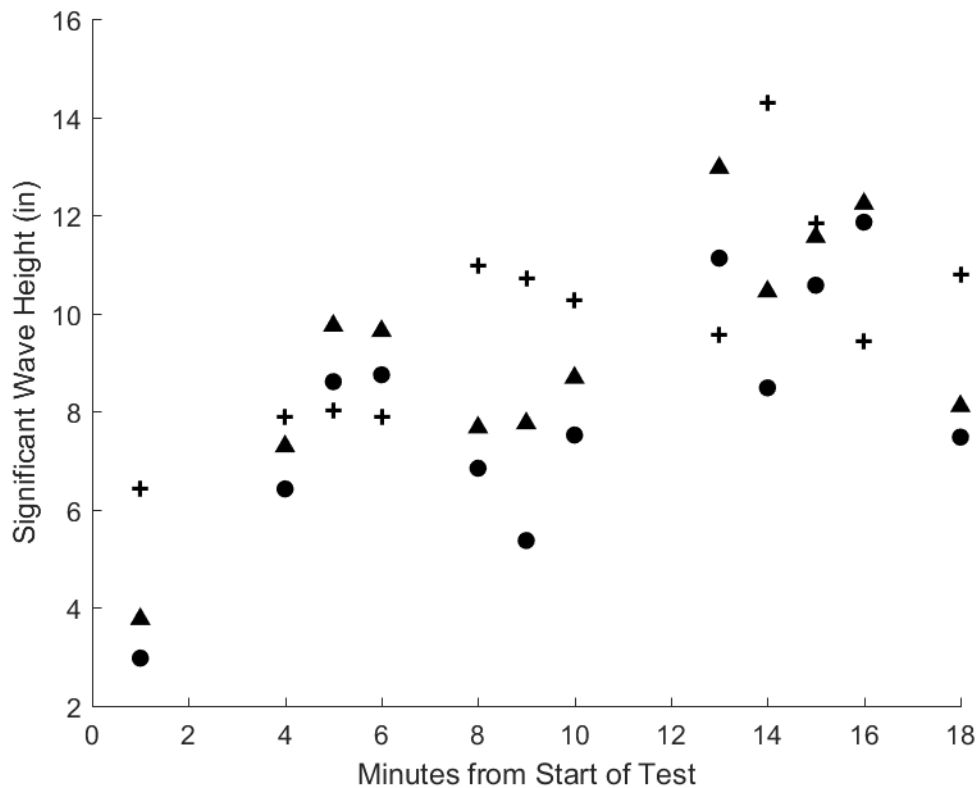


Figure G-41

Figure G-42: Plots of the significant wave heights for Test 14 of the WCM mounted to the skimmer and the raw data from the east auxiliary bridge Banner. The plus signs indicate the significant wave height (H_{m0}) calculated statistically using the raw data from the WCM mounted to the skimmer. The triangles represent the significant wave height (H_{m0}) calculated statistically using a segment of time corresponding to the WCM data from the raw Banner data. The dots represent the wave heights calculated using the average of the top third wave height from the same segments ($H_{1/3}$). Each data point represents a calculation of the significant wave height from approximately 60 seconds of raw data.

Here it can be seen that the $H_{1/3}$ calculation is lower than the H_{m0} value calculated using the Banner data for each time segment. The H_{m0} calculated using the WCM data is generally within the 4-inch performance objective with the H_{m0} from the bridge data.

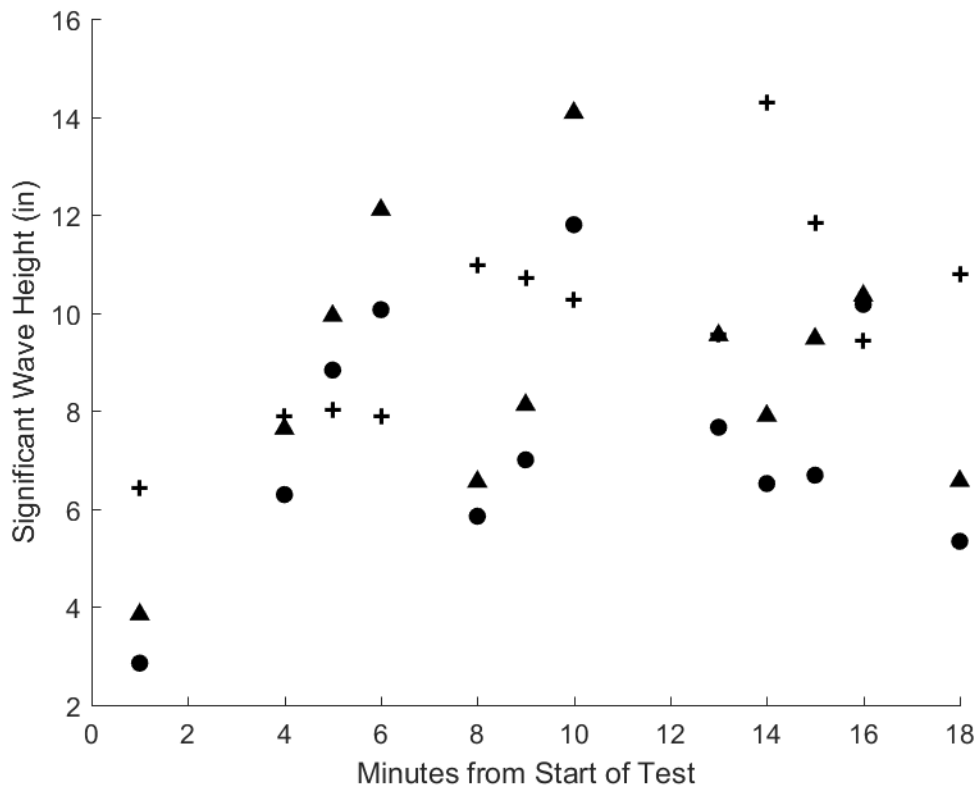


Figure G-42

Figure G-43: Plots of the significant wave heights for Test 15 of the WCM mounted to the skimmer and the raw data from the main bridge Banner. The plus signs indicate the significant wave height (H_{m0}) calculated statistically using the raw data from the WCM mounted to the skimmer. The triangles represent the significant wave height (H_{m0}) calculated statistically using a segment of time corresponding to the WCM data from the raw Banner data. The dots represent the wave heights calculated using the average of the top third wave height from the same segments ($H_{1/3}$). Each data point represents a calculation of the significant wave height from approximately 60 seconds of raw data.

Here it can be seen that the $H_{1/3}$ calculation is lower than the H_{m0} value calculated using the Banner data for each time segment. The H_{m0} calculated using the WCM data is generally within the 4-inch performance objective with the H_{m0} from the bridge data.

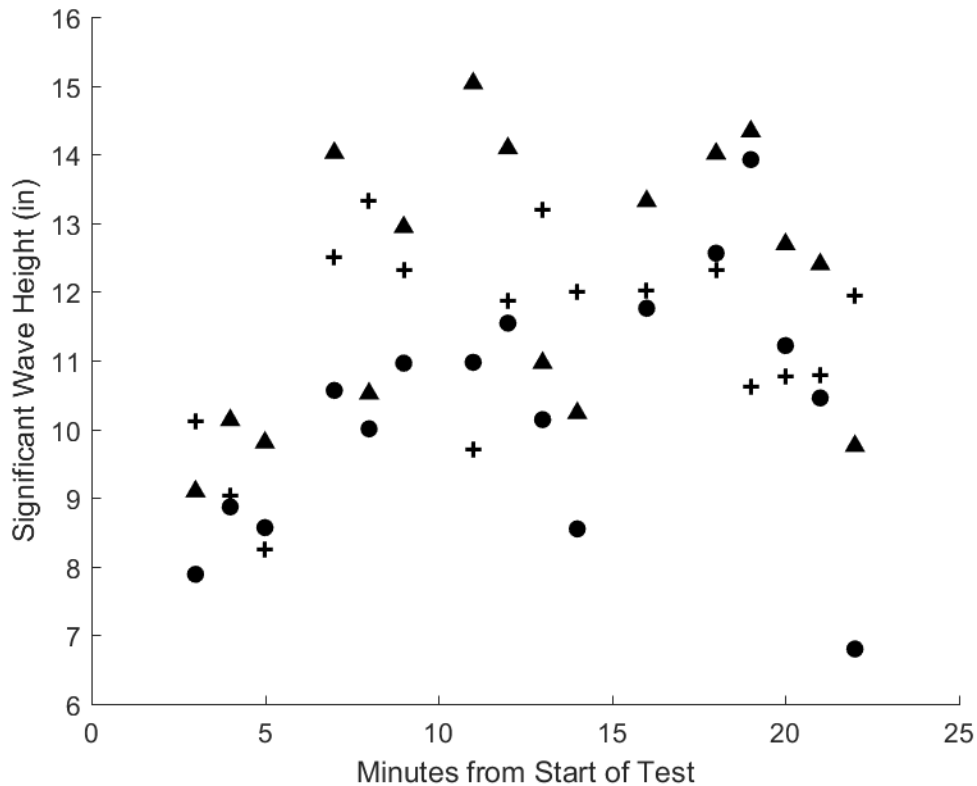


Figure G-43

Figure G-44: Plots of the significant wave heights for Test 15 of the WCM mounted to the skimmer and the raw data from the west auxiliary bridge Banner. The plus signs indicate the significant wave height (H_{m0}) calculated statistically using the raw data from the WCM mounted to the skimmer. The triangles represent the significant wave height (H_{m0}) calculated statistically using a segment of time corresponding to the WCM data from the raw Banner data. The dots represent the wave heights calculated using the average of the top third wave height from the same segments ($H_{1/3}$). Each data point represents a calculation of the significant wave height from approximately 60 seconds of raw data.

Here it can be seen that the $H_{1/3}$ calculation is lower than the H_{m0} value calculated using the Banner data for each time segment. The H_{m0} calculated using the WCM data is generally within the 4-inch performance objective with the H_{m0} from the bridge data.

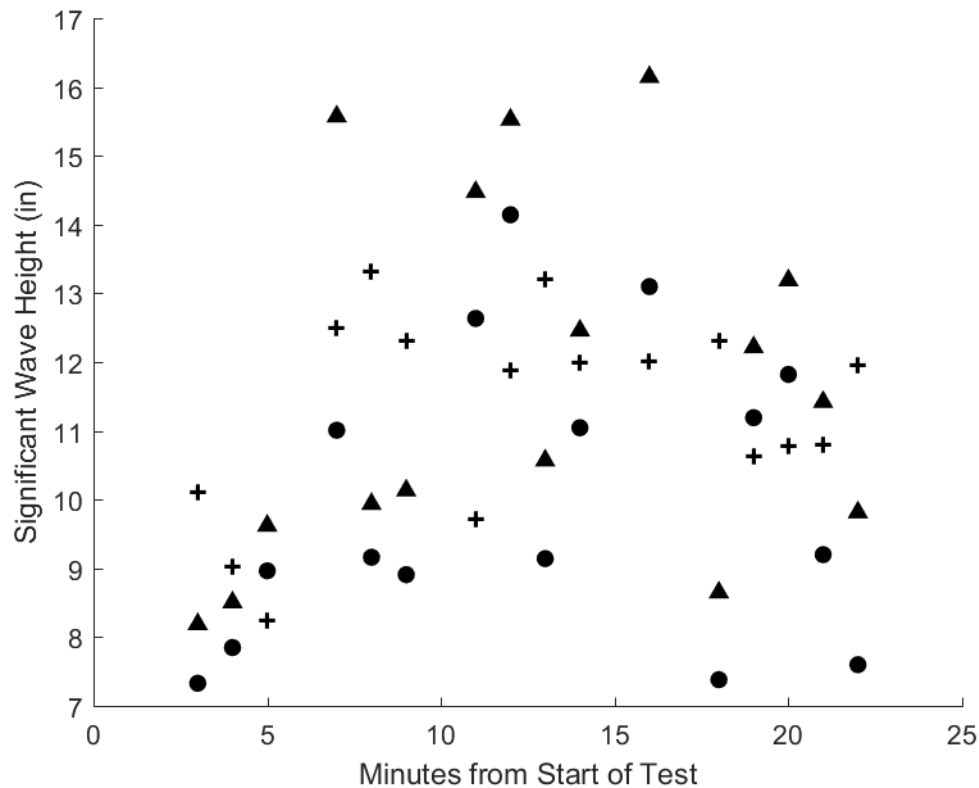


Figure G-44

Figure G-45: Plots of the significant wave heights for Test 15 of the WCM mounted to the skimmer and the raw data from the east auxiliary bridge Banner. The plus signs indicate the significant wave height (H_{m0}) calculated statistically using the raw data from the WCM mounted to the skimmer. The triangles represent the significant wave height (H_{m0}) calculated statistically using a segment of time corresponding to the WCM data from the raw Banner data. The dots represent the wave heights calculated using the average of the top third wave height from the same segments ($H_{1/3}$). Each data point represents a calculation of the significant wave height from approximately 60 seconds of raw data.

Here it can be seen that the $H_{1/3}$ calculation is lower than the H_{m0} value calculated using the Banner data for each time segment. The H_{m0} calculated using the WCM data is generally within the 4-inch performance objective with the H_{m0} from the bridge data.

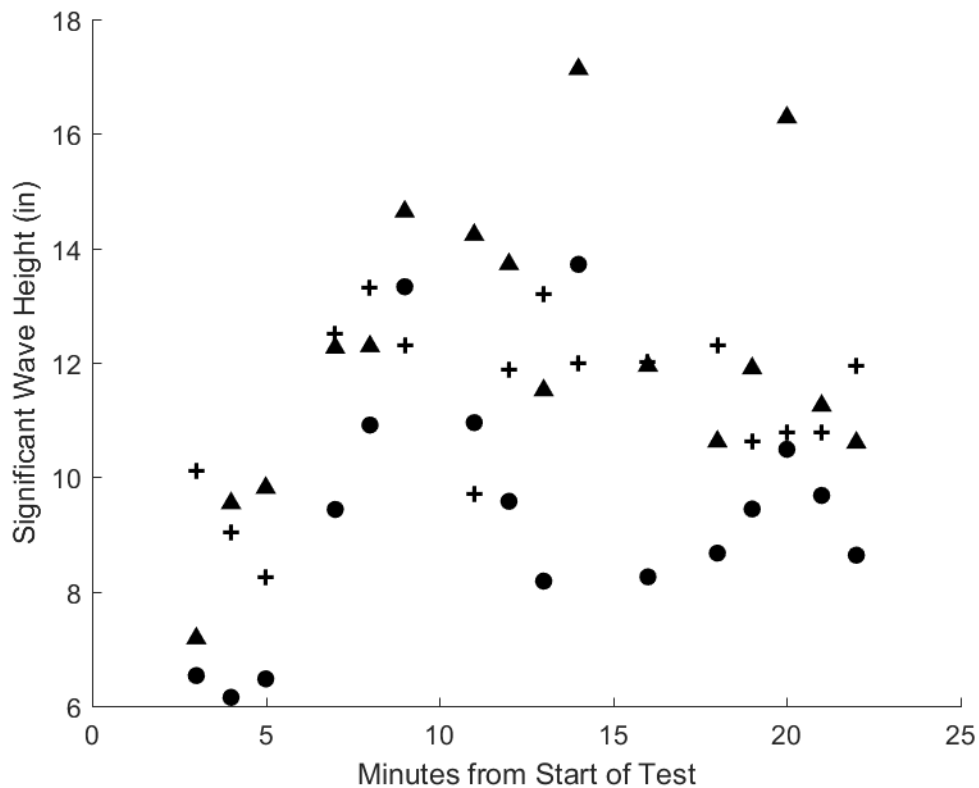


Figure G-45

Appendix H: Difference in Significant Wave Height from Skimmer-mounted WCM and Banners

This appendix contains plots showing the difference in significant wave height (H_{m0}) from the WCM mounted on the skimmer and each Banner location for each test. The plus signs indicate the difference in significant wave height (H_{m0}) from the main bridge Banner. The triangles represent the difference in significant wave height (H_{m0}) from the west auxiliary bridge Banner data. The dots represent the difference in significant wave height (H_{m0}) from the east auxiliary bridge Banner data. Each data point represents a calculation of the significant wave height from approximately 60 seconds of raw data.

Figure H-1: Plot showing the difference in significant wave height (H_{m0}) from the WCM mounted on the skimmer and each Banner location for Test 1. The plus signs indicate the difference in significant wave height (H_{m0}) from the main bridge Banner. The triangles represent the difference in significant wave height (H_{m0}) from the west auxiliary bridge Banner data. The dots represent the difference in significant wave height (H_{m0}) from the east auxiliary bridge Banner data. Each data point represents a calculation of the significant wave height from approximately 60 seconds of raw data.

Here it can be seen that most of the differences between WCM and the Banners are within the 4-inch performance objective. With the difference between significant wave height calculated from the east and west auxiliary bridge having the least time segments outside the performance objective.

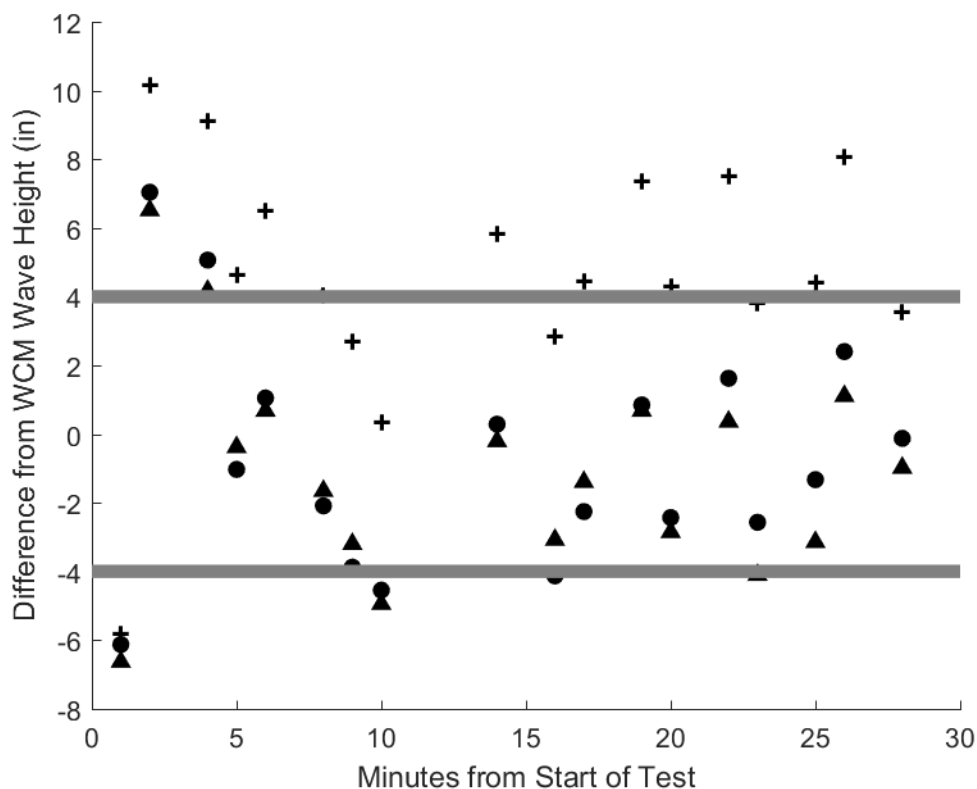


Figure H-1

Figure H-2: Plot showing the difference in significant wave height (H_{m0}) from the WCM mounted on the skimmer and each Banner location for Test 2. The plus signs indicate the difference in significant wave height (H_{m0}) from the main bridge Banner. The triangles represent the difference in significant wave height (H_{m0}) from the west auxiliary bridge Banner data. The dots represent the difference in significant wave height (H_{m0}) from the east auxiliary bridge Banner data. Each data point represents a calculation of the significant wave height from approximately 60 seconds of raw data.

Here it can be seen that most of the differences between WCM and the Banners are within the 4-inch performance objective. With the difference between significant wave height calculated from the west auxiliary bridge having the least time segments outside the performance objective.

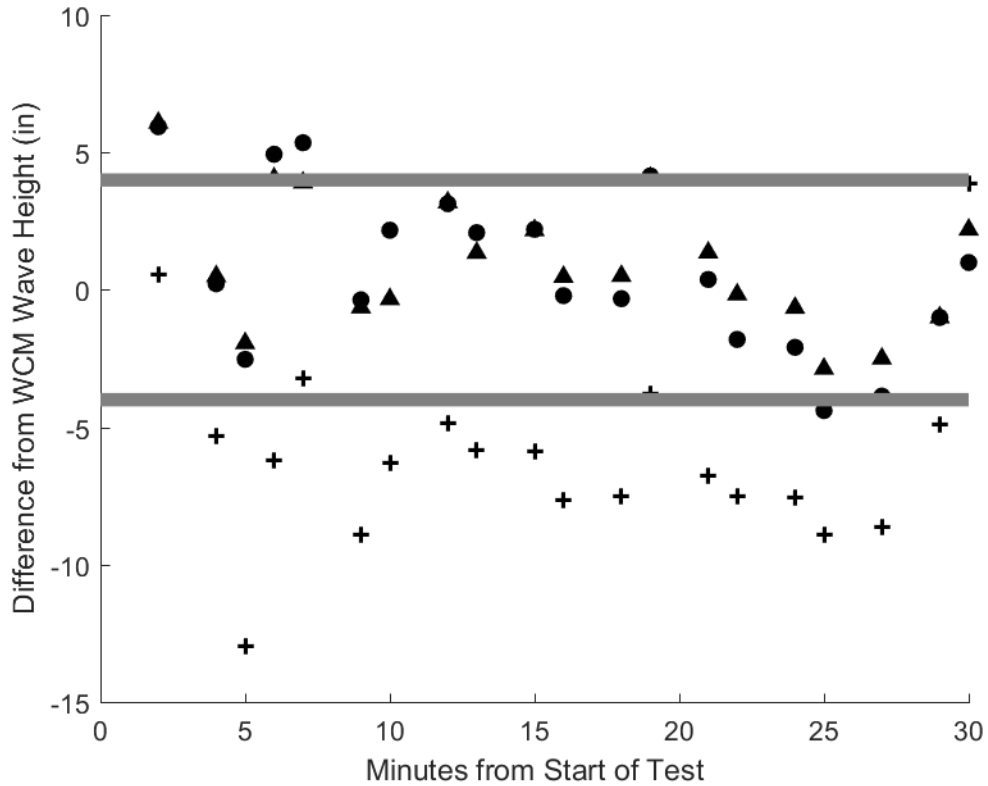


Figure H-2

Figure H-3: Plot showing the difference in significant wave height (H_{m0}) from the WCM mounted on the skimmer and each Banner location for Test 3. The plus signs indicate the difference in significant wave height (H_{m0}) from the main bridge Banner. The triangles represent the difference in significant wave height (H_{m0}) from the west auxiliary bridge Banner data. The dots represent the difference in significant wave height (H_{m0}) from the east auxiliary bridge Banner data. Each data point represents a calculation of the significant wave height from approximately 60 seconds of raw data.

Here it can be seen that most of the differences between WCM and the Banners are within the 4-inch performance objective. With the difference between significant wave height calculated from the main bridge having the least time segments outside the performance objective.

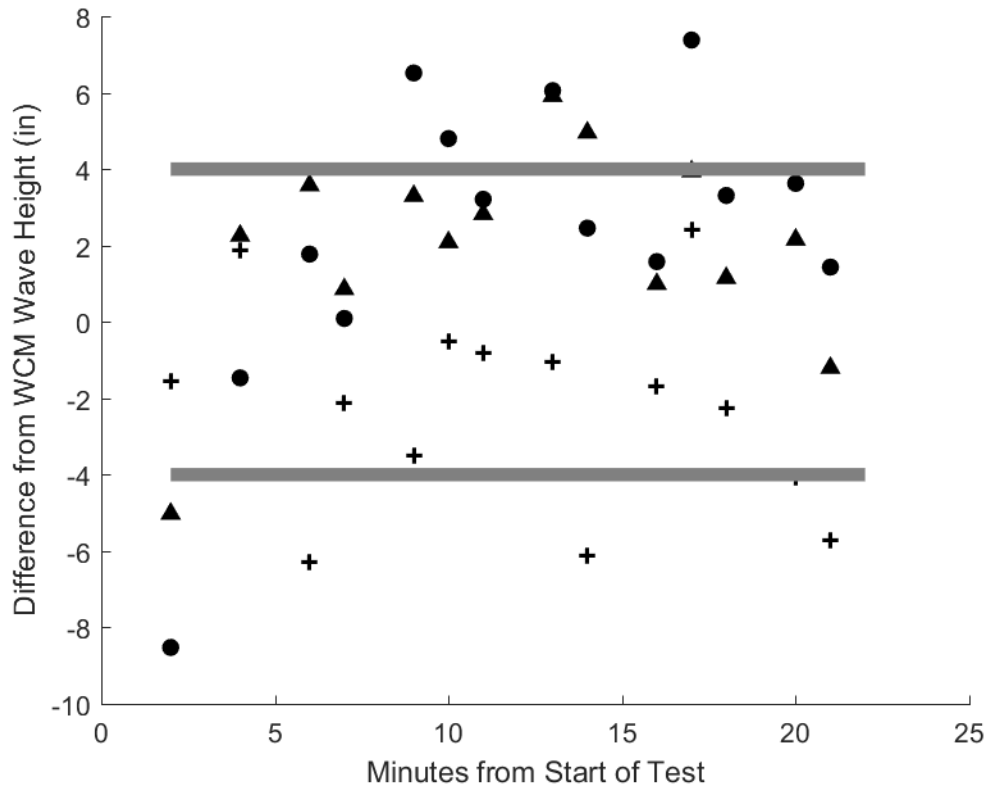


Figure H-3

Figure H-4: Plot showing the difference in significant wave height (H_{m0}) from the WCM mounted on the skimmer and each Banner location for Test 4. The plus signs indicate the difference in significant wave height (H_{m0}) from the main bridge Banner. The triangles represent the difference in significant wave height (H_{m0}) from the west auxiliary bridge Banner data. The dots represent the difference in significant wave height (H_{m0}) from the west auxiliary bridge Banner data. Each data point represents a calculation of the significant wave height from approximately 60 seconds of raw data.

Here it can be seen that most of the differences between WCM and the Banners are within the 4-inch performance objective. With the difference between significant wave height calculated from the main bridge having the least time segments outside the performance objective.

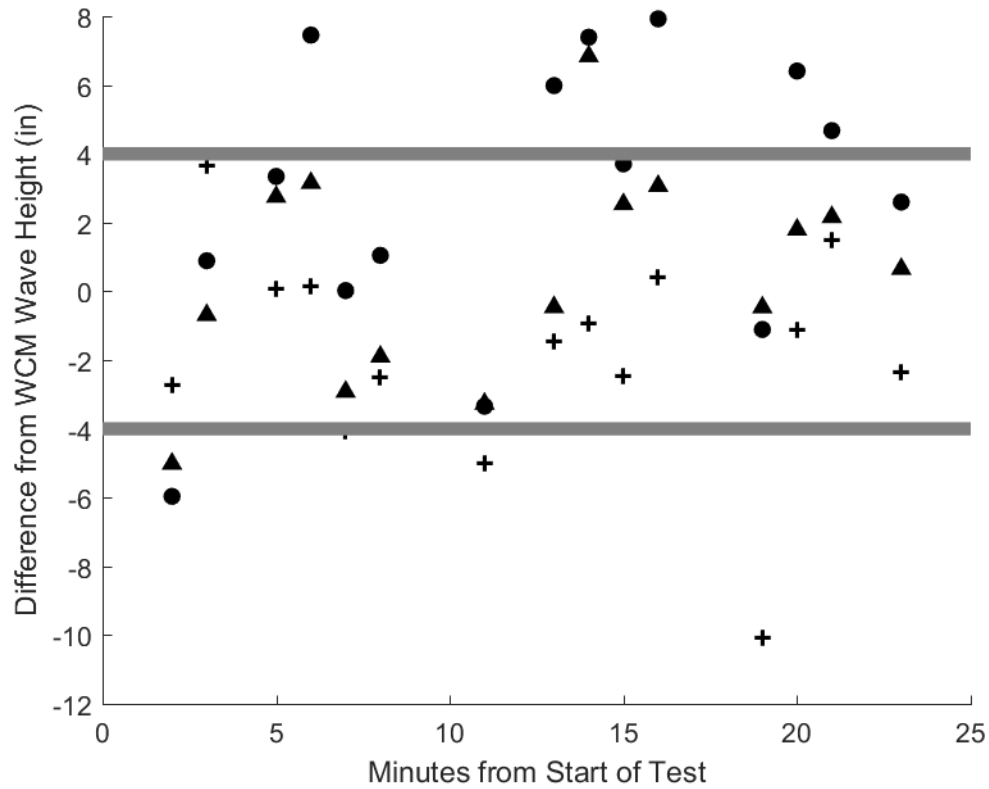


Figure H-4

Figure H-5: Plot showing the difference in significant wave height (H_{m0}) from the WCM mounted on the skimmer and each Banner location for Test 5. The plus signs indicate the difference in significant wave height (H_{m0}) from the main bridge Banner. The triangles represent the difference in significant wave height (H_{m0}) from the west auxiliary bridge Banner data. The dots represent the difference in significant wave height (H_{m0}) from the east auxiliary bridge Banner data. Each data point represents a calculation of the significant wave height from approximately 60 seconds of raw data.

Here it can be seen that one of the difference between WCM and the Banners are within the 4-inch performance objective. This test is one where the waves were created by the 18-inch stroke and 18 cycles per minute (CPM) setting of the wave generator, which creates a large sinusoidal wave. We believe the discrepancies between the WCM and Banner measurement are due to lateral motion from the large elliptical motion of the wave not being considered by the algorithms. This is because we trained them on real, complex wave motion where most of the movement is in the heave.

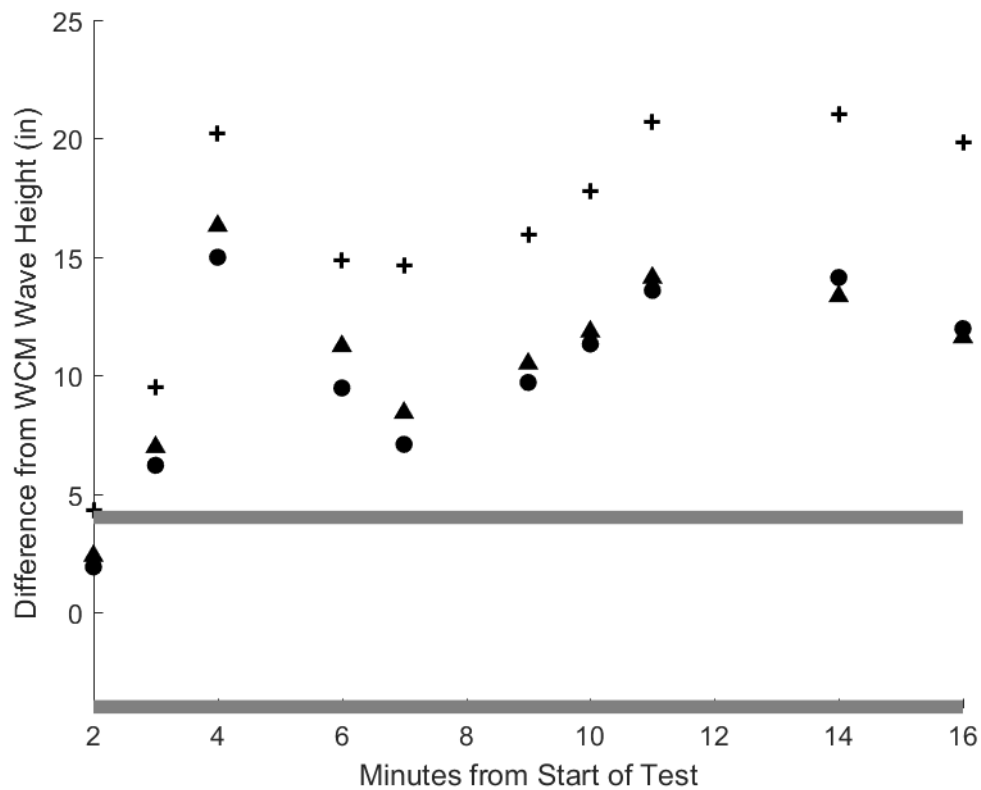


Figure H-5

Figure H-6: Plot showing the difference in significant wave height (H_{m0}) from the WCM mounted on the skimmer and each Banner location for Test 6. The plus signs indicate the difference in significant wave height (H_{m0}) from the main bridge Banner. The triangles represent the difference in significant wave height (H_{m0}) from the west auxiliary bridge Banner data. The dots represent the difference in significant wave height (H_{m0}) from the east auxiliary bridge Banner data. Each data point represents a calculation of the significant wave height from approximately 60 seconds of raw data.

Here it can be seen that a couple of the difference between WCM and the Banners are within the 4-inch performance objective. This test is one where the waves were created by the 18-inch stroke and 18 CPM setting of the wave generator, which creates a large sinusoidal wave. We believe the discrepancies between the WCM and Banner measurement are due to lateral motion from the large elliptical motion of the wave not being considered by the algorithms. This is because we trained them on real, complex wave motion where most of the movement is in the heave.

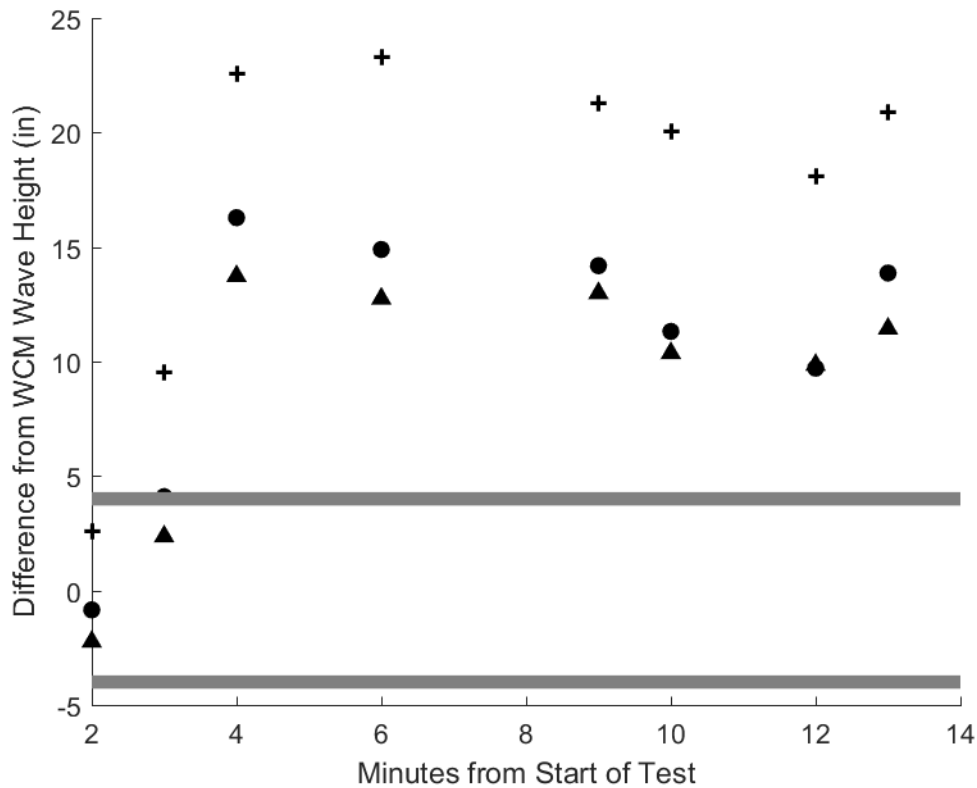


Figure H-6

Figure H-7: Plot showing the difference in significant wave height (H_{m0}) from the WCM mounted on the skimmer and each Banner location for Test 7. The plus signs indicate the difference in significant wave height (H_{m0}) from the main bridge Banner. The triangles represent the difference in significant wave height (H_{m0}) from the west auxiliary bridge Banner data. The dots represent the difference in significant wave height (H_{m0}) from the east auxiliary bridge Banner data. Each data point represents a calculation of the significant wave height from approximately 60 seconds of raw data.

Here it can be seen that many of the differences between WCM and the Banners are within the 4-inch performance objective. With the difference between significant wave height calculated from the west and east auxiliary bridge having the least time segments outside the performance objective.

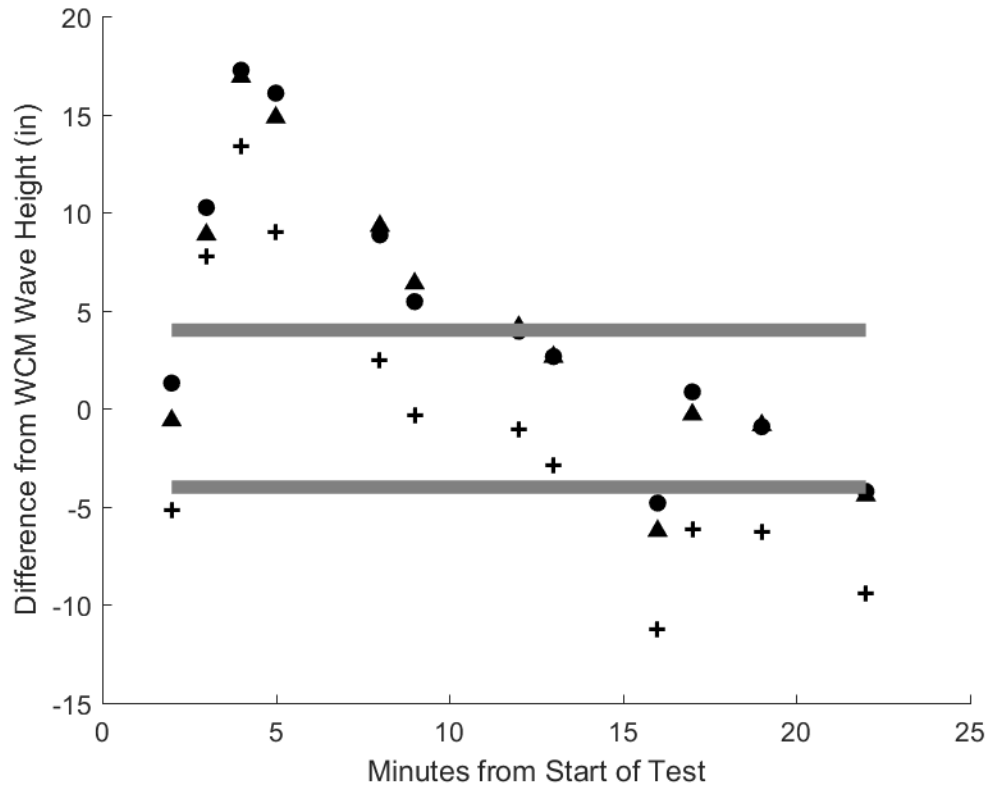


Figure H-7

Figure H-8: Plot showing the difference in significant wave height (H_{m0}) from the WCM mounted on the skimmer and each Banner location for Test 8. The plus signs indicate the difference in significant wave height (H_{m0}) from the main bridge Banner. The triangles represent the difference in significant wave height (H_{m0}) from the west auxiliary bridge Banner data. The dots represent the difference in significant wave height (H_{m0}) from the east auxiliary bridge Banner data. Each data point represents a calculation of the significant wave height from approximately 60 seconds of raw data.

Here it can be seen that most of the differences between WCM and the Banners are within the 4-inch performance objective. With the difference between significant wave height calculated from the main bridge having the least time segments outside the performance objective.

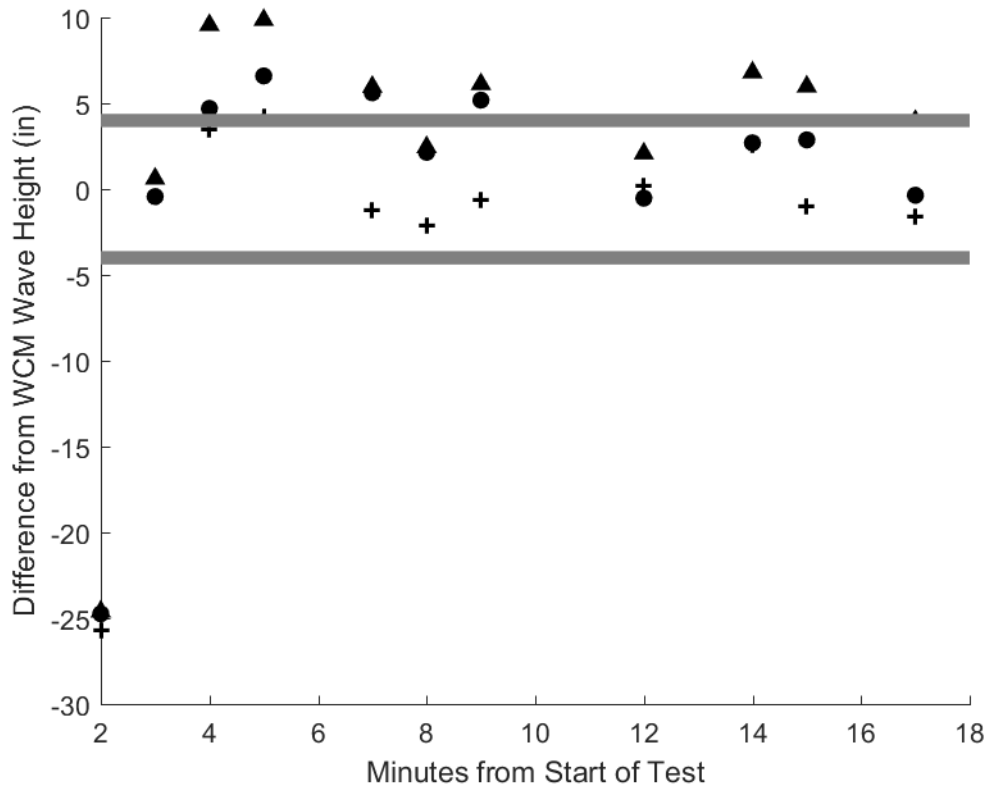


Figure H-8

Figure H-9: Plot showing the difference in significant wave height (H_{m0}) from the WCM mounted on the skimmer and each Banner location for Test 9. The plus signs indicate the difference in significant wave height (H_{m0}) from the main bridge Banner. The triangles represent the difference in significant wave height (H_{m0}) from the west auxiliary bridge Banner data. The dots represent the difference in significant wave height (H_{m0}) from the west auxiliary bridge Banner data. Each data point represents a calculation of the significant wave height from approximately 60 seconds of raw data.

Here it can be seen that most of the differences between WCM and the Banners are within the 4-inch performance objective. With the difference between significant wave height calculated from the main bridge having the least time segments outside the performance objective.

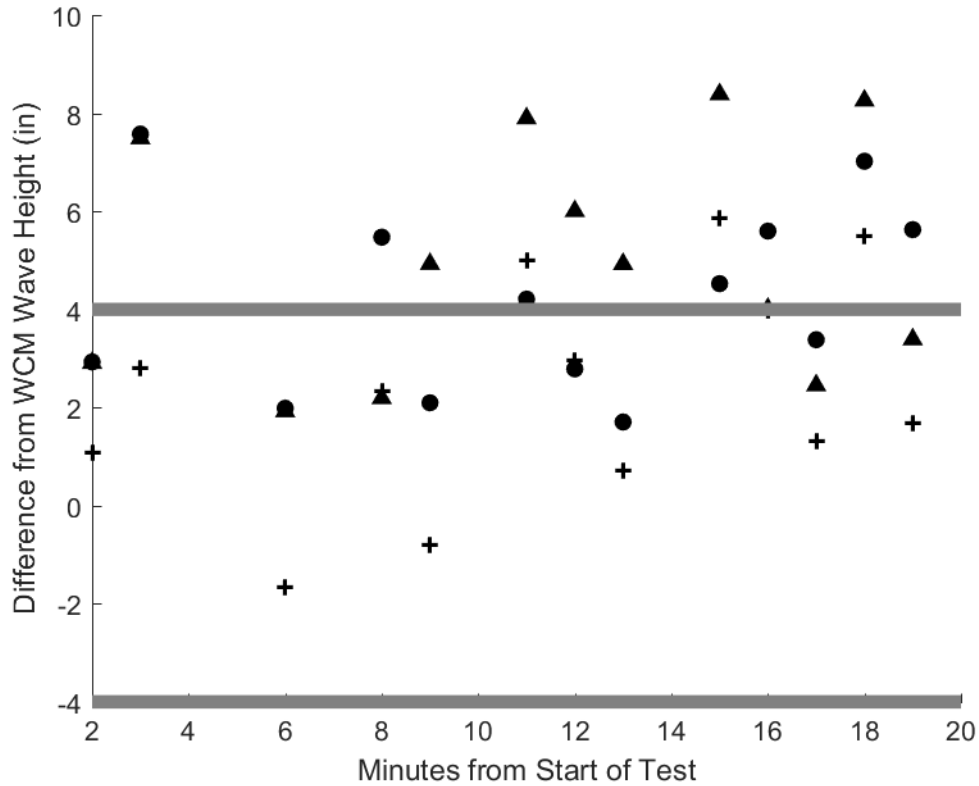


Figure H-9

Figure H-10: Plot showing the difference in significant wave height (H_{m0}) from the WCM mounted on the skimmer and each Banner location for Test 10. The plus signs indicate the difference in significant wave height (H_{m0}) from the main bridge Banner. The triangles represent the difference in significant wave height (H_{m0}) from the west auxiliary bridge Banner data. The dots represent the difference in significant wave height (H_{m0}) from the east auxiliary bridge Banner data. Each data point represents a calculation of the significant wave height from approximately 60 seconds of raw data.

Here it can be seen that most of the differences between WCM and the Banners are within the 4-inch performance objective. With the difference between significant wave height calculated from the main and east auxiliary bridge having the least time segments outside the performance objective.

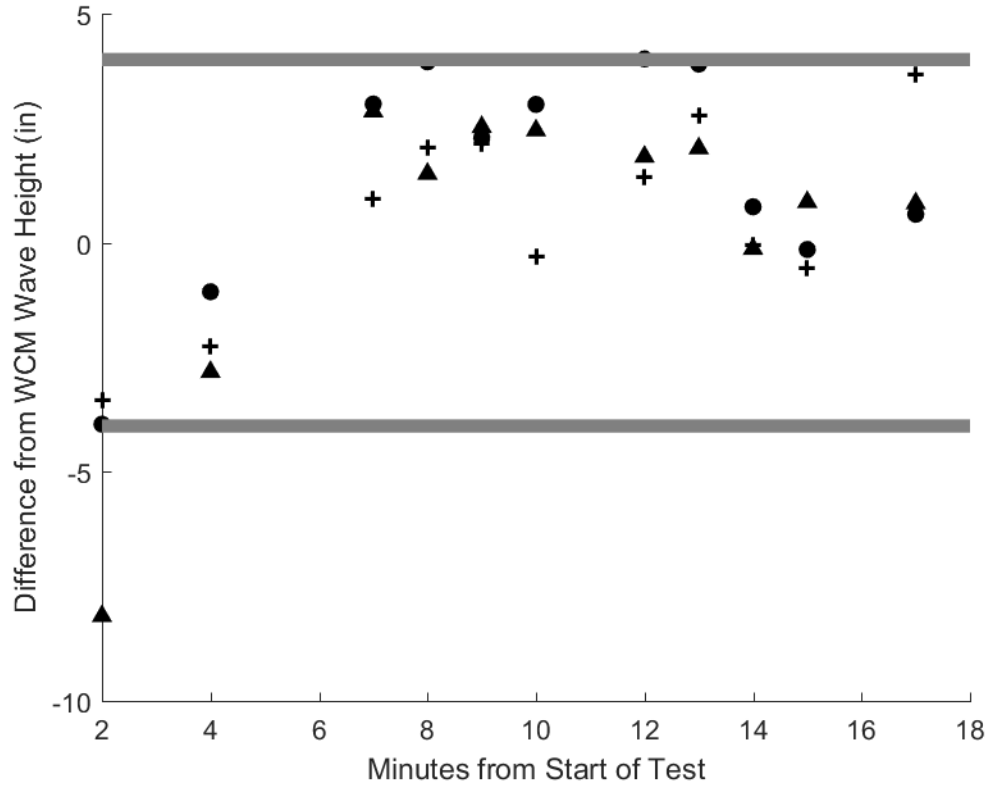


Figure H-10

Figure H-11: Plot showing the difference in significant wave height (H_{m0}) from the WCM mounted on the skimmer and each Banner location for Test 11. The plus signs indicate the difference in significant wave height (H_{m0}) from the main bridge Banner. The triangles represent the difference in significant wave height (H_{m0}) from the west auxiliary bridge Banner data. The dots represent the difference in significant wave height (H_{m0}) from the east auxiliary bridge Banner data. Each data point represents a calculation of the significant wave height from approximately 60 seconds of raw data.

Here it can be seen that most of the differences between WCM and the Banners are within the 4-inch performance objective. With the difference between significant wave height calculated from the main and east auxiliary bridge having the least time segments outside the performance objective.

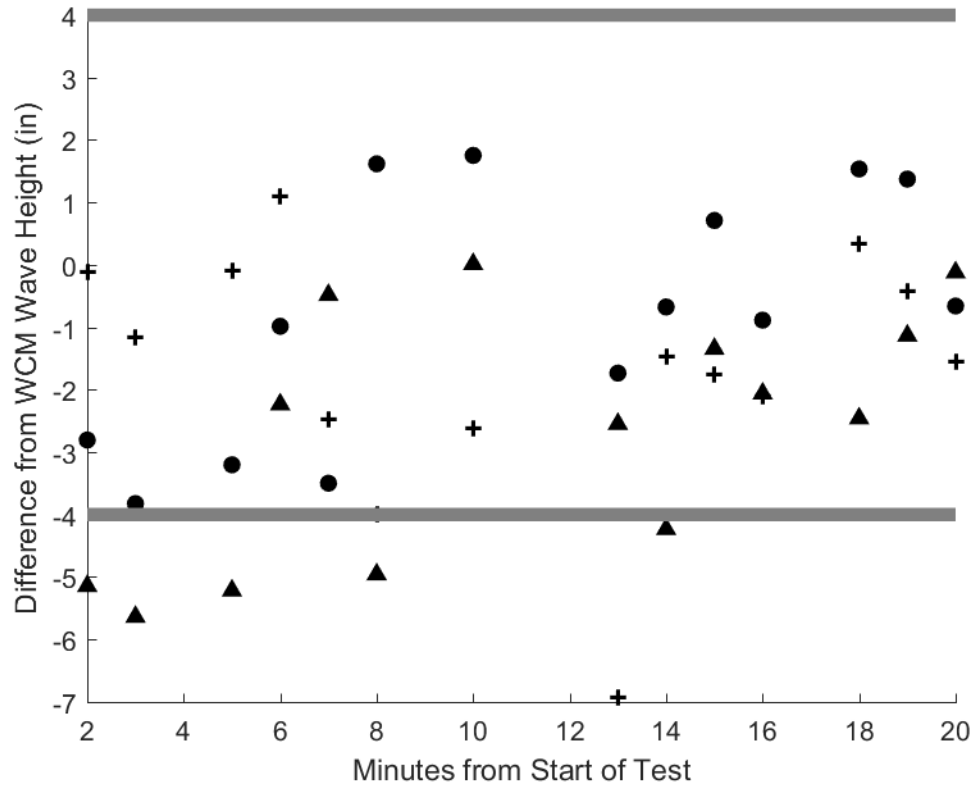


Figure H-11

Figure H-12: Plot showing the difference in significant wave height (H_{m0}) from the WCM mounted on the skimmer and each Banner location for Test 12. The plus signs indicate the difference in significant wave height (H_{m0}) from the main bridge Banner. The triangles represent the difference in significant wave height (H_{m0}) from the west auxiliary bridge Banner data. The dots represent the difference in significant wave height (H_{m0}) from the east auxiliary bridge Banner data. Each data point represents a calculation of the significant wave height from approximately 60 seconds of raw data.

Here it can be seen that most of the differences between WCM and the Banners are within the 4-inch performance objective. With the difference between significant wave height calculated from the west auxiliary bridge having the least time segments outside the performance objective.

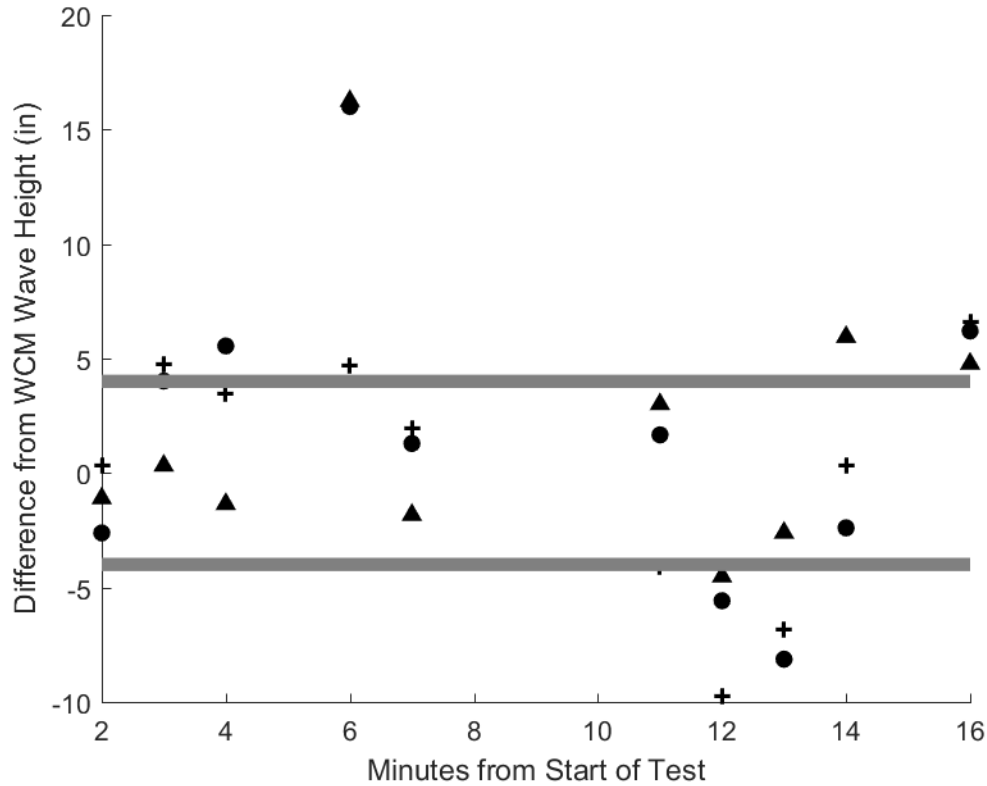


Figure H-12

Figure H-13: Plot showing the difference in significant wave height (H_{m0}) from the WCM mounted on the skimmer and each Banner location for Test 13. The plus signs indicate the difference in significant wave height (H_{m0}) from the main bridge Banner. The triangles represent the difference in significant wave height (H_{m0}) from the east auxiliary bridge Banner data. The dots represent the difference in significant wave height (H_{m0}) from the west auxiliary bridge Banner data. Each data point represents a calculation of the significant wave height from approximately 60 seconds of raw data.

Here it can be seen that most of the differences between WCM and the Banners are within the 4-inch performance objective. With the difference between significant wave height calculated from the west auxiliary bridge having the least time segments outside the performance objective.

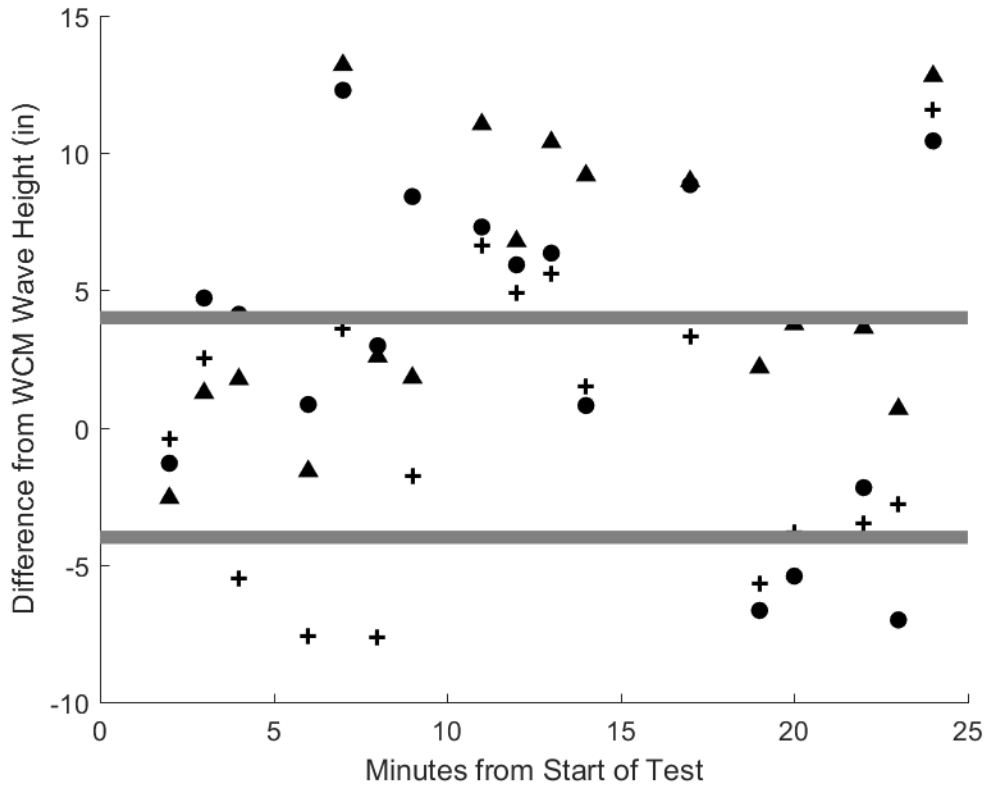


Figure H-13

Figure H-14: Plot showing the difference in significant wave height (H_{m0}) from the WCM mounted on the skimmer and each Banner location for Test 14. The plus signs indicate the difference in significant wave height (H_{m0}) from the main bridge Banner. The triangles represent the difference in significant wave height (H_{m0}) from the west auxiliary bridge Banner data. The dots represent the difference in significant wave height (H_{m0}) from the east auxiliary bridge Banner data. Each data point represents a calculation of the significant wave height from approximately 60 seconds of raw data.

Here it can be seen that most of the differences between WCM and the Banners are within the 4-inch performance objective. With the difference between significant wave height calculated from the west auxiliary bridge having the least time segments outside the performance objective.

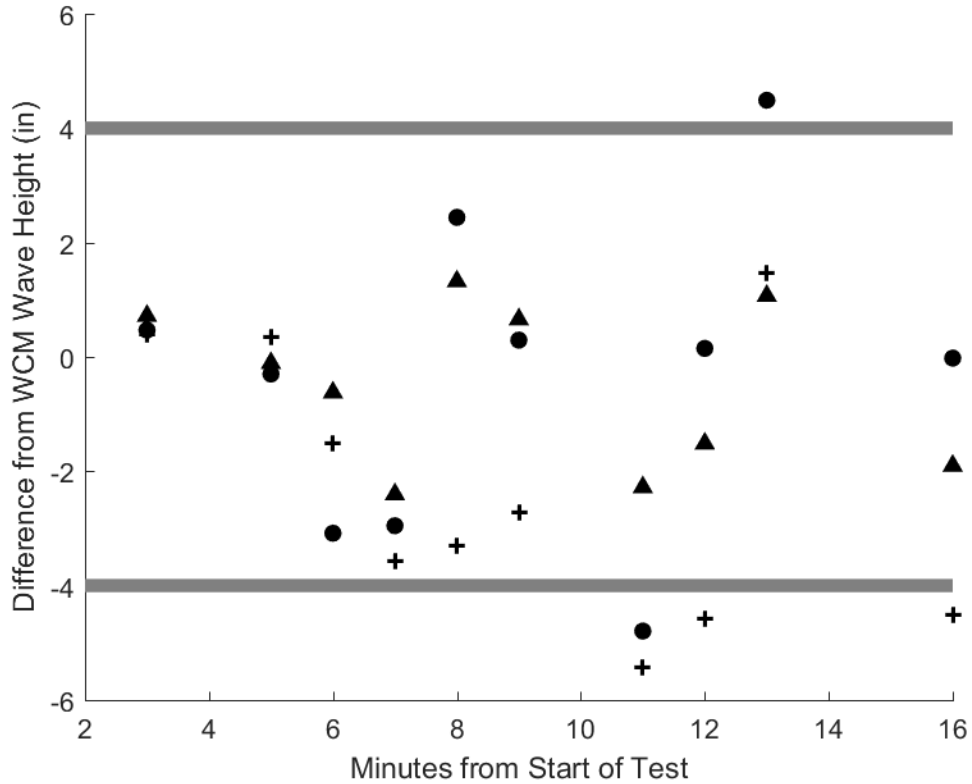


Figure H-14

Figure H-15: Plot showing the difference in significant wave height (H_{m0}) from the WCM mounted on the skimmer and each Banner location for Test 15. The plus signs indicate the difference in significant wave height (H_{m0}) from the main bridge Banner. The triangles represent the difference in significant wave height (H_{m0}) from the west auxiliary bridge Banner data. The dots represent the difference in significant wave height (H_{m0}) from the west auxiliary bridge Banner data. Each data point represents a calculation of the significant wave height from approximately 60 seconds of raw data.

Here it can be seen that most of the differences between WCM and the Banners are within the 4-inch performance objective. With the difference between significant wave height calculated from the main bridge having the least time segments outside the performance objective.

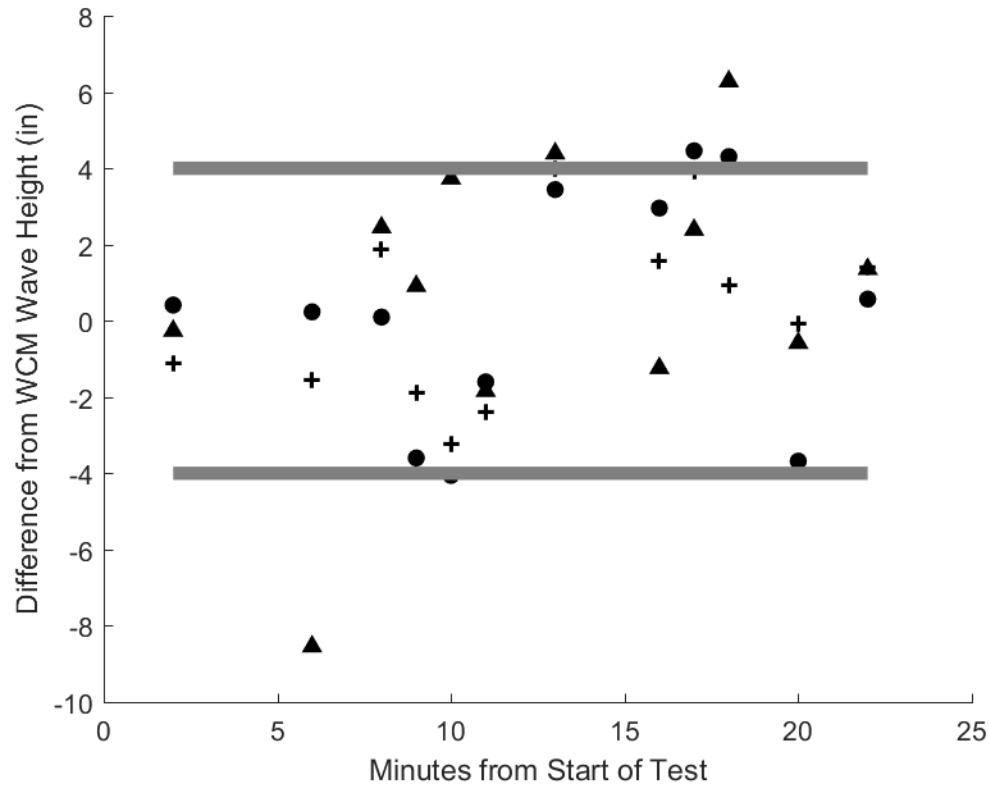


Figure H-15

Figure H-16: Plot showing the difference in significant wave height (H_{m0}) from the WCM mounted on the skimmer and each Banner location for Test 16. The plus signs indicate the difference in significant wave height (H_{m0}) from the main bridge Banner. The triangles represent the difference in significant wave height (H_{m0}) from the west auxiliary bridge Banner data. The dots represent the difference in significant wave height (H_{m0}) from the east auxiliary bridge Banner data. Each data point represents a calculation of the significant wave height from approximately 60 seconds of raw data.

Here it can be seen that most of the differences between WCM and the Banners are within the 4-inch performance objective. With the difference between significant wave height calculated from the east auxiliary bridge having the least time segments outside the performance objective.

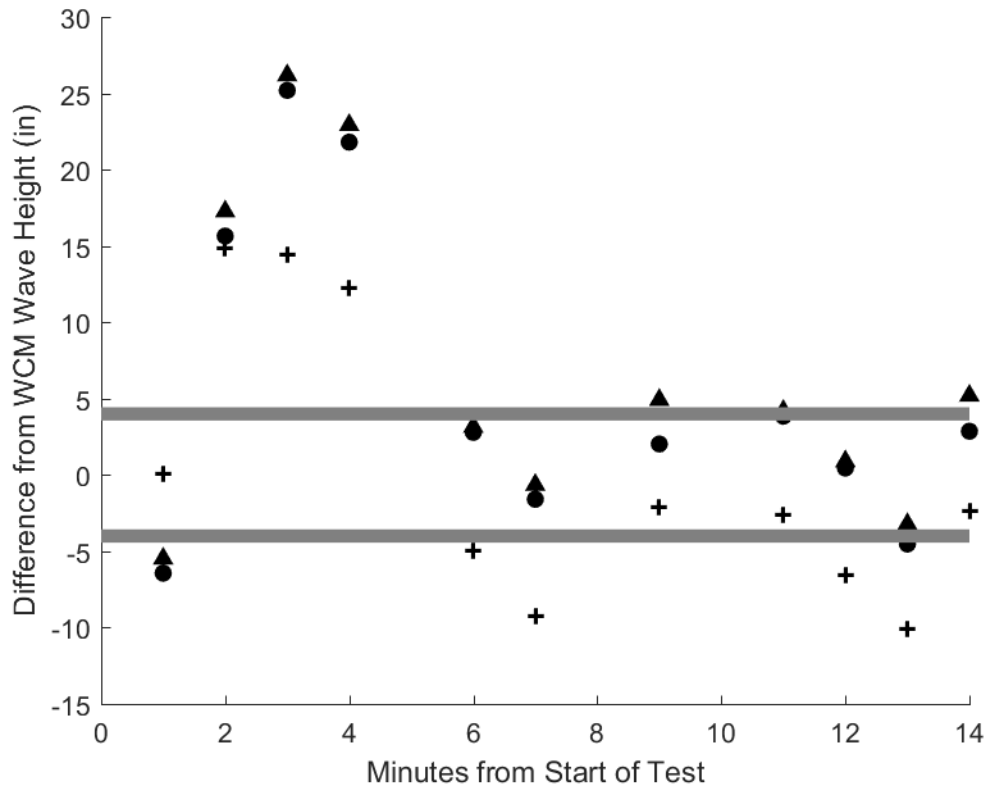


Figure H-16

Figure H-17: Plot showing the difference in significant wave height (H_{m0}) from the WCM mounted on the skimmer and each Banner location for Test 17. The plus signs indicate the difference in significant wave height (H_{m0}) from the main bridge Banner. The triangles represent the difference in significant wave height (H_{m0}) from the west auxiliary bridge Banner data. The dots represent the difference in significant wave height (H_{m0}) from the east auxiliary bridge Banner data. Each data point represents a calculation of the significant wave height from approximately 60 seconds of raw data.

Here it can be seen that all of the differences between WCM and the Banners are within the 4-inch performance objective.

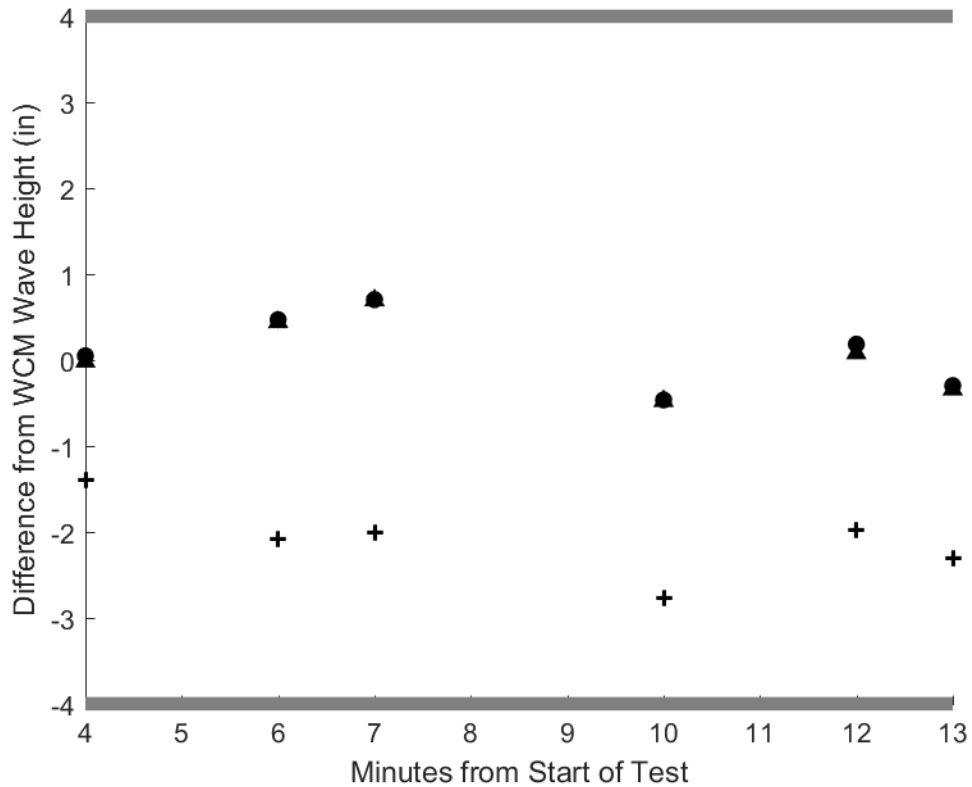


Figure H-17

Figure H-18: Plot showing the difference in significant wave height (H_{m0}) from the WCM mounted on the skimmer and each Banner location for Test 18. The plus signs indicate the difference in significant wave height (H_{m0}) from the main bridge Banner. The triangles represent the difference in significant wave height (H_{m0}) from the west auxiliary bridge Banner data. The dots represent the difference in significant wave height (H_{m0}) from the east auxiliary bridge Banner data. Each data point represents a calculation of the significant wave height from approximately 60 seconds of raw data.

Here it can be seen that some of the differences between WCM and the Banners are within the 4-inch performance objective. With the difference between significant wave height calculated from the main bridge having the least time segments outside the performance objective.

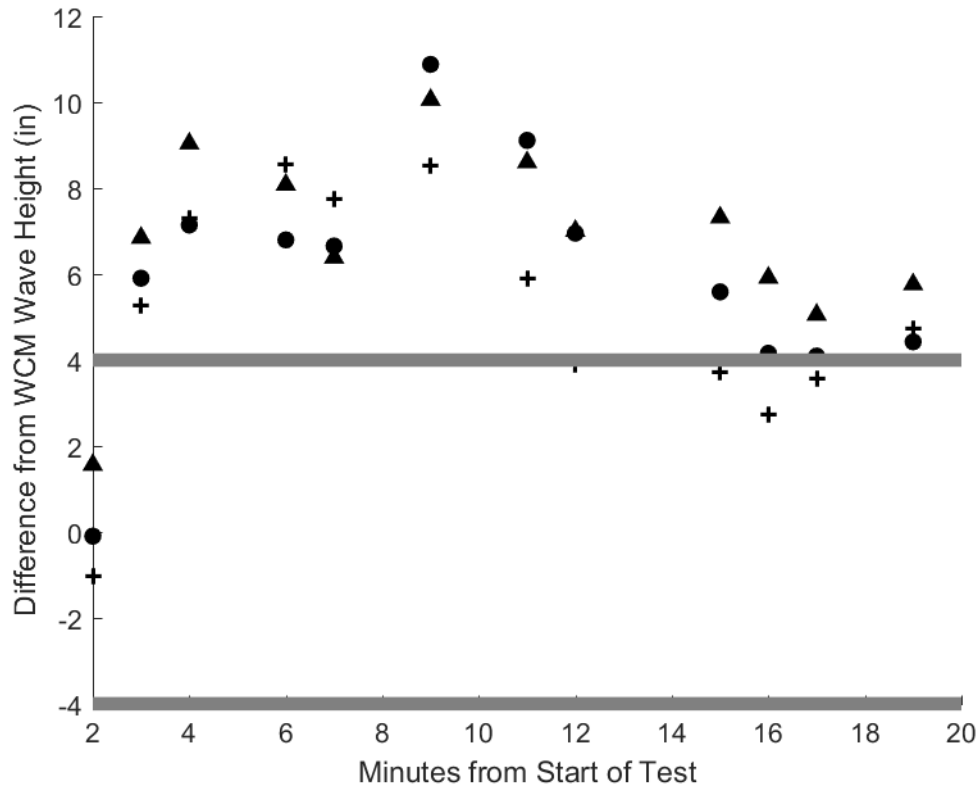


Figure H-18

Figure H-19: Plot showing the difference in significant wave height (H_{m0}) from the WCM mounted on the skimmer and each Banner location for Test 19. The plus signs indicate the difference in significant wave height (H_{m0}) from the main bridge Banner. The triangles represent the difference in significant wave height (H_{m0}) from the west auxiliary bridge Banner data. The dots represent the difference in significant wave height (H_{m0}) from the east auxiliary bridge Banner data. Each data point represents a calculation of the significant wave height from approximately 60 seconds of raw data.

Here it can be seen that most of the differences between WCM and the Banners are within the 4-inch performance objective. With the difference between significant wave height calculated from the east auxiliary bridge having the least time segments outside the performance objective.

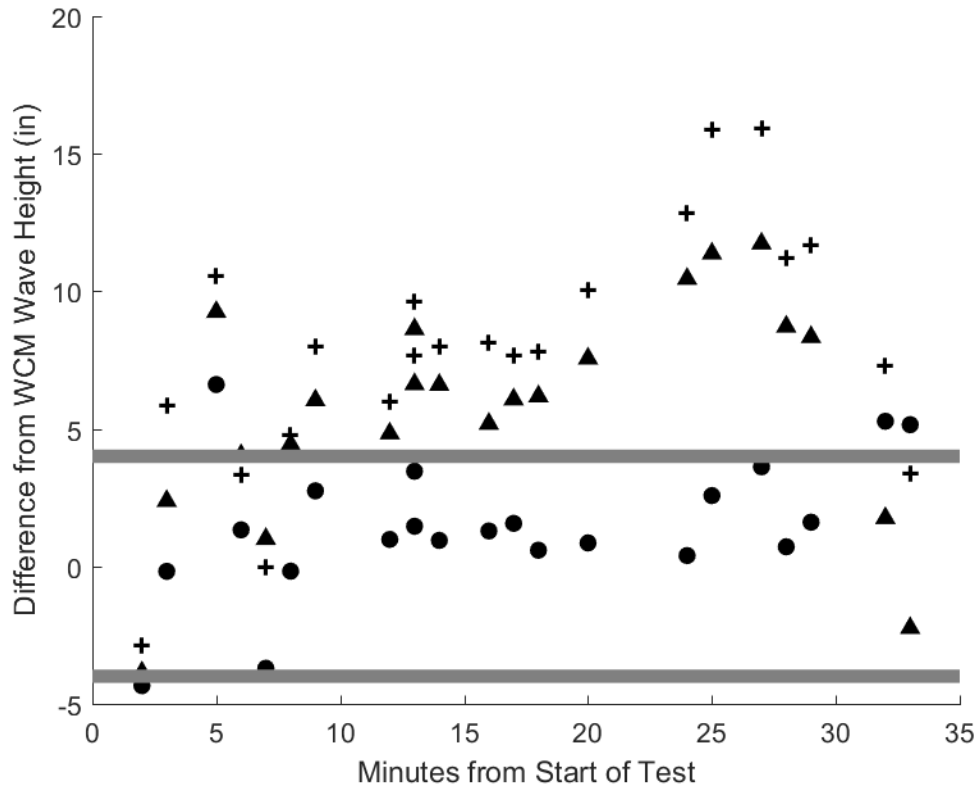


Figure H-19

Figure H-20: Plot showing the difference in significant wave height (H_{m0}) from the WCM mounted on the skimmer and each Banner location for Test 20. The plus signs indicate the difference in significant wave height (H_{m0}) from the main bridge Banner. The triangles represent the difference in significant wave height (H_{m0}) from the west auxiliary bridge Banner data. The dots represent the difference in significant wave height (H_{m0}) from the east auxiliary bridge Banner data. Each data point represents a calculation of the significant wave height from approximately 60 seconds of raw data.

Here it can be seen that most of the differences between WCM and the Banners are within the 4-inch performance objective. With the difference between significant wave height calculated from the main bridge having the least time segments outside the performance objective.

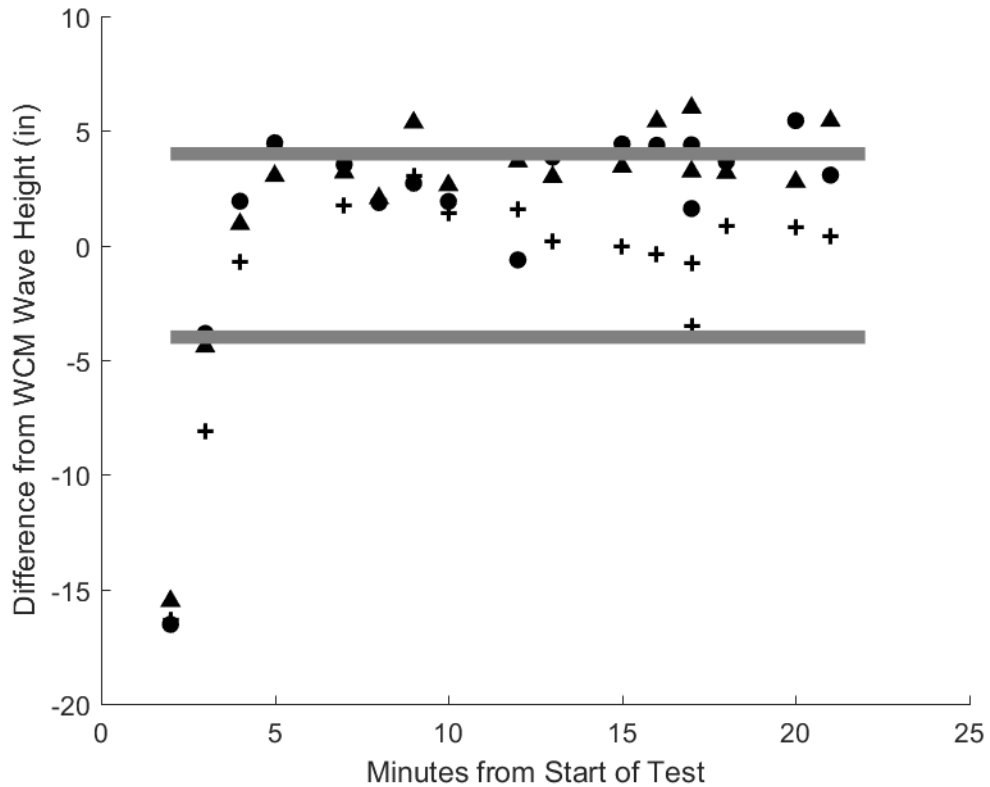


Figure H-20

Figure H-21: Plot showing the difference in significant wave height (H_{m0}) from the WCM mounted on the skimmer and each Banner location for Test 21. The plus signs indicate the difference in significant wave height (H_{m0}) from the main bridge Banner. The triangles represent the difference in significant wave height (H_{m0}) from the west auxiliary bridge Banner data. The dots represent the difference in significant wave height (H_{m0}) from the east auxiliary bridge Banner data. Each data point represents a calculation of the significant wave height from approximately 60 seconds of raw data.

Here it can be seen that some of the differences between WCM and the Banners are within the 4-inch performance objective. With the difference between significant wave height calculated from the main bridge having the least time segments outside the performance objective.

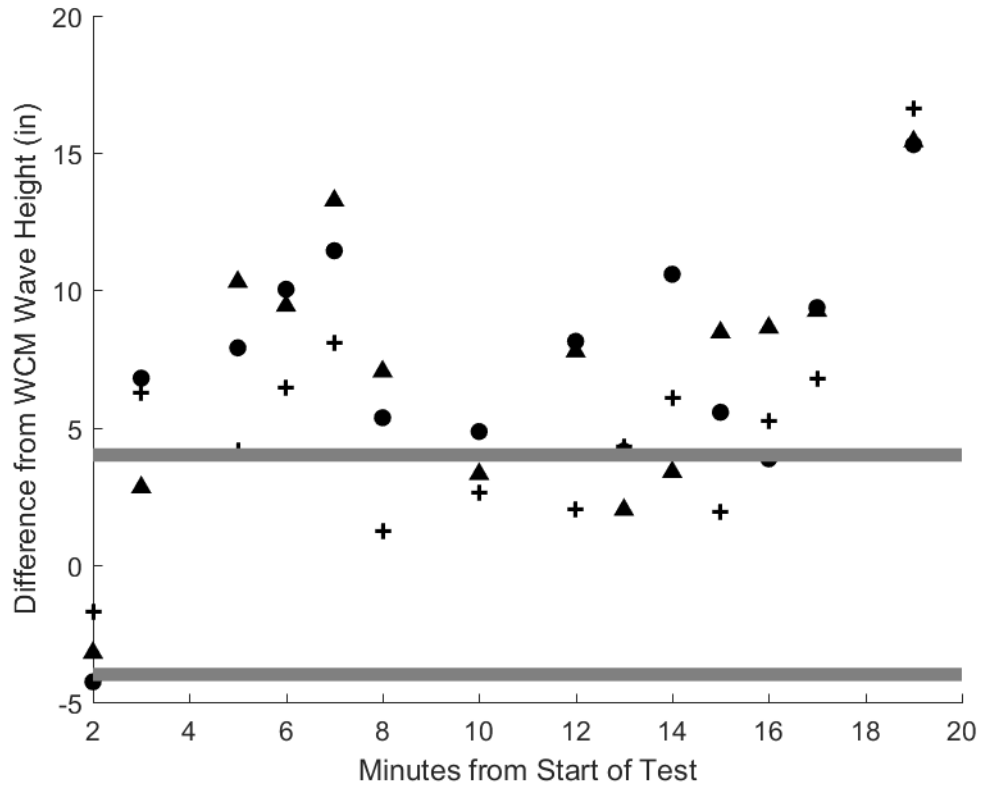


Figure H-21

Figure H-22: Plots showing the difference in significant wave height (H_{m0}) from the WCM mounted on the skimmer and each Banner location for Test 22. The plus signs indicate the difference in significant wave height (H_{m0}) from the main bridge Banner. The triangles represent the difference in significant wave height (H_{m0}) from the west auxiliary bridge Banner data. The dots represent the difference in significant wave height (H_{m0}) from the west auxiliary bridge Banner data. Each data point represents a calculation of the significant wave height from approximately 60 seconds of raw data.

Here few of the difference between WCM and the Banners are within the 4-inch performance objective. This test is one where the waves were created by the 18-inch stroke and 18 CPM setting of the wave generator, which creates a large sinusoidal wave. We believe the discrepancies between the WCM and Banner measurement are due to lateral motion from the large elliptical motion of the wave not being considered by the algorithms. This is because we trained them on real, complex wave motion where most of the movement is in the heave.

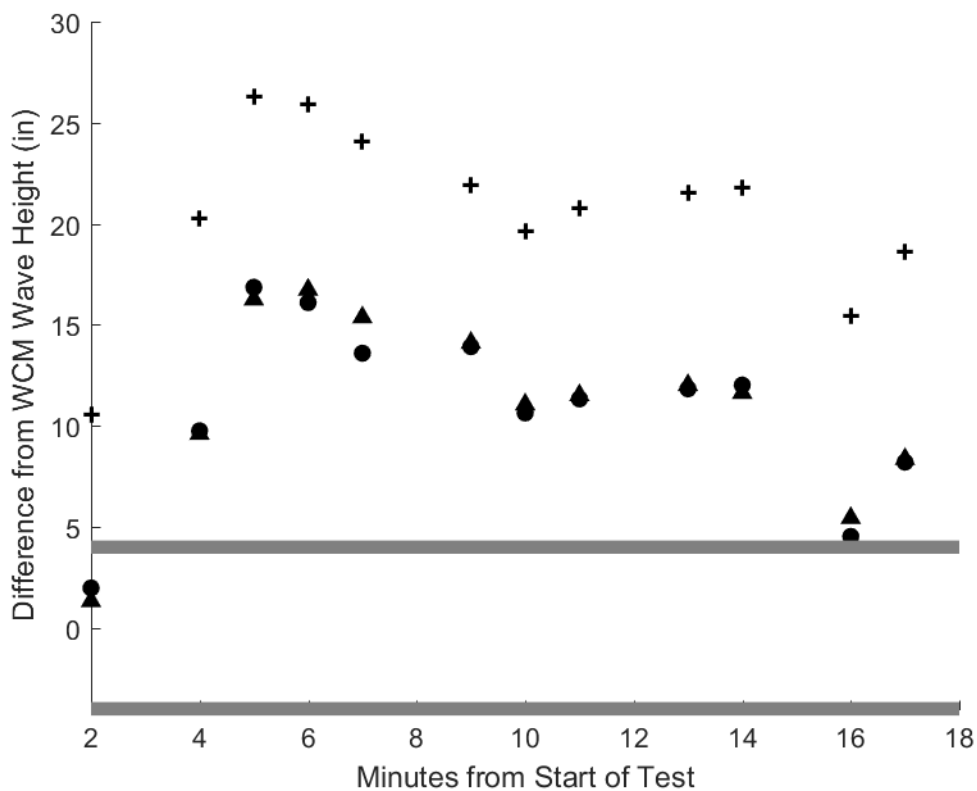


Figure H-22

Appendix I: Difference in Significant Wave Height between WCM-Buoy and Banners

This appendix contains plots showing the difference in significant wave height (H_{m0}) from the WCM buoy and each Banner location for each test.

Figure I-1: Plot showing the difference in significant wave height (H_{m0}) from the WCM buoy and each Banner location for Test 1. The plus signs indicate the difference in significant wave height (H_{m0}) from the main bridge Banner. The triangles represent the difference in significant wave height (H_{m0}) from the west auxiliary bridge Banner data. The dots represent the difference in significant wave height (H_{m0}) from the east auxiliary bridge Banner data. Each data point represents a calculation of the significant wave height from approximately 60 seconds of raw data.

Here it can be seen that the some of the difference between WCM and the Banners are within the 4-inch performance objective. This test is one in which the waves were created by the 18-inch stroke and 18 cycles per minute (CPM) setting of the wave generator, which creates a large sinusoidal wave. We believe the discrepancies between the WCM and Banner measurement are due to lateral motion from the large elliptical motion of the wave not being considered by the algorithms. This is because we trained them on real, complex wave motion where most of the movement is in the heave.

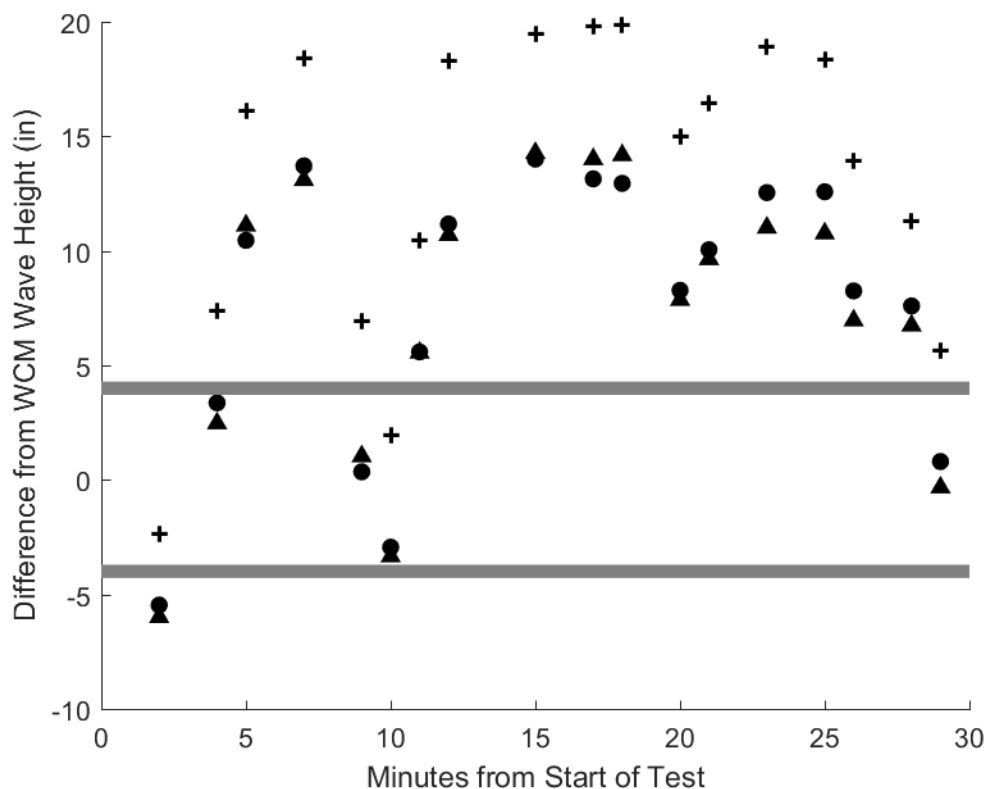


Figure I-1

Figure I-2: Plot showing the difference in significant wave height (H_{m0}) from the WCM buoy and each Banner location for Test 2. The plus signs indicate the difference in significant wave height (H_{m0}) from the main bridge Banner. The triangles represent the difference in significant wave height (H_{m0}) from the west auxiliary bridge Banner data. The dots represent the difference in significant wave height (H_{m0}) from the east auxiliary bridge Banner data. Each data point represents a calculation of the significant wave height from approximately 60 seconds of raw data.

Here it can be seen that most of the differences between WCM and the Banners are within the 4-inch performance objective. With the difference between significant wave height calculated from the east auxiliary bridge having the least time segments outside the performance objective.

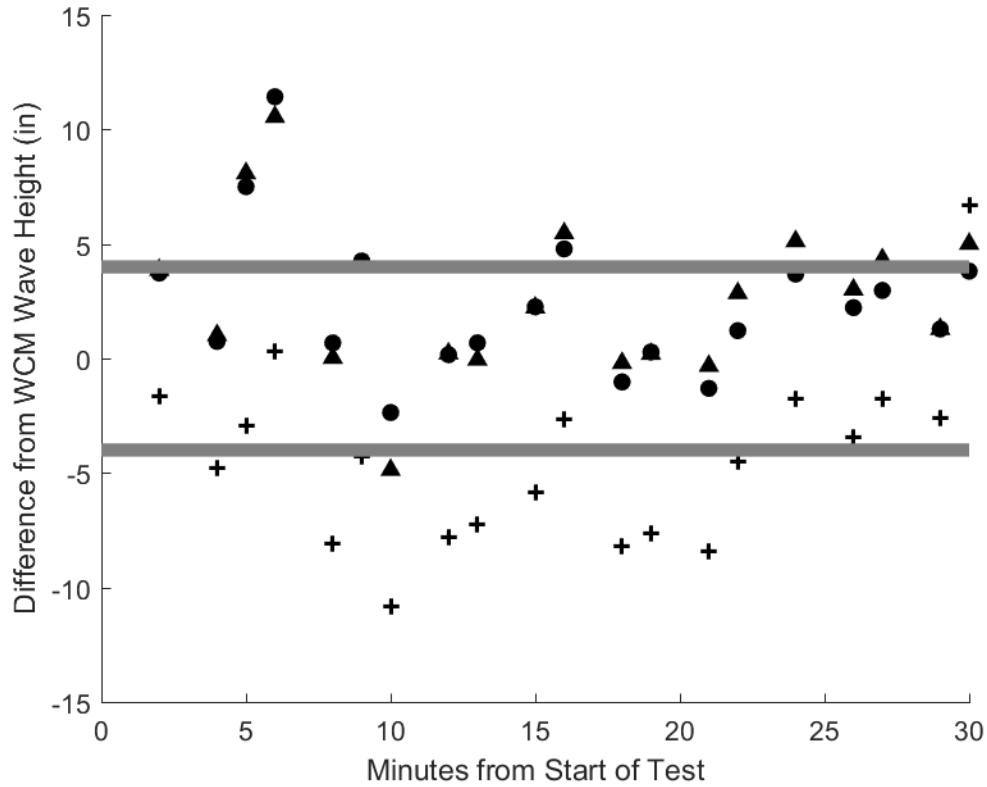


Figure I-2

Figure I-3: Plot showing the difference in significant wave height (H_{m0}) from the WCM buoy and each Banner location for Test 3. The plus signs indicate the difference in significant wave height (H_{m0}) from the main bridge Banner. The triangles represent the difference in significant wave height (H_{m0}) from the west auxiliary bridge Banner data. The dots represent the difference in significant wave height (H_{m0}) from the east auxiliary bridge Banner data. Each data point represents a calculation of the significant wave height from approximately 60 seconds of raw data.

Here it can be seen that most of the differences between WCM and the Banners are within the 4-inch performance objective. With the difference between significant wave height calculated from the west auxiliary bridge having the least time segments outside the performance objective.

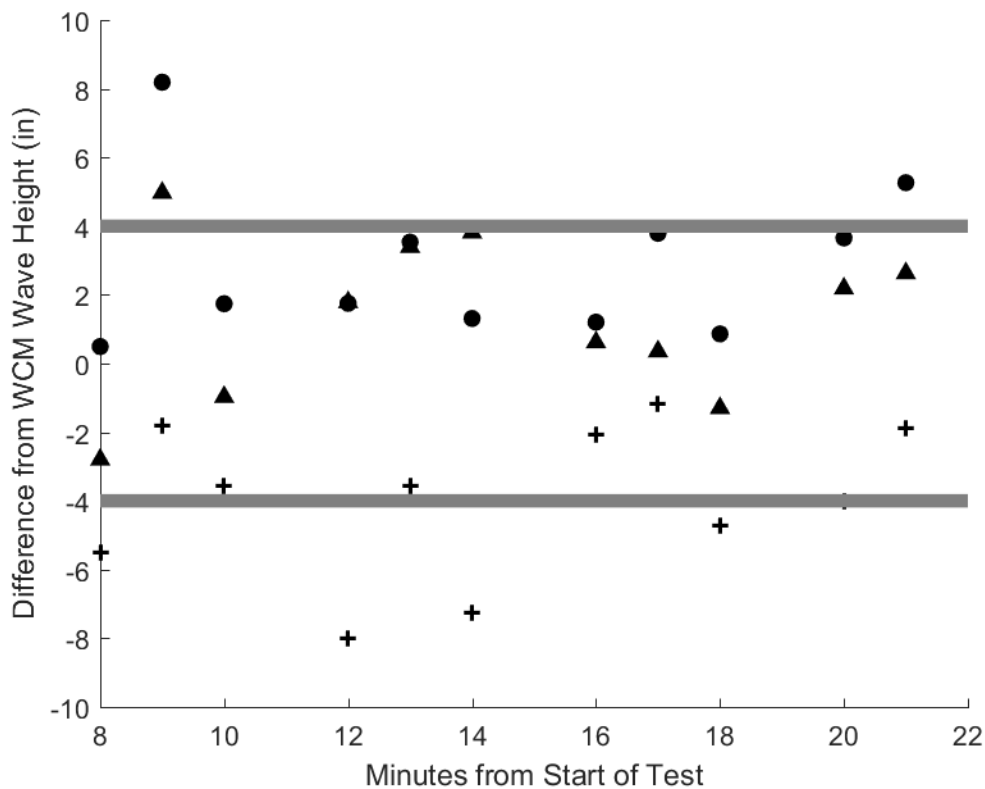


Figure I-3

Figure I-4: Plot showing the difference in significant wave height (H_{m0}) from the WCM buoy and each Banner location for Test 4. The plus signs indicate the difference in significant wave height (H_{m0}) from the main bridge Banner. The triangles represent the difference in significant wave height (H_{m0}) from the west auxiliary bridge Banner data. The dots represent the difference in significant wave height (H_{m0}) from the east auxiliary bridge Banner data. Each data point represents a calculation of the significant wave height from approximately 60 seconds of raw data.

Here it can be seen that most of the differences between WCM and the Banners are within the 4-inch performance objective. With the difference between significant wave height calculated from the east auxiliary bridge having the least time segments outside the performance objective.

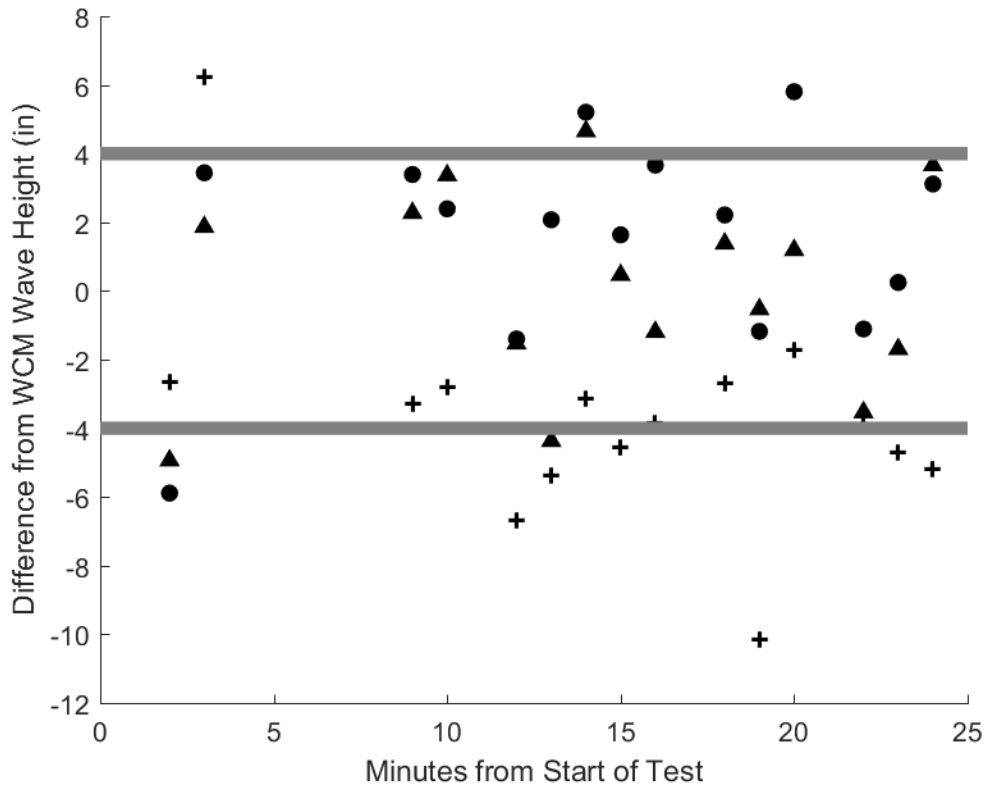


Figure I-4

Figure I-5: Plot showing the difference in significant wave height (H_{m0}) from the WCM buoy and each Banner location for Test 5. The plus signs indicate the difference in significant wave height (H_{m0}) from the main bridge Banner. The triangles represent the difference in significant wave height (H_{m0}) from the west auxiliary bridge Banner data. The dots represent the difference in significant wave height (H_{m0}) from the east auxiliary bridge Banner data. Each data point represents a calculation of the significant wave height from approximately 60 seconds of raw data.

Here it can be seen that some of the difference between WCM and the Banners are within the 4-inch performance objective. This test is one where the waves were created by the 18-inch stroke and 18 CPM setting of the wave generator, which creates a large sinusoidal wave. We believe the discrepancies between the WCM and Banner measurement are due to lateral motion from the large elliptical motion of the wave not being considered by the algorithms. This is because we trained them on real, complex wave motion where most of the movement is in the heave.

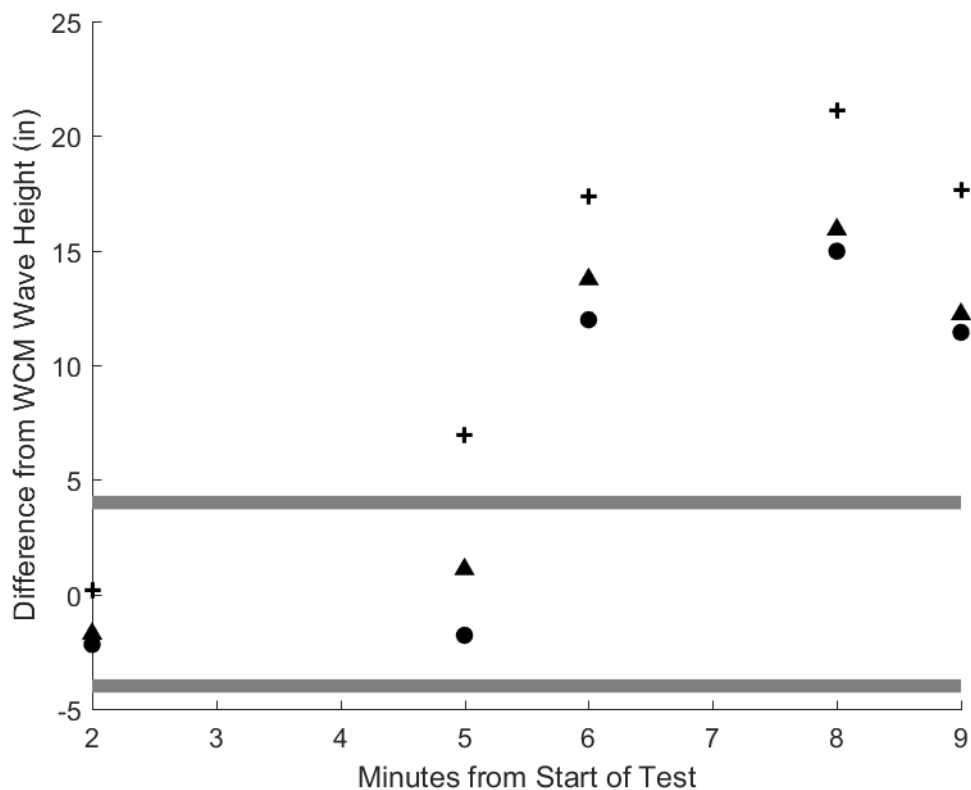


Figure I-5

Figure I-6: Plot showing the difference in significant wave height (H_{m0}) from the WCM buoy and each Banner location for Test 6. The plus signs indicate the difference in significant wave height (H_{m0}) from the main bridge Banner. The triangles represent the difference in significant wave height (H_{m0}) from the west auxiliary bridge Banner data. The dots represent the difference in significant wave height (H_{m0}) from the east auxiliary bridge Banner data. Each data point represents a calculation of the significant wave height from approximately 60 seconds of raw data.

Here it can be seen that many of the difference between WCM and the Banners are within the 4-inch performance objective. This test is one where the waves were created by the 18-inch stroke and 18 CPM setting of the wave generator, which creates a large sinusoidal wave. We believe the discrepancies between the WCM and Banner measurement are due to lateral motion from the large elliptical motion of the wave not being considered by the algorithms. This is because we trained them on real, complex wave motion where most of the movement is in the heave.

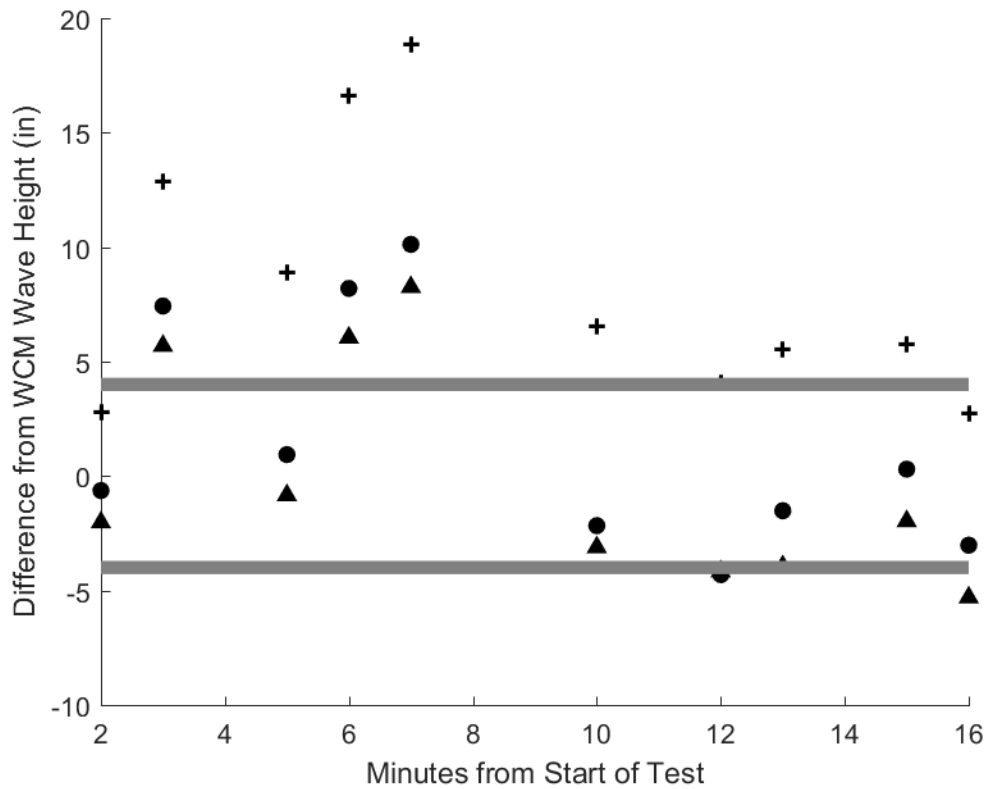


Figure I-6

Figure I-7: Plot showing the difference in significant wave height (H_{m0}) from the WCM buoy and each Banner location for Test 7. The plus signs indicate the difference in significant wave height (H_{m0}) from the main bridge Banner. The triangles represent the difference in significant wave height (H_{m0}) from the west auxiliary bridge Banner data. The dots represent the difference in significant wave height (H_{m0}) from the east auxiliary bridge Banner data. Each data point represents a calculation of the significant wave height from approximately 60 seconds of raw data.

Here it can be seen that many of the differences between WCM and the Banners are within the 4-inch performance objective. With the difference between significant wave height calculated from the main bridge having the least time segments outside the performance objective.

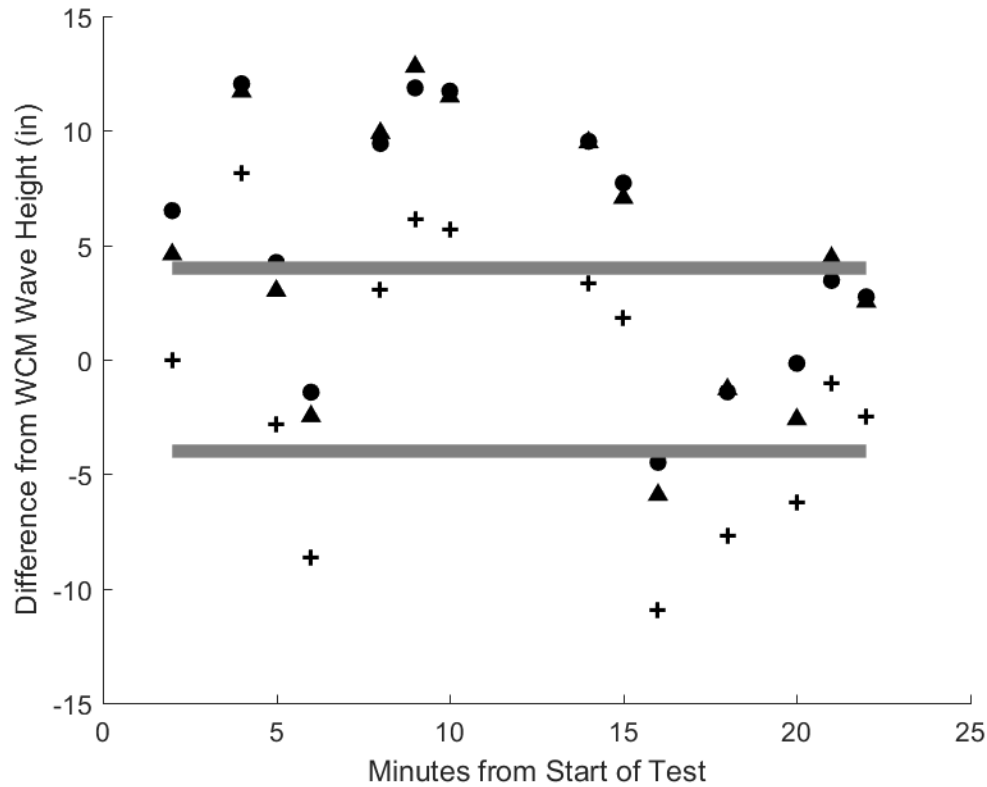


Figure I-7

Figure I-8: Plot showing the difference in significant wave height (H_{m0}) from the WCM buoy and each Banner location for Test 8. The plus signs indicate the difference in significant wave height (H_{m0}) from the main bridge Banner. The triangles represent the difference in significant wave height (H_{m0}) from the west auxiliary bridge Banner data. The dots represent the difference in significant wave height (H_{m0}) from the east auxiliary bridge Banner data. Each data point represents a calculation of the significant wave height from approximately 60 seconds of raw data.

Here it can be seen that most of the differences between WCM and the Banners are within the 4-inch performance objective. With the difference between significant wave height calculated from the west auxiliary bridge having the least time segments outside the performance objective.

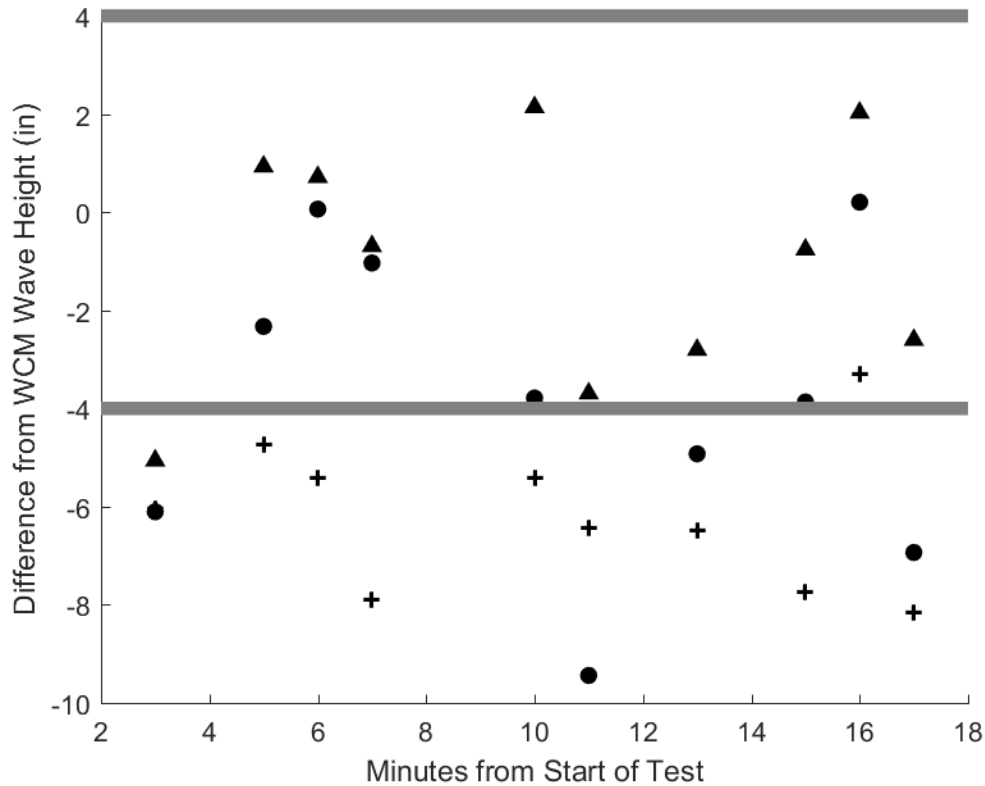


Figure I-8

Figure I-9: Plot showing the difference in significant wave height (H_{m0}) from the WCM buoy and each Banner location for Test 9. The plus signs indicate the difference in significant wave height (H_{m0}) from the main bridge Banner. The triangles represent the difference in significant wave height (H_{m0}) from the west auxiliary bridge Banner data. The dots represent the difference in significant wave height (H_{m0}) from the east auxiliary bridge Banner data. Each data point represents a calculation of the significant wave height from approximately 60 seconds of raw data.

Here it can be seen that most of the differences between WCM and the Banners are within the 4-inch performance objective. With the difference between significant wave height calculated from the main bridge having the least time segments outside the performance objective.

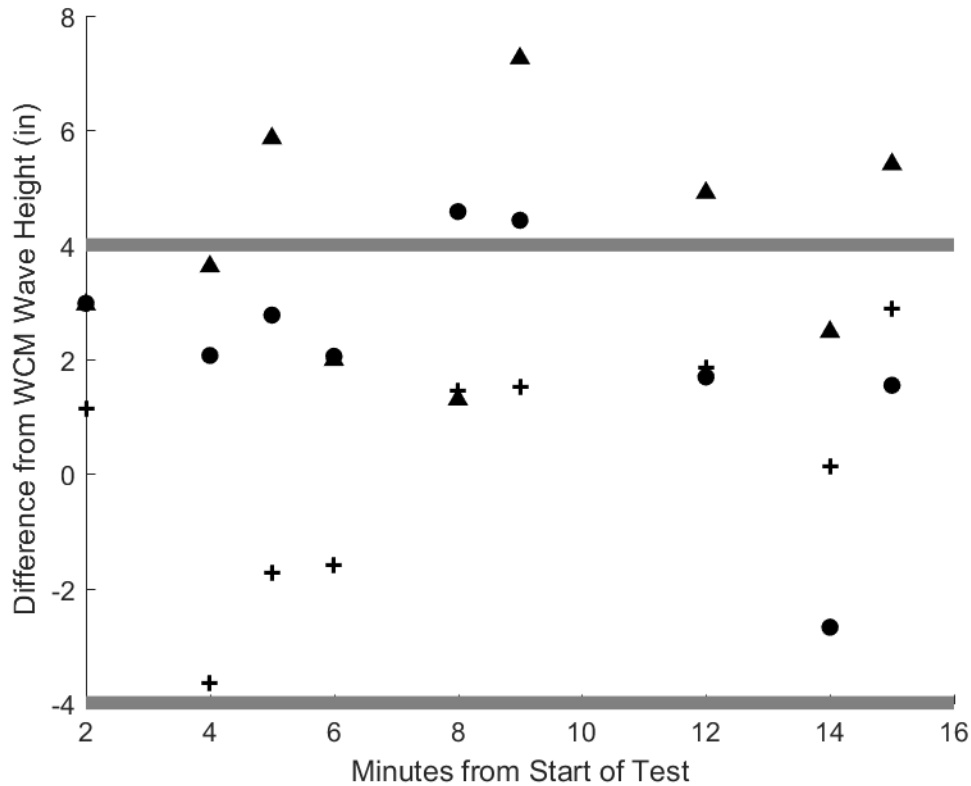


Figure I-9

Figure I-10: Plot showing the difference in significant wave height (H_{m0}) from the WCM buoy and each Banner location for Test 10. The plus signs indicate the difference in significant wave height (H_{m0}) from the main bridge Banner. The triangles represent the difference in significant wave height (H_{m0}) from the west auxiliary bridge Banner data. The dots represent the difference in significant wave height (H_{m0}) from the east auxiliary bridge Banner data. Each data point represents a calculation of the significant wave height from approximately 60 seconds of raw data.

Here it can be seen that most of the differences between WCM and the Banners are within the 4-inch performance objective. With the difference between significant wave height calculated from the main bridge having the least time segments outside the performance objective.

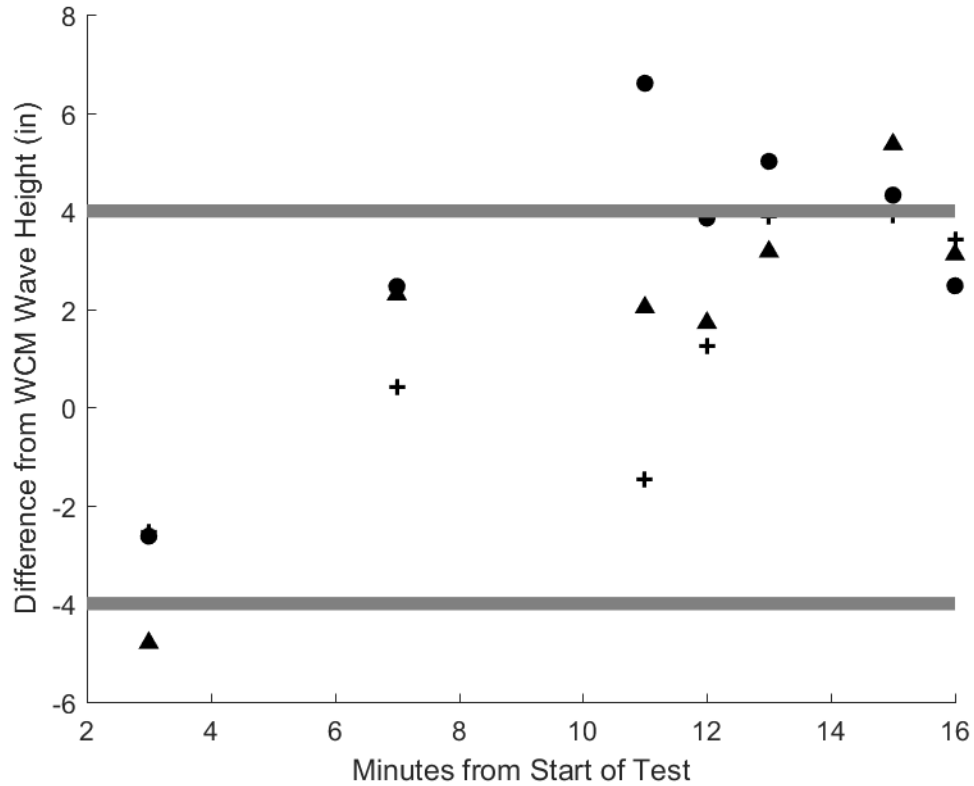


Figure I-10

Figure I-12: Plot showing the difference in significant wave height (H_{m0}) from the WCM buoy and each Banner location for Test 12. The plus signs indicate the difference in significant wave height (H_{m0}) from the main bridge Banner. The triangles represent the difference in significant wave height (H_{m0}) from the west auxiliary bridge Banner data. The dots represent the difference in significant wave height (H_{m0}) from the east auxiliary bridge Banner data. Each data point represents a calculation of the significant wave height from approximately 60 seconds of raw data.

Here it can be seen that most of the differences between WCM and the Banners are within the 4-inch performance objective. With the difference between significant wave height calculated from the west auxiliary bridge having the least time segments outside the performance objective.

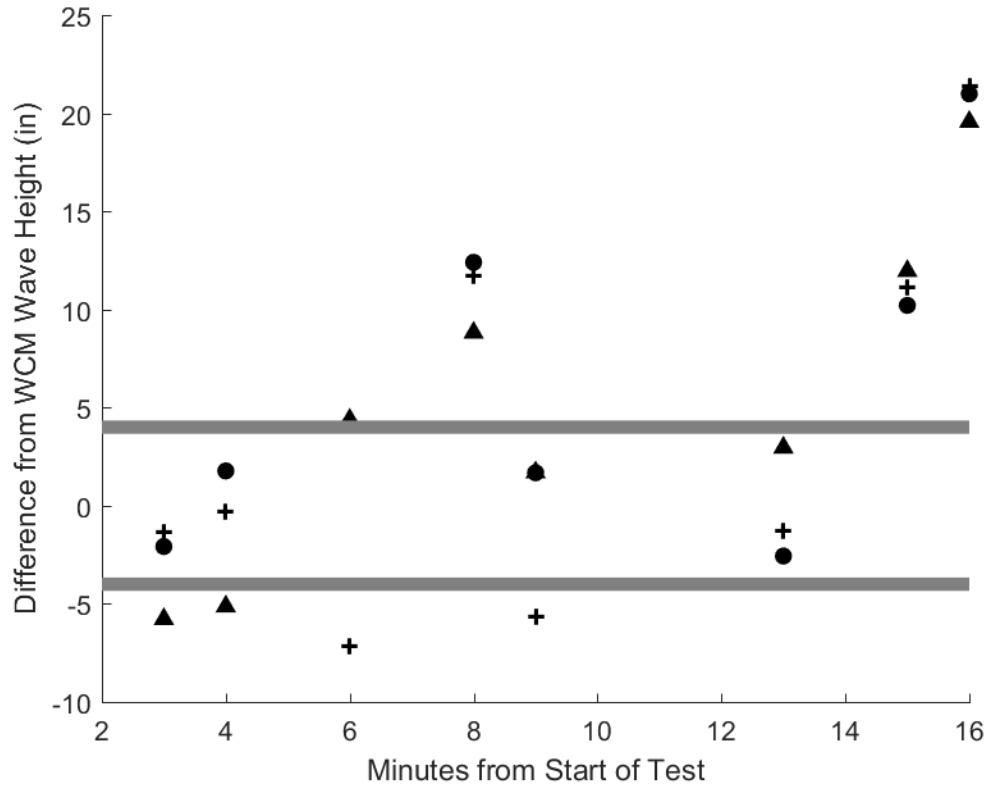


Figure I-12

Figure I-13: Plot showing the difference in significant wave height (H_{m0}) from the WCM buoy and each Banner location for Test 13. The plus signs indicate the difference in significant wave height (H_{m0}) from the main bridge Banner. The triangles represent the difference in significant wave height (H_{m0}) from the west auxiliary bridge Banner data. The dots represent the difference in significant wave height (H_{m0}) from the east auxiliary bridge Banner data. Each data point represents a calculation of the significant wave height from approximately 60 seconds of raw data.

Here it can be seen that most of the differences between WCM and the Banners are within the 4-inch performance objective. With the difference between significant wave height calculated from the east auxiliary bridge having the least time segments outside the performance objective.

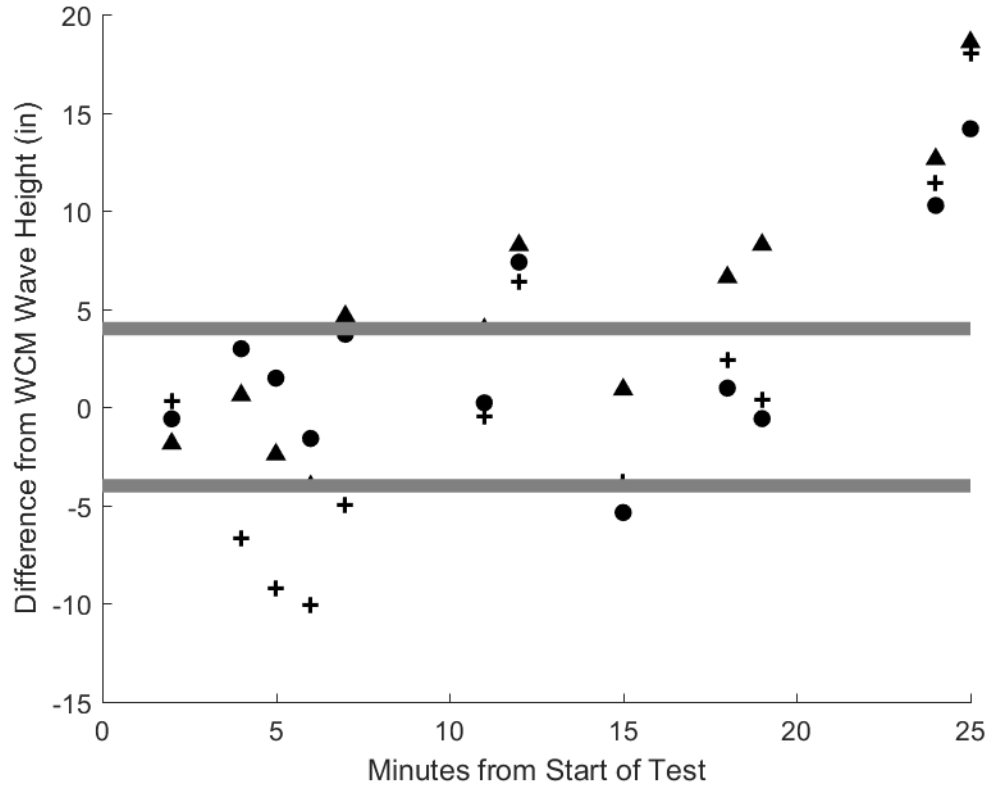


Figure I-13

Figure I-14: Plot showing the difference in significant wave height (H_{m0}) from the WCM buoy and each Banner location for Test 14. The plus signs indicate the difference in significant wave height (H_{m0}) from the main bridge Banner. The triangles represent the difference in significant wave height (H_{m0}) from the west auxiliary bridge Banner data. The dots represent the difference in significant wave height (H_{m0}) from the east auxiliary bridge Banner data. Each data point represents a calculation of the significant wave height from approximately 60 seconds of raw data.

Here it can be seen that most of the differences between WCM and the Banners are within the 4-inch performance objective. With the difference between significant wave height calculated from the west auxiliary bridge having the least time segments outside the performance objective.

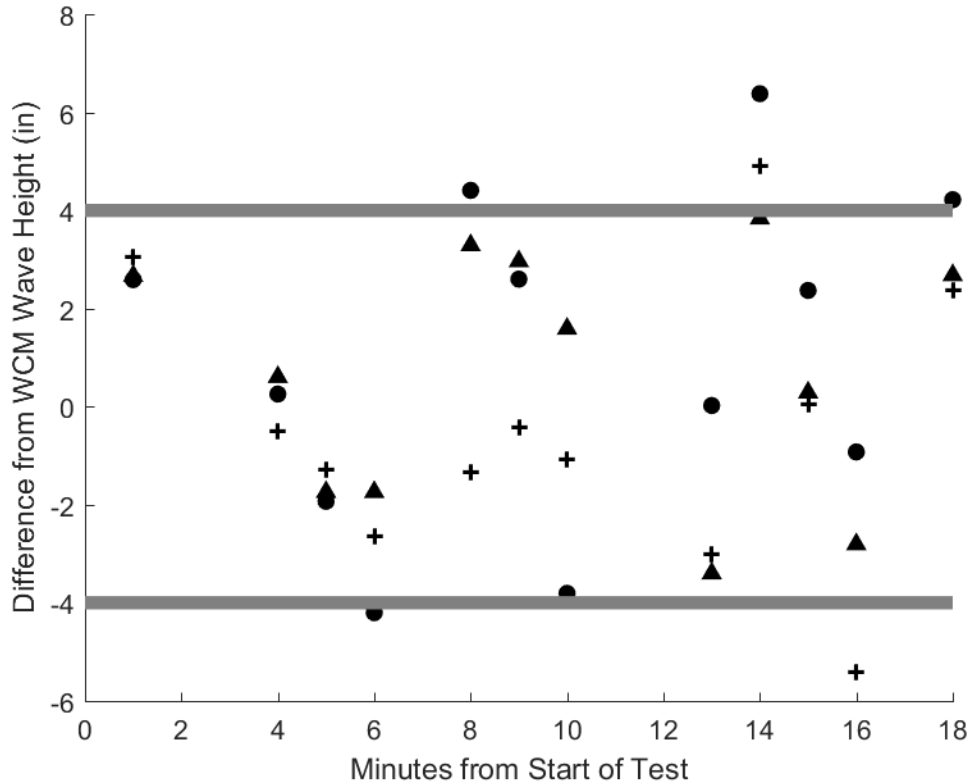


Figure I-14

Figure I-15: Plot showing the difference in significant wave height (H_{m0}) from the WCM buoy and each Banner location for Test 15. The plus signs indicate the difference in significant wave height (H_{m0}) from the main bridge Banner. The triangles represent the difference in significant wave height (H_{m0}) from the west auxiliary bridge Banner data. The dots represent the difference in significant wave height (H_{m0}) from the east auxiliary bridge Banner data. Each data point represents a calculation of the significant wave height from approximately 60 seconds of raw data.

Here it can be seen that most of the differences between WCM and the Banners are within the 4-inch performance objective. With the difference between significant wave height calculated from the main bridge having the least time segments outside the performance objective.

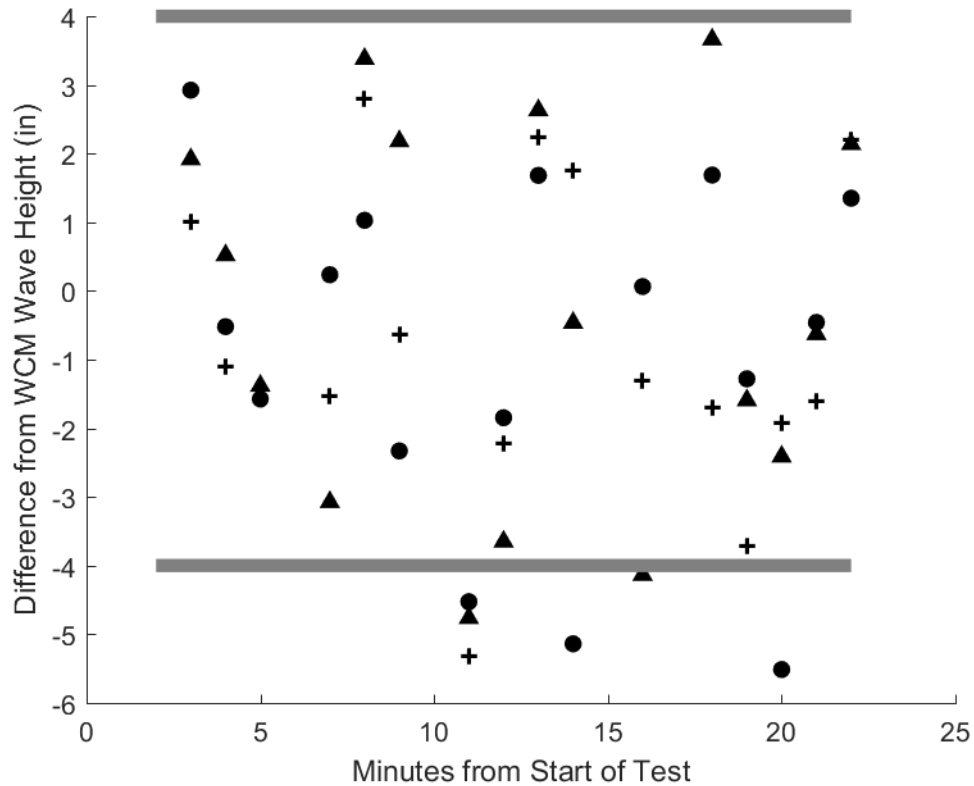


Figure I-15

Appendix J: Mean and Standard Deviation of Differences of the Significant Wave Height for WCM and WCM-Buoy Compared to Banner Data

This appendix contains plots showing the mean and standard deviation of differences of the significant wave height for each test using the WCM attached to the skimmer compared the Banner data. Each data point represents the mean of the difference between the significant wave height calculated statistically using the raw data from the WCM and the significant wave height calculated statistically using a segment of time corresponding to the WCM data from the raw Banner data for each test.

Figure J-1: Plot showing the mean and standard deviation of differences of the significant wave height for each test using the WCM attached to the skimmer compared the main bridge Banner data. Each data point represents the mean of the difference between the significant wave height calculated statistically using the raw data from the WCM and the significant wave height calculated statistically using a segment of time corresponding to the WCM data from the raw Banner data for each test.

Here it can be seen that the mean difference between most of the tests are within the 4-inch performance objective. The maximum differences are for Tests 5, 6, and 22. For these tests, the waves were created by the 18-inch stroke and 18 cycles per minute (CPM) setting of the wave generator, which creates a large sinusoidal wave. We believe the discrepancies between the WCM and Banner measurement are due to lateral motion from the large elliptical motion of the wave not being considered by the algorithms. This is because we trained them on real, complex wave motion where most of the movement is in the heave.

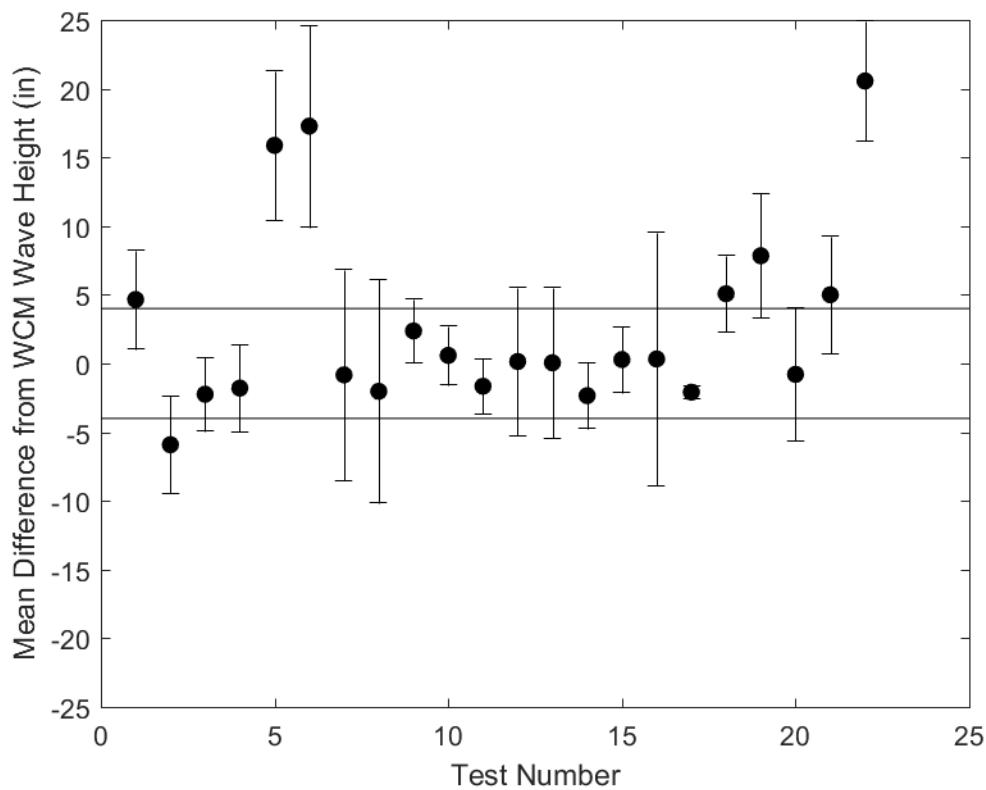


Figure J-1

Figure J-2: Plot showing the mean and standard deviation of differences of the significant wave height for each test using the WCM attached to the skimmer compared the west auxiliary bridge Banner data. Each data point represents the mean of the difference between the significant wave height calculated statistically using the raw data from the WCM and the significant wave height calculated statistically using a segment of time corresponding to the WCM data from the raw Banner data for each test.

Here it can be seen that the mean difference between most of the tests are within the 4-inch performance objective. The maximum differences are for Tests 5, 6, and 22. For these tests, the waves were created by the 18-inch stroke and 18 CPM setting of the wave generator, which creates a large sinusoidal wave. We believe the discrepancies between the WCM and Banner measurement are due to lateral motion from the large elliptical motion of the wave not being considered by the algorithms. This is because we trained them on real, complex wave motion where most of the movement is in the heave.

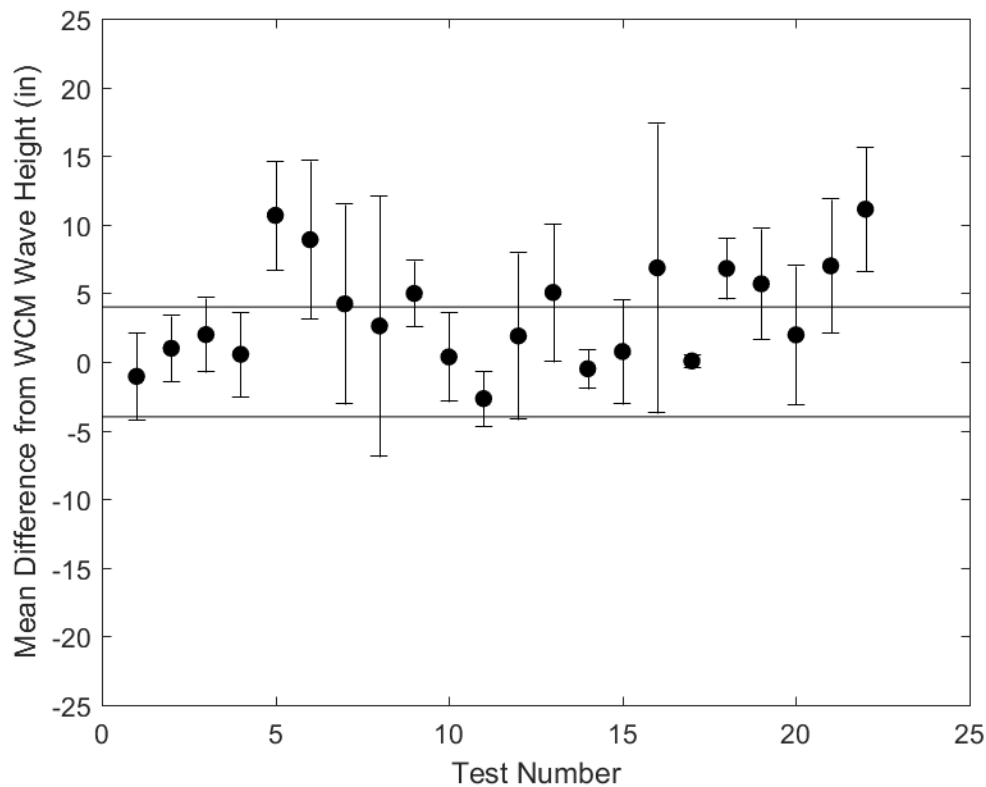


Figure J-2

Figure J-3: Plot showing the mean and standard deviation of differences of the significant wave height for each test using the WCM attached to the skimmer compared the east auxiliary bridge Banner data. Each data point represents the mean of the difference between the significant wave height calculated statistically using the raw data from the WCM and the significant wave height calculated statistically using a segment of time corresponding to the WCM data from the raw Banner data for each test.

Here it can be seen that the mean difference between most of the tests are within the 4-inch performance objective. The maximum differences are for Tests 5, 6, and 22. For these tests the waves were created by the 18-inch stroke and 18 CPM setting of the wave generator, which creates a large sinusoidal wave. We believe the discrepancies between the WCM and Banner measurement are due to lateral motion from the large elliptical motion of the wave not being considered by the algorithms. This is because we trained them on real, complex wave motion where most of the movement is in the heave.

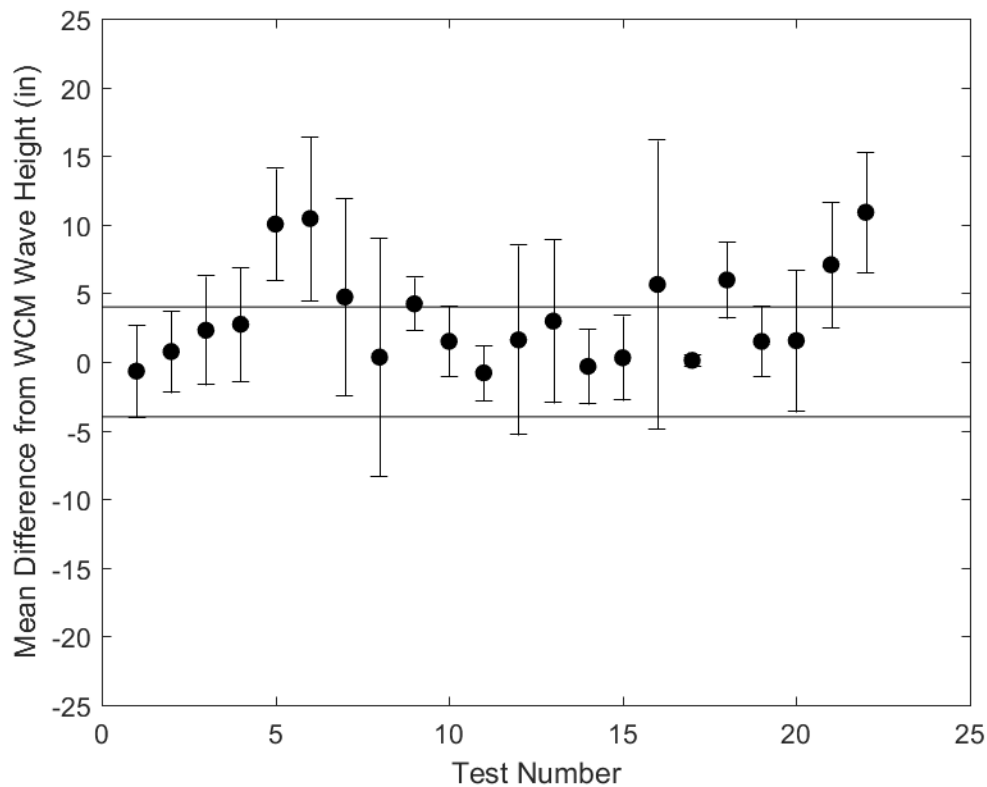


Figure J-3

This appendix contains plots showing the mean and standard deviation of differences of the significant wave height for each test using the WCM buoy compared the Banner data. Each data point represents the mean of the difference between the significant wave height calculated statistically using the raw data from the WCM and the significant wave height calculated statistically using a segment of time corresponding to the WCM data from the raw Banner data for each test.

Figure J-4: Plot showing the mean and standard deviation of differences of the significant wave height for each test using the WCM buoy compared the main bridge Banner data. Each data point represents the mean of the difference between the significant wave height calculated statistically using the raw data from the WCM and the significant wave height calculated statistically using a segment of time corresponding to the WCM data from the raw Banner data for each test.

Here it can be seen that the mean difference between most of the tests are within the 4-inch performance objective. The maximum differences are for Tests 1, 5, and 6. For these tests the waves were created by the 18-inch stroke and 18 CPM setting of the wave generator, which creates a large sinusoidal wave. We believe the discrepancies between the WCM and Banner measurement are due to lateral motion from the large elliptical motion of the wave not being considered by the algorithms. This is because we trained them on real, complex wave motion where most of the movement is in the heave.

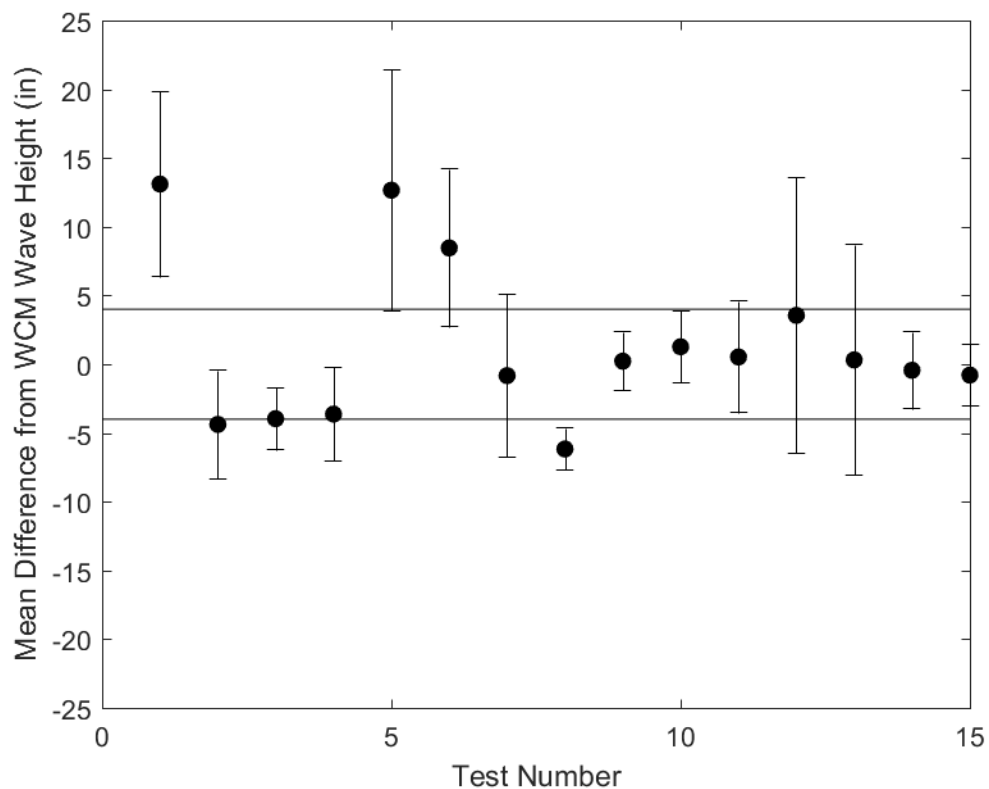


Figure J-4

Figure J-5: Plot showing the mean and standard deviation of differences of the significant wave height for each test using the WCM buoy compared the west auxiliary bridge Banner data. Each data point represents the mean of the difference between the significant wave height calculated statistically using the raw data from the WCM and the significant wave height calculated statistically using a segment of time corresponding to the WCM data from the raw Banner data for each test.

Here it can be seen that the mean difference between most of the tests are within the 4-inch performance objective. The maximum differences are for Tests 1 and 5. For these tests the waves were created by the 18-inch stroke and 18 CPM setting of the wave generator, which creates a large sinusoidal wave. We believe the discrepancies between the WCM and Banner measurement are due to lateral motion from the large elliptical motion of the wave not being considered by the algorithms. This is because we trained them on real, complex wave motion where most of the movement is in the heave.

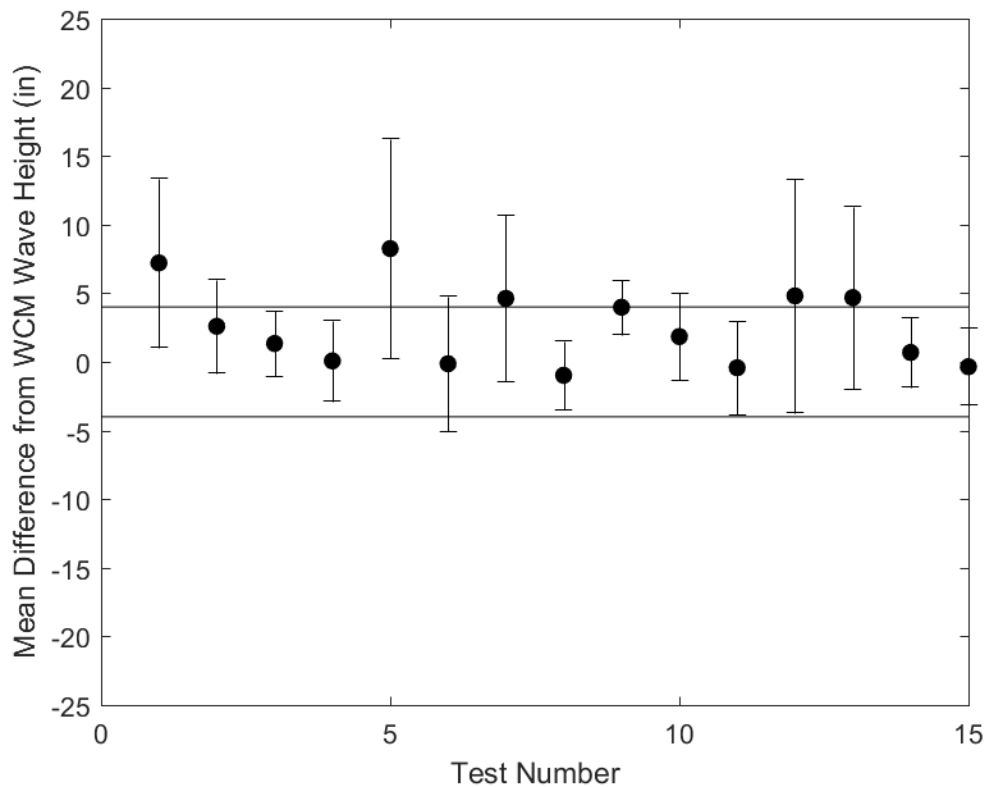


Figure J-5

Figure J-6: Plot showing the mean and standard deviation of differences of the significant wave height for each test using the WCM buoy compared the east auxiliary bridge Banner data. Each data point represents the mean of the difference between the significant wave height calculated statistically using the raw data from the WCM and the significant wave height calculated statistically using a segment of time corresponding to the WCM data from the raw Banner data for each test.

Here it can be seen that the mean difference between most of the tests are within the 4-inch performance objective. The maximum differences are for Tests 1 and 5. For these tests the waves were created by the 18-inch stroke and 18 CPM setting of the wave generator, which creates a large sinusoidal wave. We believe the discrepancies between the WCM and Banner measurement are due to lateral motion from the large elliptical motion of the wave not being considered by the algorithms. This is because we trained them on real, complex wave motion where most of the movement is in the heave.

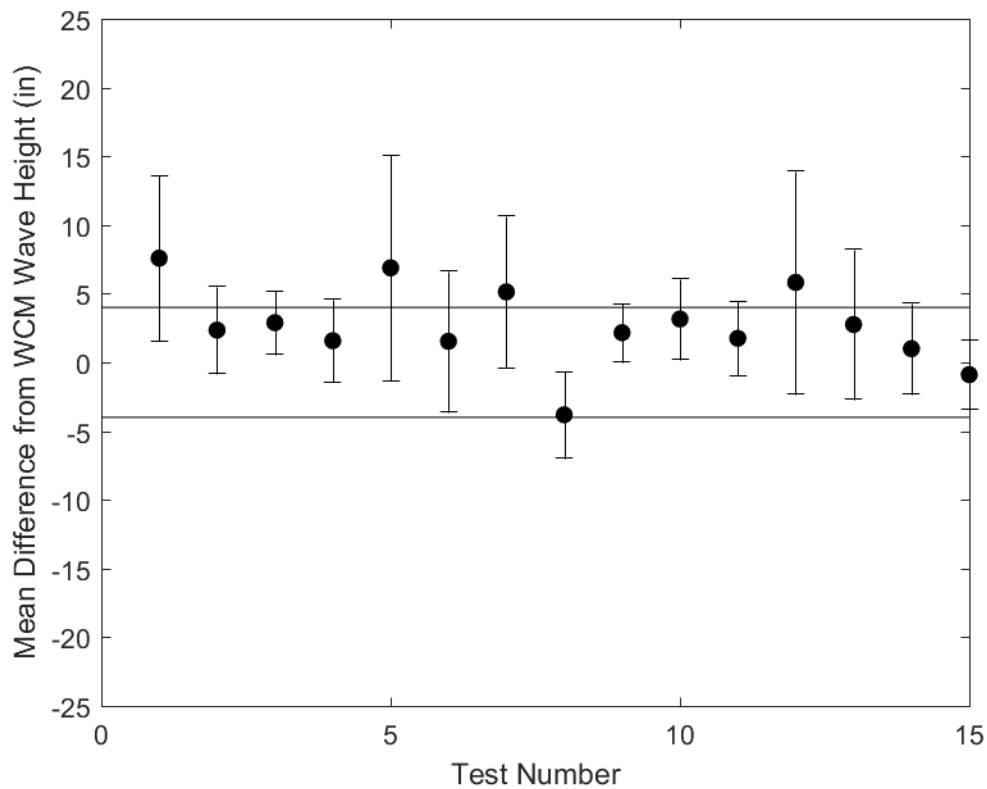


Figure J-6

Appendix K: Mean and Standard Deviation of Differences of the Significant Wave Height between Banners

This appendix contains plots showing the mean and standard deviation of differences of the significant wave height for each test between each Banner sensor.

Figures K-1a and K-1b (line at ± 4 inches): This plot shows the mean and standard deviation of differences of the significant wave height for each test between the main bridge Banner and the east auxiliary bridge Banner. Each data point represents the mean of the difference between the significant wave height calculated statistically using 80 seconds segments of the raw Banner data from Ohmsett. While there is small measurement error in the wave heights being measured by the Banner devices, there is a measurement uncertainty in the wave height due to the location of the device collecting data. This is due to the complex wave field generated in the tank.

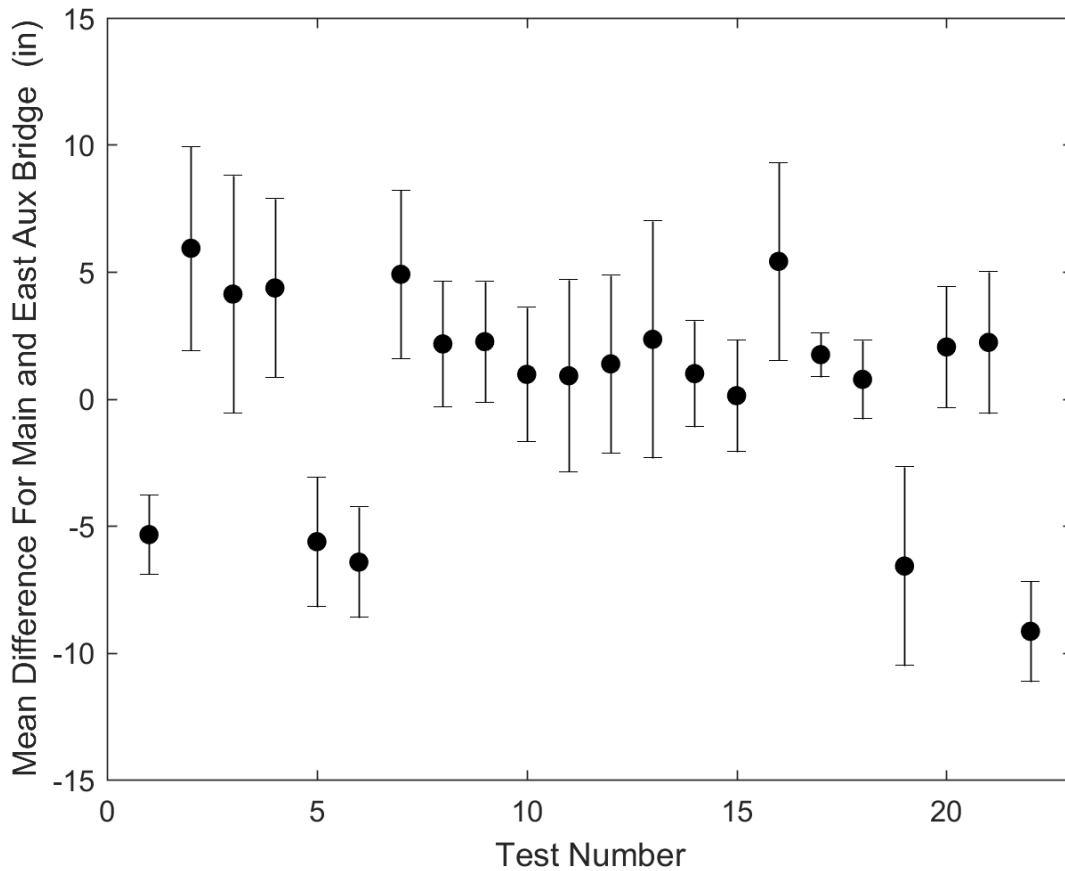


Figure K-1a

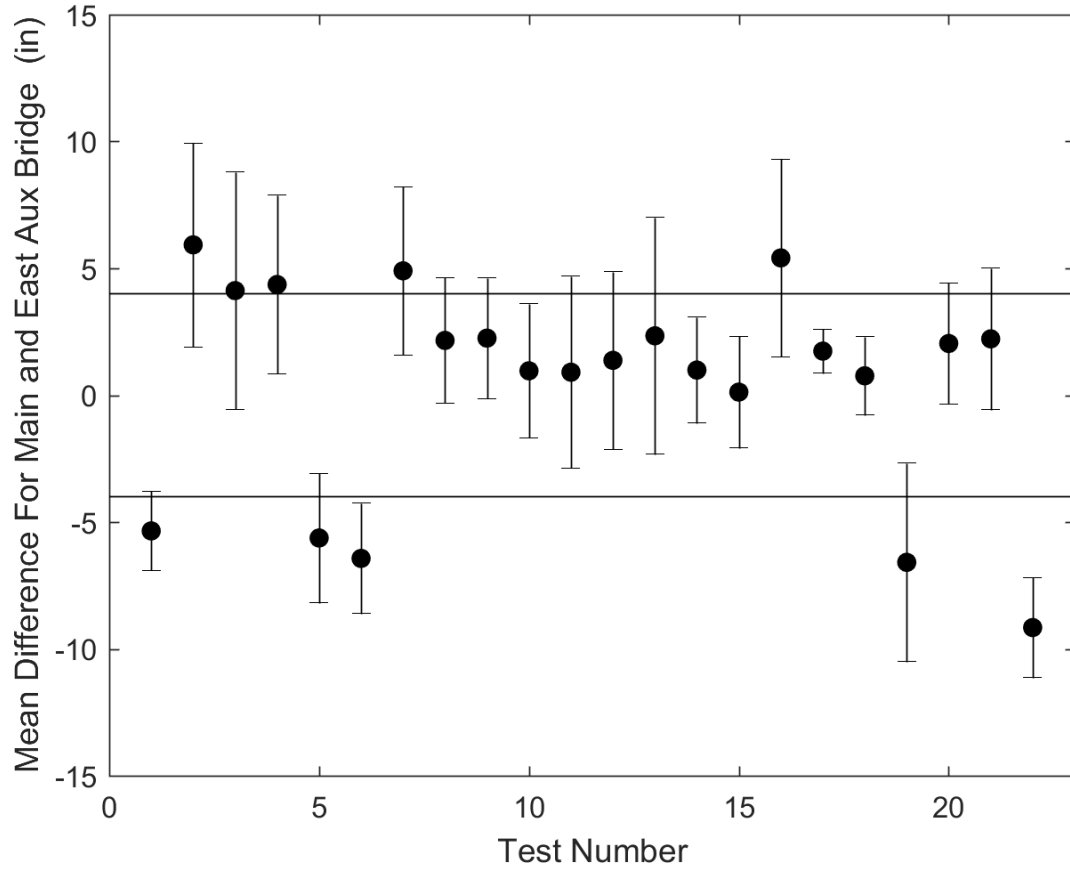


Figure K-2b

Figures K-2a and K-2b (line at ± 4 inches): This plot shows the mean and standard deviation of differences of the significant wave height for each test between the main bridge Banner and the west auxiliary bridge Banner. Each data point represents the mean of the difference between the significant wave height calculated statistically using 80 seconds segments of the raw Banner data from Ohmsett. While there is small measurement error in the wave heights being measured by the Banner devices, there is a measurement uncertainty in the wave height due to the location of the device collecting data. This is due to the complex wave field generated in the tank.

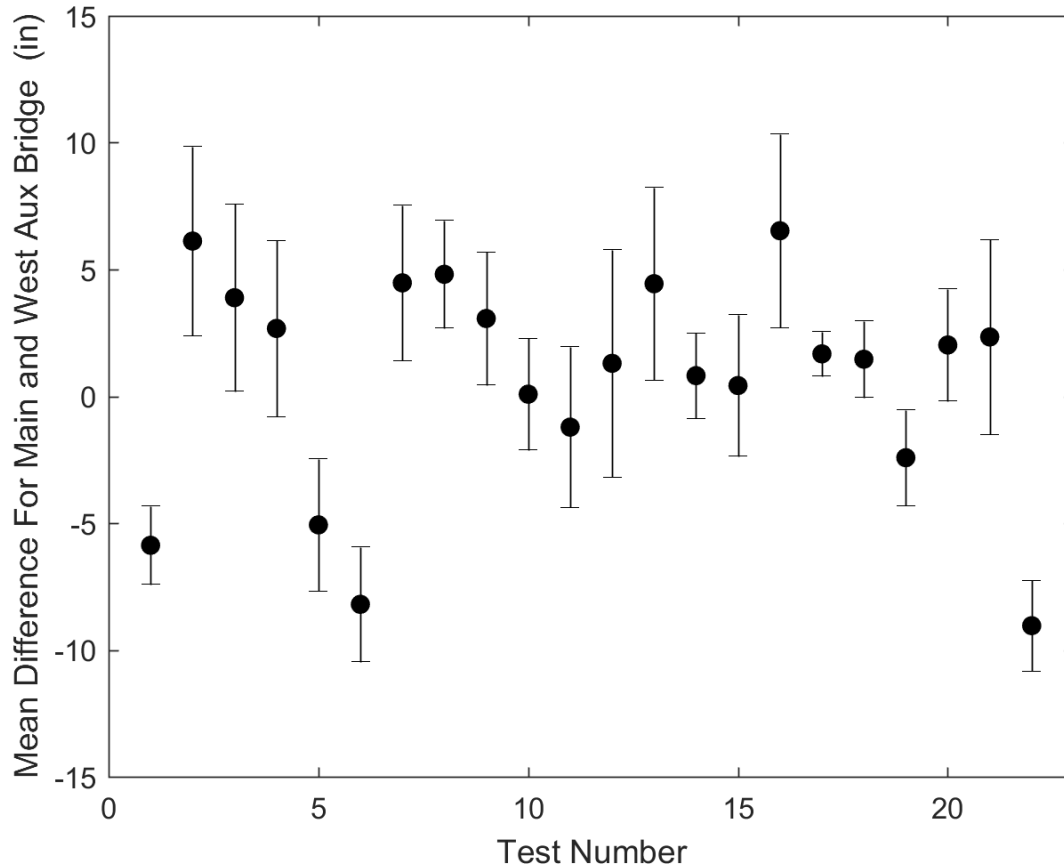


Figure K-2a

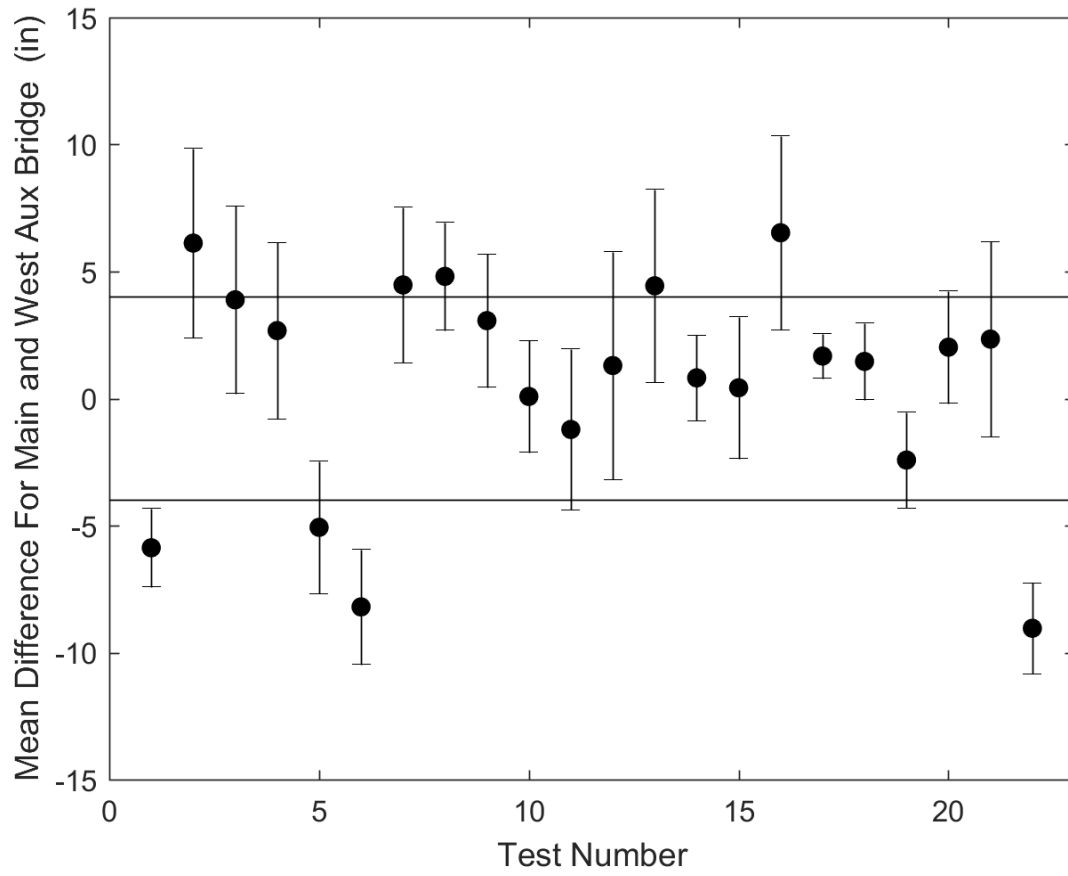


Figure K-2b

Figures K-3a and K-3b (line at ± 4 inches): This plot shows the mean and standard deviation of differences of the significant wave height for each test between the west auxiliary bridge Banner and the east auxiliary bridge Banner. Each data point represents the mean of the difference between the significant wave height calculated statistically using 80 seconds segments of the raw Banner data from Ohmsett. While there is small measurement error in the wave heights being measured by the Banner devices, there is a measurement uncertainty in the wave height due to the location of the device collecting data. This is due to the complex wave field generated in the tank. The difference between these two Banners is less than that seen between the main and auxiliary bridge. This is most likely due to the fact that the two Banners are separated by only a few feet, parallel at the same distance from the wave generator.

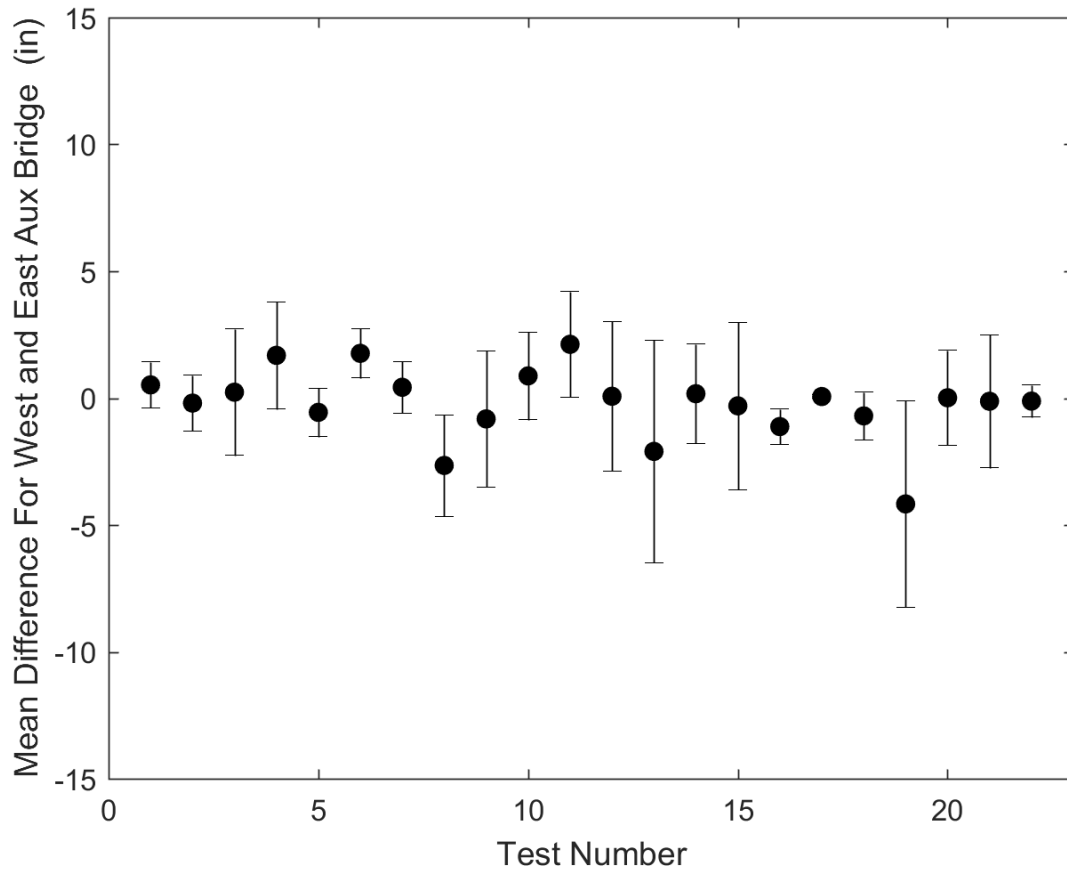


Figure K-3a

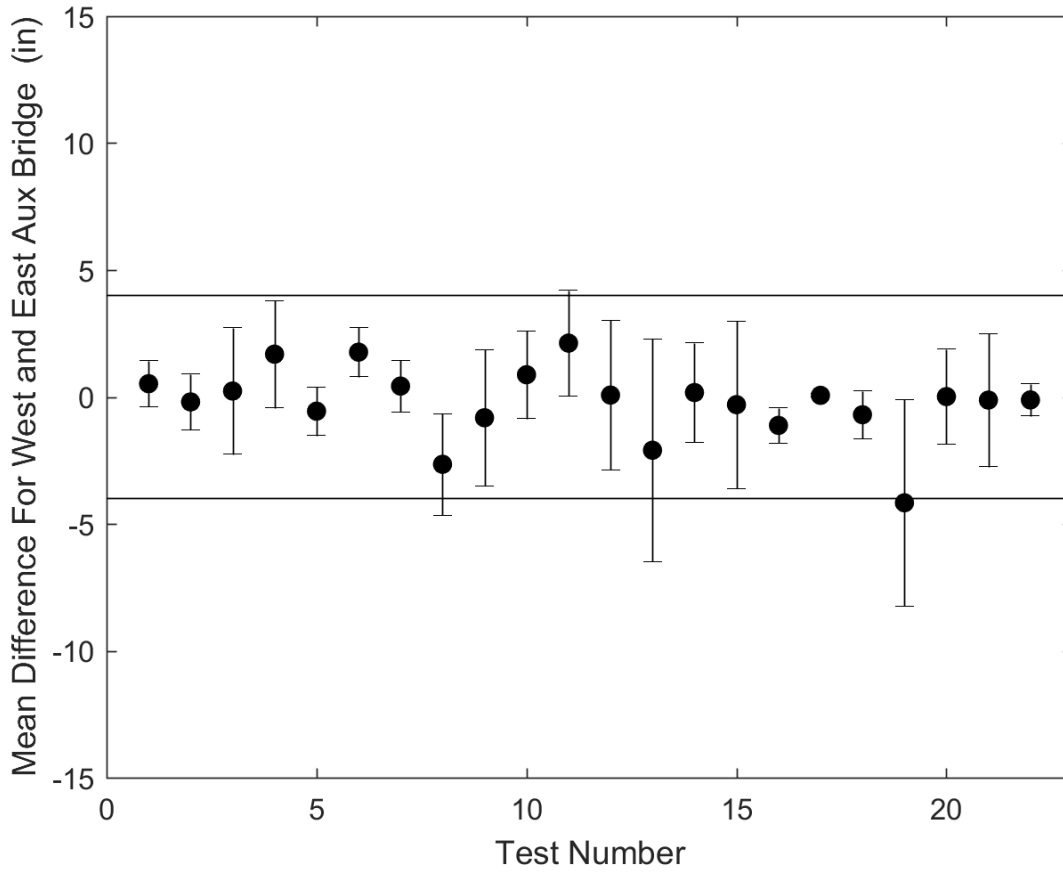


Figure K-3b

Appendix L: References

- Agilent. (2017) "Loss Tangent." http://cp.literature.agilent.com/litweb/pdf/genesys200801/elements/substrate_tables/tablelosstan.htm. Retrieved March 20, 2017.
- Banner. (n.d.). "Item Detail QT50U Series 8 M Range Chemical Resistant Ultrasonic Sensor." <https://www.bannerengineering.com/us/en/products/part.02726.html>. Retrieved November 7, 2017.
- Bishop, C. (2001, November 13). The Relationship Between Loss, Conductivity, and Dielectric Constant [PDF]. Retrieved from <http://www.electromagnetics.biz/the%20relationship%20between%20loss.pdf>
- Brodtkorb, P.A., Johannesson, P., Lindgren, G., Rychlik, I., Rydén, J., and Sjö, E. (2000). "WAFO – A Matlab Toolbox for Analysis of Random Waves and Loads." Proc. 10th Int. Offshore and Polar Eng. Conf., Seattle, USA, Vol. III, pp. 343-350.
- Chaplin, M. (2017, February 1). "Water and Microwaves." http://www1.lsbu.ac.uk/water/microwave_water.html. Retrieved March 20, 2017.
- Clarke, R.N. (2015). "Dielectric Properties of Materials." http://www.kayelaby.npl.co.uk/general_physics/2_6/2_6_5.html. Retrieved Retrieved March 20, 2017.
- CDIP (Coastal Data Information Program). (n.d.). "Wave Measurement." <https://cdip.ucsd.edu/?nav=documents&sub=index&xitem=waves>. Retrieved November 28, 2016.
- Erdogan, L. (2011). *Dielectric Properties of Oil Sands at 2.45 GHz Determined with Rectangular Cavity Resonator*. <https://publications.polymtl.ca/732/>. Retrieved March 20, 2017.
- Federici, C. and Mintz, J. (2014). *Oil Properties and Their Impact on Spill Response Options*. Retrieved from <https://www.bsee.gov/sites/bsee.gov/files/osrr-oil-spill-response-research//1017aa.pdf>.
- Fingas, M. (n.d.). *Vegetable Oil Spills: Oil Properties and Behavior* [PDF]. https://media.wix.com/ugd/183bd6_31263940630041af8118bbb2cb5ab4a3.pdf. Retrieved March 20, 2017.
- IEEE (Institute of Electrical and Electronics Engineers). (2017). "Miscellaneous Dielectric Constants." <https://www.microwaves101.com/encyclopedias/miscellaneous-dielectric-constants>. Retrieved March 20, 2017.
- Kabusa. (n.d.) *Dielectric Constants of Common Materials*. <https://www.kabusa.com/Dielectric-Constants.pdf>. Retrieved March 20, 2017.
- Komarov, V., Wang, S., and Tang, J. (2005). Permittivity and Measurements [PDF]. <http://public.wsu.edu/~sjwang/dp-rf-mw.pdf>. Retrieved March 20, 2017.
- Lund University. (2007, December 21). WAFO. <http://www.maths.lth.se/matstat/wafo/>. Retrieved November 28, 2016.
- Massel, S.R. (2013). *Ocean Surface Waves: Their Physics and Prediction (2nd Edition)*, Singapore: World Scientific, eBook Collection (EBSCOhost), EBSCOhost.
- McGill University. "Canola Oil." http://digitool.library.mcgill.ca/webclient/StreamGate?folder_id=0&dvs=1490300434236~827. Retrieved March 20, 2017.
- Park, J.H. (2014, May 9). *Complex Dielectric Properties of Crude Oils in the Wide Frequency Range 10^{-2} Hz ~ 10^9 Hz* [PDF]. http://www.npsm-kps.org/journal/download_pdf.php?doi=10.3938/NPSM.64.692. Retrieved March 20, 2017.

Pattnayak, T. and Thanikachalam, G. (n.d.). *Antenna Design and RF Layout Guidelines*, Document No. 001-91445 Rev. *D, Cypress Semiconductor [PDF]. <http://www.cypress.com/file/136236/download>. Retrieved March 20, 2017.

RF Café. (n.d.) “Dielectric Constant, Strength, & Loss Tangent.” <http://www.rfcafe.com/references/electrical/dielectric-constants-strengths.htm>. Retrieved March 20, 2017.

SAIC Canada (Science Applications International Corporation Canada). (2008, November). *Oil Spill Simulation Materials Review* [PDF]. http://www.pwsrca.org/wp-content/uploads/filebase/programs/oil_spill_response_operations/oil_spill_simulation_materials_review.pdf. Retrieved March 20, 2017.

Tadiran Batteries (Tadiran Batteries, Ltd.). (2008, May). “Guidelines for Disposal of Lithium Cells and Batteries.” Lithium Technical Notice LTN0111. <https://media.digikey.com/pdf/Other%20Related%20Documents/Tadiran/DisposalGuidelinesLithium.pdf>. Retrieved November 28, 2016.

